PHYSICO-CHEMICAL STUDIES OF GRAPHITE AND ITS COMPOUNDS

Thesis

submitted to the University of London

for the degree of

Doctor of Philosophy in the Faculty of Science

by

Joseph Charles ORR M.Sc.(Queen's University Belfast)

Chemical Engineering Department,

Imperial College,

London S.W.7

ABSTRACT.

Experiments are described in the course of which a new technique "flash sintering" was evolved. These had the purpose of exploring possible methods of sintering that avoid any recrystallisation except at contact points between particles of powder and at defect sites, thus permitting definitive measurements to be made on graphite powders where the magnitude of contact effects has hitherto been largely unknown. From this work it is believed that new light has been thrown on the mechanism of electronic conduction in such powders and that valid information can be obtained from powders on the energy levels in graphite crystal compounds.

Investigations of natural graphite crystals have led to the detection of an anisotropic thermo-electric effect and a thermo junction has been constructed between two crystals orientated along different crystallographic axis.

A compound between aluminium chloride and graphite has been prepared, its thermo-electric power determined and a value for the interplanar distance evaluated from X-ray data. Some electrical resistance measurements of this compound were made, the technique of flash sintering being employed.

Bromine-graphite was prepared and examined by X-ray diffraction. Some preliminary measurements were made of the resistance changes which occur along the two main crystallographic axis as a well-orientated block of natural graphite, reacted with bromine vapour.

The thermal expansion of aluminium chloride, bromine-graphite and potassium-graphite could not conveniently me measured by X-ray diffraction technique as the diffraction patterns did not show lines of sufficiently high angle for a shift to be measurable. The thermal expansion of graphite was measured as part of this investigation and the results are described in Appendix I. Principal findings are -

1) The greater electrical resistivity of graphite powders as compared to graphite block material can be accounted for purely in terms of constriction of current flow through interparticle contacts.

2) Powdering block graphite in air creates electron traps on the surface of the particles and increases the contribution of "holes" to electrical conduction.

3) "Flash sintering" reduces the electrical resistance of graphite powders by increasing the contact area between particles.

4) Electrons in a well-orientated graphite crystal show anisotropic energy relationships.

5) Natural graphite reacts with aluminium chloride to form a lamellar compound. The interlamellar spacing in this compound is 9.75Å. The bond between aluminium chloride and graphite is probably of the polarisation type.

Acknowledgements

The author wishes to thank Professor A.R.Ubbelohde F.R.S. for his supervision of this research and for his encouragement at all times. Thanks are also due to Dr.F.A.Lewis, Dr.G.Parry and Dr.A.Cimino for helpful discussions and to the Central Electricity Authority for financial support.

The work to be described was carried out in the Chemical Engineering Department of Imperial College between October 1954 and September 1957. Part of it has been published in

NATURE, 179, 193, (1957)

and in the

PROCEEDINGS OF THE PHYSICAL SOCIETY, 70, 928, (1957).

CONTENTS

General Introduction page

Chapter 1 Theoretical Background..... 7
: : : 2 Carbon in the solid state..... 20
: : : 3 Object and scope of the investigation..... 36

Part I

Contact resistance effects in graphite powders

Chapter 4 Introduction..... 39
: : : 5 Experimental..... 54
: : : 6 Results..... 63
: : : 7 Discussion.....110

Part II

Anisotropic thermo-electric effects in graphite

Chapter 8 Introduction.....163
: : : 9 Experimental.....169
: : : 10 Results.....174
: : : 11 Discussion.....181

Part III

The preparation and properties of some graphite compounds

Chapter 12 Introduction.....187
: : : 13 Experimental.....199
: : : 14 Results.....215
: : : 15 Discussion.....235

Appendix I..... 252
: : : II..... 258

References..... 262

GENERAL INTRODUCTION.

CHAPTER I

The following brief description of some aspects of theory taken from the work of various authors is intended to be in the nature of a definition of terms relevant to the present work.

THE BAND THEORY.

The Band model of the solid state has been successfully employed to describe the substances known as Insulators, Semiconductors and Conductors. It is an outcome of the Free-electron theory as developed by Sommerfeld. The important difference between the two approaches being that whereas in the Free-electron concept the potential due to nuclei of all the atoms in the solid is considered as smoothed out over the whole lattice, in the Band theory the treatment of Bloch, Brillouin and Wilson is incorporated by which the electrons are considered to move in a periodic field, the periodicity being that of the lattice.

ORIGIN OF THE BANDS.

It can be shown from wave mechanics that the atomic orbitals in a solid will broaden out into bands of permitted energies as the atomic nuclei are brought closer together. For maximum broadening there will be a critical separation depending upon electrostatic repulsion and attraction.

The bands are derived from the outermost atomic orbitals since it is only the outermost or valency electrons which may be considered

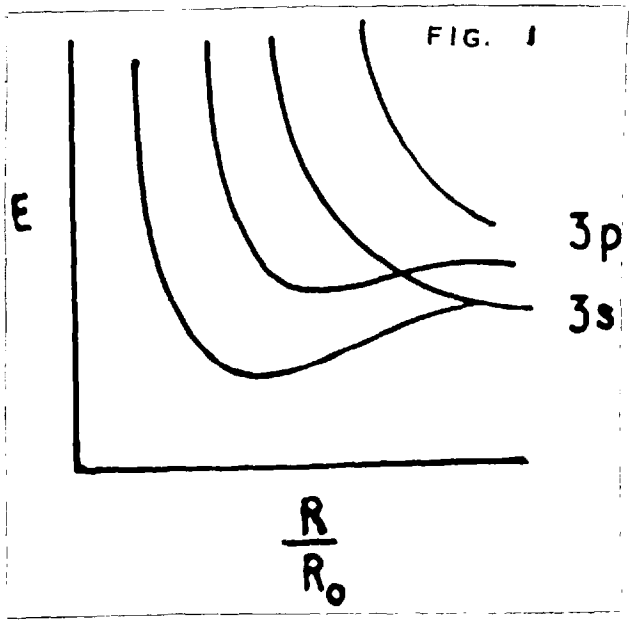


Fig. 1. The broadening of atomic orbitals of sodium into bands of permitted energies as a function of inter-atomic distance R. R_o = equilibrium distance.

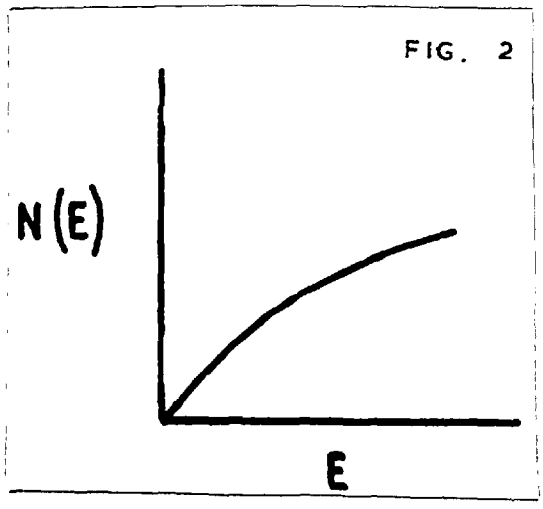


Fig. 2. Density of electronic states as a function of energy (Free Electrons).

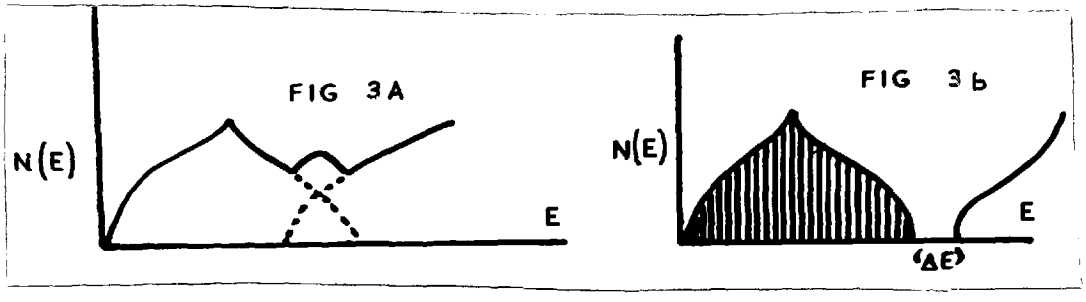


Fig. 3 (a) and (b). Density of electronic states as a function of energy (Periodic Field). (a) overlap between bands.
(b) energy gap between bands.

as delocalised. The crystals of some substances possess bands which can be shown to overlap. Fig. 1 shows the effect in sodium as an instance of this.

DENSITY OF ELECTRONIC STATES.

In the Free-electron theory the density of electronic states increases smoothly with Energy, $\int N(E)\, dE \propto E^{\frac{1}{2}}$ where $N(E)$ is the number of states with energy between E and E + dE (Fig. 2), whereas in the Periodic field model the density of states goes through a maximum in any one band. If overlap between bands occurs the density of states does not sink to zero but rises again at energies corresponding to the filling of the new band, Fig. 3(a).

CONDUCTORS.

On the Band model, conductors of electric current are considered as substances which possess an incompletely filled band or an overlapping system of bands. In the case of sodium the the overlapping of the 3S and 3p bands is of no major importance to the electrical conductivity since the 3S band is only half full. For calcium, however, a divalent metal, overlapping of bands is all important to the electrical conductivity since the valence band is completely full.

5

INSULATORS.

An insulator is considered to be a substance in which a full band is separated from a vacant band by an energy gap the crossing of which would require an activation energy which the electron under normal conditions could not possess. (Fig. 3b)

If electrons cannot be activated out of a full band on application of an electric field the electronic distribution cannot alter. The electrons within the full band may move but for every electron which moves into a higher energy state within the band an electron must drop down into the vacated level. Since electrons are indistinguishable the overall distribution cannot change and consequently no current can flow.

SEMI-CONDUCTORS.

These substances possess an appreciable electronic conductivity at room temperature which increases exponentially as the temperature rises according to the relationship $\sigma = \sigma_o e^{\frac{-E}{kT}}$

where σ = conductivity at T^oK

σ_o = conductivity at 0^oK

E = activation energy

T = temp. ^oK

A semi-conductor may be either of the intrinsic or impurity type. An intrinsic semi-conductor has a band system which is essentially that of an insulator, (Fig. 3b), the difference being that the

semi-conductor has a comparatively low electronic activation energy. The demarcation line between semi-conductors and insulators is generally placed at a conductivity of 10^{-10} ohm^{-1} cm^{-1}.

The impurity of extrinsic type of semi-conductor is technically the more important. It owes its conductivity to the presence of impurity atoms which increase the number of current carriers in the material either by injecting electrons into the vacant conduction band of the semi-conductors, (N type) or by extracting electrons from the full valence band thus creating positive holes (P type). When a sufficiently high temperature has been reached and all the impurity centres are ionised, the conductivity may become intrinsic.

ELECTRON SCATTERING.

Resistance to current flow in a solid arises because of interactions between the current carrier and force fields which are departures from the periodic field. Two causes of such fields are

1) displacement of the lattice atoms from their regular positions due to thermal oscillations,

11) the existence of imperfections due to chemical impurities, vacancies, interstitial atoms, etc.

1) may be called lattice scattering, and

11) may be referred to as impurity scattering.

Lattice scattering is responsible for the ordinary temperature dependent resistivity of pure metals. Impurity scattering produces additional resistance and is the cause of resistance at low temperatures.

HALL EFFECT.

Certain metals and certain semi-conductors behave as though they contained free electrons with a positive charge. This was discovered in 1880 by E.H. Hall whose name is linked with the Hall effect. The phenomenon is due to the fact that electrons travel in a curved path in a magnetic field. If an electric current is passed through a conductor in a direction normal to a superimposed magnetic field the Hall effect is the voltage difference which is observed across the conductor normal to both the Electric and Magnetic field.
The Hall Co-efficient R is defined by the relation

$$R = \frac{Ed}{IH}$$

where E is the transverse potential difference, d is the thickness of the sample parallel to the magnetic field of strength H. I is the total current.

There are metals for which the sign of the Hall effect implies that the current is borne by drifting positive carriers, e.g. Zn Be Cd Fe Co (1).

Quantum mechanics avers that the semblance of positive electrons in a conductor with positive Hall Effect is due to a singular attribute of a collectivity of negative electrons. A collectivity of negative electrons in a valence band which is short by X electrons of the number required to fill the band behaves as though it were a gas of X positive electrons pervading the metal or semi-conductor, provided that the vacant states all lie close to the top of the band.

This statement can be clarified somewhat if the electron

distribution in a solid is considered. It is important to the present work since Thermo-electric power measurements yield similar information as those of Hall Effect and in the results to be described positive values were obtained implying the existance of these "positive" electrons or holes.

The relationship between the energy E of the electrons and the wave number k (the number of waves/unit length) is illustrated in Figs. 4 and 5.

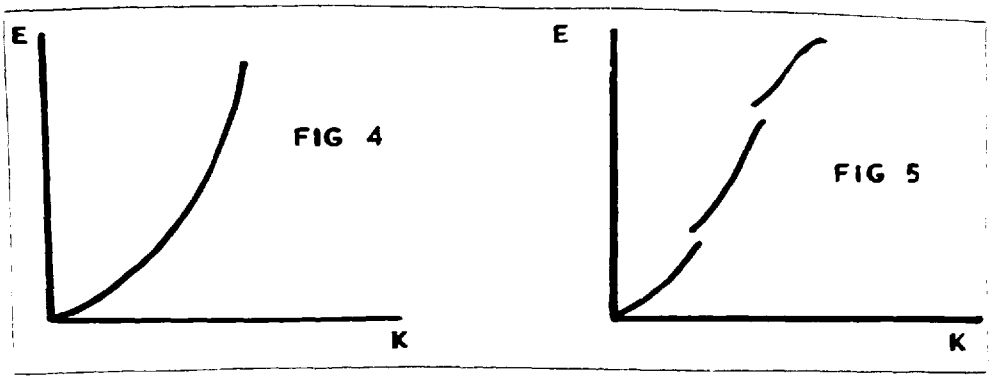


Fig. 4 illustrates the relationship for Free electrons and Fig. 5 that for electrons moving in a periodic field. Only Fig. 5 need be considered.

The velocity v of any electron is given by

$$V = \frac{2\pi e}{h} \frac{dE}{dk} \quad \text{(in one dimension)}$$

Where e is the charge on the electron E and k its energy and wave number respectively, h is Plancks constant.

Under the influence of an electric field the wave number in the

direction of the field increases uniformly with time and its variation is

$$\frac{dk}{dt} = \frac{2\pi eF}{h} \quad \text{where F is the field.}$$

The rate of change of velocity is

$$\frac{dv}{dt} = \frac{2\pi e}{h} \cdot \frac{d}{dt}\left(\frac{dE}{dk}\right) = \frac{d^2E}{dk^2} \cdot \frac{4\pi^2}{h^2} \cdot eF$$

This is an equation relating acceleration and force and if it is compared with the classical expression F = m.a. it will be seen that the mass is replaced by

$$\frac{h^2}{4\pi^2} \Big/ \frac{d^2E}{dk^2}$$

This is called the "effective" mass of the electron.

It can be seen from Fig. 5 that the E v k curve goes through a point of inflexion, such that in the upper region of any band $\frac{d^2E}{dk^2}$ is negative. In the upper part of any band the electron has then a negative acceleration and a negative "effective" mass. Such an electron has been called a "positive hole".

THERMO-ELECTRIC EFFECTS IN METALS AND SEMI-CONDUCTORS.

If two metals A and B are joined in contact to form a circuit, electrons will flow from the metal of higher electron density to the other until the Fermi level throughout the circuit is the same. The Fermi level may be defined as the energy at which the Fermi

distribution function is $\frac{1}{2}$. The distribution function $f_o(E)$ is given by $f_o(E) = \frac{1}{e^{(E-W)/kT}+1}$ where W is the energy of the electrons at the absolute zero and E is the energy of a quantum state of which $f_o(E)$ is the average occupation number.

THE SEEBECK EFFECT.

If one of the junctions is heated, the potential energy of the electrons at that junction will be increased and an electric current will be set up in the circuit to minimise this increase in energy.

The Peltier Effect.

Peltier showed that when a current is passed through a function of two different metals heat is absorbed or liberated depending on the direction of the current. This heat is often referred to as "Peltier heat" and it is produced at a rate proportional to the current flowing, i.e. Peltier heat per second = $\pi_{AB}I$ where π is the Peltier coefficient measured in calories per coulomb or volts, and I is the current in amperes.

THERMO-ELECTRIC POWER.

If the temperatures at the two junctions of the metals A and B in a closed circuit are T_1 and T_2 where $T_1 > T_2$, then $E_{AB}\ (T_1\ T_2)$ is the symbol for the EMF of the metal couple. If T_2 is kept fixed $E_{AB}\ (T_1\ T_2)$ often varies with T_1 according to a parabolic law

$$E_{AB}\ (T_1\ T_2) = a\ (T_1 - T_2) + b\ (T_1 - T_2)^2$$

This is not always true, but its approximate validy for many couples can be shown by plotting $\frac{dE_{AB}}{dT_1}$ against T_1. Some graphs are, however, straight. The quantity $\frac{dE_{AB}}{dT_1}$ depends only on the nature of A and B and on T_1.

The quantity is usually written $\frac{dE_{AB}}{dT}$ and is called the thermo-electric power of a junction.(2)

CONTACT BETWEEN A METAL AND A SEMI-CONDUCTOR.

If there are electrons in the conduction band of the semi-conductor, i.e. it is N type, and it is placed in contact with a metal, electrons will flow from the semi-conductor to the metal. This is due to electrons in a semi-conductor conduction band having energies greater than those of the valence band in a metal. In the metal the electrons in the valence band are conducting because the band is not full or because overlap with an empty band has yielded levels to which electrons may be raised. If the semi-conductor has a deficit of electrons in its valence band, i.e. it is P-type, when contact is established with the metal, electrons will flow from the metal to the semi-conductor because in this instance the semi-conductor has vacant levels of lower potential energy which the electrons of the metal may occupy.(3)

Fig.6

Diagram illustrating the thermo-electric power convention

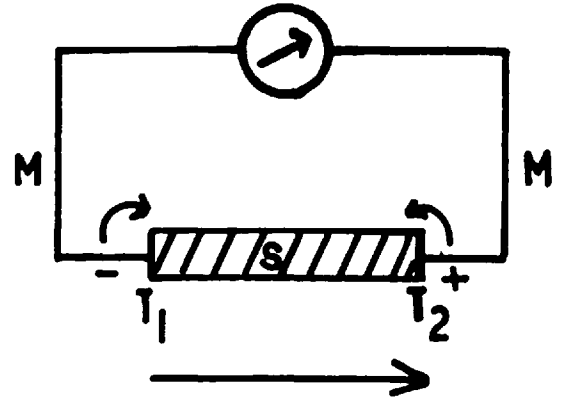


FIG. 6

ELECTRON FLOW
FOR
$T_1 > T_2$

M = METAL

S = P-TYPE (HOLE) SEMI CONDUCTOR

THE SIGN OF THE THERMO-ELECTRIC POWER.

In a metal semi-conductor circuit the sign of the thermo-electric power is the instrument sign at the cold junction. Fig. 6 represents a metal semi-conductor circuit where "M" is the metal and S a "P" type semi-conductor.

When contact is established with the metal electrons will flow from the metal to the semi-conductor as indicated by the arrows. If T_1 and T_2 are the temperatures at each contact and if T_1 is greater than T_2 the overall electron flow will be in the direction indicated since the electrons at T_1 because of the higher temperature there are at a greater potential than at T_2. Electron flow in this direction will make the colder junction positive with respect to the indicating strument.

For N-type (electron conduction) semi-conductors electrons will pass from the semi-conductor to the metal at each contact. For $T_1 > T_2$ the colder junction will be negative.

GENERAL INTRODUCTION

CHAPTER 2.

CARBON IN THE SOLID STATE.

Carbond may be considered as constituting a series of compounds - the series of condensed polynuclear aromatic solids - with graphite as its limit. These materials are compounds, for other bonded elements - mainly hydrogen - are always present, but such impurities occur in very small and variable amounts and no uhique stoichiometry can be ascribed to any particular compound. The term "Carbons" was coined at a time when the presence of hydrocarbon impurities was not detected or their significance overlooked, but in the interpretation of solid state properties, especially electronic ones, these impurities play a crucial role.

All organic substances, whether consisting of chain-like or ring-like molecules, when heated above 600°C condense and form polynuclear aromatic solids and although there exists a fundamental structural similarity between the solid state properties, in general they depend upon the extent to which the aromatic ring system had been developed. The ring system may be cross-linked through hydrocarbon side chains and through the linking up of freed valencies, and as the heat-treatment temperature is increased, lateral growth occurs and the islands of fused rings are laid down parallel with respect to one another.

When X-ray diffraction photographs of carbon are examined it is

found that for solids prepared at low temperatures (700 - 1000°C), the patterns are diffuse and resemble bands rather than diffraction lines. These bands, however, approximate to the positions which some graphite lines would occupy. As the temperature of heat treatment increases, and reflections become sharper indicating a more ordered structure with larger crystallites. However, until a heat treatment temperature around 1700°C has been reached corresponding to a crystallise size of ~ 150Å, one very important set of graphite reflections is absent. These reflections correspond to the h k l indices and they are significant because they indicate the onset of 3 dimensional order. Before they appear reflections such as the o o l show that the layer planes are lying parallel, but since no h k l reflections are present they are randomly orientated with respect to one another. Above ~ 1700°C the true graphite lattice is present in which the lamellae are not merely parallel but take up definite positions in space. Carbons without this three dimensional order are called turbostratic. On further heat treatment above 1700°C the lines sharpen up with crystallite growth until at about 2800°C a sharp diffraction pattern is obtained corresponding to well ordered polycrystalline graphite, (4) (5) (6) (7) (8) (9). The artificial graphite used in the present work showed good three dimensional order.

~~Fig.~~ PLATE 2

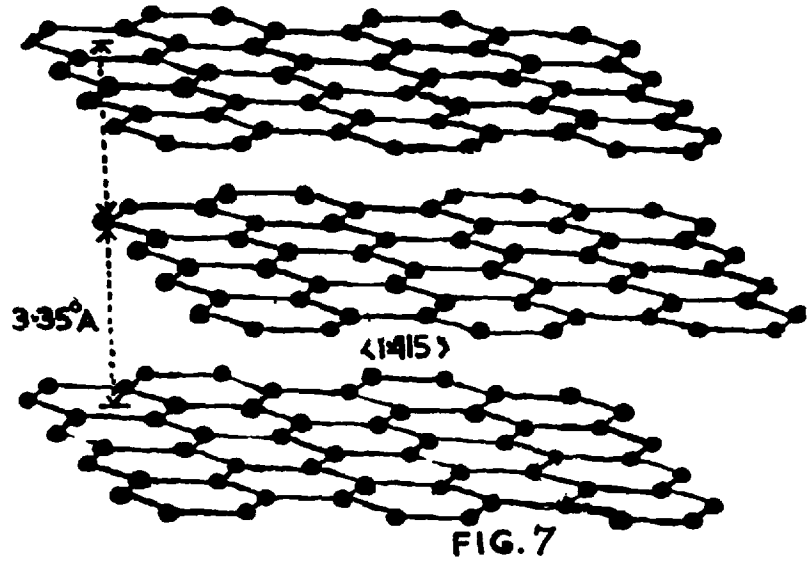


FIG. 7

HEXAGONAL FORM

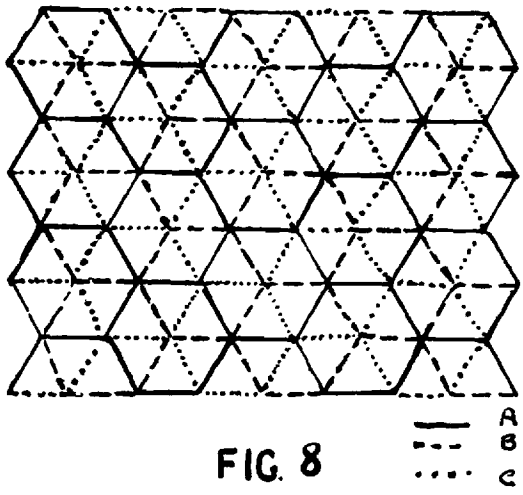


FIG. 8

RHOMBOHEDRAL FORM

CRYSTAL STRUCTURE OF GRAPHITE.

The crystal structure of graphite was one of the first to be investigated by X-rays and to the present day it has been the subject of investigation of increasing precision. It has been shown that graphite has a layer lattice structure possessing hexagonal symmetry. The atoms in each layer are arranged in hexagonal array with an interatomic distance of 1.415Å and an interlayer distance of 3.354Å (10). The layers are so arranged that half the number of atoms in one layer lie above half the number of atoms in the layer beneath and the pattern repeats in an AB AB series (11) (12). Fig. 7.

There exists, however, another structure which graphite may exhibit but which is usually only found in natural graphites and here only making up at most about 15% of the total structure. This is the Rhombohedral modification, (13) (14). For this a third layer is inserted making an ABC series. Fig. 8.

The Rhombohedral form can, however, be introduced into synthetic graphites by grinding to very small crystallites. It can be removed by boiling with hot concentrated acids. (15).

Valence Bonding in the Aromatic Lattice.

Each carbon has four electrons (2S, $2p^3$). In the aromatic lattice three of them are hybridized (2S, 2px, 2py) to give three co-planar orbitals at an angle of 120° to one another. The undisturbed 2pz orbital is at right angles to the σ orbitals and is referred to as the π orbital. The π orbitals of neighbouring

carbon atoms coalesce to form streamer-like orbitals which allow motion of the electrons over the entire molecule. The σ orbitals of neighbouring atoms interact to form a single bond and fractional bonding results from π electron interaction (16).

Bonding in Graphite.

The carbon atoms within any layer plane of graphite are valence bonded to one another. Each bond is a sigma bond and each carbon atom has three sigma bonds all lying within the same plane and inclined at 120° to one another. The bond between any two neighbouring carbon atoms is strengthened by the fractional bonding due to the overlap of the orbitals of the unhybridized 2Pz (π) electrons.

No valence bonds can exist between the layers; (ideal graphite only is considered here: valence defects must exist in all graphites above the absolute zero of temperature and defect structures involving valence bonding between layers are likely to be present, e.g. bonding resulting from a different type of hybridization such as is present in the diamond structure). The force holding the layers together results from an equilibrium of forces. These forces are those of attraction and repulsion. The attractive ones arise from a correlation of the motions of electrons in each π electron envelope due to the creation of instantaneous dipoles. The interpenetration of these envelopes would tend to place electrons in the same quantum state in the same region of space which is forbidden by the Pauli Exclusion principle. This is the origin of the repulsive force.

The distances between the layers are determined by the radii of the π electron envelopes and this gives the aromatic ring in graphite an effective thickness of 3.35Å.

Because of the amphoteric nature of graphite in compound formation (see part III) another type of interaction may occur which could lead to an additional attractive force between the layers. Each layer approximates to a large aromatic molecule and since each "molecule" may accept or donate electrons, e.g. the reaction with potassium, bromine, and aluminium chloride, there is the possibility that some form of charge transfer or polarisation might occur between such "molecules" resulting in increased binding. (17).

Theoretical Models.

Coulson and Wallace (18) (19) have derived a wave mechanical model for graphite. They consider only an ideal single crystal where the fused ring systems are considered to be of infinite extension and derive a band system considering only the π electrons in two dimensions. This simplification is permissable in view of the delocalization of the π electrons along the basal plane and the lack of evidence for quantum mechanical interaction along the hexagonal axis. The model has been successfully employed in interpreting many solid state properties. A full band of π electrons is considered to be contiguous with an empty band of higher energy so that as the temperature increases electrons can pass smoothly into the upper one without activation. The electrical resistance should

consequently increase with temperature like a metal. More recently it has been suggested that the bands overlap to a small extent (20). However, this only strengthens the metallic analogy. Experimentally it has been shown that when electrical resistance measurements are carried out along the basal plane of a single crystal of graphite the electrical resistance does increase with temperature (21) (22).

It is known that there is an energy gap between the electronic ground state of an aromatic molecule and its first excited state, and a Van der Waals solid formed from such a molecule has an energy gap between the full band of π electrons and the next higher band (conduction band) of about the same magnitude (23). According to Mrozowski (24) as the molecules grow in size, during the graphitisation process the energy gap diminishes tending towards the zero gap of the Coulson and Wallace model of ideal graphite, this reduction of gap width being the exact analogue of the shift in the absorption spectrum to the red for molecules with increasing numbers of benzene rings or with increasing length of chains.

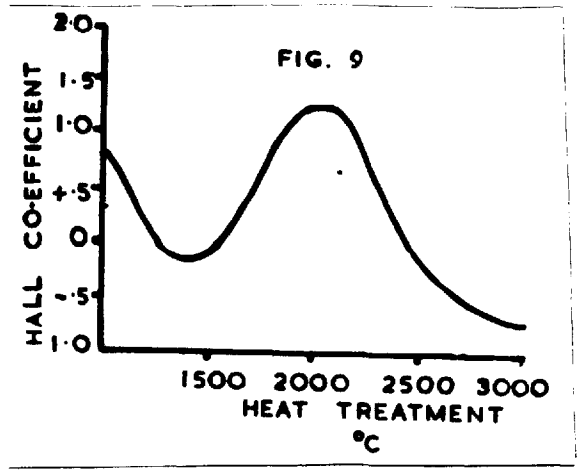
Some experimental results for carbons of different heat treatments are shown in Table I.

TABLE I

Heat Treatment Temperature	600°C	500-700°C	900-1700°C	2200	Ref.
Crystallite Diam.	20Å	15 - 25Å	25 - 80Å	150Å	23
Activation Energy (e.v.)	0.3	0.5 - 0.2	0.15-0.03	0.01	"
Specific Resistance ohm. cm.	10^5	10^7 - 1.0	0.005	10^{-3}	"
Sign of Hall Coefficient		+	-	+ to -	"

HALL EFFECT IN THE CONDENSED AROMATIC SERIES

The Hall Effect curve for the series gives considerable insight into the conduction mechanisms of carbons. Fig.9 represents values of the Hall Co-Efficient obtained for carbons of different heat-treatment temperatures.



It can be seen that graphite(heat-treatment temp.,3000°C) has a negative co-efficient implying that electrical conduction is by electrons. Polycrystalline graphite is an intrinsic semi-conductor due to the conduction band not being far above the valence or π band and thermal activation is sufficient to promote electrical conduction. When an electron is activated to the conduction band it leaves a "hole" in the valence band and thus the number of conducting "holes" and electrons is the same. It might be expected then that there should be zero Hall Effect.Electron mobility however is

greater than that of holes (25) and so electron conduction predominates.

For carbons prepared at 1000°C it has been shown from electrical conduction measurements that the energy gap between the π and conduction bands is so large that $\Delta E >> kT$. Thus since no electrons are likely to be present in the conduction band and since the carbon is a conductor, the π Band cannot be full. Under these conditions "hole" conduction would be expected and the positive value of the Hall co-efficient shows that this is the case. To account for the depleted π band it has been suggested that in the heat treatment process as hydrogen is evolved it removes an electron from this band. (24). As the heat treatment temperature is increased the progressive evolution of more and more hydrogen depletes the band still further and the magnitude of the positive co-efficient decreases as the number of holes increases. On further heat treatment crystal growth by diminishing the number of electron traps causes the π band to fill up again until the maximum at 2000°C. At this point according to the model the energy gap is of the order of kT so that electrons may be thermally activated from the π band. Electrical conduction in material prepared above 2000°C is therefore by means of "holes" and electrons with electron conduction predominating at the higher heat treatments because of its greater mobility.

Electrical conduction in polycrystalline carbons and graphite.

There is a continuous increase in the electrical conductivity of carbons as the temperature of heat-treatment increases. Between a temperature of 600°C and 2,200°C the specific resistance decreases from 10^5 ohm. cm. to 10^{-3} ohm. cm. Table I.

Individual carbons whatever their heat-treatment temperature show a similar type of resistance-temperature variation. The resistance in each case decreases with increase of temperature in the manner of a semi-conductor and activation energies may be evaluated from log ρ versus $\frac{1}{T^{o}_{k}}$ plots where ρ is the resistivity. When this is done throughout the aromatic series it is found that the values continually decrease (Table I). This has been interpreted as the narrowing of the gap width between the valence and conduction bands in the solid as a result of crystal growth (23) (24).

MAGNETIC PROPERTIES IN THE CONDENSED AROMATIC SERIES.

The magnetic susceptibility of carbons if plotted against heat treatment temperature shows a large increase in the range 1600°C - 2400°C. The susceptibility which is diamagnetic does not increase appreciably above the temperature corresponding to a crystallite size of about 150Å although crystal growth continues. In the initial stages of heat treatment of aromatic chars i.e. between 500°C and 1000°C there is a decrease in the susceptibility which involves a temperature dependent paramagnetism. This is attributed to free radicals with unpaired spins trapped in the solid (26). Fig. 10 shows the trend in magnetic susceptibility for carbons of increasing crystallite size (27).

Anisotropy of the Magnetic Susceptibility.

For aromatic hydrocarbons, the diamagnetism is very large along an axis normal to the aromatic rings as compared to that measured in the plane of the rings (28).

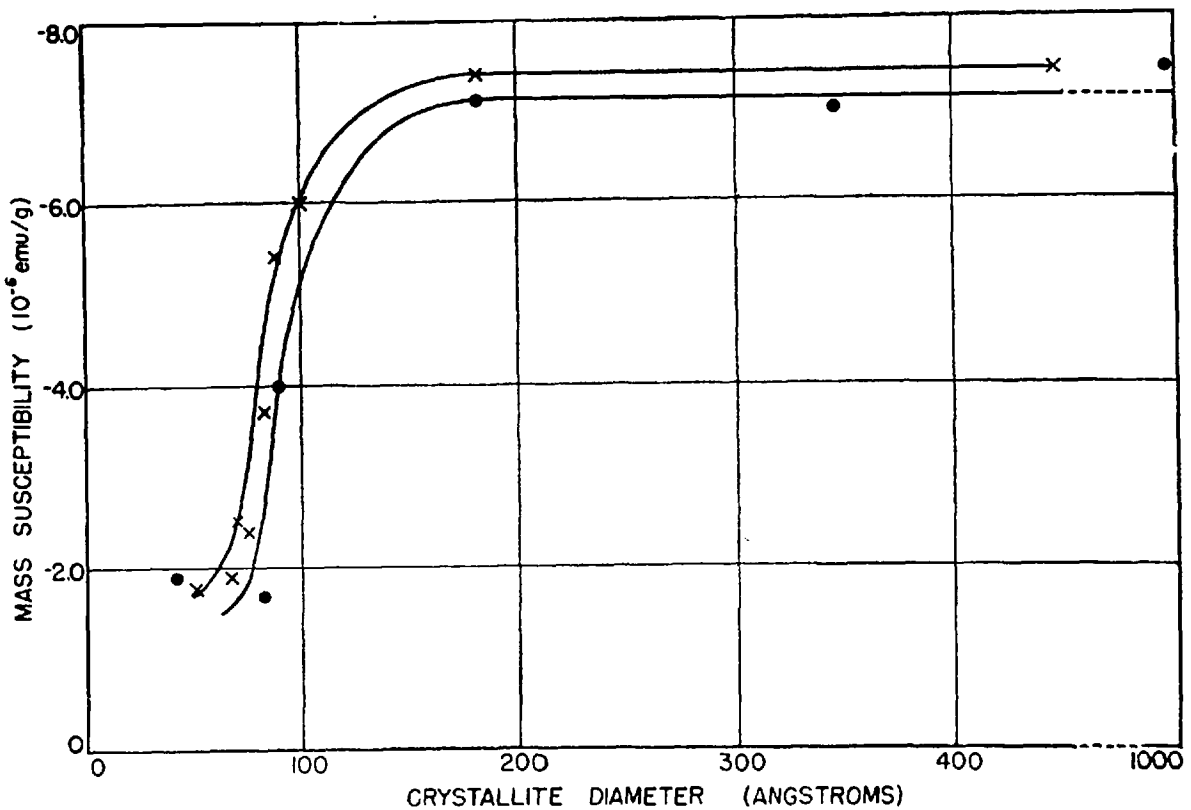
In Langevin's theory the total molecular magnetism is obtained by a summation over all the orbits of the closed electron shells

$$\chi_m = \frac{-Ne^2}{6mc^2} \sum \overline{r}^2$$

The large diamagnetism found for aromatic molecules arises from the fact that these molecules contain $\overline{\pi}$ electrons, which because of their delocalisation have very large orbits. This involves large

FIG. 10
x National carbon rods
• Thermax carbon black powder

Ref. (27)



values of the term $\sum \bar{r}^2$ which is a summation of the projected areas of the electronic orbits on a plane normal to the direction of the magnetic field. Delocalisation of π electrons occurs only along the basal plane, hence the effective electron orbits are much larger when the magnetic field is applied perpendicular to the basal plane than when the field is applied parallel to it.

For a graphite single crystal the magnetic susceptibility has been found to be

$$\chi^{\perp} = -22.0 \times 10^{-6} \text{ e.m.u./g.}$$

$$\chi^{\parallel} = -0.5 \times 10^{-6} \text{ e.m.u./g.}$$

giving an anisotropy ratio of 44. (29).

THERMO-ELECTRIC POWER.

Loebner (30) demonstrated that the sign and magnitude of the thermo-electric power of carbons and graphite was a function of their heat-treatment and in general followed the same trends as the Hall Effect, Fig. 9.

Values observed for natural graphites show considerable variation (31) (32) which is probably due to the presence of naturally occurring impurities.

HEAT PHENOMENA OF CARBONS AND GRAPHITE.

In non-metallic crystals heat is transmitted by lattice vibrations. As described above, the degree of crystalline perfection played an important role where electronic and physical properties of carbons and graphite were concerned, and the same consideration is important in dealing with various thermal properties.

Specific Heat.

The simple Debye model is unable to explain the temperature dependence of the specific heat of graphite and it has been suggested that the specific heat of layer lattices falls into a special category. Hove and Smith (33) consider that the main contribution to heat transfer comes from an in-plane mode of vibration which should result in a T^2 temperature dependence.

Thermal Conductivity.

Fig. 11 illustrates the temperature variations of the thermal conductivity at low temperatures for a number of graphites. It can

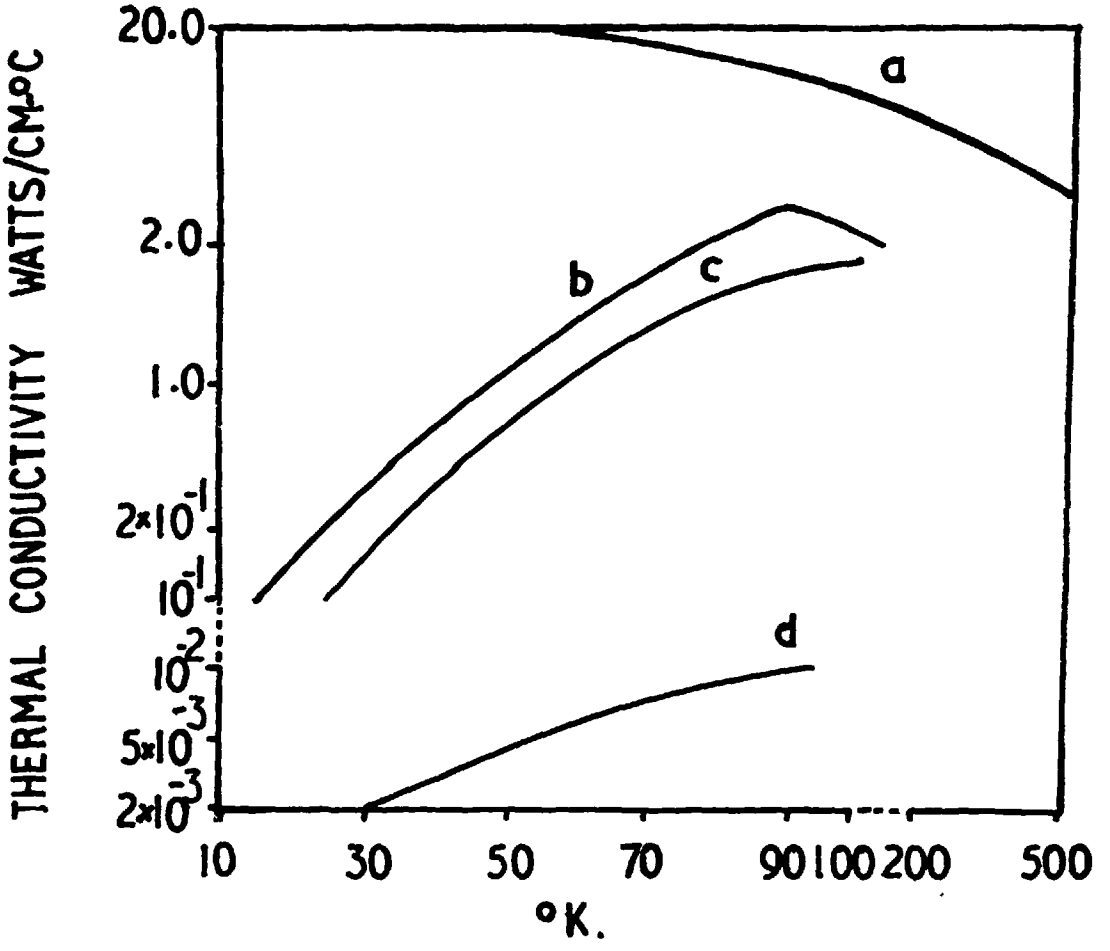


FIG. 11

a, b } NATURAL GRAPHITE REF. (34)

c SYNTHETIC GRAPHITE REF. (35)

d CARBON RESISTOR REF (35)

be seen that the conductivity increases with temperature until a maximum is reached. The temperature at which this maximum occurs depends upon the size, purity and degree of perfection of the crystallites. At higher temperatures the conductivity decreases with increasing temperature. Where carbons are concerned, however, the conductivity continues to rise until a broad maximum is attained at temperatures corresponding to those which mark the conversions of carbon into graphite. As a general rule, the thermal conductivity of carbons increases with temperature from room temperatures while that of graphite decreases.

The maximum in the thermal conductivity curve is due to the interaction of lattice waves with one another (phonon-phonon scattering) finally predominating and the consequent reduction of the conductivity with increase of temperature. At low temperatures thermal conduction is limited by the scattering of lattice waves at crystallite edges and this effect diminishes with increasing temperature thus increasing the conductivity.

Carbons of small crystallite size have low thermal conductivities which increase with temperature to a broad maximum. As the crystallite size increases, the thermal conductivity increases and the maximum occurs at lower temperatures and tends to become sharper.

CHAPTER 3

OBJECT AND SCOPE OF THE INVESTIGATION.

One of the most characteristic properties of graphites is its ability to absorb a number of substances such as potassium bromine and ferric chloride between the layers of fused hexagons. Such layers are generally known as lamellae and the compounds are referred to as lamellar compounds. These reaction products are true crystal compounds since their X-ray diffraction patterns show them to have characteristic structures.

McDonnell, Pink and Ubbelohde (35) first examined the electronic properties of potassium and bromine-graphite. Their compounds were true lamellar compounds having maximum intercalation. One of the most striking features of their results was the marked decrease of electrical resistance which the compounds exhibited as compared to the original graphite. Since compound formation always caused the graphite to crumble, the above authors carried out all their work with graphite powder. In view of the low electrical resistivity of the compounds it is important to establish whether crystalline powders of graphite exhibit large contact resistances between particles as with some metal powders. If this were so, compound formation might merely reduce this contact resistance and the large decrease of resistivity found would have a trivial explanation. Because of this unknown nature of the contacts between particles of graphite and because the extent of their influence on the band structure of graphite was not known, it was therefore difficult to interpret the properties of the lamellar compounds. The problem is aggravated by the low electrical resistance

of graphite; changes in the order of packing in powders as well as electrode contact resistance might be expected to influence this property profoundly. The object of Part I of this investigation was to elucidate the nature of the intercrystalline contacts and to develop a technique for the measurement of electronic properties in graphite powders.

Thermo-electric power measurements give important information concerning changes in the band structure of a solid. Since it was intended to measure the thermo-electric power of graphite powders and block material it was thought that the same measurement on highly crystalline material might provide an interesting comparison. The object of Part II then was to investigate thermo-electric effects in single crystal or well orientated graphite.

The ability of graphite to intercalate such widely differing chemical species as potassium, bromine and ferric chloride creates a field where research is called for to elucidate the nature of the bonds formed in such compounds. It also provides the impetus for attempts to prepare new compounds.

The object of Part III was to prepare and investigate new compounds of graphite and to measure the thermal expansion of graphite at low temperatures with a view to making similar measurements on the compounds, low temperatures ensuring that the compound would not decompose. Thermal expansion data should give some indication of the strength of bonding between the graphite lamellae and the intercalated species.

PART I

CONTACT RESISTANCE EFFECTS IN GRAPHITE POWDERS.

CHAPTER 4

INTRODUCTION TO PART I

CONTACT RESISTANCE EFFECTS IN POWDERS.

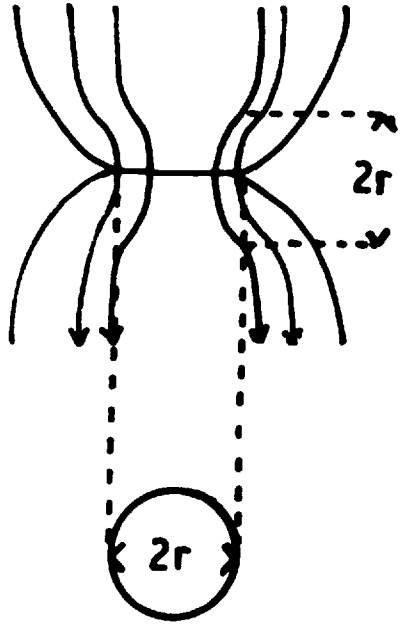
The electrical resistance of a powder is composed of different parts. Resistance to current flow is not only due to lattice vibrations but factors such as

1) poorly conducting films of adsorbed or chemisorbed molecules on crystalline surfaces,
2) disorder at inter-crystalline boundaries,
3) constriction of current flow through the small contact region between particles,

may also contribute to it.

If the powder is not "ideally" packed such that the maximum number of contacts is not realised, the resistance will also be a function of the packing.

With metals 1) often playes a large part in determining the electrical resistance, (37). Intercrystalline disorder, however, is not as great a barrier to current flow in metals as in molecular solids. The electrons in a metal may be considered as completely delocalised and the effect of intercrystalline boundaries is to cause only a small perturbation of electron waves. The molecular solids, however, where the forces of attraction between molecules are Van der Waals forces, boundaries contribute significantly to the resistance since there is no electron overlap between molecules.



CONTACT AREA.

FIG. 12

Considered as a macro molecular solid, graphite with its extensive π electron system represents a transition between metallic and Van der Waals systems.

The Nature of the Constriction Resistance.

If an electric current is passed between two contacting surfaces the flow of charge will be greatly constricted in passing from one to the other as only a very small fraction of the solids will be in electrical contact. Fig. 12. Because of this constriction in the current flow the potential difference across the interface will exceed that which would have been produced by the same current flowing uniformly across the boundary. This disturbance in the current stream will give rise to an additional resistance in the electric circuit.

The region in which the current flow is constricted extends into the bulk of the materials for a distance equal to several times the diameter of the contact area (38), but the constriction is most severe in the material close to the interface and a very large fraction of the potential drop occurs there.

Strout (39) showed that when a current passes between two large conductors across an interface of which only a circle of radius r is conducting the extra resistance due to constriction is given by

$$R = \frac{\rho}{2r}$$

where R = resistance
and ρ = specific resistance of the material

If more than one region is in contact but if the radius of each contact is the same the total constriction resistance is $R = \frac{\rho}{n2r}$ where

n = the number of contacts.

This may be re-written as $R = \frac{1}{2} \rho(\frac{\pi}{A})^{\frac{1}{2}}$ where A is the total contact area. The area of contact is determined by the load W operating on the surfaces and Pm the mean yield pressure of the asperities in contact, such that $A = \frac{W}{P_m}$.

This model of constriction resistance assumes that over the circle of contact the surfaces are within range of one anothers fields of force, so that from the point of view of electrical conduction, the two specimens behave as a continuous single conductor of uniform conductivity. Those portions of the two specimens which are a few Angstroms apart will also be partly conducting because of the tunnel effect. For portions of the surfaces more than 5Å apart the tunnel effect is negligible. (37) Consequently the contact resistance if the region of contact is essentially metallic provides a reasonably close measure of the real area of contact between the surfaces, i.e. the area over which one surface is within molecular range of the other.

The Constriction Resistance when adsorbed films are present.

It is clear that if adsorbed films are present on the surfaces of the materials in contact the above considerations will be greatly complicated. Only a small part of the contact area for example may be in true electrical contact. It was part of the object of the work to be described to determine whether such films were present in graphite compacts.

FIG. 13.

The effect of pressure on the conductivity and apparent density of graphite compacts. These results were obtained concurrently with the present investigation by another worker, (Dr. F.A. Lewis) in the same laboratory.

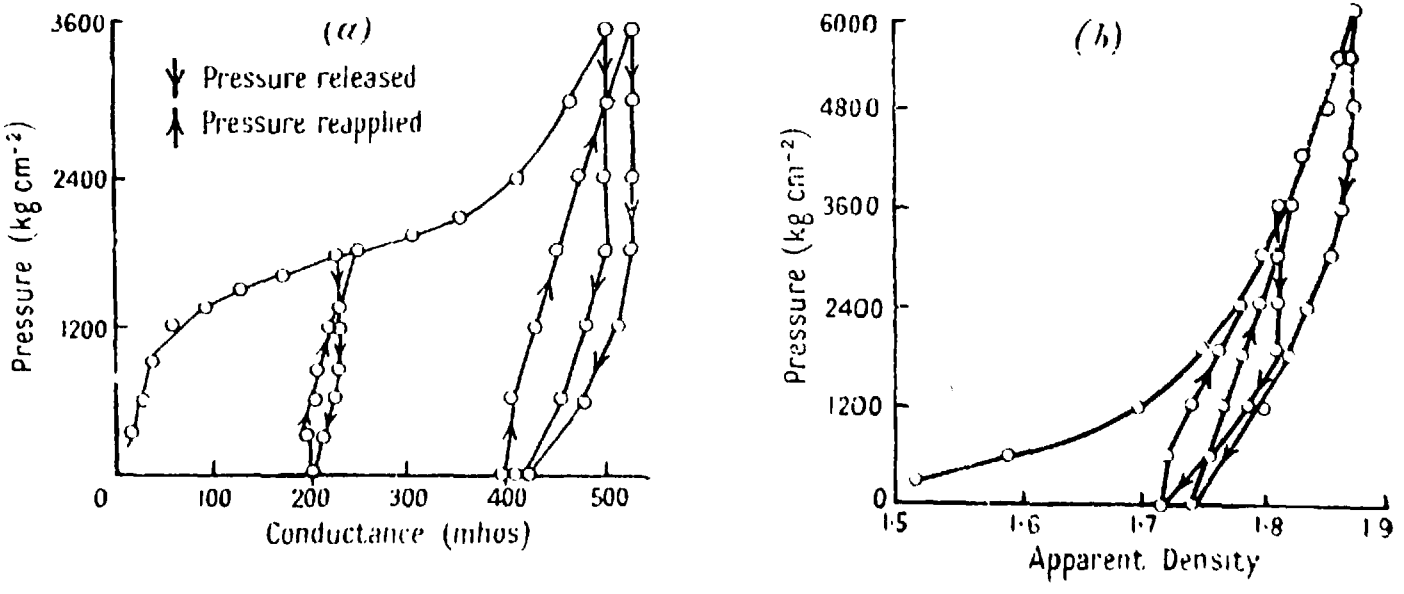

(a)
Pressure released
Pressure reapplied
Pressure (kg cm⁻²)
3600
2400
1200
0
100
200
300
400
500
Conductance (mhos)
(b)
Pressure (kg cm⁻²)
6000
4800
3600
2400
1200
0
1·5
1·6
1·7
1·8
1·9
Apparent Density

Figure 13

The contact resistance of carbon under pressure.

Knowles (40) investigated the electrical contact resistance between two blocks of carbon as a function of the pressure holding them together. He found that the resistance decreased with increase of pressure and that this change was reversible. Reproducible results were obtained over a number of pressure cycles, pressures up to 20 kg/cm^2 were employed. These results suggest that the controlling forces should be due to the inherent physical properties of the crystal structure and not to surface film breakdown. In a column of powder, however, the contacts are both in parallel and in series and pressure induced packing variations are likely to be irreversible and hence cause irreversible resistance changes.

Work carried out concurrently in the same laboratory as the present work and using the same graphite powders showed the effect of increasing pressure on the electrical conductance (the reciprocal resistance) and density of a column of powder, Fig. 13. The conductance increased irreversibly with pressure and this effect was reflected by irreversible density changes. It seems clear that the increased conductivity of compressed powders is due mainly to tighter packing of the particles and consequently the realization of more parallel contacts.

The number of parallel current paths through the interface between two blocks of carbon will,depend upon the load applied, for as the load increases more asperities on the two surfaces will interlock. This is the explanation Knowles suggests for his results which show that the interface resistance decreases with increasing load.

Increase of pressure will bring more surface asperities into contact with one another; this, however, will only occur if the asperities in contact in the first instance either break, deform elastically or deform plastically. Since Knowles observed that the electrical resistance changed reversibly with pressure, the most reasonable explanation would be that elastic deformation of carbon occurred.

DEFORMATION OF A SURFACE UNDER LOAD.

If two solid surfaces are pressed together under a load W they will at first deform elastically. The region of contact will be bounded by a circle of radius "a" where

$$a = 1.1 \left\{ \frac{Wr}{2} \left(\frac{1}{E_1} + \frac{1}{E_2} \right) \right\}^{\frac{1}{3}} \qquad (41)$$

where r is the radius of curvature of the asperity and E_1 and E_2 are Youngs module for the asperity and the surface respectively. At this stage therefore the area of contact, $A = \pi a^2$, will be proportional to $W^{\frac{2}{3}}$ whilst the mean pressure (Pm) over the area of contact — $Pm = W/\pi a^2$ — will be proportional to $W^{\frac{1}{3}}$. In the region of elastic deformation if the load is removed the surfaces return to their original configuration. As the load "W" is increased the mean pressure Pm increases until it reaches such a value that at a critical point within the softer material the elastic limit is exceeded. The material then yields plastically and irreversibly.

Surface Flow and Friction.

The characteristic frictional properties of metals are due largely to their ability to flow plastically and to weld together under load. The welded junctions so formed are sheared during the sliding process. The friction depends upon the intimacy of contact, the yield pressure and the shear strength of the junctions. If one of these factors is altered there will be a corresponding alteration in the frictional force. For example, at extremely slow speeds of sliding, these factors vary in such a way that the resultant strength of the metallic junctions is often greater than that occurring at higher speeds of sliding. This means that static friction is often higher than kinetic friction. If therefore one of the sliding surfaces has a certain degree of elastic friction, the motion may not be continuous but may be intermittent and proceed by a process of "stick-slip". The "stick" is due to the higher static friction between the surfaces and the "slip" to the lower kinetic friction during the "slip" itself. Surface damage is caused by ploughing and fragmentation due to hot spots. With similar metals the friction is very much higher and there are large fluctuations but no rapid slips are observed. In this case both surfaces flow equally and contribute in comparable measure to the formation and shearing of the metallic junctions. Consequently the changes are less marked and less abrupt than with combinations of dissimilar metals. (42).

The Friction of Graphite.

With graphite, friction is very low and it remains low up to high temperatures. On one view the low friction is due to the marked anisotropy of the crystal structure. Graphite has a layer structure and the bonding between layer planes is very weak. Shearing between the layers occurs readily and hence the low friction co-efficient (about 0.15) may be explained.

Another theory attributes the good lubrication properties of graphite to adsorbed water molecules. Savage (43) found that when graphite is out gassed by heating in vacuo its friction co-efficient increases and wear is very heavy. Friction was reduced by the admission of small traces of water vapour to the system.

The influence of surface films on the friction and electrical contact resistance between metals.

Although the area of contact under given conditions is determined primarily by the mechanical properties of the solid, the intimacy of the contact and the strength of adhesion at the points of contact will be greatly influenced by the strength of surface films. It can be demonstrated that under most experimental conditions metal surfaces are covered with a thin oxide layer and other contaminating films. During sliding these oxide and surface films are torn and some metallic contact occurs. The adhesion and shear strength of these junctions which consist of metal plus torn fragments of oxide and other contaminents is less than that of the pure metals and removal of the surface film leads to a large increase in friction. (44).

The electrical resistance of a surface film may readily determine the contact resistance between two metals. If the two metal surfaces are placed under load the resistance decreases somewhat. The same effect may be produced by holding a tuning fork against one of the metals. It is probable that this process breaks through the contaminating film at the region of contact.

If a lubricant film, e.g. paraffin oil, is placed between metal surfaces under loads sufficient to cause plastic flow at the regions of real contact, the electrical resistance between the surfaces is essentially the same as that observed with unlubricated surfaces. This suggests that the high pressure is sufficient to squeeze out the oil film. Although metallic oxide film is considerably more regid there must be a similar breaking through of the oxide layer. There may, however, be small quantities of oxide left between the surfaces which may play a less significant role in this type of measurement but a more important role in others. (42). This latter observation by Bowden is particularly relevant to the present work where it will be shown that thermo-electric power measurements indicate the presence of contaminent surface groups on particles of graphite powder which do not, however, affect the electrical resistance to any significant extent.

DRIFT WITH TIME OF THE ELECTRICAL RESISTANCE OF CARBON UNDER PRESSURE.

Both Knowles (40) and Mrozowski (45) found that under constant loading conditions there was a period during which the electrical resistance "settled down", that is, it decreased with time. Knowles as described earlier, was working with a simple system, i.e. two carbon blocks and the interface between. Mrozowski was working with carbon powders. The same phenomenon was observed with graphite powders in the present work, Fig. 17 and is described later. The type of measurement carried out in this work - temperature variation of electrical resistance for example - involving very small changes of magnitude necessitated that the drift of resistance should be eliminated.

Surface flow below the melting point.

It is well known that the mechanical strength of many metals and solids falls to a low value at temperatures well below the melting point. The rounding of sharp metal crystals and the low value of the tensile strength, hardness and other mechanical properties at these temperatures show that metals may lose their rigidity and resistance to shear at comparatively low temperatures. For such solids flow would be expected to occur at temperatures well below the melting point and experiment shows this can occur, (42). In the work to be described it is suggested that surface flow of carbon occurred during the process of flash sintering.

The drift with time of the electrical resistance of the powder seemed likely to be the result of growth of the contact area between particles. For example, if two metals are brought together under loading conditions the pressure is first transmitted through very small regions of each material which project from the surface. Because of the intense pressure on these regions they yield either elastically or plactically until the number and area of contacting surfaces is large enough to support the load.

Between the particles of a powder the same type of mechanism is possible. However, if packing is not perfect, movement of whole particles into different positions is likely. The material is not rigidly fixed and the yielding of small asperities under stress may lead to slip of the whole particle. This new position will be held until yield occurs elsewhere in the compact when co-operative movement may again take place.

The contact sites between particles are likely to play a considerable role in determining the overall electrical resistance of the compact. This is due to the high resistance they offer to current flow either because of the presence of impurity films on the surfaces of particles or in the case of "clean" contacts to constriction of the current path. A method of sintering was sought which would lead to improved stability at the contact sites.

SINTERING OF SOLIDS.

The process of "sintering" comprises the agglomeration of a powdered solid into a more or less compact mass by heating at a temperature below the melting point. It may therefore be regarded as a solid-solid reaction involving particles of a single reactant. Surface energy considerations show that small particles of solid (or small droplets of liquid) will always have some tendency to agglomerate into larger units. Among the most important factors which govern the degree of sintering in solids is the rate at which atomic diffusion may occur between two particles in contact. Activation energies calculated for sintering processes are often the same as those found for self diffusion in the same media. Foreign films on the surface of the particles influence the rate and degree of sintering profoundly and in these cases the relationship between diffusion and sintering processes is not so clear. (46).

The usual sequence of operations in commercial powder metallurgy is to compact metal powders in a die at room temperature and sinter the compact in a furnace. In hot pressing, the compacting and the sintering are combined. The loose powder, or in many cases a cold formed compact is inserted into the die which is held at the hot pressing temperature, the compact is left in the die until it attains its temperature and then pressure is applied and maintained for a given length of time. One of the principle difficulties in hot pressing is the lack of suitable die materials which will have adequate strength at the hot pressing temperature.

CHAPTER 5.

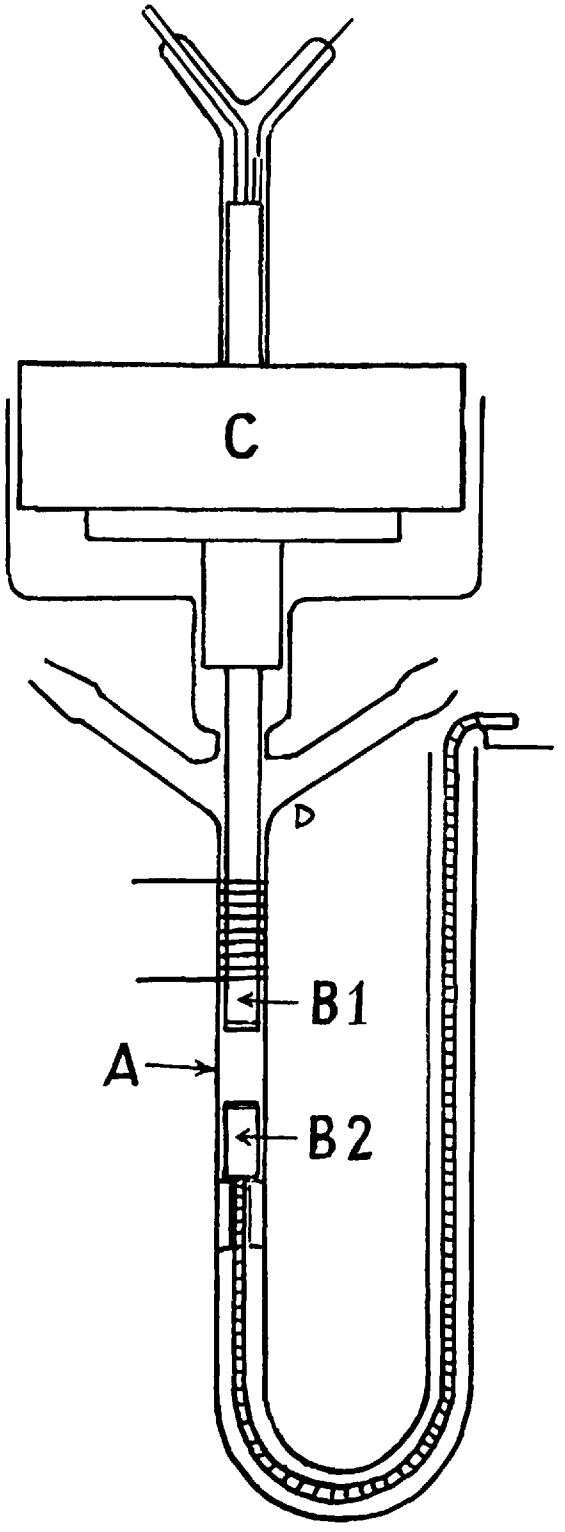
PART I : EXPERIMENTAL.

Choice of Sintering Method.

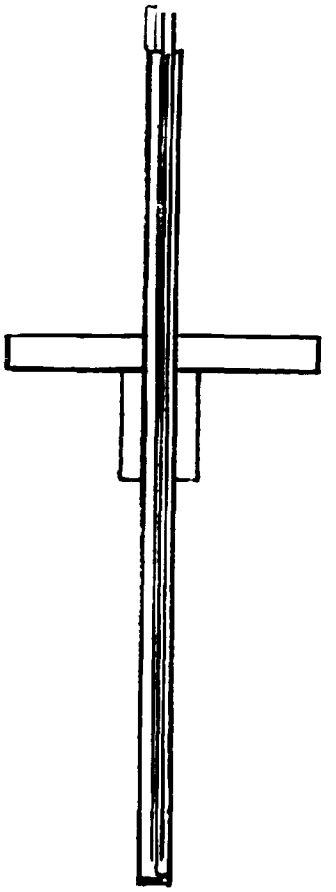
It was considered that the decrease of electrical resistance with time was due to a slow growth of the contact area between particles. The electrical resistance of these regions is likely to be higher than elsewhere in the compact for the reasons given in the Introduction - adsorbed impurity film and/or constriction of current flow. If an electric current is passed through a powder compact Joule heating will be greatest in these contact regions. What was required then, was a current large enough to cause recrystallisation or other change in the contact region which would physically stabilize one particle with respect to another by Joule heating but which would not appreciably heat the rest of the powder.

The techniques of sintering described in Chapter 4 could not be employed since they involved high temperatures and prolonged heating times which when applied to the graphite compounds would lead to decomposition.

Joule heating depends upon the square of the current and the first power of the time and therefore a condensor discharge appeared to be the best means of heating points of high resistance since the peak current of the discharge could be arranged to be very great. The short discharge time would ensure that general heating of the compact was not significant. This technique of discharging condensors charged to different voltages through a powder compact is referred to hereafter as flash sintering.



(a)



(b)

FIG. 14

Apparatus for Flash Sintering.

Condensors having a total capacitance of 100 micro-farads were employed. They were charged by rectified A.C. current to different voltages and discharged through a mercury switch into the resistance cell. A switch having a very low contact resistance was necessary to keep the resistance heating to a minimum outside the cell. Because of the unavoidable vaporization of some mercury on the passage of the high currents used, the switch was constructed from a closed ampoule of pyrex glass having thick platinum rods sealed into each end as electrodes. The ampoule was clamped in the centre to a spindle and switching was effected by rotating it in the manner of a simple "egg-timer".

Apparatus for the measurement of electrical resistance and thermo-electric power.

Fig. 14a illustrates the apparatus used for columns of powdered materials. The powder was packed in a pyrex tube A and was maintained between two cylindrical copper electrodes B_1 and B_2 of cross-sectional area 0.085 sq. cm. These electrodes were a sliding fit in the pyrex tube and were faced with a thin platinum sheet, hard soldered to the copper, so that the barrier contact was between bright platinum and the powder. Each of these electrodes also formed one arm of a copper-eureka thermocouple so that the temperature of each electrode could be determined. In the case of the top electrode, the eureka wire passed down the centre of it and was insulated by means of a glass capillary.



PLATE I

A section through this electrode is shown in Fig. 14b. Measurements were carried out under constant compression by means of a lead weight C which exerted a pressure of 13.5 kg. cm.^{2} on the tip of the upper electrode. For resistance measurements, most of the cell could be immersed in the bath which was thermostated to $\pm$ 0.05°C. Materials unstable in air could be maintained under oxygen free nitrogen by means of the inlets D attached to the cell. To measure the thermo-electric voltage a coil of "Brightray" wire was wound on the outside of the glass cell in the vicinity of the top electrode so that a controlled temperature difference could be maintained between the two electrodes. The cell dipped into a thermostated bath A shown in Plate 1, so that the temperature of the bottom electrode, which was determined accurately, did not fluctuate greatly from that of the bath. Resistances were measured to 0.0001 ohm. by a Smiths low resistance Bridge and a sensitive galvonometer. Voltages were measured by a Doran potentiometer reading to $\pm$ 0.05 millivolts. Column heights were measured by a cathetometer to 0.005 cm.

PREPARATION OF MATERIALS.

Artificial Graphite.

High purity reactor graphite was obtained from the Atomic Energy Research Establishment, Harwell, in the form of a bar 3" square and 12" long. The bar had been produced by extrusion and the extrusion axis lay along the longest dimension of the bar. Small cylindrical rods were cut from the bar along and across the extrusion axis. The rest of the material was powdered in a ball mill and sieved. Only the fraction passing 300 mesh was used. This was to permit comparisons to be made between the work now described and that of a colleague who was investigating the effect of high pressure on graphite powder and who found that only the fraction passing 300 mesh could be used without damage to the high pressure cell.

Two types of compact were used -

1) That in which the powder was progressively tamped as it was poured into the resistance cell.

2) That in which the powder was admitted into the cell without tamping.

These two methods were employed because it is difficult to reproduce the degree of tamping from one sample to the next and results might vary because of this. The reproducibility of values of the electrical resistance in untamped columns was therefore investigated. This was important for the future measurement of the electrical properties of those graphite compounds which are best investigated under vacuum

conditions due to their instability in air. Tamping in these conditions is usually difficult.

Some thermo-electric measurements were made on a bar of Acheson graphite obtained commercially. X-ray diffraction photographs were taken of graphite powder packed in special thin walled pyrex tubes. The purpose of this was to see if the particles of the powder exhibited orientation effects.

Natural Graphite.

Natural graphite was obtained through the courtesy of the Natural History Museum, South Kensington. It consisted of small flakes about 2 mm. in diameter. The ash content of these flakes was about 5% by weight. After refluxing with concentrated hydrochloric acid the ash content was reduced to not greater than 1%. The acid purified material was outgassed at 400°C in vacuo.

X-RAY DIFFRACTION

Preparation of thin walled specimen tubes.

A pyrex tube about half inch diameter was closed at one end and the other end connected to an aspirator by rubber tubing which could be rotated through a brass valve. A pressure of two cm. of water was maintained inside the pyrex tube by this means. The centre of the tube was then heated in a "fish-tail" burner and as the glass softened and the walls swelled outwards the two ends of the tube were pulled apart. By this method specimen tubes were prepared with internal diameter from 0.3 mm. - 1.0 mm. and wall thicknesses of 0.03 mm.

Filling of specimen tubes.

The most convenient method of filling the tubes was to leave them connected to the tube from which they were drawn down and then to pour in the powder. This powder was then tamped with a fine platinum wire and the tube sealed off.

Measurement of films.

The diffraction patterns were measured by means of an electronic scanner which activated photo-electric multipliers, the signal then being fed to two cathode-ray tubes which gave an image of the line profile and an image of the line itself as it occurred on the film. The film was mounted on a carriage which travelled along a fixed scale. When the peak of the line profile was in the centre of the cross wires on the C-R tube the relative position of the line was read off from the scale. Readings could be made to $\pm$ 0.001 cm.

X-ray source.

X-rays were produced using a Raymax (Newton-Victor) rotating anode instrument. The radiation was CuKα and most exposured were taken at 45 Kv and 50 m.a.

The camera was the Ubbelohde multiple exposure instrument with a diamater of 14 cm.

CHAPTER 6

PART I

Results

Electrical resistance measurements on powder compacts.

Fig. 15 shows column height versus resistance plots for tamped and untamped columns of artificial graphite powder. It can be seen that at short column heights - up to 0.4 cm. - the curves coincide. Above this point untamped columns have higher resistances. Between a column 0.2 cm. high and zero the curves especially the one connecting the points after flash sintering must change slope considerably and descend almost vertically. This means that specific resistance of the powder decreases considerably, at column heights less than 0.2 cm. It is important to note that if a contact resistance between electrodes and powder exists, the minimum resistance must have a value equal to this electrode contact resistance.

Where flakes of natural graphite were concerned reproducibility of electrical resistance was impossible to obtain. Fig. 16 shows the scatter of points in a plot of column height versus resistance. Only tamped columns were used. If the columns were not tamped, the packing of the flakes could visually be seen to be irregular, some flakes lying flat and others on end. The current will flow preferentially along the plane of the flake and variations in orientation of one flake relation to the next would be expected to influence the specific resistance profoundly.

FIG. 15.

Plots of column height versus electrical resistance (A.E.R.E./graphite powder) N.B. divergence between the curves for tamped and untamped columns decreases as the column height diminishes, indicating that for low columns, tamping does not significantly increase the degree of packing.

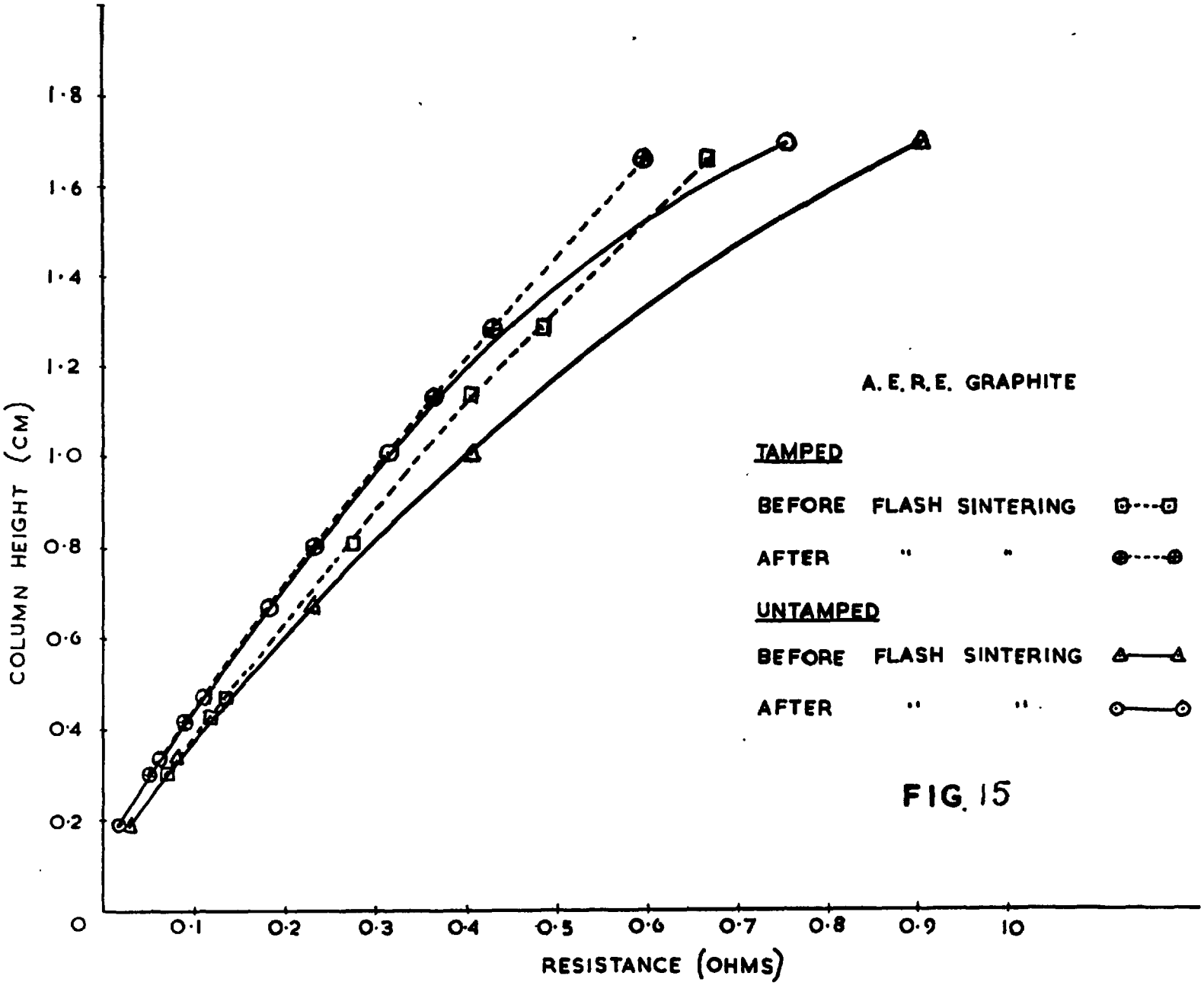

COLUMN HEIGHT (CM)
1·8
1·6
1·4
1·2
1·0
0·8
0·6
0·4
0·2
0
0·1
0·2
0·3
0·4
0·5
0·6
0·7
0·8
0·9
10
RESISTANCE (OHMS)
A. E. R. E. GRAPHITE
TAMPED
BEFORE FLASH SINTERING
AFTER " "
UNTAMPED
BEFORE FLASH SINTERING
AFTER " "

FIG. 15

Fig.16

Plots of column height versus electrical resistance for natural flake graphite.

N.B. the scatter of points.

Conduction in graphite takes place primarily along the aromatic layer planes(see PART II) Large natural flakes exhibit this anisotropy. Small variations in orientations of the flakes with respect to one another, may then be expected to lead to significant variations in resistance per unit length of column.

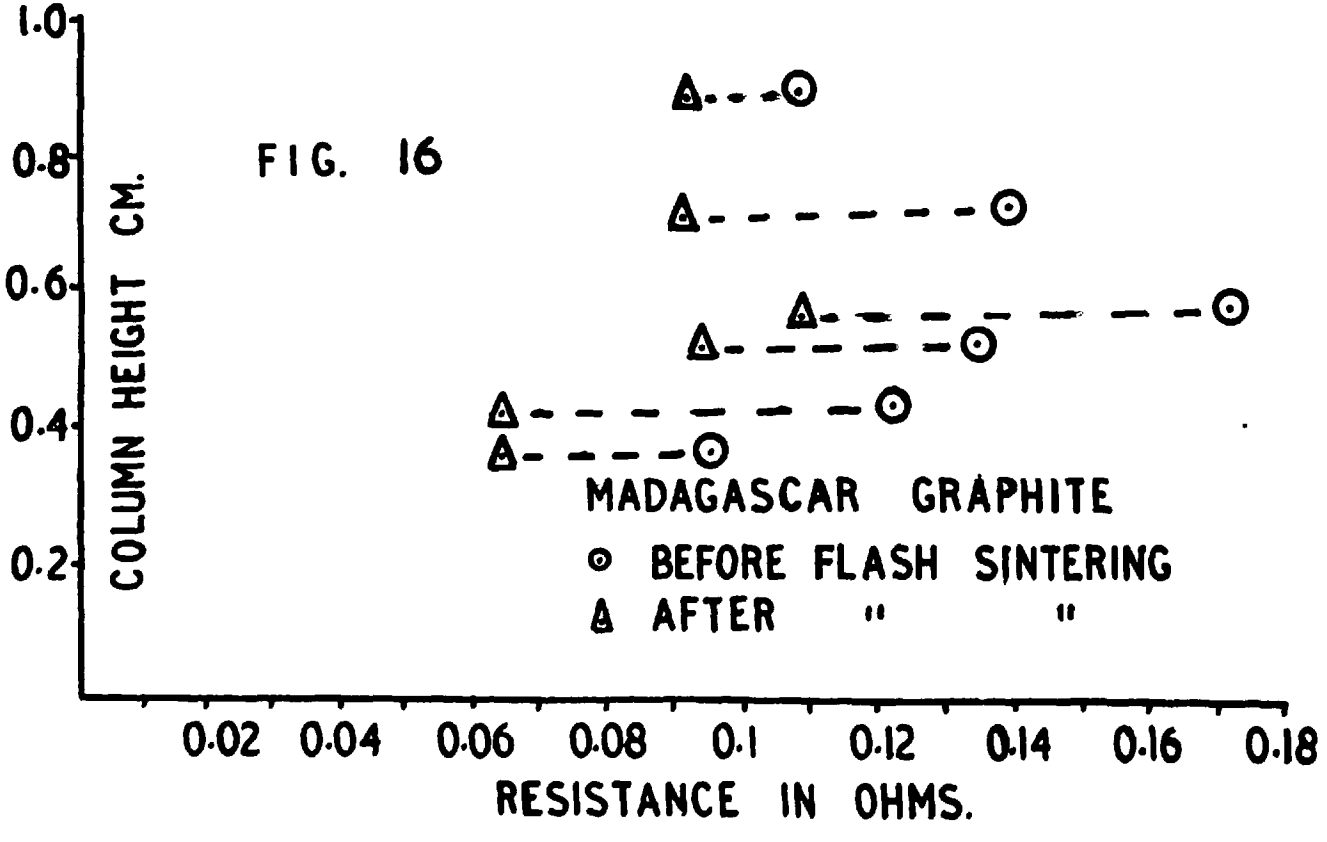

1.0
0.8
0.6
0.4
0.2
COLUMN HEIGHT CM.
MADAGASCAR GRAPHITE
⊙ BEFORE FLASH SINTERING
Δ AFTER " "
0.02 0.04 0.06 0.08 0.1 0.12 0.14 0.16 0.18
RESISTANCE IN OHMS.

FIG. 16

Fig.17-20

Drift of the electrical resistance with time under constant loading conditions, and its elimination by "flash sintering".

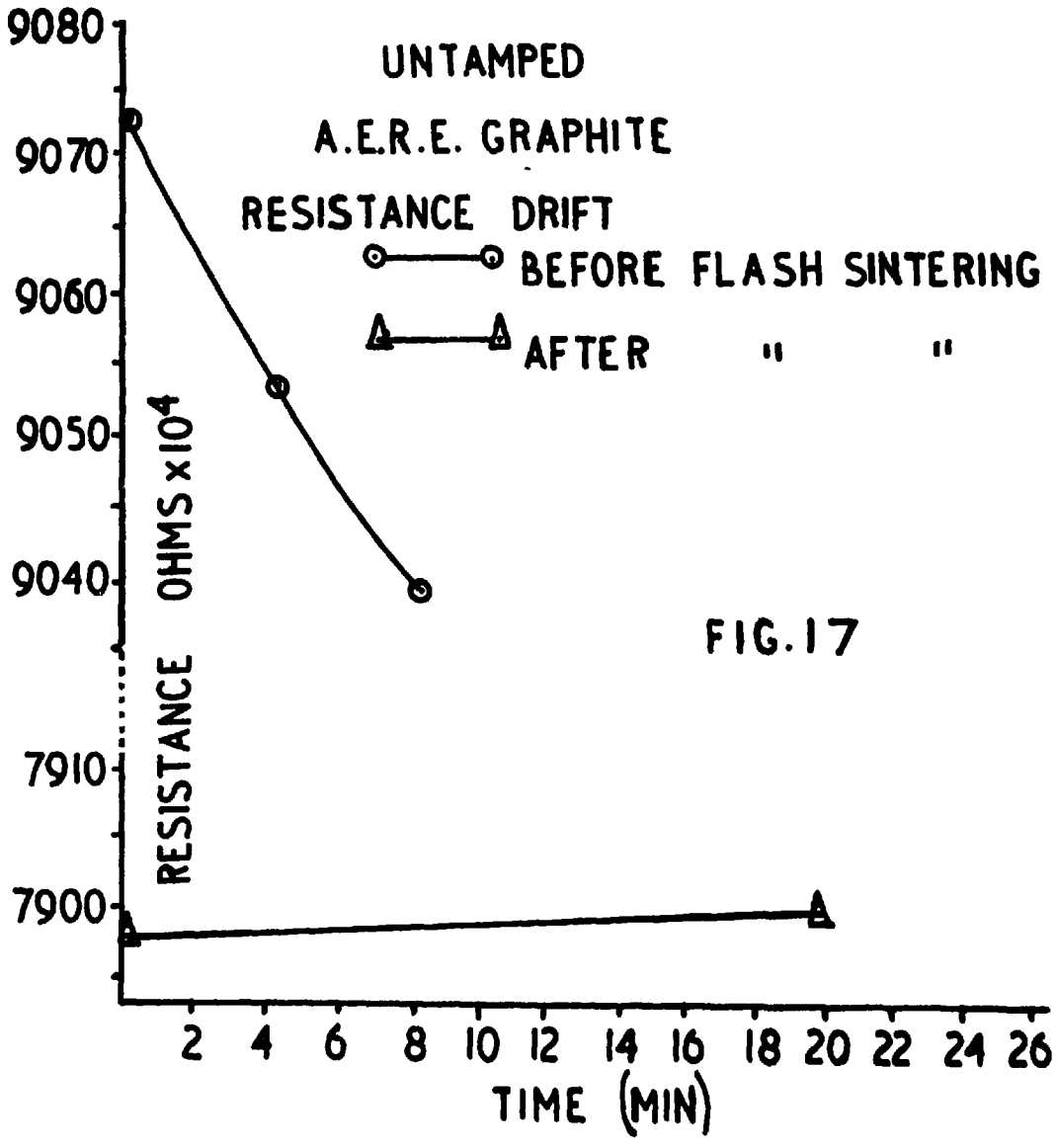

UNTAMPED
A.E.R.E. GRAPHITE
RESISTANCE DRIFT
BEFORE FLASH SINTERING
AFTER " "
RESISTANCE OHMS x10⁴
9080
9070
9060
9050
9040
7910
7900
2 4 6 8 10 12 14 16 18 20 22 24 26
TIME (MIN)

FIG. 17

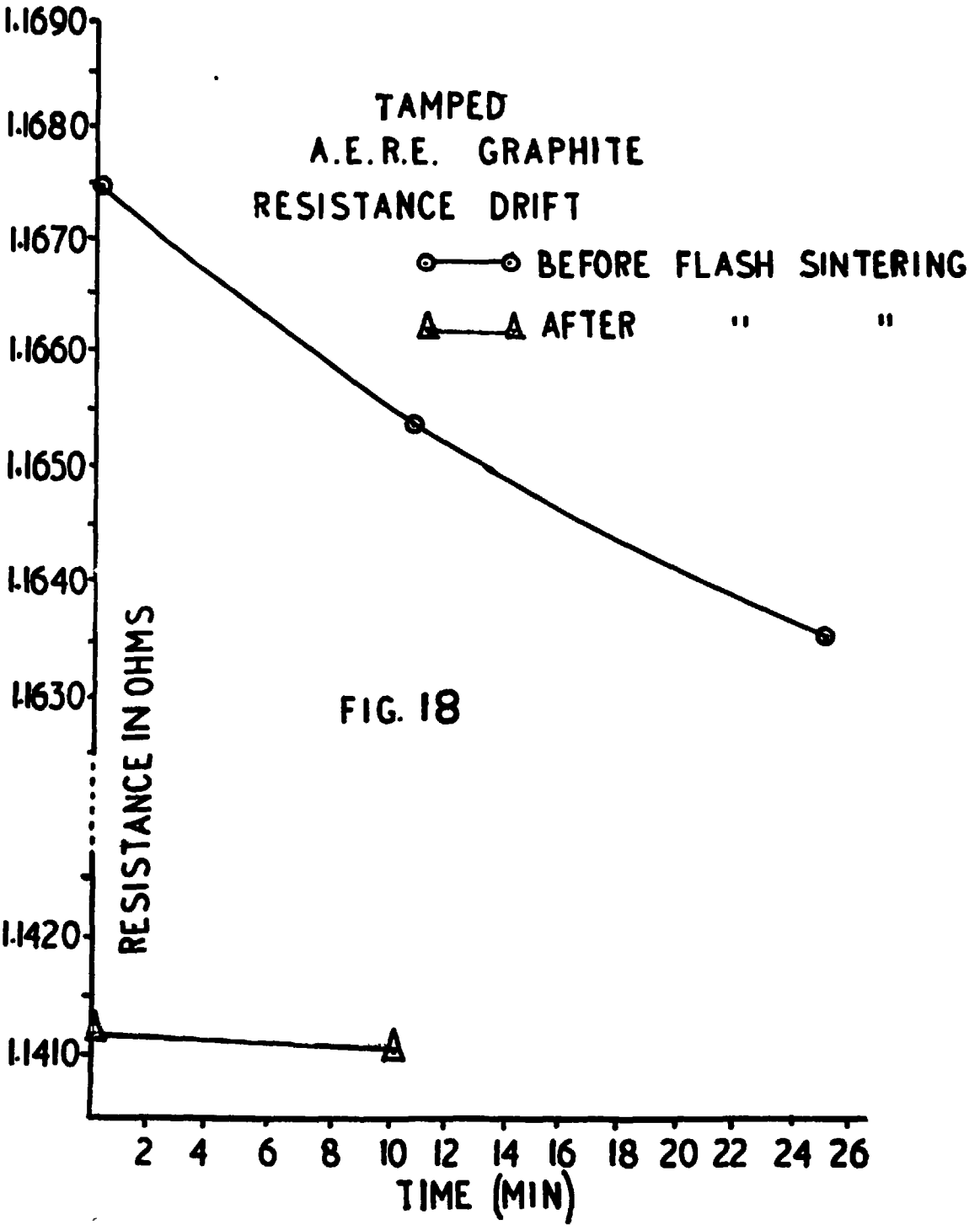

TAMPED
A.E.R.E. GRAPHITE
RESISTANCE DRIFT
BEFORE FLASH SINTERING
AFTER " "
1.1690
1.1680
1.1670
1.1660
1.1650
1.1640
1.1630
1.1420
1.1410
RESISTANCE IN OHMS
2 4 6 8 10 12 14 16 18 20 22 24 26
TIME (MIN)

FIG. 18

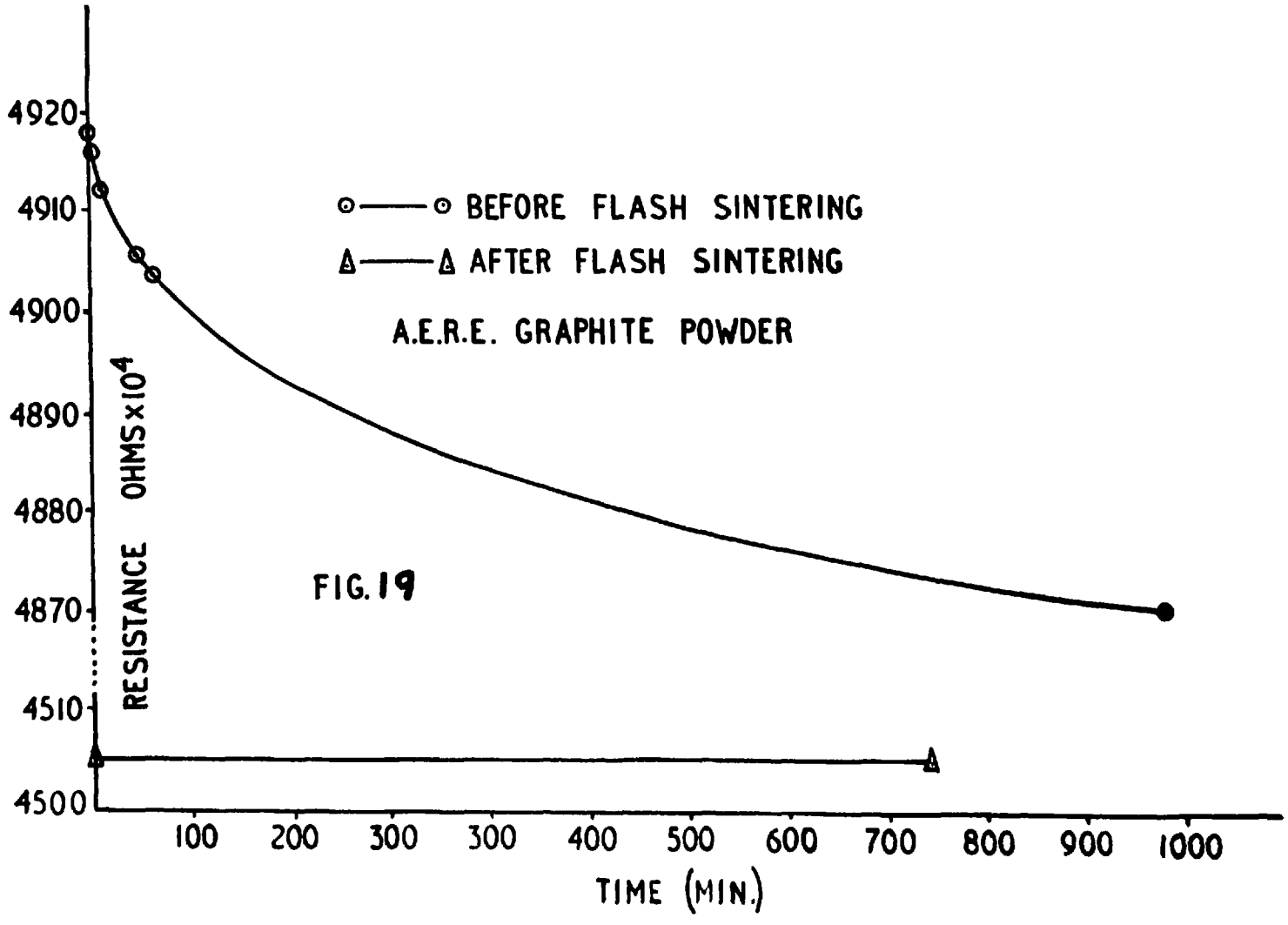

4920
4910
4900
4890
4880
4870
4510
4500
RESISTANCE OHMS x 10^4
⊙——⊙ BEFORE FLASH SINTERING
Δ——Δ AFTER FLASH SINTERING
A.E.R.E. GRAPHITE POWDER
100
200
300
300
400
500
600
700
800
900
1000
TIME (MIN.)

FIG. 19

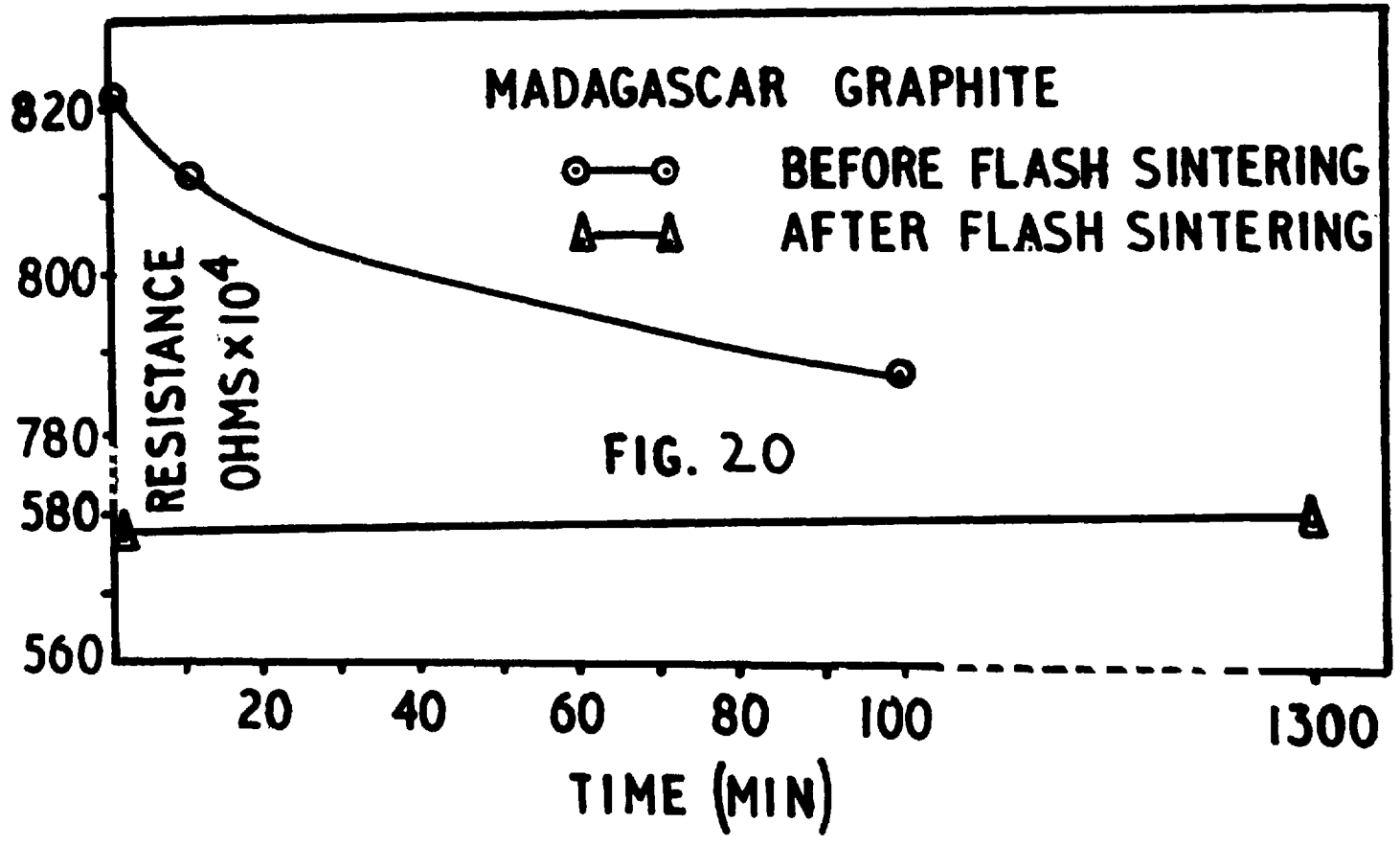

MADAGASCAR GRAPHITE
BEFORE FLASH SINTERING
AFTER FLASH SINTERING
RESISTANCE OHMS x 10^4
820
800
780
580
560
20
40
60
80
100
1300
TIME (MIN)

FIG. 20

Resistance drift with time.

Figs. 17, 18, 19, 20 show the manner in which the electrical resistance varied with time for both artificial and natural graphites. The rate of drift varied from one specimen to the next but the trend was always to lower resistances. This drift made measurements of the temperature variation of resistance difficult since it could mask the temperature effect. The drift of resistance, however, slowed down with time, and temperature variation measurements were made when the resistance had become fairly steady. Change of temperature, however, caused the drift to increase once more. In an attempt to obtain significant results, the measurements were carried out as quickly as possible, the thermostat water being syphoned off after each measurement and water at a different temperature admitted.

Fig. 21a shows the results obtained with artificial graphite, the divergence between the heating and cooling points can be taken to be the result of drift. With natural flake graphite increase of temperature decreased the resistance but the divergence between the heating and cooling curves was often more marked than in the case of artificial graphite, i.e. Fig. 22a.

Figs. 21 - 23.

Reproducible measurements of the temperature variation of the electrical resistance (co-incidence of heating and cooling curves) resulting from flash sintering stabilisation.

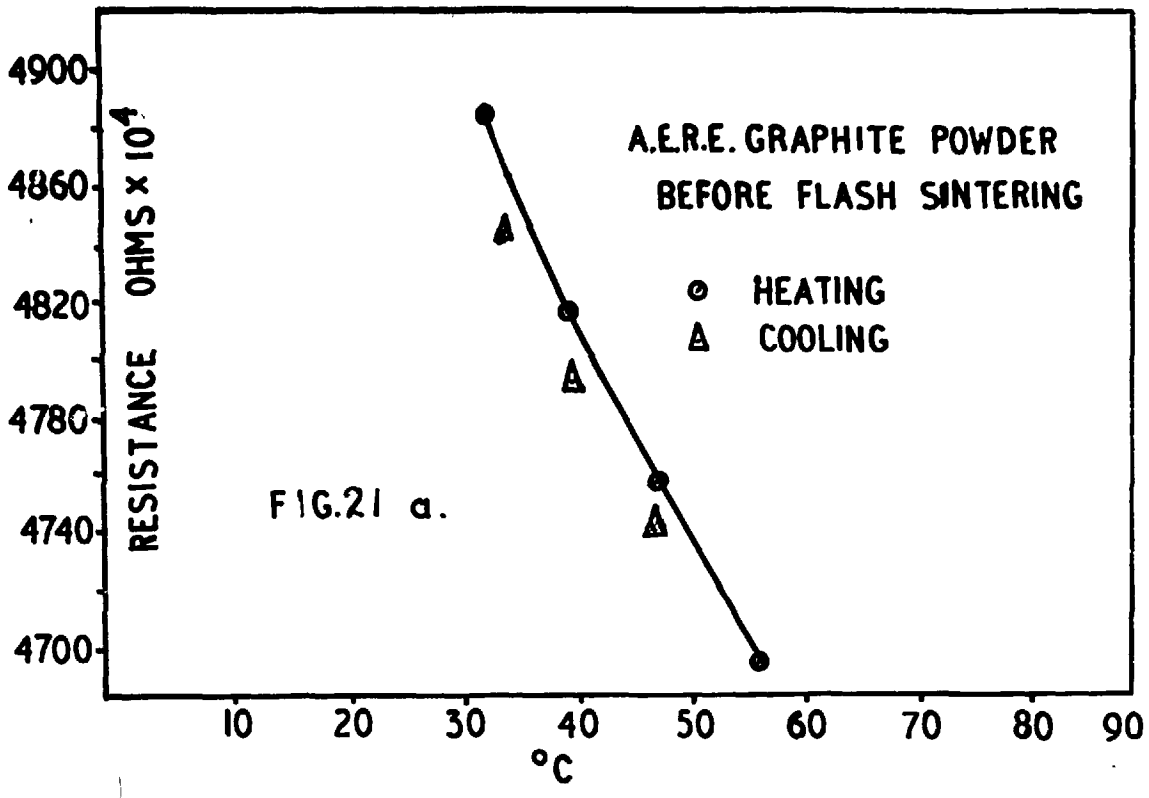


FIG.21 a.

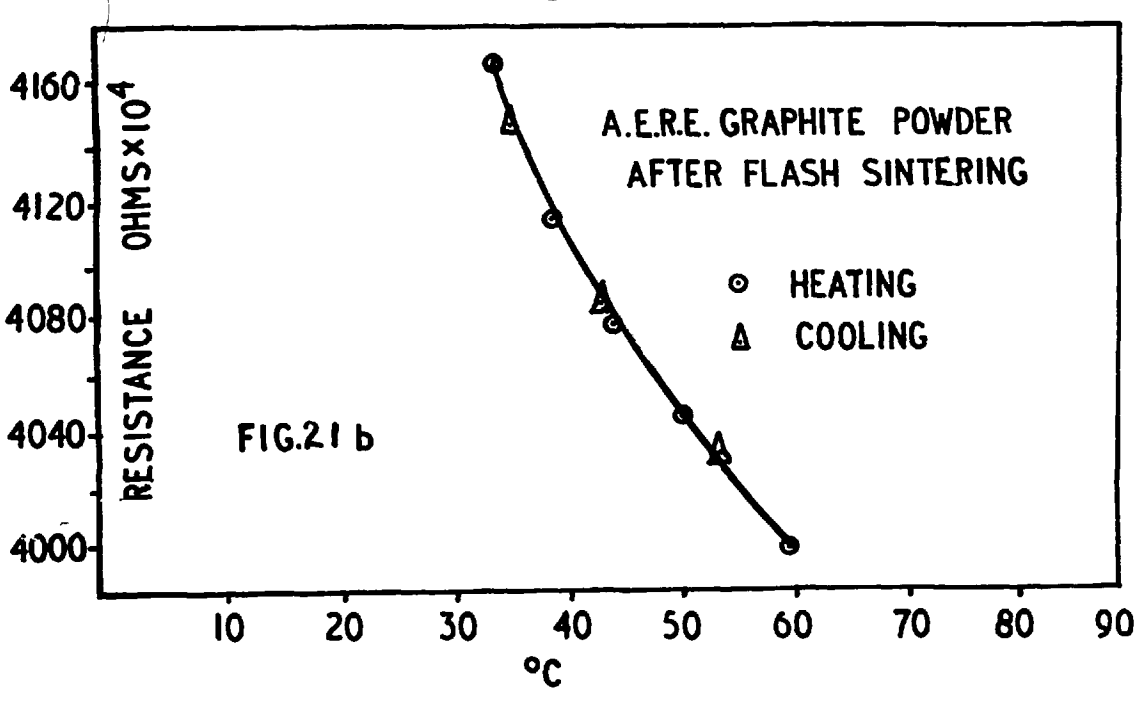
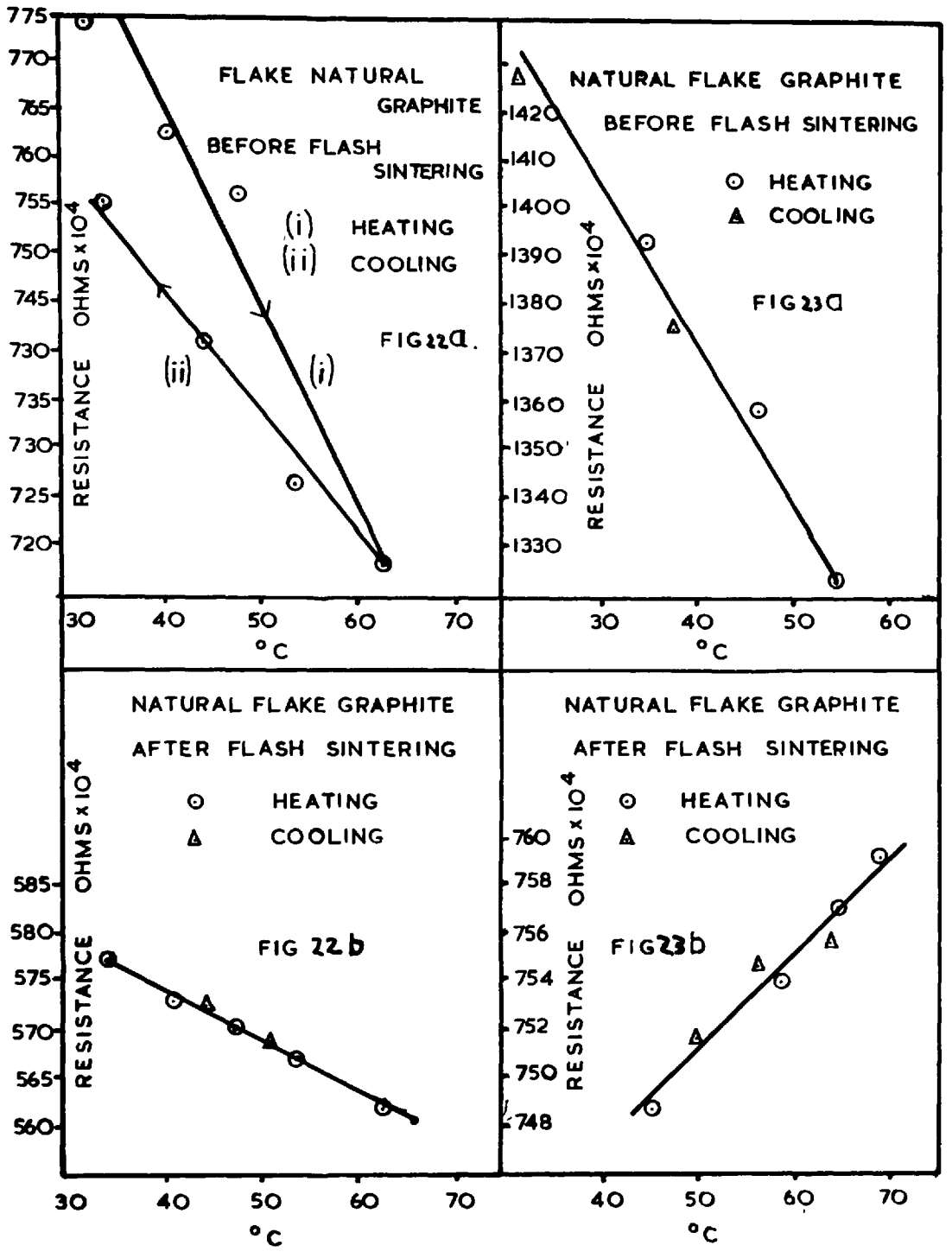


FIG.21 b


FLAKE NATURAL GRAPHITE
BEFORE FLASH SINTERING
(i) HEATING
(ii) COOLING
FIG 22a.
RESISTANCE OHMS x 10^4
°C
NATURAL FLAKE GRAPHITE
BEFORE FLASH SINTERING
HEATING
COOLING
FIG 23a
NATURAL FLAKE GRAPHITE
AFTER FLASH SINTERING
HEATING
COOLING
FIG 22b
NATURAL FLAKE GRAPHITE
AFTER FLASH SINTERING
HEATING
COOLING
FIG 23b

THE EFFECTS OF FLASH SINTERING

The discharge time of a condensor depends upon the time constant (CR) of the circuit which is the product of capacitance and resistance. After one time constant the charge Q_o on a condensor falls to $\frac{Q_o}{e}$, the decay of charge with time t being represented by $Q = Q_o e^{\frac{-t}{CR}}$. The product of farads (C) and ohms (R) is measured in units of time. In the present work the condensor capacitance was 10^{-4} farads and time constants usually lay between 10^{-5} and 10^{-6} secs. Discharge times and energies are considered more fully in the Discussion.

1) Reduction in the overall electrical resistance.

When a series of high current pulses of short duration was passed through compacts of both artificial and natural graphite, the electrical resistance was reduced. Figs. 24 - 39 show this effect. It can be seen that for most columns there was a voltage beyond which the resistance decreased more rapidly tending to level off to a plateau value beyond which increasing the voltage produced only a small decrease. Fig. 33b shows the influence of repeated discharges of different voltages on a column where the plateau had not been attained. The overall change of resistance in different columns varied considerably. Untamped columns shows changes of greater magnitude.

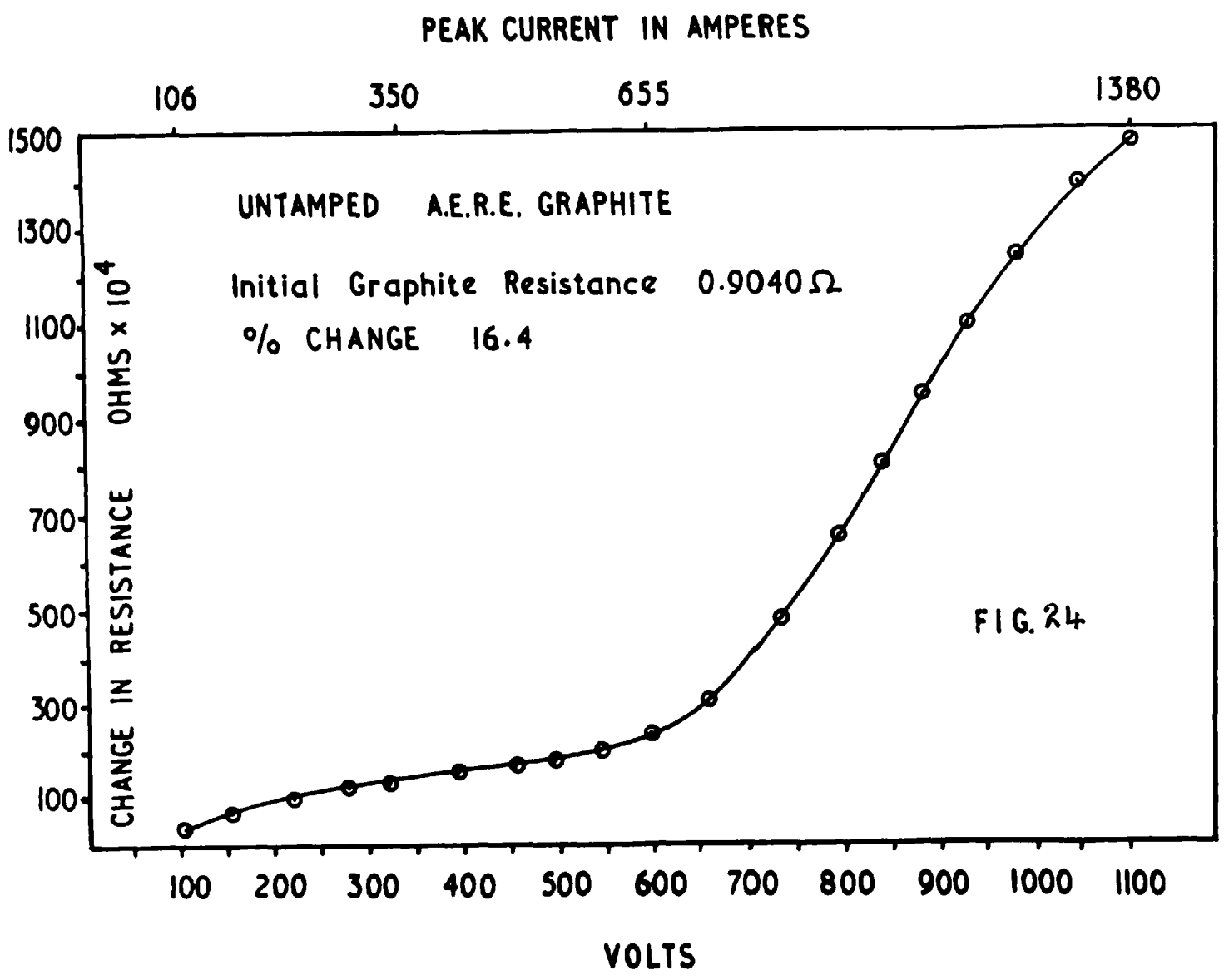
Where natural graphite was concerned the percentage change of resistance was on the average considerably greater than that observed

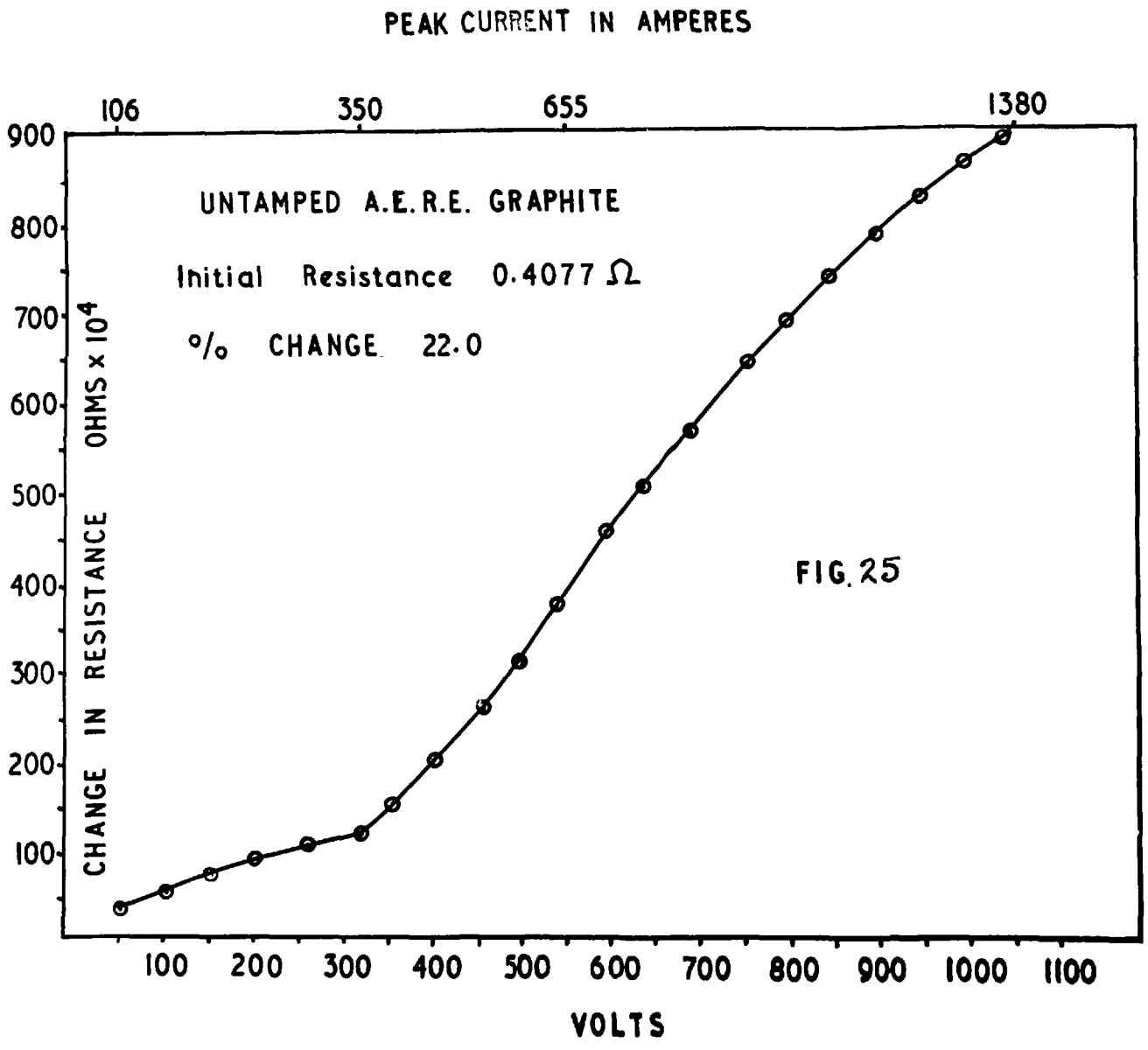
with synthetic graphite powder. A plateau resistance was also more often attained. At high voltage discharges the resistance sometimes increased. The 1150 volt discharge of Fig. 33b shows this effect. This increase of resistance never occurred before a plateau had been reached. After the application of these post plateau voltages a very fine deposit of carbon was found ingrained on the glass wall of the cell. This carbon could not be removed either by brushing or by boiling water. Acid treatment was not feasible because the bottom copper electrode was a permanent fixture in the cell. Photomicrographs of the polished platinum tip of the electrode before and after flash discharges failed to reveal any change of contact surface.

Figs. 24 - 39.

Plots of graphite resistance decrease v. condensor voltages.

Note especially the threshold effect in AERE graphite and the series of steps in natural flake graphite curves.


PEAK CURRENT IN AMPERES
106
350
655
1380
UNTAMPED A.E.R.E. GRAPHITE
Initial Graphite Resistance 0.9040Ω
% CHANGE 16.4
CHANGE IN RESISTANCE OHMS x 10^4
1500
1300
1100
900
700
500
300
100
100 200 300 400 500 600 700 800 900 1000 1100
VOLTS
FIG. 24


PEAK CURRENT IN AMPERES
106
350
655
1380
UNTAMPED A.E.R.E. GRAPHITE
Initial Resistance 0.4077 Ω
% CHANGE 22.0
CHANGE IN RESISTANCE OHMS x 10^4
900
800
700
600
500
400
300
200
100
100 200 300 400 500 600 700 800 900 1000 1100
VOLTS
FIG. 25

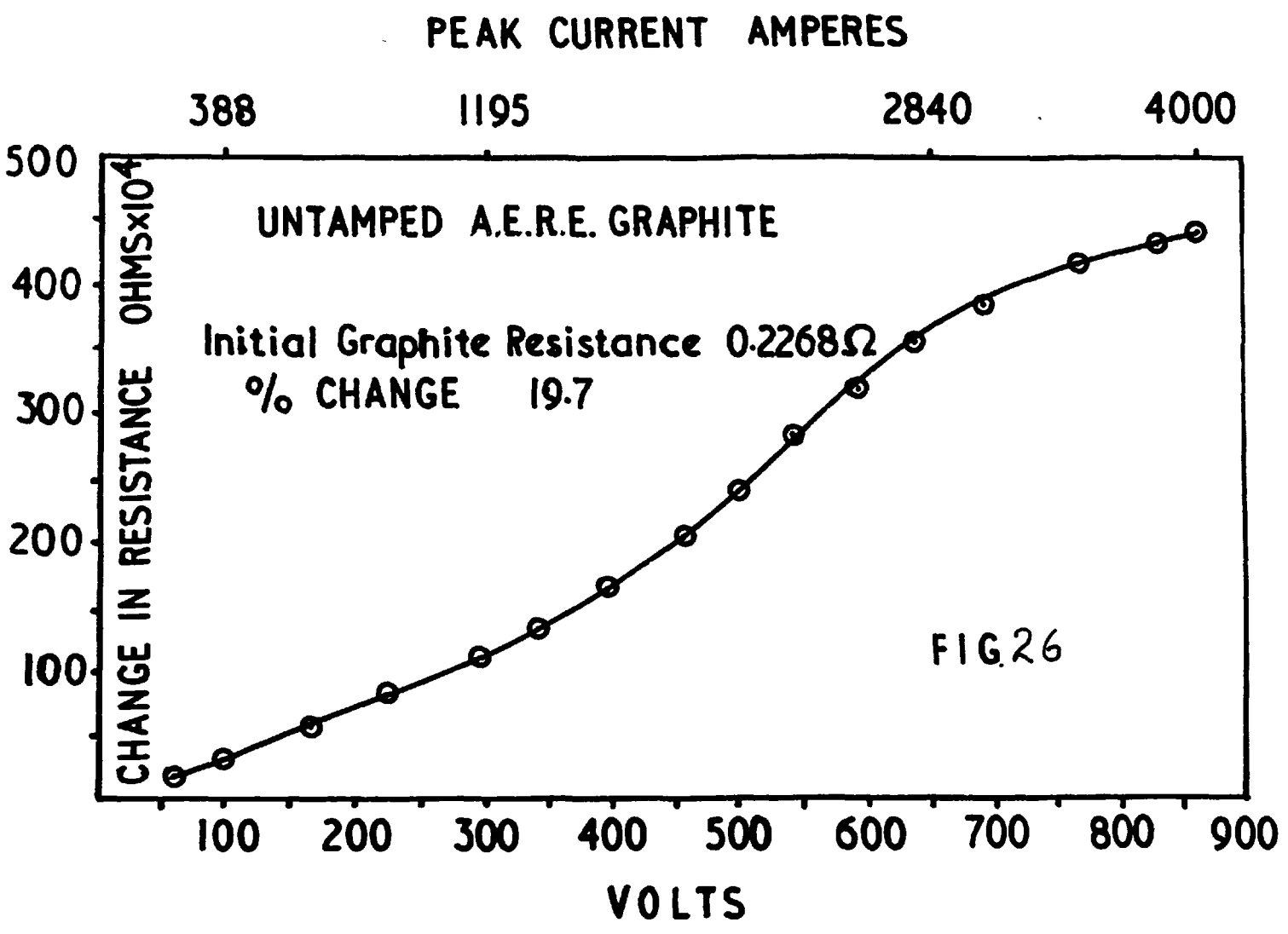

PEAK CURRENT AMPERES
388
1195
2840
4000
500
400
300
200
100
CHANGE IN RESISTANCE OHMS x 10⁴
UNTAMPED A.E.R.E. GRAPHITE
Initial Graphite Resistance 0.2268Ω
% CHANGE 19.7
100
200
300
400
500
600
700
800
900
VOLTS

FIG. 26

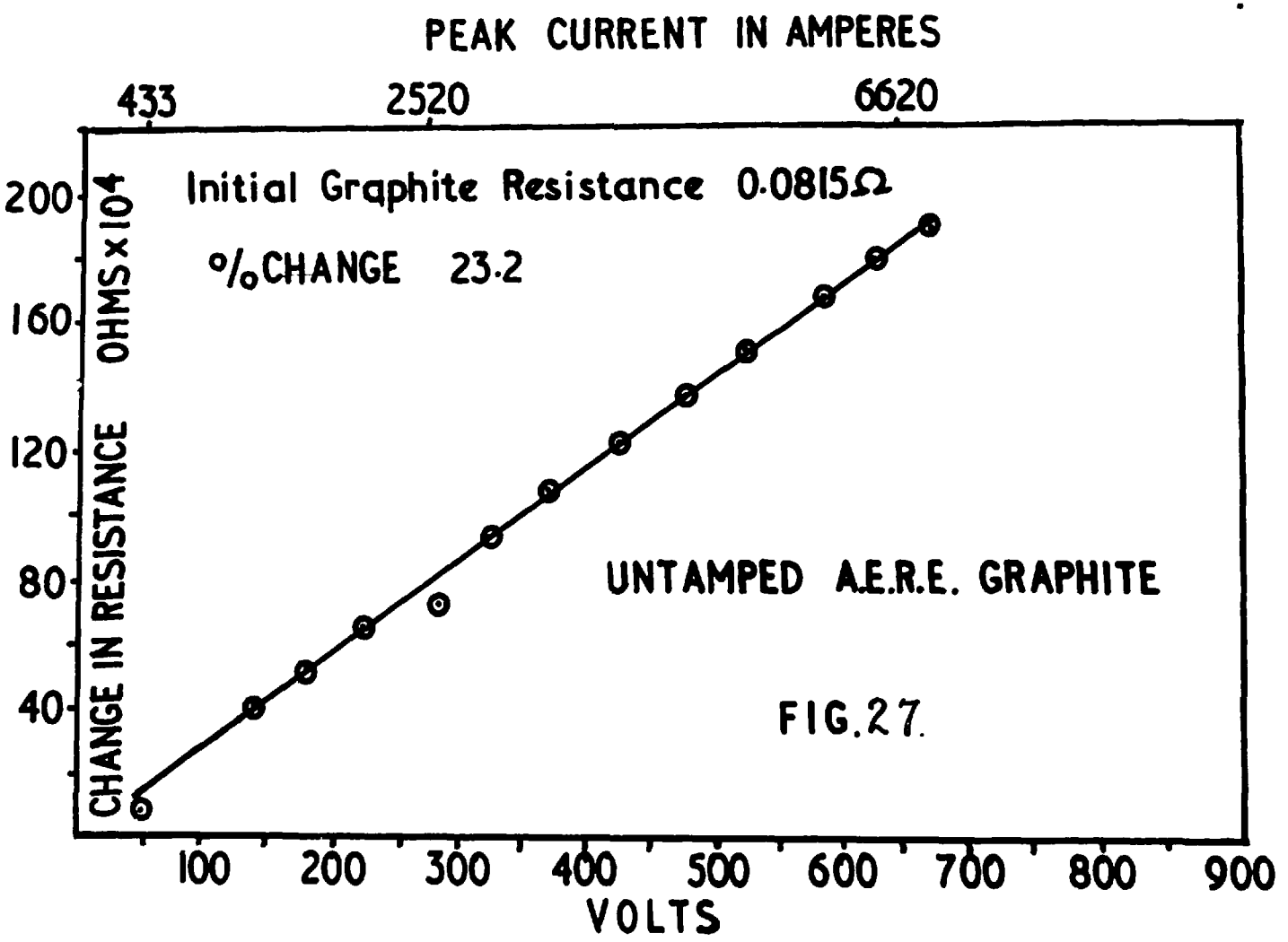

PEAK CURRENT IN AMPERES
433
2520
6620
Initial Graphite Resistance 0.0815Ω
%CHANGE 23.2
UNTAMPED A.E.R.E. GRAPHITE
CHANGE IN RESISTANCE OHMS x 10⁴
200
160
120
80
40
100
200
300
400
500
600
700
800
900
VOLTS

FIG. 27.

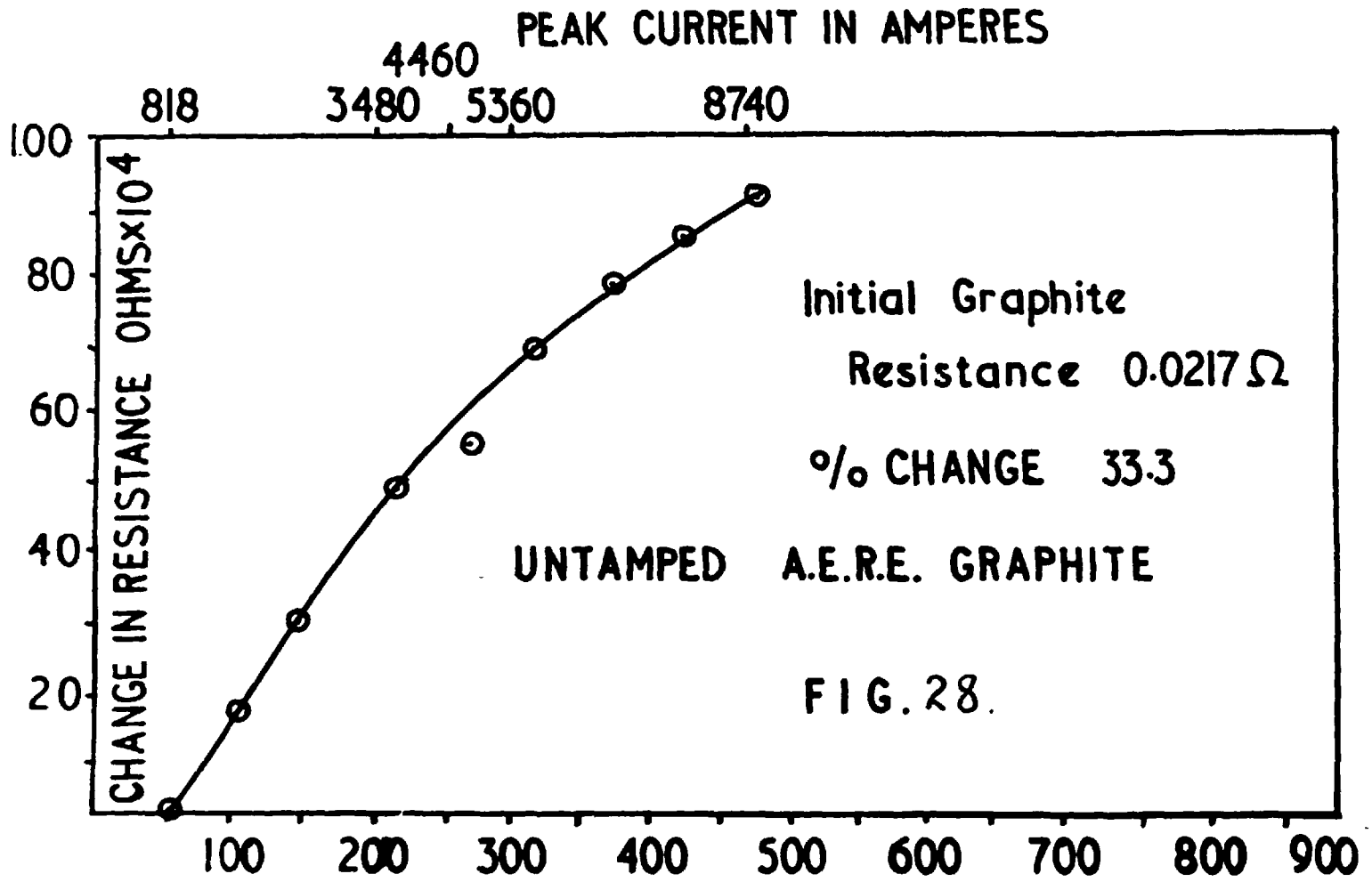

PEAK CURRENT IN AMPERES
818
3480
4460
5360
8740
CHANGE IN RESISTANCE OHMS x 10⁴
100
80
60
40
20
100
200
300
400
500
600
700
800
900
Initial Graphite
Resistance 0.0217 Ω
% CHANGE 33.3
UNTAMPED A.E.R.E. GRAPHITE

FIG. 28.

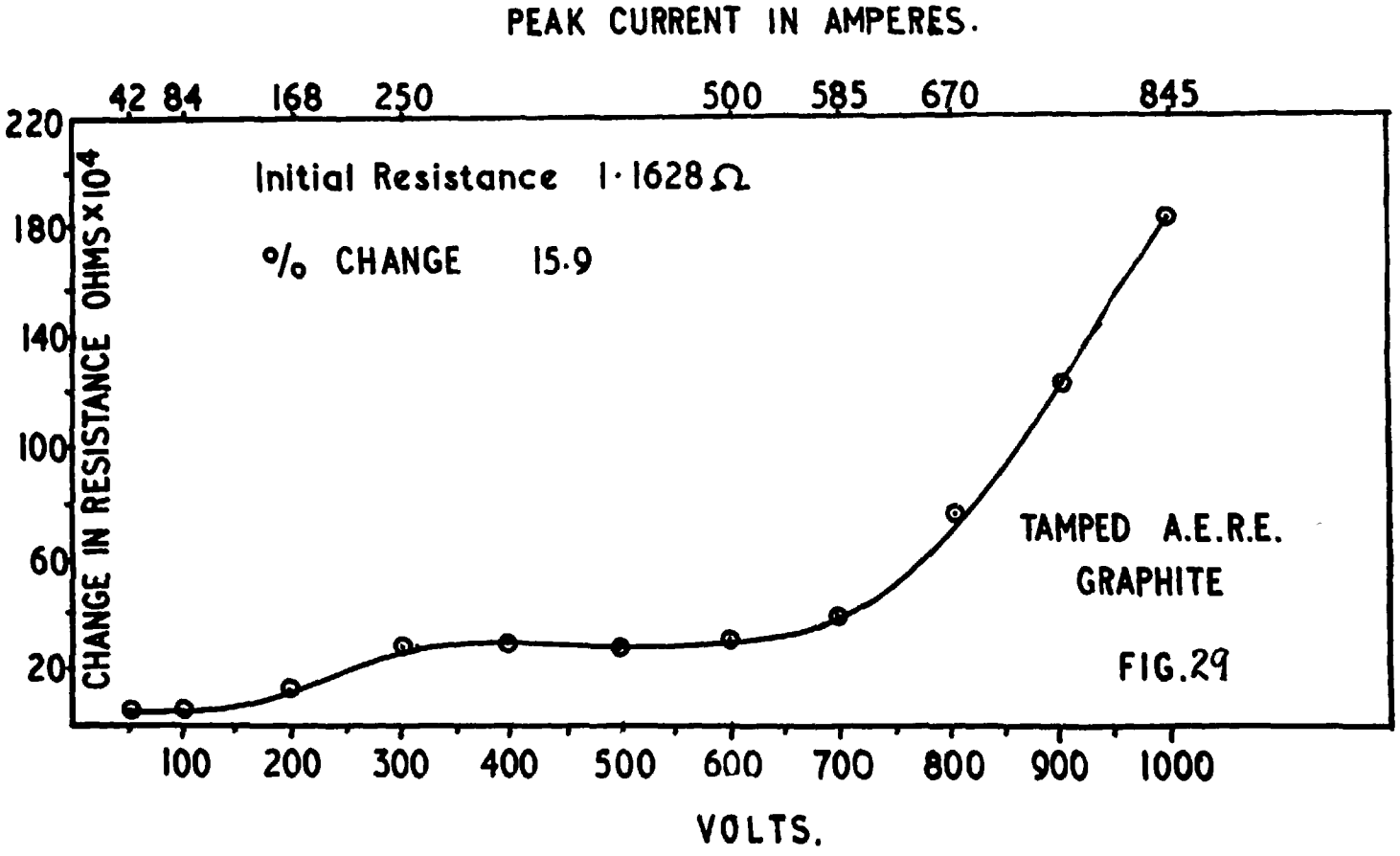
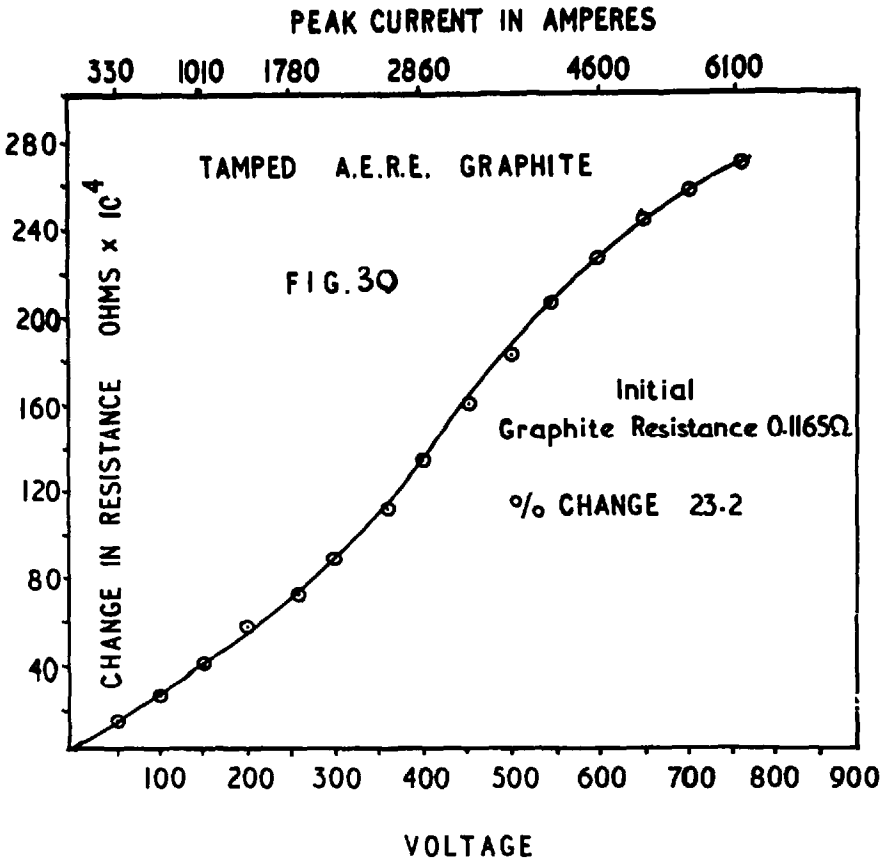
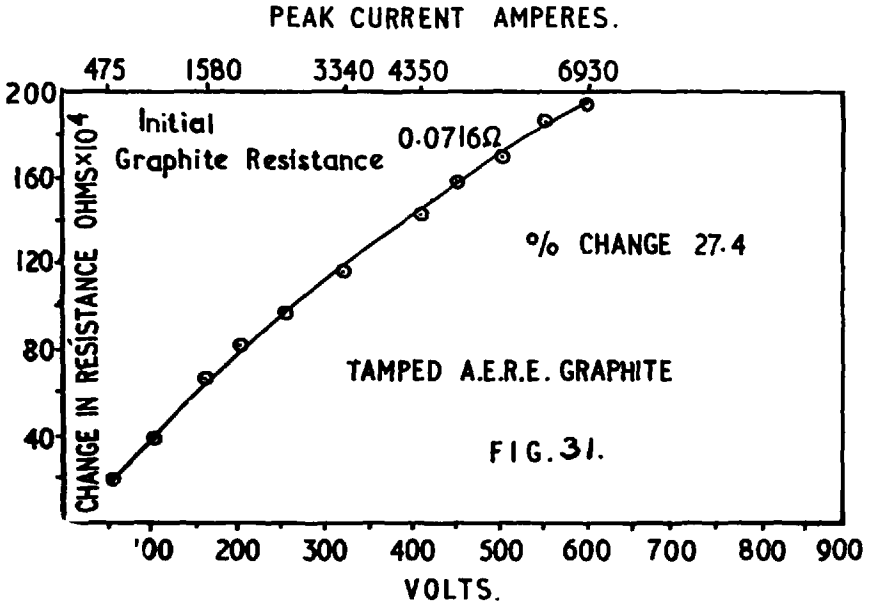

PEAK CURRENT IN AMPERES.
42 84 168 250 500 585 670 845
220
180
140
100
60
20
CHANGE IN RESISTANCE OHMS×10⁴
Initial Resistance 1·1628Ω
% CHANGE 15·9
TAMPED A.E.R.E.
GRAPHITE
100 200 300 400 500 600 700 800 900 1000
VOLTS.

FIG.29


PEAK CURRENT IN AMPERES
330
1010
1780
2860
4600
6100
280
240
200
160
120
80
40
TAMPED A.E.R.E. GRAPHITE
FIG.30
CHANGE IN RESISTANCE OHMS x IC4
Initial
Graphite Resistance 0.1165Ω
% CHANGE 23.2
100
200
300
400
500
600
700
800
900
VOLTAGE


PEAK CURRENT AMPERES.
475
1580
3340
4350
6930
200
160
120
80
40
CHANGE IN RESISTANCE OHMS×10⁴
Initial
Graphite Resistance
0.0716Ω
% CHANGE 27.4
TAMPED A.E.R.E. GRAPHITE
FIG.31.
'00
200
300
400
500
600
700
800
900
VOLTS.

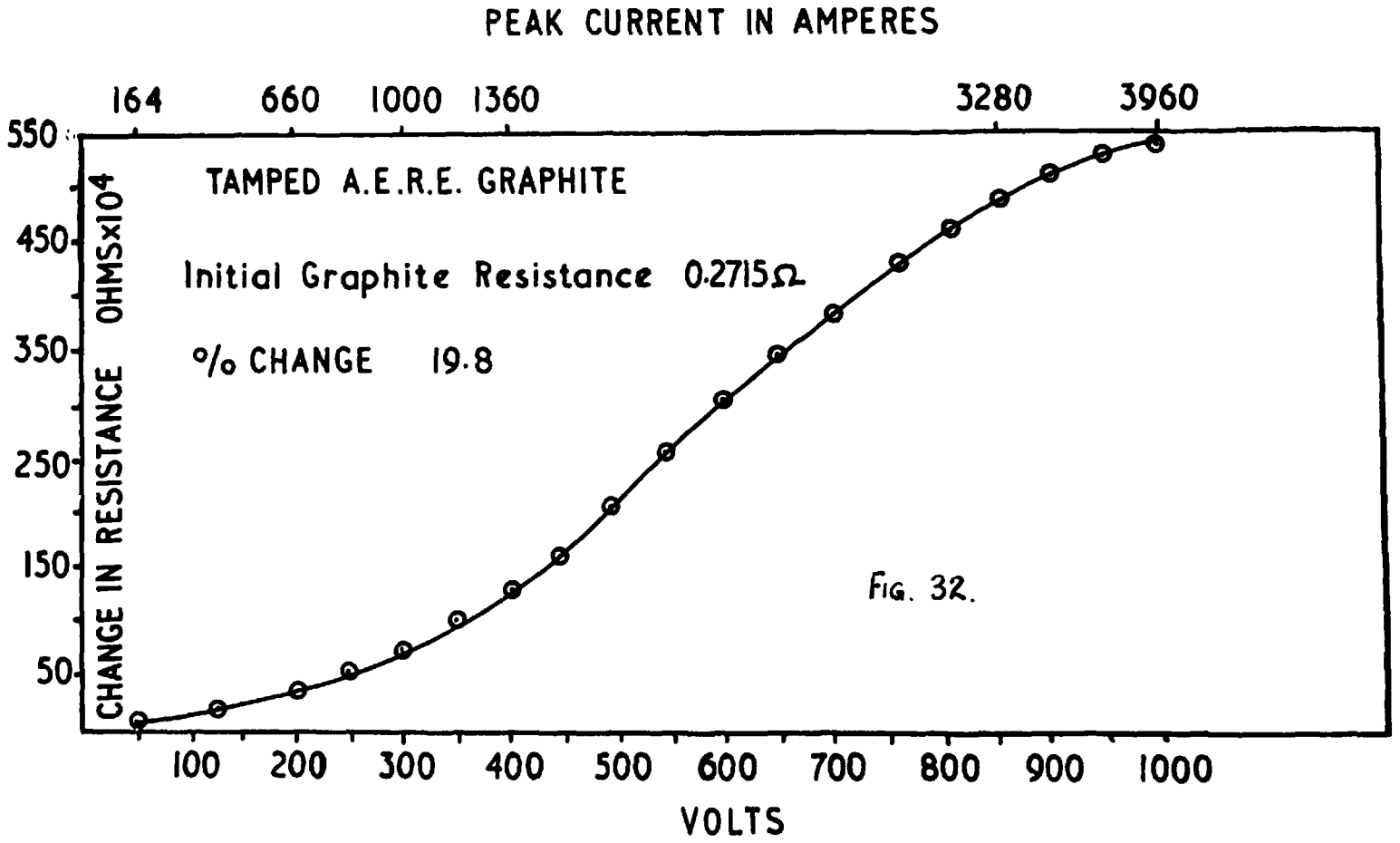
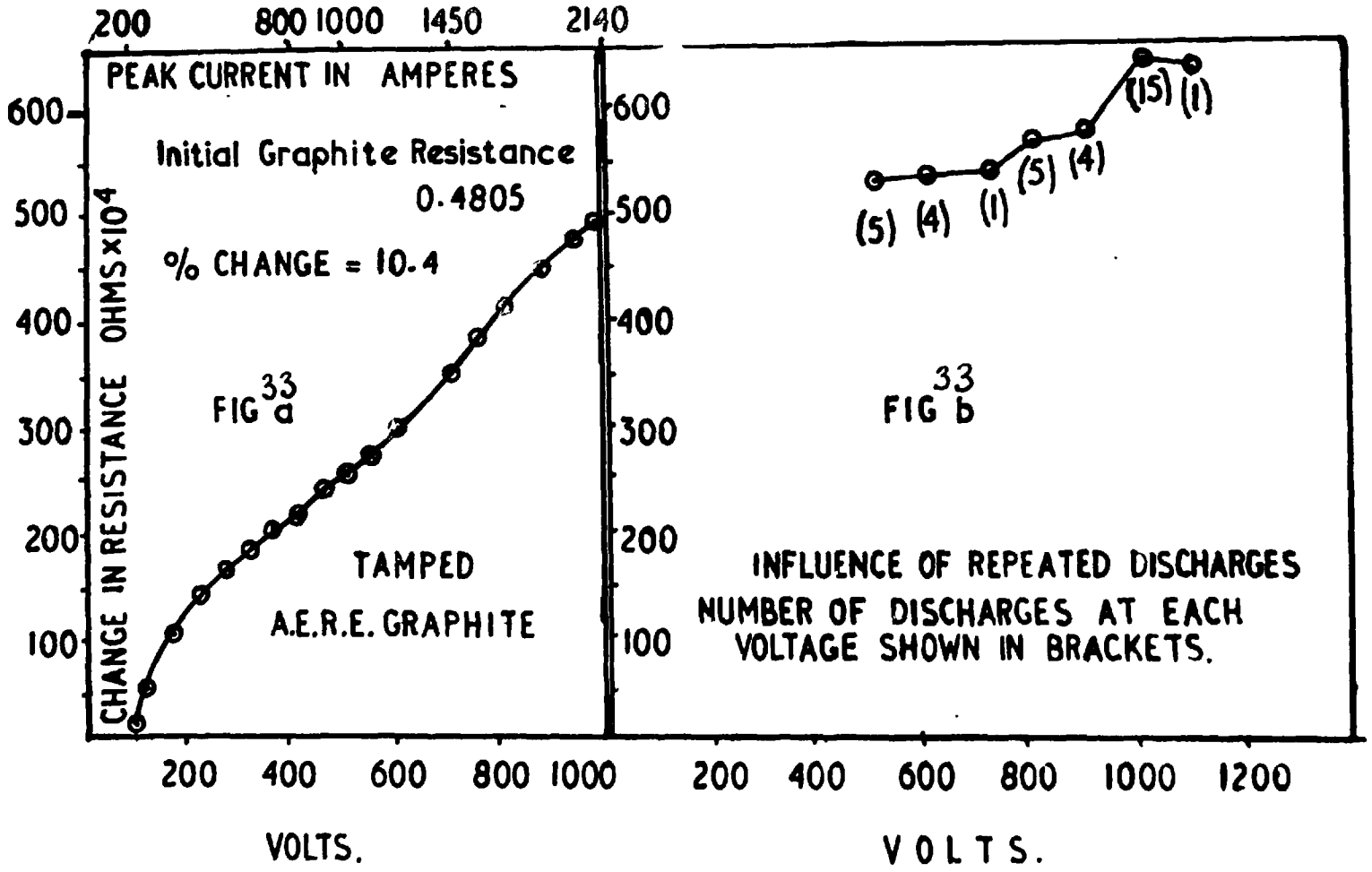
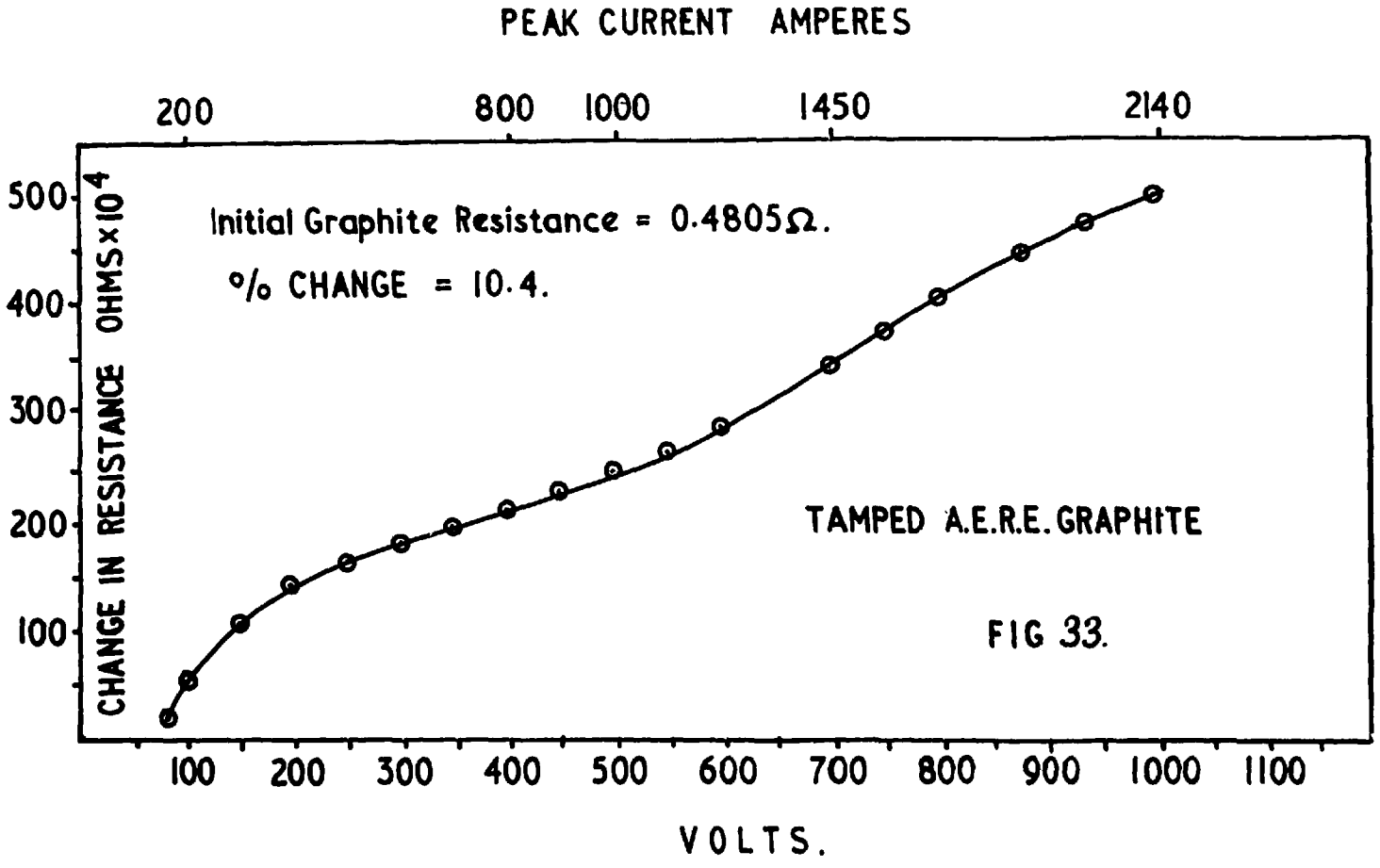

PEAK CURRENT IN AMPERES
164
660
1000
1360
3280
3960
550
450
350
250
150
50
CHANGE IN RESISTANCE OHMS x 10⁴
TAMPED A.E.R.E. GRAPHITE
Initial Graphite Resistance 0.2715Ω
% CHANGE 19.8
100
200
300
400
500
600
700
800
900
1000
VOLTS

FIG. 32.

Fig. 33b.

The compact which gave the curve shown in Fig. 33a was subjected to repeated discharges at the voltages illustrated. The number in brackets refers to the number of discharges given at the particular voltage. It can be seen that voltages lower than voltages already employed have little effect on the resistance.


200
800 1000
1450
2140
PEAK CURRENT IN AMPERES
Initial Graphite Resistance
0.4805
% CHANGE = 10.4
CHANGE IN RESISTANCE OHMS x10^4
600
500
400
300
200
100
TAMPED
A.E.R.E. GRAPHITE
200 400 600 800 1000
VOLTS.
FIG 33 a
(5) (4) (1) (5) (4) (15) (1)
INFLUENCE OF REPEATED DISCHARGES
NUMBER OF DISCHARGES AT EACH VOLTAGE SHOWN IN BRACKETS.
200 400 600 800 1000 1200
VOLTS.
FIG 33 b


PEAK CURRENT AMPERES
200
800
1000
1450
2140
CHANGE IN RESISTANCE OHMS x 10⁴
500
400
300
200
100
Initial Graphite Resistance = 0.4805Ω.
% CHANGE = 10.4.
TAMPED A.E.R.E. GRAPHITE
FIG 33.
100
200
300
400
500
600
700
800
900
1000
1100
VOLTS.

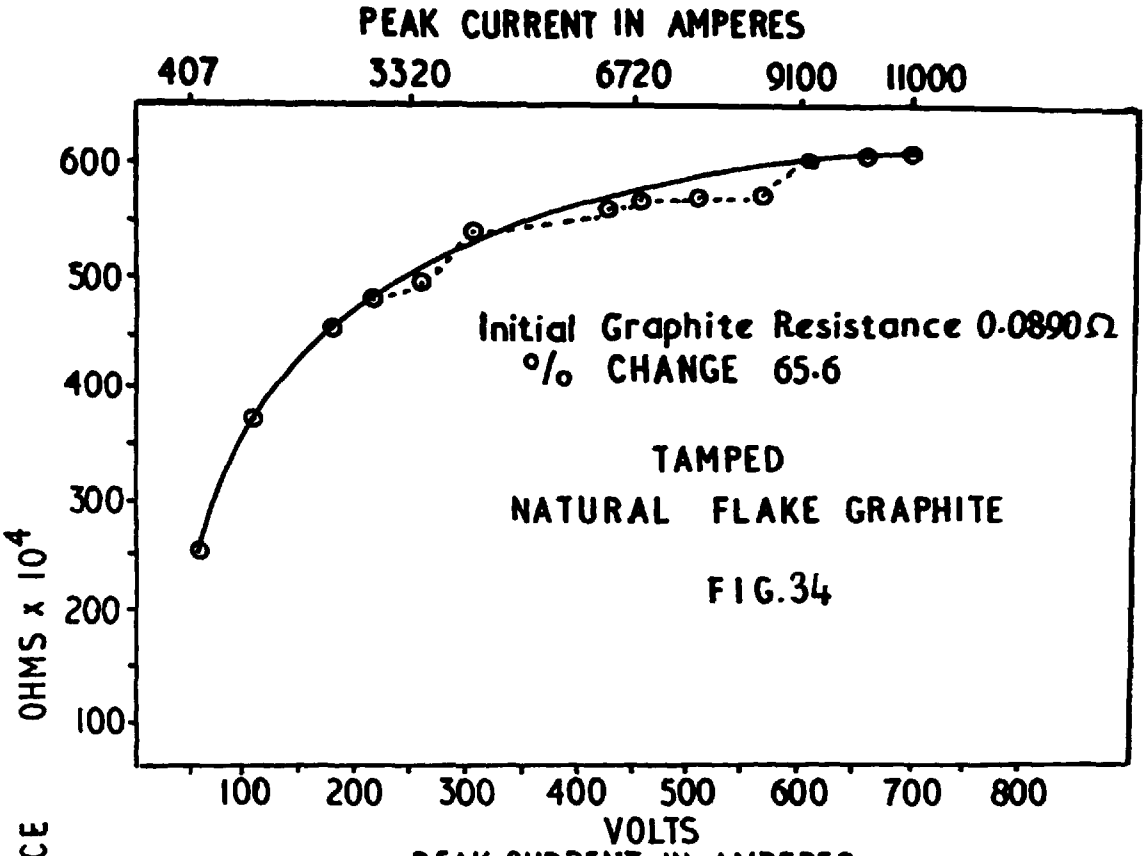

PEAK CURRENT IN AMPERES
407
3320
6720
9100
11000
600
500
400
300
200
100
OHMS x 10^4
Initial Graphite Resistance 0.0890Ω
% CHANGE 65.6
TAMPED
NATURAL FLAKE GRAPHITE
100
200
300
400
500
600
700
800
VOLTS

FIG.34

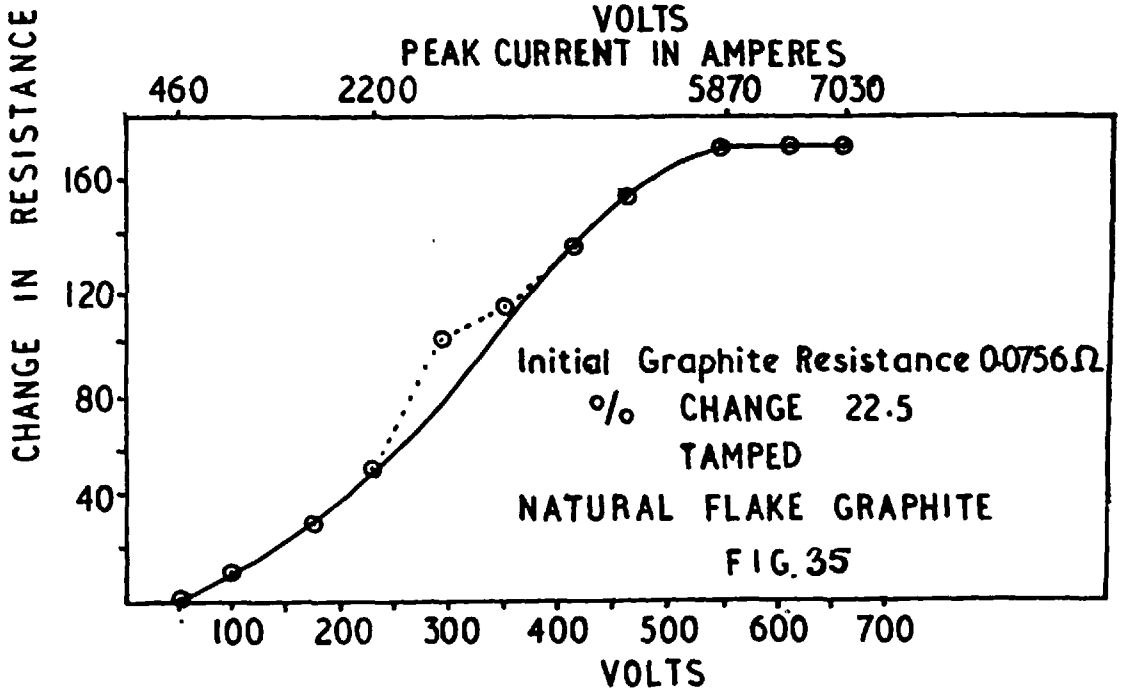

PEAK CURRENT IN AMPERES
460
2200
5870
7030
CHANGE IN RESISTANCE
160
120
80
40
Initial Graphite Resistance 0.0756Ω
% CHANGE 22.5
TAMPED
NATURAL FLAKE GRAPHITE
100
200
300
400
500
600
700
VOLTS

FIG.35

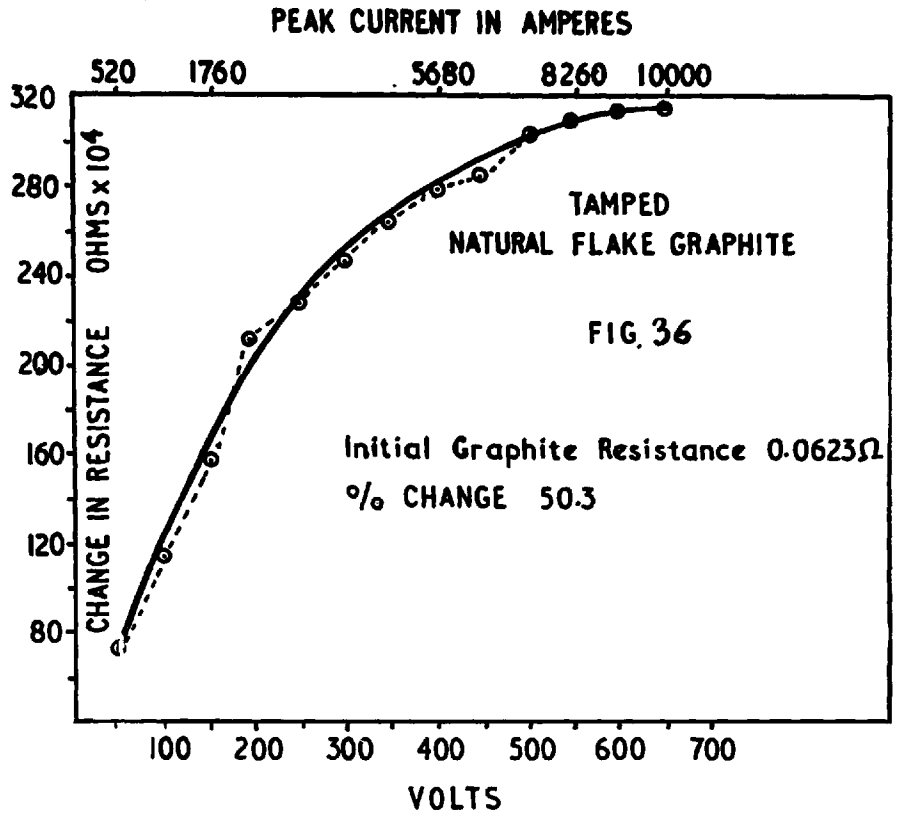

PEAK CURRENT IN AMPERES
520
1760
5680
8260
10000
320
280
240
200
160
120
80
CHANGE IN RESISTANCE OHMS x 10⁴
TAMPED
NATURAL FLAKE GRAPHITE
Initial Graphite Resistance 0.0623Ω
% CHANGE 50.3
100
200
300
400
500
600
700
VOLTS

FIG. 36

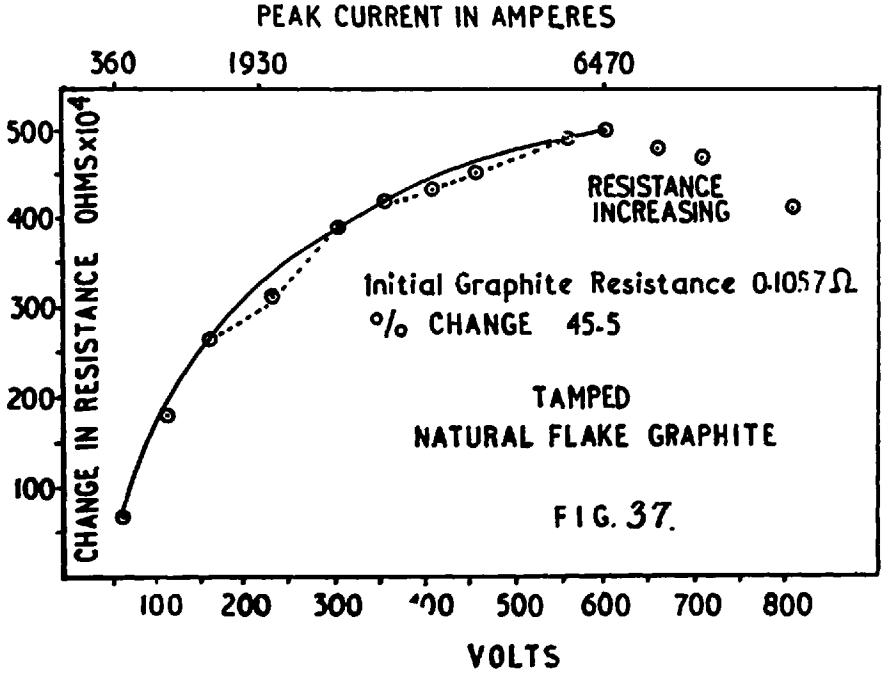

PEAK CURRENT IN AMPERES
360
1930
6470
500
400
300
200
100
CHANGE IN RESISTANCE OHMS x 10⁴
RESISTANCE INCREASING
Initial Graphite Resistance 0.1057Ω
% CHANGE 45.5
TAMPED
NATURAL FLAKE GRAPHITE
100
200
300
400
500
600
700
800
VOLTS

FIG. 37.

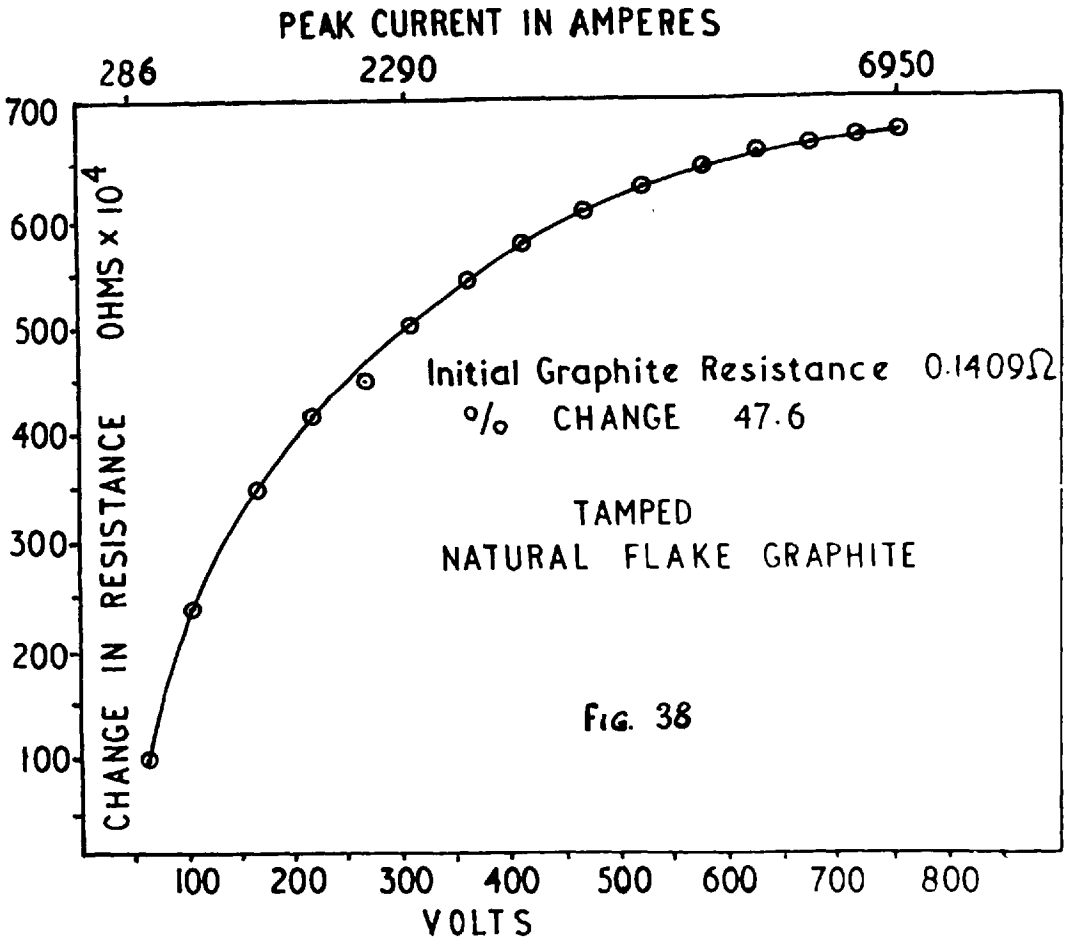

PEAK CURRENT IN AMPERES
286
2290
6950
700
600
500
400
300
200
100
CHANGE IN RESISTANCE OHMS x 10^4
Initial Graphite Resistance 0.1409Ω
% CHANGE 47.6
TAMPED
NATURAL FLAKE GRAPHITE
100 200 300 400 500 600 700 800
VOLTS

FIG. 38

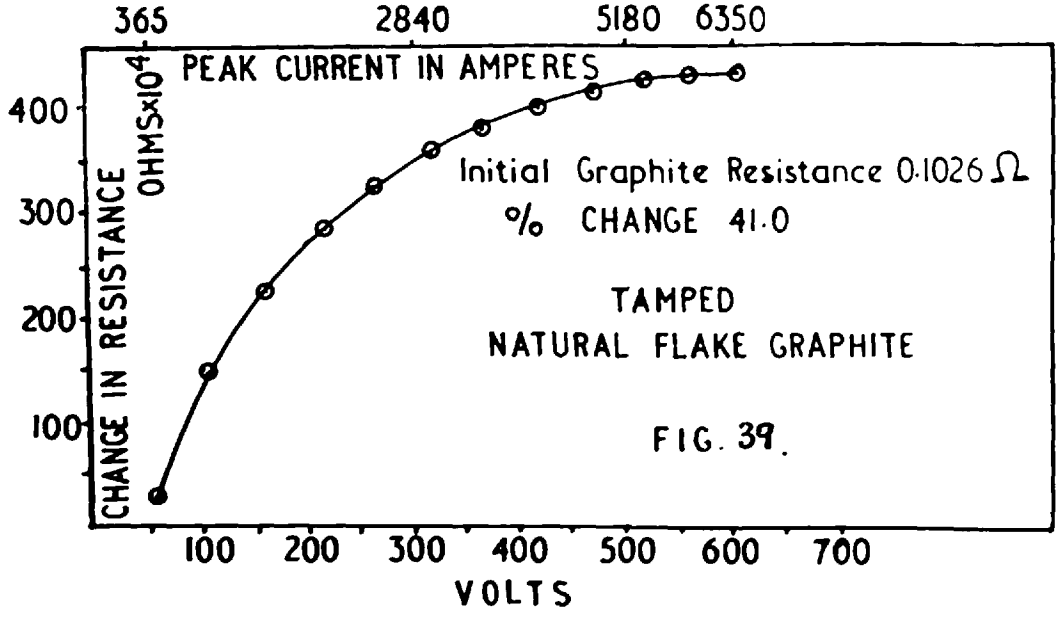

365
2840
5180
6350
PEAK CURRENT IN AMPERES
400
300
200
100
CHANGE IN RESISTANCE OHMS x 10^4
Initial Graphite Resistance 0.1026Ω
% CHANGE 41.0
TAMPED
NATURAL FLAKE GRAPHITE
100 200 300 400 500 600 700
VOLTS

FIG. 39.

2) Stabilisation of the electrical resistance by flash sintering.

Flash sintering stabilised the electrical resistance, Figs. 17-20. The close agreement between the heating and cooling points of Figs. 21b and 22b is another illustration that the drift had been stopped and had not been initiated again by changing the temperature.

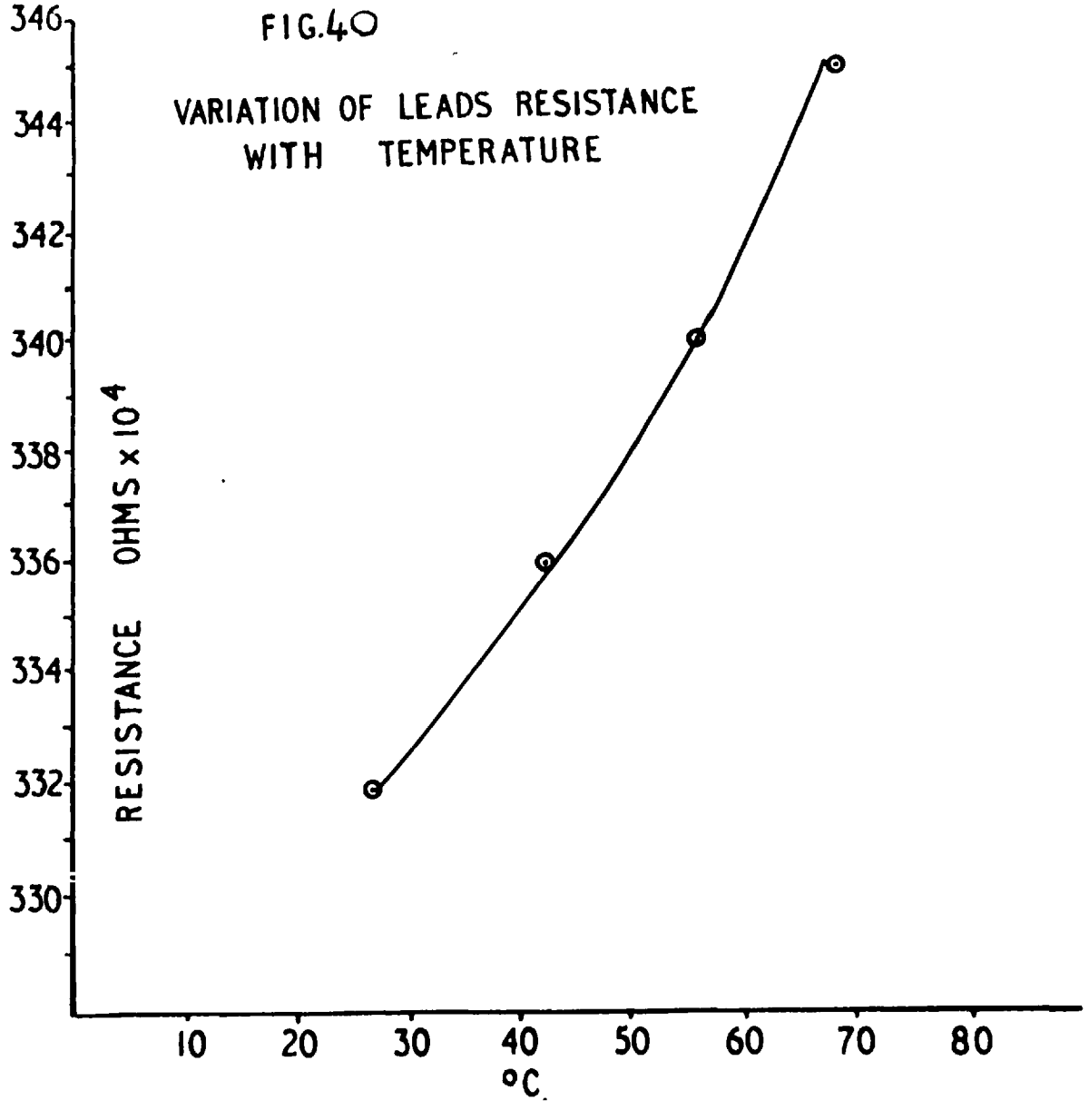
Temperature variation of the electrical resistance after flash sinterin

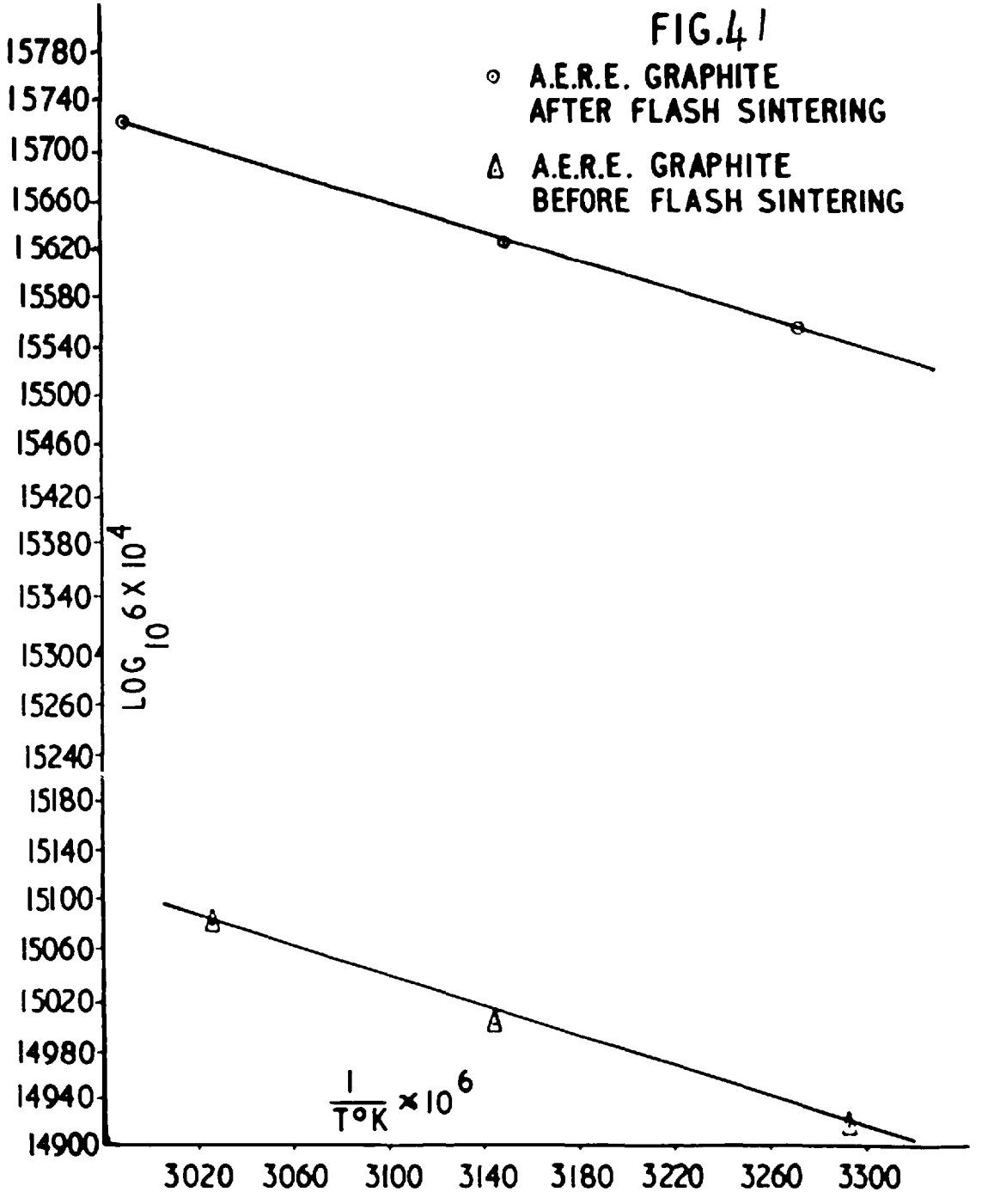
Fig. 40 shows the variation of the electrical resistance of the leads as a function of temperature. Account was taken of this variation in carrying out similar measurements on graphite. The heating and cooling points of Fig.21b correspond to one another and the curve can be taken to represent a true temperature effect on the electrical resistance of artificial graphite. The resistance is seen to decrease with increasing temperature. The effect of flash sintering on the temperature and resistance curves of natural graphite was again to bring the heating and cooling points closer together, Fig.22b. As in the case of artificial graphite, the resistance decreased with increasing temperature. However the temperature effect was not always the same in the case of natural graphite. Fig.23b shows a striking variation which occasionally occurred after flash sintering in which the temperature dependence of the electrical resistance is in the positive, i.e. "metallic" sense.

Activation energies ΔE calculated from log conductivity (σ) v $\frac{1}{T^{\circ}K}$ plots, Fig. 41 are given in Table II. The conductivity σ is the reciprocal of the resistance ρ and is the specific conductance Λ is given by

$$\sigma \text{ (mhos)} = \frac{\text{length of column (cm.)}}{\text{cross-sectional area (sq.cm.) x observed resistance (ohms)}}$$

FIG.4O


VARIATION OF LEADS RESISTANCE
WITH TEMPERATURE
RESISTANCE OHMS x 10^4
346
344
342
340
338
336
334
332
330
10
20
30
40
50
60
70
80
°C


FIG.41
A.E.R.E. GRAPHITE
AFTER FLASH SINTERING
A.E.R.E. GRAPHITE
BEFORE FLASH SINTERING
15780
15740
15700
15660
15620
15580
15540
15500
15460
15420
15380
15340
15300
15260
15240
15180
15140
15100
15060
15020
14980
14940
14900
LOG10 6X10^4
1/T°K ×10^6
3020
3060
3100
3140
3180
3220
3260
3300

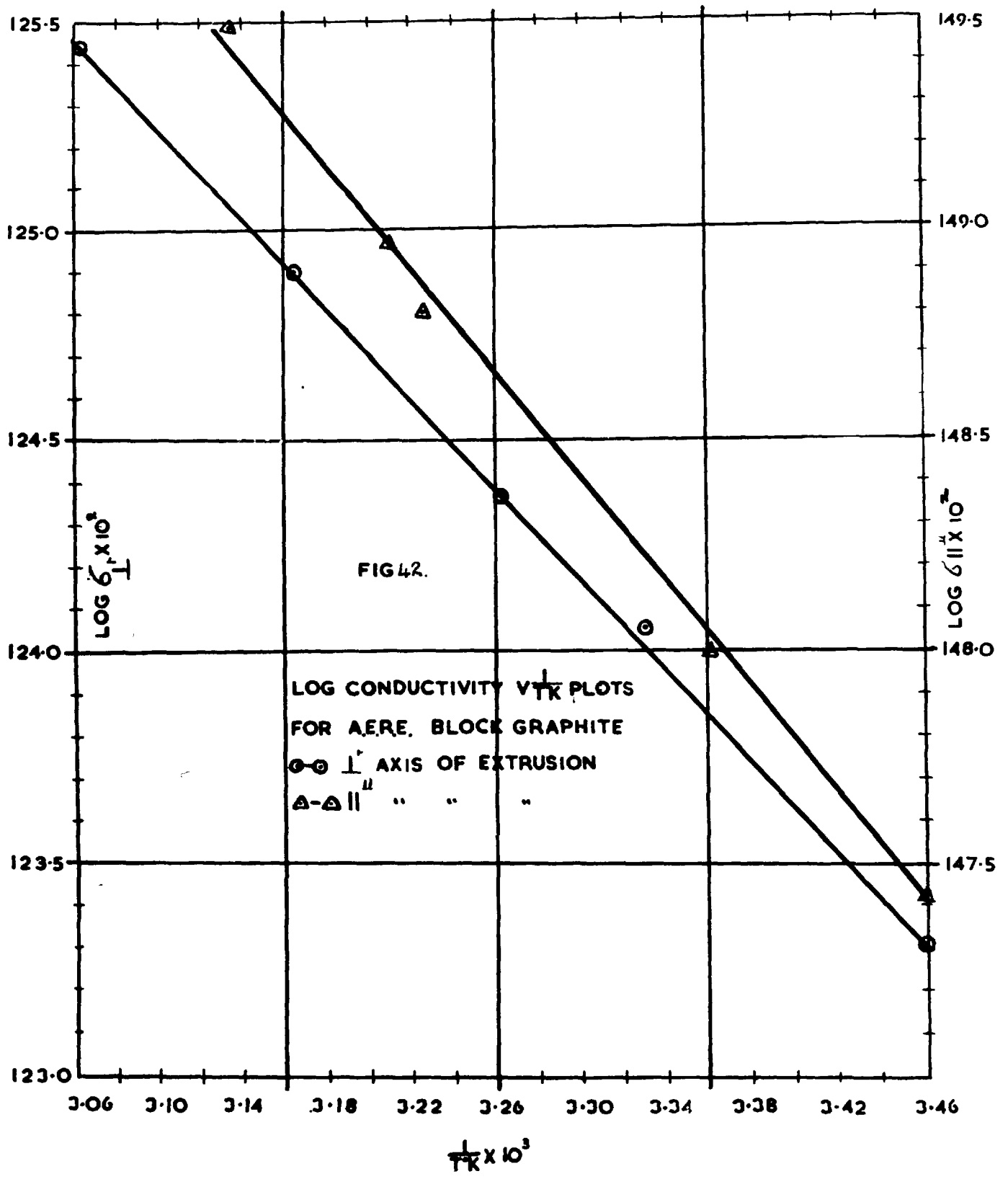

125·5
125·0
124·5
124·0
123·5
123·0
149·5
149·0
148·5
148·0
147·5
LOG $\sigma_{\perp}$ X 10^{8}
LOG $\sigma_{\parallel}$ X 10^{8}
3·06
3·10
3·14
3·18
3·22
3·26
3·30
3·34
3·38
3·42
3·46
$\frac{1}{T_K}$ X 10^{3}
FIG 42.
LOG CONDUCTIVITY V $\frac{1}{T_K}$ PLOTS
FOR A.E.R.E. BLOCK GRAPHITE
⊙-⊙ $\perp^{r}$ AXIS OF EXTRUSION
△-△ $\parallel^{ll}$ " "

TABLE II

	ΔE Before flash sintering	ΔE After flash sintering
AERE Powder	0.024 Fig. 41 e.v.	0.023 Fig. 41 e.v.
Natural flake graphite	0.031 Fig.22a "	0.016 Fig. 22b "
	0.040 Fig.23a "	*

* The electrical resistance in this case increased with increase of temperature giving a positive temperature co-efficient of 5.4×10^{-4}. In calculating activation energies it was assumed that the equation $\sigma = \sigma_o \; e^{-\frac{\Delta E}{2kT}}$ applied, where σ is the conductivity ΔE the activation energy and k and T Boltzmann's constant and the absolute temperature respectively. If m is the slope of the log σ v $\frac{1}{T}$ plot then

$$E = 2.303.2.k.m$$
$$= m.\ 3.98 \times 10^{-4} \text{ electron volts}$$

since $k = 1.38047 \times 10^{-16}$ erg. deg.$^{-1}$

and 1 e.v. $= 1.60203 \times 10^{-12}$ erg.

The electrical resistance and its temperature variation of the original block graphite.

Block graphite was investigated because it represents a completely sintered material. If an appreciable barrier resistance exists between particles of a graphite powder because the particles are not bonded to one another, then in completely sintered material this barrier will be absent. It could be expected that the presence or

absence of such a barrier to current flow in powder would be evident by comparing estimates of activation energies obtained from resistance versus temperature plots for both powder and block material. Specimens were cut from graphite block both parallel to and perpendicular to the extrusion axis. The electrical resistance and its temperature dependence were then measured. Fig. 42 shows $\log \sigma$ v $\frac{1}{T}$ plots. The activation energies and specific conductivities measured are shown in Table III.

Table III.

	Δ E	Specific conductivity $OHM^{-1} CM^{-1}$
Parallel to extrusion axis	0.025 e.v.	1000
Perpendicular to extrusion axis	0.022 "	333

It can be seen that while there was an anisotropy ratio of 3:1 in conductivity, the activation energies measured were not appreciably different.

The density of the block material was determined by flotation in a mixture of bromoform and carbon tetrachloride as 2.0 g./cc. The bulk density was measured as 1.6 g./cc.

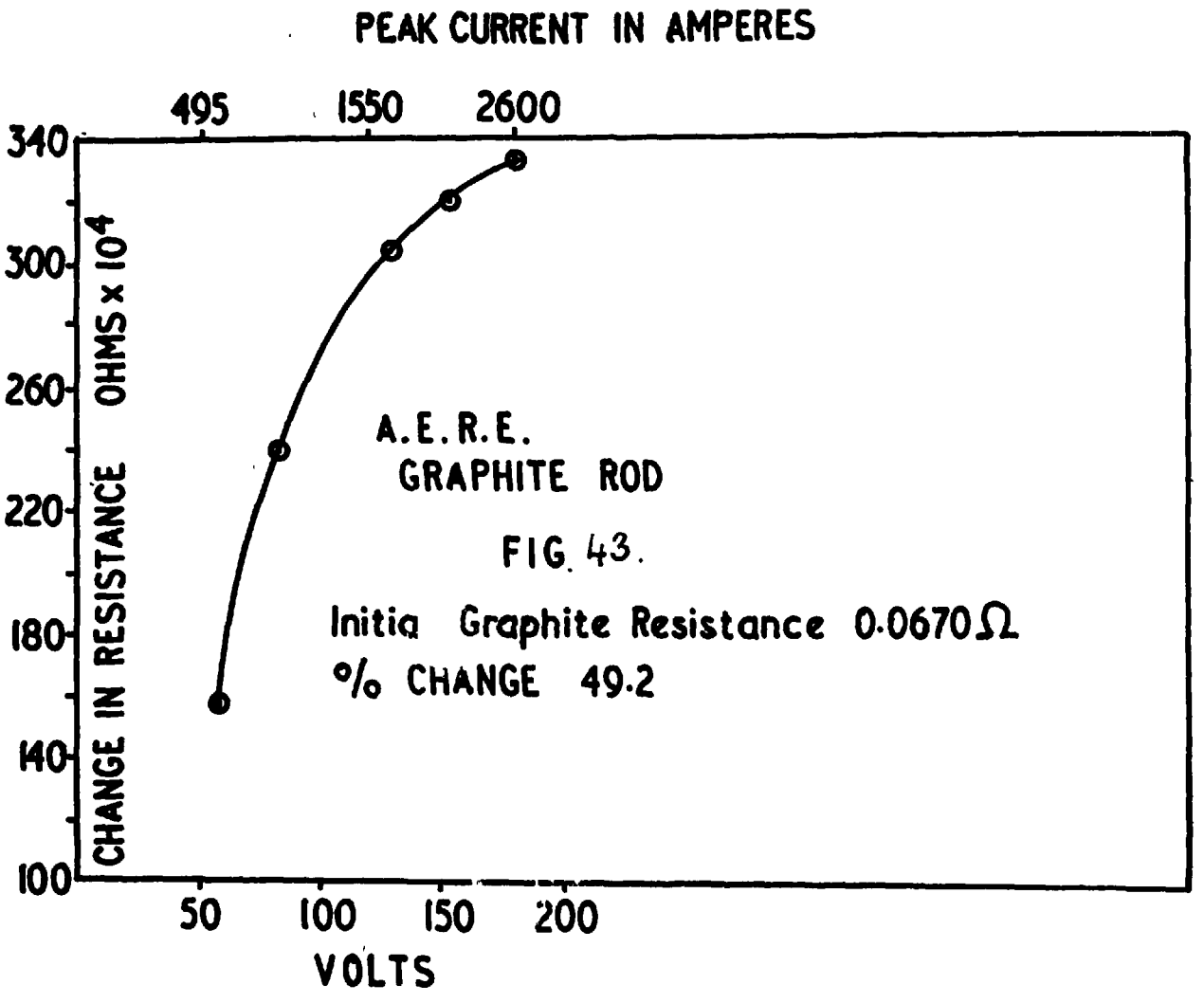
The effect of flash sintering on the bulk density of the powder.

Measurements before and after flash sintering rarely showed any change in column height and hence bulk density. For columns above 1 cm. in height a contraction of about 0.01 cm. was occasionally observed. However, since the column heights could not be measured to better than 0.005 cm. the changes observed were so close to the limits of measurement that little reliance could be placed upon them.

In an attempt to detect some change in column height induced specifically by flash sintering, a column of artificial graphite powder was carefully tamped and left for twenty four hours to allow any possible settling down of the particles to take place. The column height was recorded and the compact flash sintered to 1100 volts.

Column height before flash sintering	=	1.285 cm.
Column height after flash sintering	=	1.270 cm.
Mass of Graphite	=	0.156 g.
Cross-sectional area of cell	=	0.085 sq. cm.
Bulk Density before flash sintering	=	1.42
Bulk Density after flash sintering	=	1.44

The increase in density was thus between one and two per cent. To study density changes induced by flash sintering in a quantitative manner more refined apparatus would be necessary.


PEAK CURRENT IN AMPERES
495
1550
2600
340
300
260
220
180
140
100
CHANGE IN RESISTANCE OHMS x 10⁴
A.E.R.E.
GRAPHITE ROD
FIG. 43.
Initia Graphite Resistance 0.0670Ω
% CHANGE 49.2
50
100
150
200
VOLTS

The Contact between a platinum tipped electrode and a graphite surface.

The passage of an electric current through a solid block of graphite is unlikely to have any permanent effect on the specific resistance of the material provided that the temperature is not increased to a point where crystallite growth can occur. The peak current of a condensor discharge can be very high, but since the discharge time is very short - in the present work it is of the order of microseconds - resistance heating, measured as i^2Rt where i is the current, R the resistance of the block and t the time of current flow, cannot produce any significant overall heating. Significant heating might occur at points of high resistance provided the current was obliged to traverse such points but within a solid block of material such barrier resistances are unlikely to be present. However, high resistance points which fall directly in the path of current flow will not be entirely absent since no surface is perfectly smooth and points of high resistance may be expected in the electrode contact region. Fig. 43 shows the change of resistance observed on increasing the voltage of the condensor discharge. The change of resistance versus voltage tends to a plateau at high voltages as with graphite powders.

The Peak current of the Discharge.

Values of the Peak current in amperes calculated using Ohms Law from the voltage applied and the total electrical resistance of the circuit are indicated on each curve. Calling the threshold resistance R, the resistance of the powder at the point where the rate of change of

resistance with applied voltage sharply increased, and the current at this point the threshold current i, the following table was drawn up.

TABLE IV

AERE Graphite	Threshold Resistance R	Threshold Current i	i^2R
Untamped	0.8860 ~	655	3.8×10^5
	0.3977 "	740	2.17×10^5
	0.2188 "	1195	3.13×10^5
	0.0753 "	2520	4.76×10^5
	0.0223 "	4440	4.4×10^5
Tamped	1.1598 ~	585	3.97×10^5
	0.4580 "	913	3.82×10^5
	0.2645 "	1170	3.62×10^5
	0.1109 "	1780	3.52×10^5
	0.0616 "	3340	6.82×10^5

Where the very low resistances are concerned, e.g. Figs. 27, 28, 31, the threshold resistance was not easy to distinguish. R for these samples was taken to be the value at the point where a step in the curve was indicated. However, not much reliance may be placed on values of the threshold resistance obtained from these figures. The other figures clearly show the threshold effect.

An attempt was made to find some relationship between the threshold resistance and threshold current. The square of the threshold peak current multiplied by the threshold resistance is seen to be approximately

constant suggesting that the threshold resistance is inversely proportional to the square of the threshold current. A summary of the results of flash sintering on the electrical resistance is given in Table V.

TABLE V

Sample	Initial Resistance ohms.	Change in Resistance ohms.	% Change	Specific Conductance ohm^{-1} cm^{-1}	
AERE Powder Tamped	1.1628	0.0184	1.59	21.4	
	0.4805	0.0500	10.4	36.0	
	0.2715	0.0539	19.8	44.0	P
	0.1165	0.0271	23.2	50.5	
	0.0716	0.0196	27.4	62.0	
Untamped	0.9040	0.1480	16.4	23.0	
	0.4077	0.0922	22.0	37.7	
	0.2268	0.0447	19.7	43.5	P
	0.0815	0.0189	23.2	63.5	
	0.0217	0.0090	33.3	125.0	
Natural Flake	0.1409	0.0672	47.6	94.2	P
	0.1057	0.0479	45.5	150.0	P
	0.1026	0.0422	41.0	105.0	P
	0.0890	0.0594	65.6	172.0	P
	0.0756	0.0170	22.5	183.0	P
	0.0623	0.0313	50.3	147.0	P

P signifies that a plateau was reached.

THERMO-ELECTRIC POWER MEASUREMENTS.

The thermo-electric power was measured under three types of condition.

1) Without the weight C Fig. 14 in place (referred to as zero pressure),

2) With weight C in place - equivalent to a pressure of 13.5 kg/cm^2,

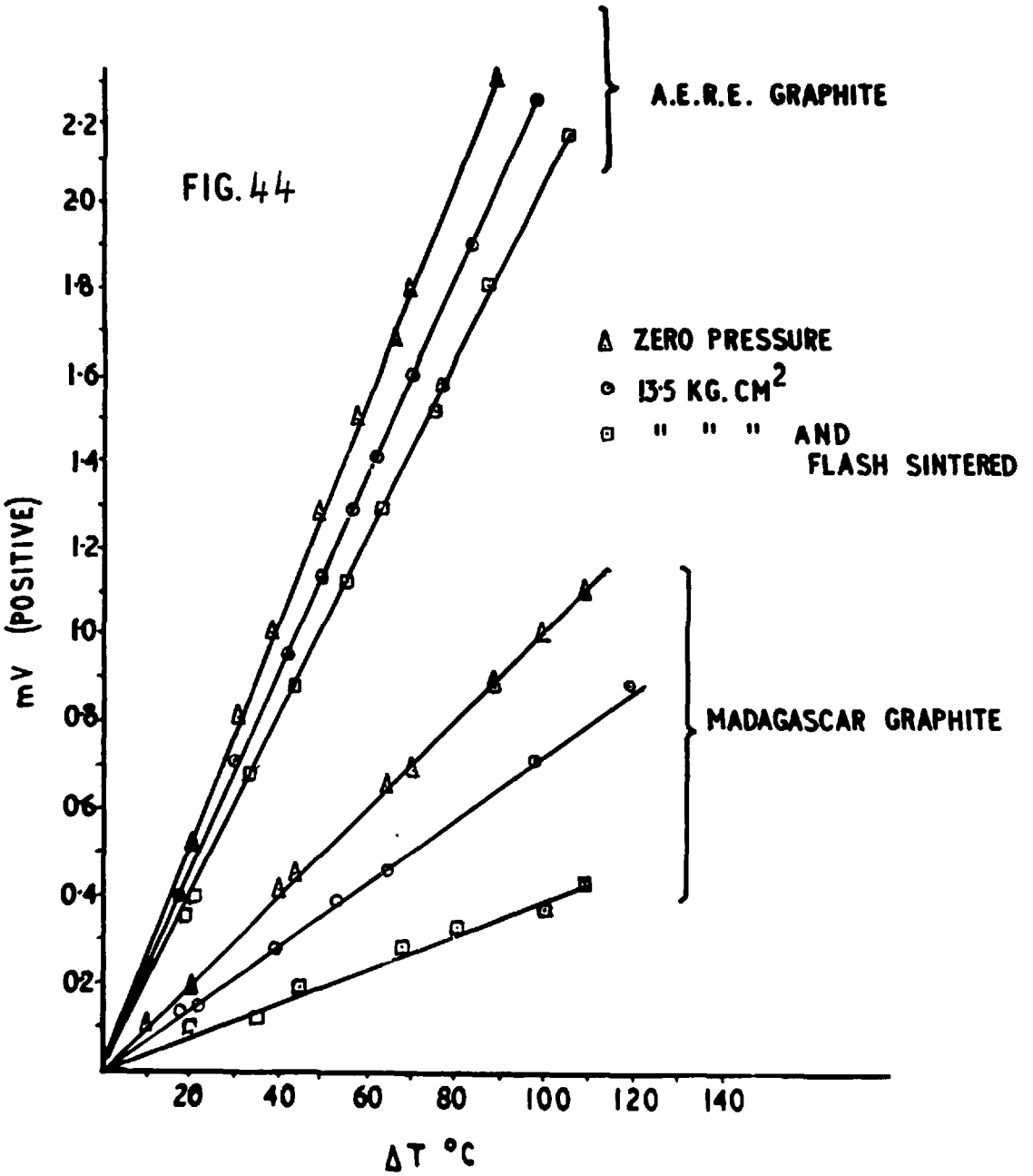
3) With weight C in place and after flash sintering.

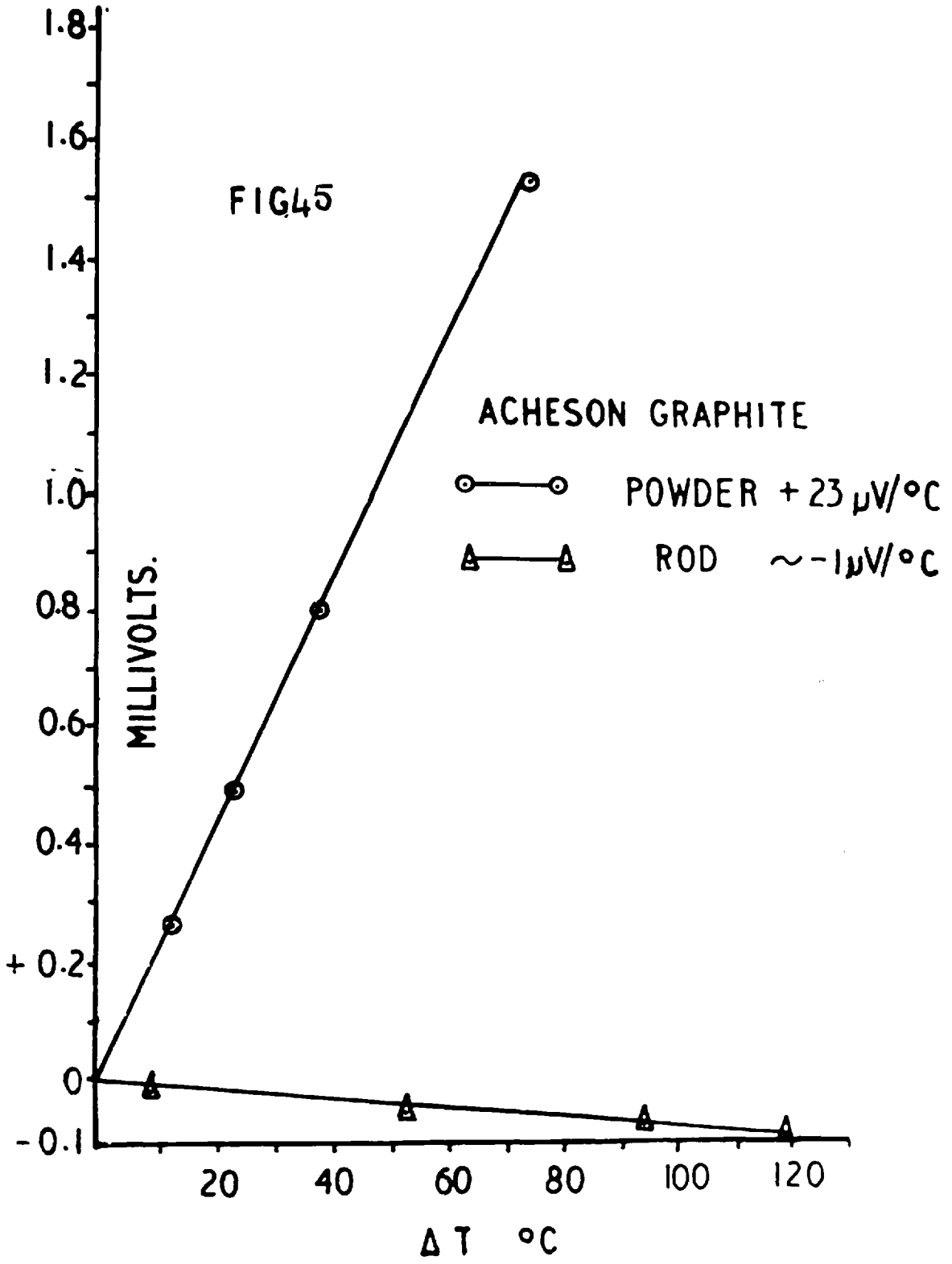
Fig. 44 shows that the thermo-electric power became less positive on increased pressure and also after flash sintering. The results are recorded in Table VI.

TABLE VI

Material	Fig.	Zero pressure $\mu v/^o c$	$\mu v/^o c$ 13.5 kg.cm.^{2}	
			before	after flash sintering
AERE Powder	44	+ 25	+ 23	+ 20
Acheson Powder	45		+ 23	
Natural flake (Madagascar)	46	+ 10	+ 7.0	+ 4
AERE Block 11	See Part II		- 0.1	
" " 1	See Part II		+ 1.9	
Acheson Block 11			- 1.0	

The striking effect of powdering on the thermo-electric power can be seen from the above table by considering the values obtained for AERE and Acheson graphite. Powdering always caused the thermo-electric power to become markedly positive.


FIG. 44
A.E.R.E. GRAPHITE
Δ ZERO PRESSURE
○ 13·5 KG. CM²
□ " " " AND FLASH SINTERED
MADAGASCAR GRAPHITE
mV (POSITIVE)
2·2
2·0
1·8
1·6
1·4
1·2
1·0
0·8
0·6
0·4
0·2
20
40
60
80
100
120
140
ΔT °C


FIG45
ACHESON GRAPHITE
POWDER +23 μV/°C
ROD ~-1μV/°C
MILLIVOLTS.
1.8
1.6
1.4
1.2
1.0
0.8
0.6
0.4
+0.2
0
-0.1
20
40
60
80
100
120
ΔT °C

X-RAY DIFFRACTION INVESTIGATION.

The X-ray diffraction photographs of the artificial graphite powder used in the work on electrical resistance showed only powder lines and these were of uniform intensity, Plate 2. No spottiness was present and the lines were of uniform intensity indicating that the powder was truly polycrystalline and that preferred orientation effects were absent.

The reflections were indexed by calculating all possible reflections on the basis of the known symmetry and unit cell of graphite.

For the hexagonal lattice

$$\mathrm{Sin}^2\theta_{hkl} = \frac{\lambda^2}{3a^2}(h^2 + hk + k^2) + \frac{\lambda^2}{4c_o^2} \cdot l^2$$

Taking $a = 2.45\text{Å}$ and $c = 6.69\text{Å}$

h	k	l	$\mathrm{Sin}^2\theta$	θ
0	0	1	0.0132	6.5
0	0	2	0.0528	13.3
0	0	3	0.1188	20.1
0	0	4	0.2112	27.44
0	0	5	0.3300	35.1
0	0	6	0.4752	43.6
0	0	7	0.6469	53.54
0	0	8	0.8449	66.81
1	0	0	0.1307	21.2
1	0	1	0.1439	22.3

etc.

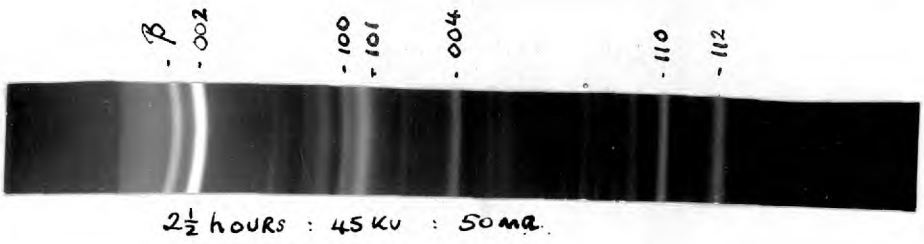


PLATE II

Poly-crystalline graphite

Diffraction rings of uniform density
(unfiltered radiation)

CHAPTER 7

PART I : DISCUSSION

In the following discussion the first topic to be considered is the observed decrease of the electrical resistance with time and its elimination by flash sintering. The electrical resistances of the compacts are then considered with regard to the main types of contact which may exist in an electrode - powder - electrode system and with each of which a significant contact resistance may be associated. It is concluded that the extra resistance which a graphite powder exhibits as compared to block material can be accounted for purely in terms of constriction of current flow in passing from one particle to the next. The effect of flash sintering in decreasing the overall electrical resistance of the compact is attributed to an increase in the contact area between particles. Then follows an interpretation of the marked thermo-electric power changes observed when block graphite was powdered in air and the fact that while flash sintering had a striking effect on the electrical resistance of the powder its effect on the thermo-electric power was not so pronounced.

Using the Strout model of constriction resistances described in the Introduction to Part I, an estimate is then made of the radius of contact between particles and its change on flash sintering.

The flash sintering curves are next considered in detail, attention being drawn to the existence of a threshold effect.

The next section of the Discussion is concerned with calculating temperature distributions in the contact region assuming the centre of the contact area to be raised instantaneously to any given temperature. The energies required for such temperature distributions are also calculated. In making an estimate of the temperature distribution attainable from the energy of a condensor discharge, attention is drawn to the fact that itmis the rate at which energy is supplied and not the total energy which determines what distribution shall be attained.

Melting and surface flow of graphite are discussed and assuming a flow temperature for graphite, a temperature distribution involving this temperature is chosen in the light of the energy available. From this an estimate is made of the area of contact after flash sintering and compared with that obtained from electrical resistance measurements.

DECREASE OF THE ELECTRICAL RESISTANCE WITH TIME.

If extensive impurity films were present on the surface of the graphite particles it is unlikely that a smooth resistance decrease with time would have been observed. Such films would present a barrier to electron flow and although they could rupture if they were thin enough, a resistance decrease brought about by such processes occurring throughout the compact is not likely to show the smooth continuous charge as was observed Figs. 17, 18, 19, 20. A process which would exhibit such behaviour would be the growth of a contact area under pressure. The contact area will grow until it is capable of supporting the load. In such a process the rate of change of resistance would be expected to decrease rapidly at first and then slow down as the contact area became progressively greater. This was the effect observed. Assuming that the resistance drift with time was due to growth of contact areas between particles if this growth were speeded up the resistance drift could be expected to cease. The technique of flash sintering was devised to achieve this by causing a large amount of heat to be liberated at the contact points which might soften the graphite and allow a rapid increase of contact area to occur. The results of flash sintering are in accordance with these expectations. The drift of resistance with time was stopped and the overall resistance decreased.

The effect of tamping on the electrical resistance of the powder.

From Table V it may be seen that tamped columns exhibit higher specific conductances than untamped columns. The plot for untamped columns also shows greater curvature. These results may be reasonably interpreted on differences in degree of packing. Tamped columns would be expected to have more particles in contact per unit area than untamped columns. This would increase the specific conductance.

For short columns of untamped material the degree of packing and therefore the number of contacts per unit area is likely to be greater than that of longer columns. In the preparation of untamped columns the powder was simply poured into the cell and the electrode carrying the lead weight set on top of the powder. As the column increased in height it would be expected that the pressure of the electrode would not be evenly transmitted through the powder, that in certain regions it would become "locked in" and that the degree of packing would therefore not be uniform throughout the column. The specific conductance would therefore decrease with column height leading to a curve of the type found. This effect would be less marked with tamped columns since in this case the powder was tamped periodically as it was admitted into the cell.

At the lower column heights it may be seen from Fig. 15 that the plots for tamped and untamped material coincide indicating that for these columns packing is not improved by tamping.

The fact that at short column heights tamping does not significantly

improve the degree of packing, and that untamped columns will give reproducible results, could prove useful when resistance measurements are required under vacuum conditions. Tamping in these circumstances is a cumbersome process.

CONTACT RESISTANCES IN POWDERS.

In the system investigated two main types of contact are to be distinguished; they are

a) Electrode/particle, and

b) particle/particle

In each case if an impurity film of significant dimensions intervenes between the two surfaces such that they no longer come within the range of one anothers force fields then condiction within this barrier layer must be considered as well as conduction within the material under investigation. With a high resistance barrier layer present, e.g. an oxide film, the overall resistance would not only be determined to a considerable extent by this film but also, important parameters such as conduction activation energies would reflect the nature of the impurity film rather than that of the "substrate"

a. Electrode contact resistance.

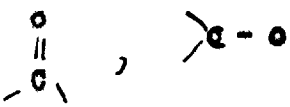
When a condensor discharge was passed through a column of graphite powder it was found that at a particular condensor voltage, the electrical resistance of the powder decreased sharply. The resistance continued to decrease with increasing voltage but levelling off at higher voltages and tending to a plateau. Before discussing the process of flash sintering in detail the overall change of resistance which it effected will be considered in relation to electrode contact resistance.

For a series of electrical resistance measurements on different column heights of the same powdered material a plot of column height versus resistance would be a straight line if the degree of packing was constant for all columns. If an electrode contact resistance was present, the straight line plot would intersect the resistance axis at a value equal to this quantity. The leads resistance is constant and it is reasonable to suggest as above that the electrode contact resistance would not vary for all powdered compacts of the same material. If the effect of flash sintering were to be explained solely in terms of decrease in the contact resistance between the platinum surface of the electrods and the surfaces of the graphite particles, then the same absolute resistance change in ohms. might reasonably be expected for all powdered columns. When Table V is consulted it can easily be seen that the overall changes of resistance observed on flash sintering vary considerably. Artificial graphite powder and natural flake graphite are best considered separately since the particle and flake sizes are not comparable. However, within each group significant variation of the overall resistance change is evident. If it is again assumed that the electrode/graphite contact resistance is constant for all compacts of the same material, no compact may then exhibit a total electrical resistance less than the resistance of this contact. From Table V it can be seen that there are some cases where the absolute change of resistance found with one compact was significantly greater than the total resistance of another. Compare for example the first and last rows of figures listed under untamped columns. In the first case the

the overall change of resistance observed on flash sintering was 0.1480 ohmn., while the total resistance of the other was 0.0217 ohms. On the basis of the assumption that an electrode/graphite contact resistance if present remains constant throughout a series of measurements on the same material the decrease of resistance observed on flash sintering clearly cannot be satisfactorily explained as elimination or even significant reduction in the resistance of this contact. The evidence suggests that the resistance changes observed occur by some process wrought in the body of the powder. It is worth noting that to extrapolate the curves, Fig. 15, to zero column height from the smallest columns measured involves a considerable change of slope. The extrapolated portion of the curves must descent almost vertically to the resistance axis. This demonstrates that there can be no appreciable contact resistance between the platinum surface of the electrodes and the particles of graphite powder because the curves would have to intersect the resistance axis at the value of this contact resistance. The lack of evidence for the presence of an electrode-graphite contact resistance is important. It suggests that a metallic bond is set up between the graphite and the platinum tip of the electrode.

b. Contact resistance between particles.

A contact resistance between metals is usually due to the presence of oxide films on the surface. Such a contact resistance is very often the greatest single factor in determining the electrical resistance between metals. (42). It can hardly be supposed that the surface of

the graphite particles was completely free from impurities. On powdering the graphite block chemical bonds must have been ruptured. Since the powdering was carried out in air the free valencies produced could not have remained unsatisfied for long and groups such as  could be expected to exist on the surface. This type of impurity however could not give rise to a film in any way comparable to the oxide film which can cover most metals. Where metals are concerned a layer can be built up and oxidation can still occur by diffusion of defects through the oxide lattice, (47). In the case of graphite, however, such a solid oxide structure is difficult to envisage since the quinone type group is firmly fixed at the point where a chemical bond was ruptured and once the freed valency is satisfied there will be no further reaction between carbon and oxygen unless the temperature is raised to the oxidation temperature which for graphite is about 500°C. Even at these temperatures no appreciable oxide film will be built up since the products of oxidation are mainly gaseous, e.g. CO and CO_2 (48).

The presence of impurity groups on the surface of the graphite has not been proved and while it seems probable that they are present there is no evidence to suggest that they significantly impede the flow of current from one particle to the next.

At the lowest column height measured the conductivity of the powder can be seen from Table V to be 125. If this is compared with block graphite (Table III), it is seen that this value is one eighth

That measured along the extrusion axis and about one third of that measured across this axis. Since the conductivity was calculated in terms of the dimensions of the resistance cell and since as described in Chapter 4 only part of each particle could be in contact, the extra constriction resistance must lead to a value which is smaller than the true value. It does not seem necessary to invoke a barrier contact resistance between particles or between electrodes and particles to account for the lower conductivity of powdered as opposed to block graphite. This hypothesis is supported by the work on cold pressing Fig. 13, where a conductance of 500 $ohm.^{-1}cm.^{-1}$ was obtained for powder compressed to 3000 kg/cm^2. At this applied pressure the contact area between particles will be much larger than that existing in the experiments described above which were carried out at 13.5 $kg.cm.^2$. Since the powder is isotropic (Plate II) a figure of 500 $ohm.^{-1}cm.^{-1}$ would be a reasonable value to expect for the specific conductance of a block of isotropic graphite if it could be obtained.

Activation Energies of Conduction.

It is very significant that while there was a considerable difference between the conductivities of powdered and block artificial graphite, the activation energies measured in both cases were not appreciably different.

viz.	AERE Block 11[11]	0.025 e.v.
	1	0.023 e.v.
and	AERE Powder before flash sintering	0.024 e.v.
	AERE Powder after flash sintering	0.023 e.v.

These figures strongly support the hypothesis that in both powder and block material the mechanism of conduction is the same and that the powdering process does not introduce significantly new barriers to electron flow.

The decrease of resistance observed on flash sintering can hardly be due to the removal of an oxide barrier from the surface of the graphite particle since the crossing of such a barrier would require an activation energy measurably different from that obtaining in the barrier's absence. Hence the fact that the activation energies measured before and after flash sintering were effectively the same suggests that flash sintering did not alter in any significant way the mechanism of conduction but simply decreased the resistance by increasing the contact area between particles. However, this does not exclude the possibility of scattered impurity groups being present on the surface of the particle.

THERMO-ELECTRIC POWER MEASUREMENTS.

The argument for the presence of impurity groups on the surface arises from the fact that on powdering, free valencies must be created and that these valencies may satisfy themselves by removing certain atoms or groups of atoms from the atmosphere. That some process occurs on powdering which disturbs the electron distribution in graphite can be seen from the thermo-electric data presented in Table VI.

The thermo-electric power of AERE block graphite along and across the axis of extrusion was -0.1 and +1.9μV/$^{\circ}$C respectively. Acheson graphite which was only measured along the extrusion axis had a value of -1.0μV/$^{\circ}$C. When AERE and Acheson materials were powdered in air the thermo-electric power of both became +23μV$^{\circ}$C, Figs. 44 and 45.

From these values it is clear that in the powder positive "holes" play a greater role in conduction than do electrons. In the block materials both contribute approximately to the same extent giving a very small thermo-electric voltage with the electron contribution just predominent. (The positive value observed across the extrusion axis will be considered in Part II; it does not affect the present argument) This is in agreement with measurements of the Hall Co-efficient (25). To produce this positive value on powdering, electron traps must have been introduced into the graphite. This could be brought about in a number of ways. Electro-negative species such as O_2 or H_2O could have become adsorbed on the surface of the particles causing a drift of electrons to a particular region of the particle. This local

polarisation of electrons will constitute an electron trap and the overall mobility of the electrons will be reduced. The thermo-electric power depends both on the number and mobility of electrons and if "holes" are also present as in graphite, on the number and mobility of holes. Thus if the mobility of electrons is reduced the contribution of "holes" to the conduction will be greater. If the electro-negative species forms a chemical bond such as a quinone group as discussed earlier, removal of an electron from the graphite π band will occur and the resultant increase in the number of holes will lead to their predominance in conduction.

Because of the strain imposed on powdering, free valencies may be created in the body of the graphite particle and while the distance between such a free valency and a neighbouring macro-molecule may be great enough to prevent link-up occurring, space requirements may forbid the satisfaction of these valencies by foreign atomic species. Thus giant free radicals such as occur at "hole" and "claw" defects may be created on powdering (17). These unsatisfied valencies would lead to the polarisation of electrons in their vicinity and such a polarisation by reducing electron mobility would enhance the role played by holes in conduction.

There remains another possible mechanism by which freed valencies could satisfy themselves and lead to hole conduction in graphite. If when a sigma bond is ruptured a π electron is picked up, the free valency could in this way become "internally" satisfied. This is the

type of mechanism proposed by Mrozowski to account for the depletion of the π Band electrons as carbons are heat-treated to higher temperatures with the evolution of hydrogen (24).

The influence of pressure and flash sintering on the thermo-electric power.

It can be seen that the effect of pressure and of flash sintering on the thermo-electric power was similar. In each case, the value became less positive by a few microvolts. This suggests that both pressure and flash sintering slightly reduce the number of electron traps. If the traps are considered to by surface traps, of the type considered earlier, - OH groups, etc., they will be distributed over the whole surface of the particle. Flash sintering and pressure will exert their effects only on the contact regions and this is only a small part of the total surface. If both these processes cause heat to be generated in the contact region, the first by Joule heating and the second by friction and this leads to expulsion of the adsorbed impurity, then the number of impurity groups expelled will only be a fraction of the total number present on the particle's surface. Thus the small change of thermo-electric power to a more positive value could be explained.

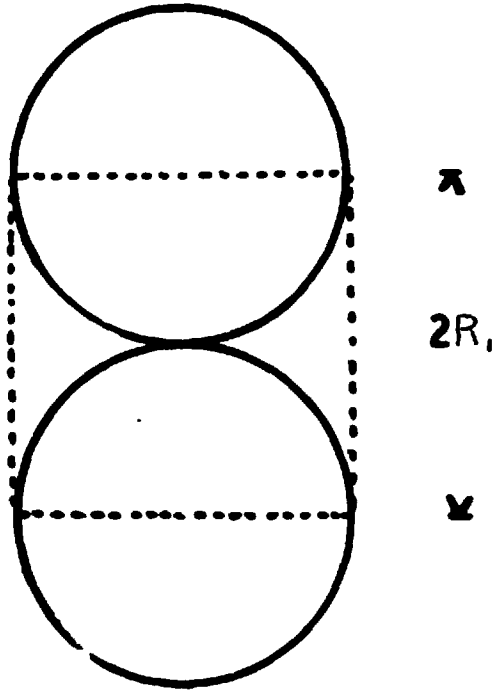
The small effect of both pressure and flash sintering on the thermo-electric power may also be taken as evidence that a well developed impurity layer does not exist on the surface of the graphite particles. The amount of heat liberated by flash sintering is clearly in excess of that produced by pressure since it can produce

an immediate increase of the contact area (compare the slow increase of the contact area with pressure as indicated by decrease resistance with time which still never achieves the low resistance - large contact areas - attained by flash sintering.) Despite the large differences in heat liberated by both processes, their effect on the thermo-electric power is comparable. This may be understood by considering the following:-

If only scattered impurity sites exist on the surface of the graphite particles, i.e. impurity atoms which are not linked up to form a film, within any area as small as the contact area the number of adsorbed impurities will not be large. Pressure may be considered to remove about half this number and flash sintering the remainder. The procedure adopted was always to flash sinter the compact under compression and under these circumstances flash sintering while potentially capable of expelling all impurities from the final contact area could only expel such as remained after pressure had been applied.

The thermo-electric power is sensitive to the whole surface condition of the particle and not just the contact area. Foreign species chemisorbed on any part of the surface will influence the electronic levels of the solid as a whole. In flash sintering since almost all of the energy of the discharge is liberated in the contact region, only surfaces within this region will be affected. Only some of the electron traps will then be removed and the still strongly positive value of the thermo-electric after flash sintering can be understood. Bowden points out that when an oxide film between two

metals is ruptured the small pieces of oxide scattered over the surface do not influence significantly the electrical contact resistance but that they may play a more important role in other types of measurements (42).



UNIT CELL VOLUME $\pi R_1^2 2R_1$

FIG. 46

CALCULATION OF THE RADIUS OF CONTACT AND ITS CHANGE ON FLASH SINTERING.

The results of flash sintering can most conveniently be discussed in terms of the contact radius between particles and constriction of current flow through these contacts.

If the path of an electric current is constricted by flow through a contact, there is an extra resistance - the constriction resistance - be to considered over and above the intrinsic resistance of the material. The Strout Equation for this constriction resistance is

$$W = \frac{\rho}{2nr}$$ (See Instroduction to Part I)

When ρ = specific resistance of the material, n = number of parallel contacts and r = contact radius.

For the lowest column measured 0.19 cm., considering the untamped material, it is assumed that the maximum number of contacts is realised. This appears a reasonable assumption in view of the very short column and the fact that tamping did not produce a lower resistance. The value of the specific resistance of this column was 8 times that of block graphite as measured along the extrusion axis and about 3 times that as measured across this axis, Table III. The particle diameter was taken as 4×10^{-3}cm. corresponding to British standard sieve grade 300 mesh. (49).

To calculate the maximum number of contacts in the column 0.19 cm. high spherical particles 4×10^{-3}cm. in diameter were considered in open packing. The "unit cell", i.e. the smallest repeating unit in the system made up of particles and contacts, will consist of two half particles and a contact, Fig. 46. The volume of this unit cell is

$\pi R_1^2 2R_1$ where $2R_1$ is the particle diameter and equal to 4×10^{-3} cm. The area of the resistance cell was 0.084 cm.

The Strout Equation applies to parallel contacts and hence the number of parallel contacts is

$$\frac{0.084 \times 4 \times 10^{-3}}{(2 \times 10^{-3})^2 \, 4 \times 10^{-3}} = 6.67 \times 10^3$$

This is the number of contacts in a volume determined by the area of the resistance cell and the length of the unit cell. This volume will be called unit volume. For the purpose of these calculations it is essential to assume that the area of contact between two spherical particles results from a single contact. When the diameter of the particles is considered this does not seem unreasonable.

The number of contacts in unit volume for perfect packing is now known. Since it is assumed that for the shortest column height measured all contacts are realised and that no impurity films which constitute a barrier resistance exist, if the value of the electrical resistance which block graphite would exhibit having the same dimensions of this column of powder is subtracted from the measured value of the powder, the difference will represent the total constriction resistance in the powder and the constriction resistance/unit volume can thus be calculated.

Thus knowing "n" the number of contacts/unit volumn and "W" the constriction resistance/unit volume, by substituting in the Strout Equation, r the contact radius may be evaluated. Thus for column

height 0.19 cm.

Total Constriction Resistance = 0.0247

$$W = \frac{0.0247 \times 4 \times 10^{-3}}{0.19} = \text{constriction resistance/unit volume}$$

$\rho = 10^{-3}$ ohm.cm. (specific resistance)

$$W = \frac{\rho}{2r \times n} = \frac{10^{-3}}{6.67 \times 10^{3} \times 2r}$$

$r = 1.44 \times 10^{-4}$ cm.

Throughout the series of untamped columnsthe contact radius is assumed to remain constant but the number of contacts/unit volume, i.e. the degree of packing is considered to vary leading to the curve found experimentally, Fig. 15.

From the experimentally determined values of the Constriction Resistance at each column height the number of contacts/unit volume was determined, Table VII.

Table VII

col.Ht. cm.	W	n	r
0.19	5.21×10^{-4}	6.67×10^{3}	1.44×10^{-4}cm.
0.34	9.1×10^{-4}	3.84×10^{3}	...
0.66	1.33×10^{-3}	2.60×10^{3}	...
1.0	1.58×10^{-3}	2.19×10^{3}	...
1.69	2.09×10^{-3}	1.65×10^{3}	...

Contact radii after flash sintering.

If flash sintering decreases the electrical resistance solely by increasing the contact area then the new radius of contact can be calculated from the decreased value of the constriction resistance assuming the number of contacts/unit volume for each column before and after flash sintering to be the same.

While dealing with the series of columns before flash sintering, for the purpose of calculating the number of contacts/unit volume it was assumed that the contact radius remained constant throughout the series; this assumption will not hold after flash sintering since it can be seen from the change of resistance versus voltage plots that for some columns the resistance was still decreasing rapidly at the highest voltages which could be used. A constant radius of contact might be assumed if a plateau resistance had been reached in all cases.

The radii calculated after flash sintering are shown in Table VIII.

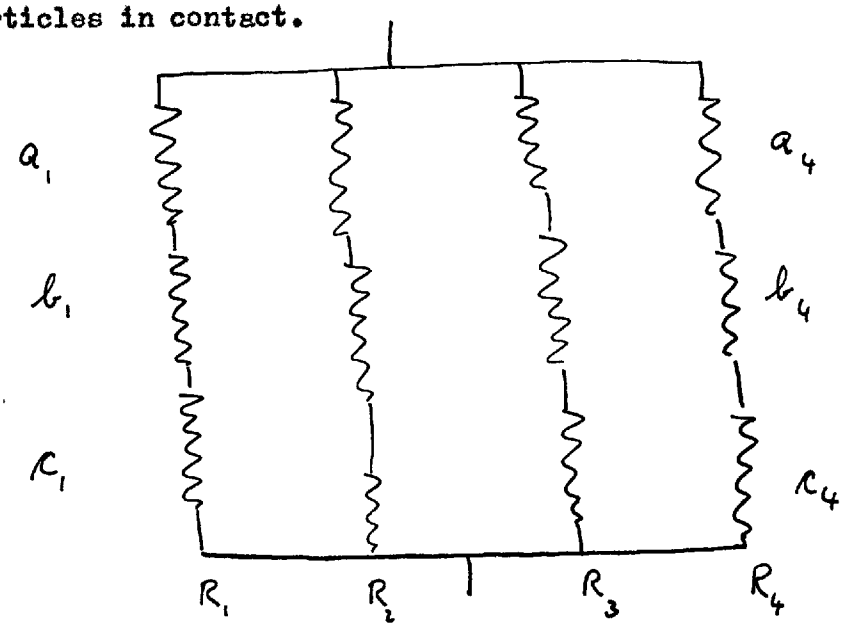
TABLE VIII

Col. Ht. cm.	W∧	r cm.
0.19	3.25×10^{-4}	2.3×10^{-4}
0.34	6.82×10^{-4}	1.92×10^{-4}
0.66	1.04×10^{-3}	1.84×10^{-4}
1.0	1.22×10^{-3}	1.89×10^{-4}
1.69	1.74×10^{-3}	1.74×10^{-4}

ANALYSIS OF THE FLASH SINTERING CURVES.

The most striking feature of the curves, Figs. 24, 25, 26, 29, 30, 32, is that there was a critical voltage above which the rate of decrease of resistance increased sharply tending to level off again at higher voltages.

The powder may be considered as made up of a number of series resistances joined in parallel. If the total resistance observed is mainly the result of constriction resistance then each individual resistance in each series is the constriction resistance between two particles in contact.



If the total resistance observed is R_o

$$\frac{1}{R_o} = \frac{1}{R_1} + \frac{1}{R_2} + \frac{1}{R_3} + \frac{1}{R_4} + \cdots\cdots$$

and $R_1 = a_1 + b_1 + c_1 + \cdots\cdot$

$R_2 = a_2 + b_2 + c_2 + \cdots\cdot$

etc.

If the a, b, c, etc.resistances are constriction resistances as suggested, their magnitude depends upon the contact radius between particles. If this contact radius is constant throughout the powder $a = b = c = d$ etc.

The cessation of resistance drift with time and the overall decrease of resistance on flash sintering was considered to be due to growth of the contact area which was caused by the heating effect of the discharge current. The amount of heat liberated at the constriction will depend upon both the resistance of the constriction and the current flowing through it. The time for which the current flows will be the same for every constriction in the one powder compact. It is determined by the Time constant of the circuit which is the product of the capacitance of the condensors and the total resistance. If there is a particular quantity of heat or rate of heat supply which causes the graphite in the vicinity of the constriction to flow or melt, thereby increasing the contact area, for any one compact there will be a particular current at which this occurs if all the contact points have the same constriction resistance.

Since the majority of the decrease of resistance versus voltage curves show a point at which the resistance decreased sharply it would appear that the above suggestion is substantially correct.

The flash sintering curves for natural graphite are somewhat different to those found for artificial graphite powder. This is to be expected. With natural graphite the particles are flat and not spherical and the contacts are likely to be quite different from those of the artificial material. Again, because of their flat shape and appreciable size, the type of contact between flakes might be expected to show more variation than was apparent with the very small particles of artificial graphite powder. A flake lying sideways on its neighbour would be likely to have contacts of different dimensions than those existing between two flakes lying flat one on top of the other. This irregularity in packing would also affect measurement of specific conductance. The current will flow preferentially along the hexagon planes, i.e. in the direction of the longest flake dimension, and any two flakes lying end to end will provide a low resistance path. If two flakes lying end to end or with the edge of one touching the face of the other are considered as defects in packing, perfect packing being the case when layers of flakes lie flat on top of each other, the number of defects in any two compacts having the same column height may not be the same. This is because of the size of the flakes. For the number of defects in each compact to be the same the flakes would require to be very small so that a statistical distribution of defects could be achieved. Fig. 16 shows the results of a series of resistance measurement made on different column heights of natural flake graphite. The values of resistance obtainedbear no relation to one another. This is

considered to be due to variations in packing of the type described above.

Such variation could lead to variation in contact areas and therefore the constriction resistance of the contacts would not all be the same. The current required to produce flow or melting, following the argument outlined above would then be different for some contacts. A high resistance contact, provided that it lay in the path of the current would flow or melt at a lower current than a contact of lower resistance, (the heat produced = $i^2R't$ where i = current in amps, R' = resistance in ohms, t = time in secs.)

If the flash sintering curves of natural graphite are studied, it is seen that a sharp turning point in the curves is not usually present and the subsequent curve is often composed of a series of small steps. This suggests that not all the constriction resistances are the same. As the voltage is increased the contact areas grow larger. In the growth of this contact two factors are determinent. The first is the heat released due to the current flowing and the second is the pressure on the contact. If two constriction resistances in series are considered W_1 and W_2 and if W_1 is greater than W_2 due to a smaller circle of contact, the critical current for W_1 will be lower than that for W_2. As the current is increased to the critical current for W_1 and beyond W_1 will decrease. Were if not for the pressure W_1 would be reduced until it equalled W_2, i.e. until they both had the same contact area when they both would flow for the passage of the same current. However, since initially

W_1 is flowing first the point could be reached, just before the contact area of W_1 equalled W_2 where under the influence of pressure the area of W_1 exceeds that of W_2. While the pressure exerted on both W_1 and W_2 is about the same, since the yield temperature of W_1 has been attained, the contact area of W_1 could increase beyond that of W_2. Further increase of current brings W_2 to the yield temperature and it flows. The overall resistance would decrease but the slope of the resistance decrease versus voltage curve would change since what is happening is not only the uniform increase of the contact area of W_1, but also that of W_2 which when it starts to flow is smaller than W_1. Such a mechanism could be responsible for the small steps observed in the flash sintering curves of natural graphite. Figs. 34, 35, 36, 37 are a good example of this. Another possible explanation is a "shunt" effect. The powder represents a system of parallel resistances. If some of the branches had higher resistances than others the current would travel preferentially along the low resistance path. Even for the low resistances, however, a critical current would be reached when the contacts would flow. This would account for the sharp decrease of resistance observed at a particular voltage. As the voltage increased these contacts would continue to grow but the current through the high resistances in parallel would also increase. It would still not be as great as that along the low resistance path but the critical current would be lower. Thus when the critical current in the high resistance path was reached there would be flow and a further decrease of resistance leading to a change in slope of the curve.

The Plateau.

As the radius of contact increases, the resistance decreases. To increase the radius from r to $r + \Delta r$ a volume $\frac{4}{3}\pi (r + \Delta r)^3$ must be melted, the region of constriction being a sphere the centre of which is the centre of the contact area. Thus it requires progressively more energy to produce a given increase in radius and subsequent decrease in resistance as the contact area grows. This would lead to the plateau effect observed. When it was possible to increase the voltage beyond the plateau it sometimes happened that the resistance increased again. This effect could not be systematically examined because the condensors could not be charged above 1150 volts. If the plateau occurred well within the range of the condensors, e.g. about 500 volts, the resistance for the compact which showed a plateau effect at this voltage was so low that currents greater than plateau currents caused a discharge which occasionally shattered the resistance cell.

The increase in resistance frequently observed at voltages higher than plateau voltages (fig. 37) could be due to physical scattering of the particles by the discharge or to the volatillisation of carbon giving a non-graphitic carbon deposit on the surface of the particles. After these high voltages had been applied a black deposit was found firmly embedded in the glass walls of the cell.

TEMPERATURE DISTRIBUTION IN THE NEIGHBOURHOOD OF THE CONTACTS BETWEEN SPHERES.

In Chapter 4, following Strout (39), a contact between two graphite spheres was associated with a smaller sphere whose diameter was the contact diamater, Fig. 12. It was shown that the decrease of electrical resistance observed on flash sintering could be explained in terms of an increased contact area. In this section as estimate is made of the temperature distribution around each contact considering the energy available.

For any particular temperature distribution to be attained, the energy required by it must be supplied within a certain time, which depends upon the thermal conductivity, specific heat and density of the material. This is because heat is being conducted away from the hottest point and if the rate of cooling is greater than the rate of heating the temperature at the heat source must fall. This in considering Joule heating by means of condensor discharges it is not the total amount of energy supplied but rather the rate at which it is supplied which is important.

If, after a condensor discharge the existing contact radius increases from r_1 to r_2, a volume $\frac{4}{3} \pi r^3_2$ must melt or flow. The initial contact radius r_1 may be ignored and an estimate of r_2 made from a knowledge of the energy available and that required to raise a given mass of graphite to a temperature when melting or flow might be anticipated. This value of the contact radius calculated purely from energetic considerations may then be compared with the value arrived at from electrical resistance measurements.

The temperature distribution throughout a sphere when its surface temperature is changed suddenly to a different temperature can be related to $\frac{Kt}{r^2}$ where "K" is the diffusivity of the material and is equal to the thermal conductivity divided by the product of specific heat and density; "t" is the time in seconds after the sudden change in surface temperature and "r" is the radius of the sphere.
If "Ta" is the temperature at any point within the sphere, "Tm" the new temperature of the surface and "To" the original uniform temperature, the relationship is

$$\frac{Ta - To}{Tm - To} = \frac{2}{\pi} \cdot \sum_{m=1}^{m=\infty} \frac{\frac{1}{a} \sin \frac{m\pi a}{r}}{m(-1)^{m+1}} \cdot e^{-\frac{Km^2 \pi^2}{r^2} \cdot t}$$

where "m" is any integer and "a" is any radius inside the sphere. Williamson and Adams (50) provide a table giving values of $\frac{Ta - To}{Tm - To}$ for different distances from the centre of the sphere and for different values of $\frac{Kt}{r^2}$.
In this case these authors consider the sphere is at a uniformly high temperature and is suddenly cooled by plunging into an ice bath. The Williamson and Adams Table is reproduced below.

TABLE IX

Values of $\frac{Ta - To}{Tm - To}$

$\frac{a}{r}$	$\frac{Kt}{r^2}$								
	0.0000	0.004	0.0160	0.0360	0.0640	0.100	0.1960	0.2560	0.400
0.00	1.000	1.000	1.000	0.9943	0.9103	0.7071	0.2881	0.1598	0.0386
0.25	1.000	1.000	0.9997	0.979	0.8577	0.6466	0.2596	0.1439	0.0347
0.33	1.000	1.000	0.9994	0.9611	0.8133	0.6005	0.2386	0.1321	0.0319
0.50	1.000	1.000	0.9896	0.8752	0.6755	0.4745	0.1840	0.1018	0.0246
0.66	1.000	0.9997	0.9063	0.6788	0.4727	0.3162	0.1197	0.0661	0.0160
0.75	1.000	0.9931	0.7921	0.5312	0.3537	0.2319	0.0869	0.0480	0.0116
0.95	1.000	0.3935	0.1791	0.1030	0.0644	0.0411	0.0152	0.0084	0.0020
1.0	1.000	0.0000	0.0000	0.0000	0.0000	0.0000	0.0000	0.0000	0.0000

This table may be used for a sphere of any material provided the diffusivity and radius are known.

For the case where the sphere is heated suddenly from the outside, the above values of $\frac{Ta - To}{Tm - To}$ should be subtracted from unity, e.g. considering the case when $\frac{Kt}{r^2} = 0.036$

$\frac{a}{r}$	$\frac{Kt}{r^2}$ = 0.036
0.00	0.0037
0.25	0.021
0.33	0.0389
0.50	0.1248
0.66	0.3212
0.75	0.4688
0.95	0.8970
1.0	1.0

These are the figures used by Copp and Ubbelohde (51) in considering the heating of spheres by a hot gas. To adjust these figures to heating from the centre of the sphere towards the ourside, the values of $\frac{a}{r}$ should also be subtracted from unity. Thus considering again the temperature distribution at $\frac{Kt}{r^2} = 0.036$

$\frac{a}{r}$	$\frac{Kt}{r^2}$ = 0.036
1.0	0.0057
0.75	0.0210
0.67	0.0389
0.50	0.1248
0.34	0.3212
0.25	0.4688
0.05	0.8970
0.00	1.000

In calculating $\frac{Kt}{r^2}$, 'K' the diffusivity, given as $\frac{k}{\sigma d}$ where k K = thermal conductivity 'σ' = specific heat and 'd' the density, was equal to $\frac{0.3 \text{ cal/}}{0.185 \times 2.0} = 0.81$ cal/sec. The density determined by flotation was 2.0 g./cc, the specific heat as 0.185 cals/g. (52) and the thermal conductivity 0.3 cal/cm/cm°C/sec. (53). 'r' the radius of the contact sphere was taken as its limiting value, 2×10^{-3}cm., i.e. the radius of a single particle. Different values of $\frac{Kt}{r^2}$ were obtained by multiplying by different time intervals t. Thus when $t = 5 \times 10^{-8}$ secs. $\frac{Kt}{r^2} = 0.01$

$t = 1 \times 10^{-7}$ " " = 0.02

$t = 1 \times 10^{-6}$ " " = 0.20

etc.

Fig. 47.

The curves represent the temperatures at different points throughout a sphere when the centre has been raised instantaneously to T_m °C. With the radius of the sphere as r the temperature distribution is given for various radii (fractions of r) as a function of $\frac{Kt}{r^2}$. Since for any one material $\frac{K}{r^2}$ is constant the curves represent the temperature attained at points throughout the sphere as a function of time.

$K = \left(\frac{\text{thermal conductivity}}{\text{specific heat x density}}\right)$

r = radius of sphere

t = time

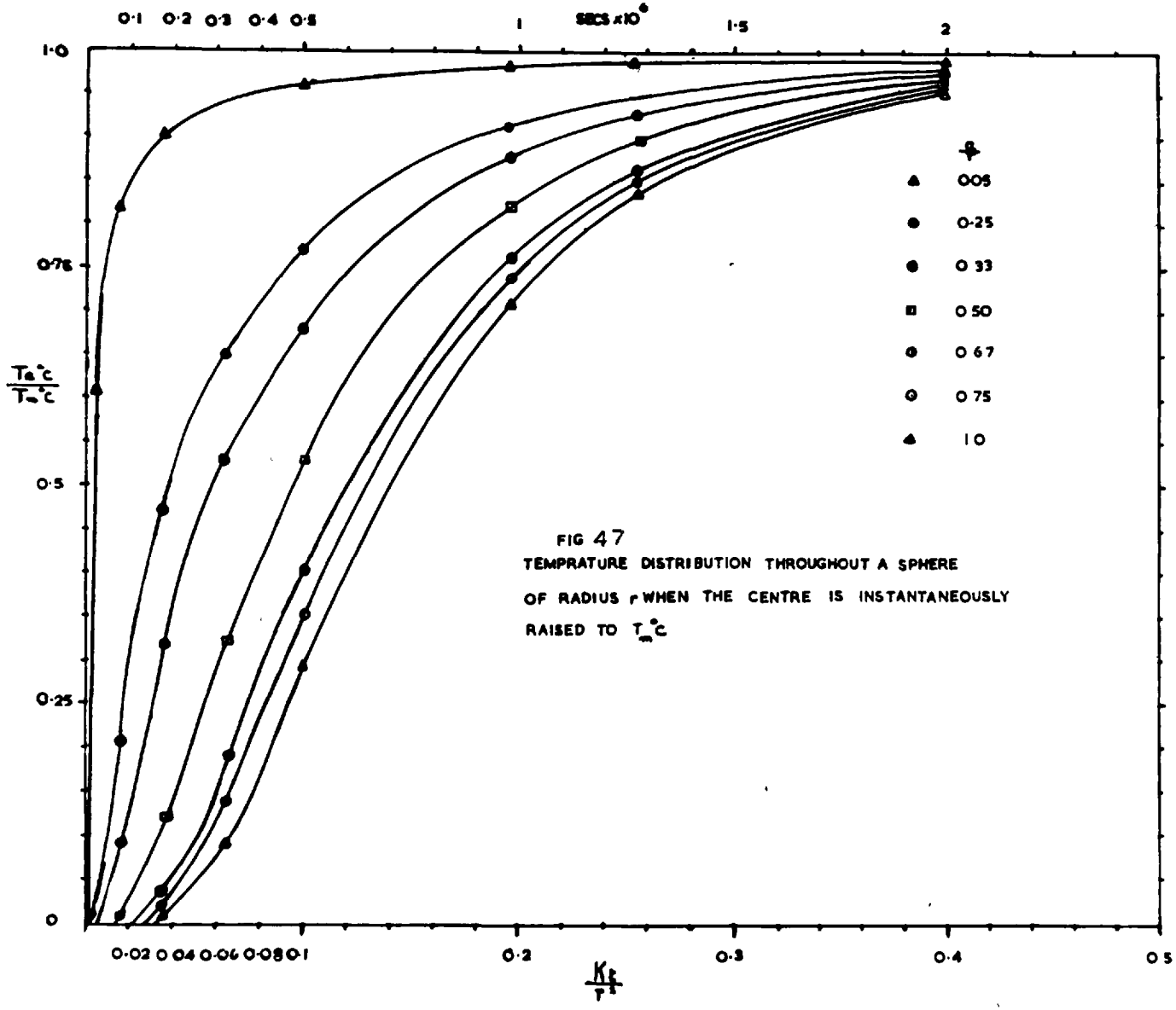


FIG 47

TEMPRATURE DISTRIBUTION THROUGHOUT A SPHERE OF RADIUS r WHEN THE CENTRE IS INSTANTANEOUSLY RAISED TO T_m°C

Values of $\frac{Ta - To}{Tm - To}$ where Tm is the temperature to which the centre of the contact sphere is raised, Ta is the temperature at any other point and To is the original uniform temperature, are plotted against $\frac{Kt}{r^2}$ in Fig. 47.

Surface flow of graphite in the powder compacts.

Little is known about the melting processes of graphite. Melting points of 3800°K (54) and 4200°K (55) have been reported and a triple point is said to exist at 4000°K and at pressures of 105 kg./cm.^{2} (56). While the pressure transmitted by the electrode to the powder in the present work was only 13.5 kg./cm.^{2}, the pressure on contact sites within the compact must have been considerably greater. An approximate calculation of the pressure is as follows.

From electrical resistance measurements the contact radius before flash sintering was 1.44×10^{-4}cm. Considering perfect open packing as was suggested for the shortest column height, the total number of contacts per unit volume was 6.67×10^3, unit volume being the area of the cell muptiplied by the diameter of one particle. The effective area across which pressure is transmitted is then

$$6.67 \times 10^3 \times (1.44 \times 10^{-4})^2 = 4.35 \times 10^{-4} \text{sq. cm.}$$

The area of the cell was 0.084 sq. cm. and the load exerted on this area a pressure of 13.5 kg./cm.^{2} The same load on 4.35×10^{-4} sq. cm. will then exert a pressure of 2,600 kg./cm.^{2} For greater column heights of material, the number of contacts/unit volume decreased, so that as the

column height increased, the pressure across the contact area also increased.

If pressures of this order are present in the compact, then provided there is sufficient heat input melting will occur before vaporisation, taking the Basset figure of 105 kg./cm.^{2} as the lower limit necessary to prevent direct vaporisation.

The temperature at which plastic flow of graphite could occur may be appreciably below the melting point because of the considerable pressures which exist within the compact. Such flow is likely to involve polyphenyl-like groupe of hexagons moving into new positions and then interlocking. By this means defects on the surface could be annealed.

In the following calculations, the centre of the contact mass is considered to be raised to 4000°C (Tm). The temperature at any other point (Ta) is then estimated from Fig. 47.)

Fig. 48.

The heat required for any particular temperature distribution defined by $\frac{Kt}{r^2}$ is obtained by first estimating the temperatures T_a at various radii from the centre for the given value of $\frac{Kt}{r^2}$ from Fig. 47 and then plotting $(T_a - T_o)$ where T_o is the original temperature against $(\frac{a}{r})^3$, "a" being measured as a fraction of "r". The heat required for 1 gram of spheres of radius "r" is then given by the area under the curve times the specific heat of the material.

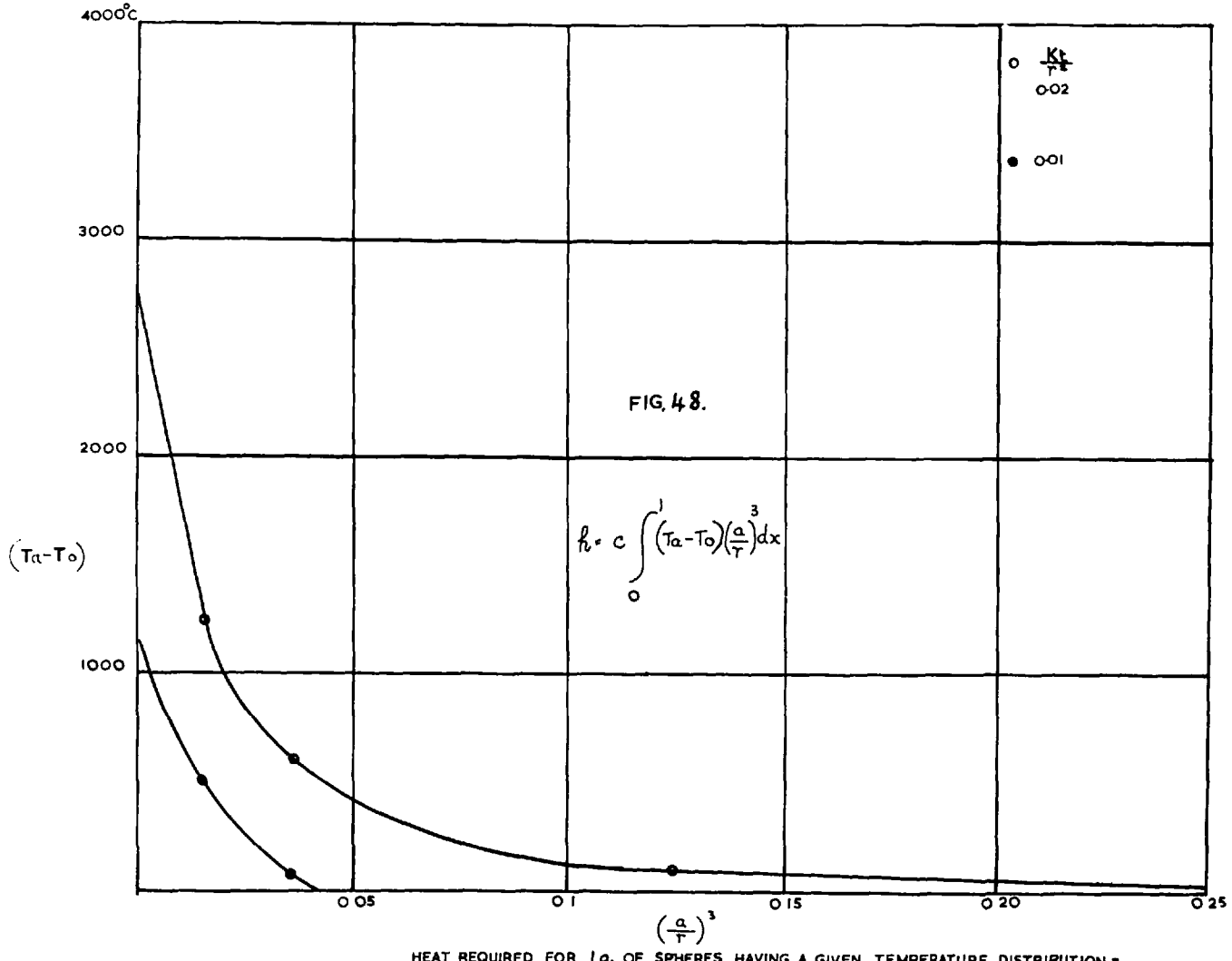


FIG. 48.

HEAT REQUIRED FOR 1g OF SPHERES HAVING A GIVEN TEMPERATURE DISTRIBUTION = AREA UNDER THE CURVE X SPECIFIC HEAT

HEAT REQUIREMENTS FOR PARTICULAR TEMPERATURE DISTRIBUTIONS.

The heat required for 1 g. of spheres having the temperature distribution defined by any given value of $\frac{Kt}{r^2}$ is

$$h = c \int_0^1 (T_a - T_o) \left(\frac{a}{r}\right)^3 dx$$

Where 'c' is the specific heat, T_a the temperature at radius 'a' T_o the original uniform temperature of the sphere (30°C) and 'r' its overall radius in cm. In Fig. 48 $T_a - T_o$ is plotted against $\left(\frac{a}{r}\right)^3$. The area under the curve multiplied by the specific heat given the amount of heat in calories required for 1 g. of spheres of radius 2×10^{-3} cm. to have any particular temperature distribution. In Fig. 48 the curves are drawn for $\frac{Kt}{r^2} = 0.01$ and 0.02.

The values of the heat required are

TABLE X

	$\frac{Kt}{r^2}$ 0.01	$\frac{Kt}{r^2}$ 0.02
Heat required for 1 g.	3.28 cals.	13.15 cals.

The Contact Mass.

Since only particles in electrical contact may be heated electrically, the mass of graphite to be considered is the mass of the total number of electrical contacts (the mass of a contact is the mass of two half particles, i.e. the mass of a single particle, the volume of a contact is, however, larger than that of a single particle - see

Fig. 46. It is because of volume considerations that a contact is described in terms of two half-particles.)

The total number of contacts in the different compacts was calculated by multiplying the number of contacts/unit volume - Table VII by the ratio of total volume to unit volume, e.g.

for column height 0.19 cm.

total volume = 0.084 sq. cm. x 0.19 cm.

(area of cell) col. ht.

unit volume = 0.084 sq. cm. x 4×10^{-3} cm.

(diameter of one particle)

number of contacts/ unit volume = 6.67×10^{-3} - Table VII

Total number of contacts = $\frac{6.67 \times 10^{3} \times 0.084 \times 0.19}{0.084 \times 4 \times 10^{-3}}$

= 3.18×10^{5}

This number was multiplied by the mass of one sphere of radius 2×10^{-3} cm., taking the density of graphite as 2.0 g/cm.^{3} to give the total "contact mass". The "contact masses" of the series of untamped columns of powder are given in Table XI.

TABLE XI

Column height	Total number of contacts	Contact Mass
0.19	3.18×10^5	2.1×10^{-2} g.
0.34	3.28×10^5	2.2×10^{-2}
0.66	4.36×10^5	2.92×10^{-2}
1.0	5.55×10^5	3.68×10^{-2}
1.69	7.1×10^5	4.75×10^{-2}

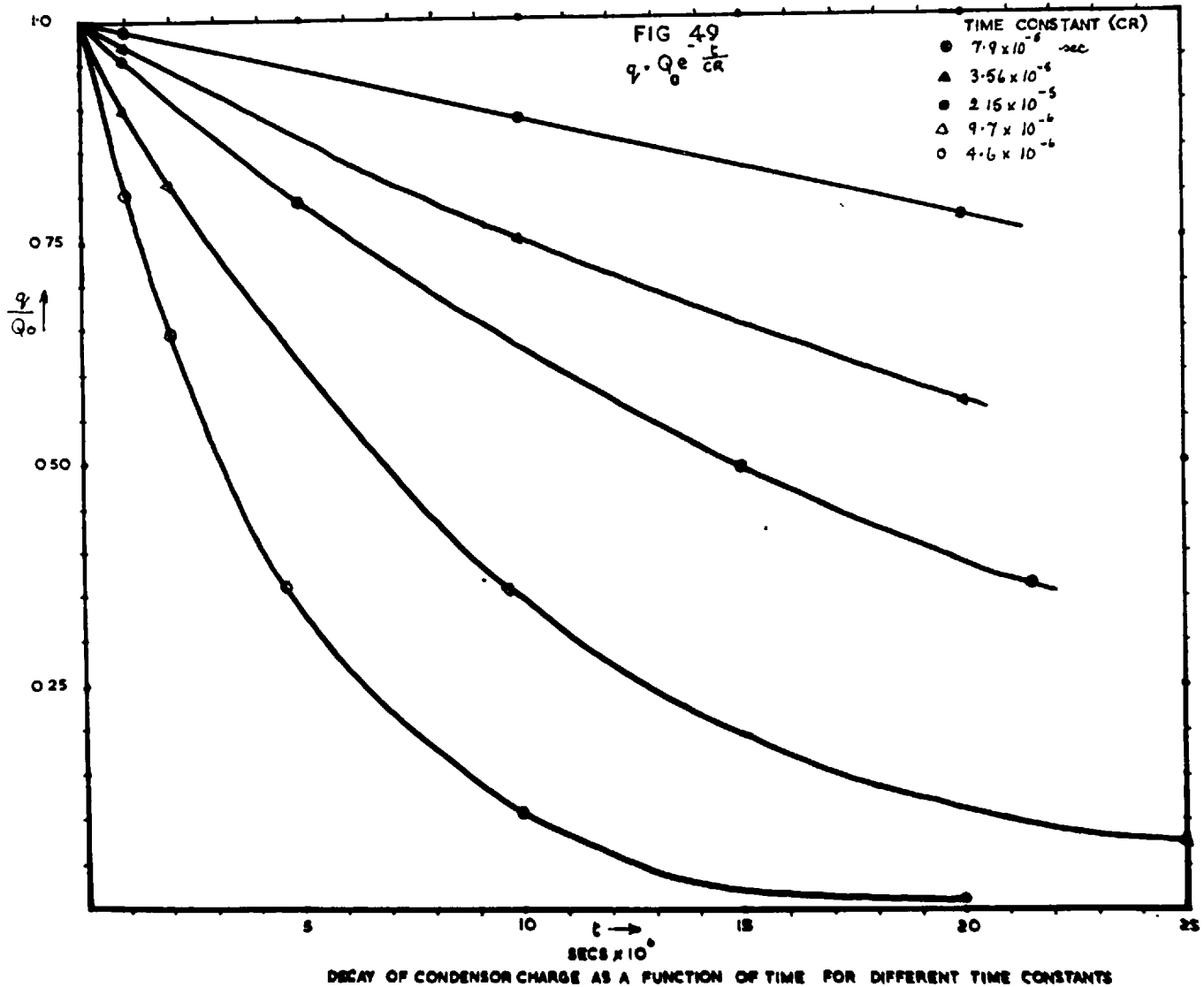
The heat required for 1 g. of graphite spheres having the temperature distributiond defined by $\frac{Kt}{r^2} = 0.01$ and 0.02 was 3.28 cals. and 13.15 cals. respectively.

The heat required for each contact mass having these temperature distributions is shown in Table XII.

TABLE XII

Contact Mass	Heat required $\frac{Kt}{r^2} = 0.01$	Heat required $\frac{Kt}{r^2} = 0.02$
2.1×10^{-2} g.	0.068 cals.	0.27 cals
2.2×10^{-2}	0.072 "	0.29 "
2.92×10^{-2}	0.096 "	0.38 "
3.68×10^{-2}	0.121 "	0.48 "
4.75×10^{-2}	0.156 "	0.62 "

Since $t = 5 \times 10^{-8}$ and 1×10^{-7} sec. when $\frac{Kt}{r^2} = 0.01$ and 0.02 respectively, if either of these temperature distributions is to be attained the above quantities of heat must be released in 5×10^{-8} and 1×10^{-7} secs. respectively.



DECAY OF CONDENSOR CHARGE AS A FUNCTION OF TIME FOR DIFFERENT TIME CONSTANTS

CALCULATIONS OF ENERGIES OBTAINED FROM CONDENSOR DISCHARGES.

In the discharge of a condensor, the charge of the condensor decays exponentially with time according to the equation $q = Q_o e^{\frac{-t}{CR}}$

where Q_o = initial charge

q = charge after time t secs.

CR = time constant, i.e. capacity in Farads multiplied by the total electrical resistance of the circuit, (57).

The capacity of the condensor used was 100 μF and when the charging voltage was 1000 volts $Q_o = CV = 3 \times 10^8$ E.S.U.

The Energy E_o of the charge in ergs is

$$E_o = \tfrac{1}{2} Q_o V$$

For $Q_o = 3 \times 10^8$ E.S.U. and V = 1000 volts

$$E_o = \frac{10^9}{2} \text{ergs} = \frac{10^9}{2 \times 4.2 \times 10^7} \text{ calories} = \underline{11.93 \text{ calories}}.$$

The Quantity of Heat Available.

The energies for the maximum voltages employed were:-

Column height cm.	Maximum Voltage volts	Energy cals.
0.19	475	2.7 cals.
0.34	650	5.05 "
0.66	870	8.6 "
1.0	1050	13.2 "
1.69	1100	14.45 "

TABLE XIII

Rate of heating.

The rate at which heat is liberated depends both upon the energy of the discharge and the time constant (CR) of the circuit. For each of the graphite columns the resistance was different and therefore the time constant was also different. The amount of heat liberated after different time intervals can be calculated from $E = E_o e^{\frac{-t}{CR}}$

where $E_o = \frac{1}{2} Q_o V$ as before and E is the energy remaining in the condensor after t secs. The energy liberated in t secs. is therefore $E_o - E$ calories. Fig. 49 shows the fraction of energy remaining in the condensors as a function of time for different time constants. Table XIV gives the heat supplied to the different compacts in 5×10^{-8} secs., 1×10^{-7} secs. and 1×10^{-6} secs.

TABLE XIV

Column height cm.	Time Constant (CR)	Heat supplied in 5×10^{-8} cal.	1×10^{-7} cal.	1×10^{-6} secs. cal.
0.19	4.6×10^{-6} sec.	0.04	0.067	0.52
0.34	9.7×10^{-6} "	0.025	0.05	0.48
0.66	2.15×10^{-5} "	0.019	0.038	0.38
1.0	3.56×10^{-5} "	0.017	0.034	0.34
1.69	7.9×10^{-5} "	0.009	0.018	0.18

Table XV summarises the calculations so far.

TABLE XV

Column height cm.	Total number of contacts	Total contact mass g.	Heat required (cals) for temperature distribution		Heat supplied (cals) in		
			$\frac{Kt}{r^2} = 0.01$ a	$\frac{Kt}{r^2} = 0.02$ b	5×10^{-8} secs.	1×10^{-7} secs.	1×10^{-6} secs.
0.19	3.18×10^5	2.1×10^{-2}	0.068	0.27	0.04	0.067	0.52
0.34	3.28×10^5	2.2×10^{-2}	0.072	0.29	0.025	0.05	0.48
0.66	4.36×10^5	2.92×10^{-2}	0.096	0.38	0.019	0.038	0.38
1.0	5.55×10^5	3.68×10^{-2}	0.121	0.48	0.017	0.034	0.34
1.69	7.1×10^5	4.75×10^{-2}	0.156	0.62	0.009	0.018	0.18

N.B. Distribution "a" must be attained in 5×10^{-8} secs. and "b" in 1×10^{-7} secs.

The preceding calculations of temperature distribution were performed on the basis of graphite having a thermal conductivity of 0.3 cals. (cm./cm.^{2}/$^\circ$C/sec.) It is known, however, that the thermal conductivity of graphite decreases with increasing temperature. At 1000°C it is approximately one third of its room temperature value, (58). If the average thermal conductivity is taken as 0.1 and not 0.3 cals./cm/cm^2/$^\circ$C/sec. the time taken for any particular temperature distribution to be attained will be three times as long.

$$\left(K = \frac{\text{thermal conductivity}}{\text{specific heat} \times \text{density}}\right)$$

Previously $\frac{Kt}{r^2}$ = 0.01 when $t = 5 \times 10^{-8}$ secs.

and $\frac{Kt}{r^2}$ = 0.02 when $t = 1 \times 10^{-7}$ secs.

on the basis of a reduced thermal conductivity

$\frac{Kt}{r^2}$ = 0.01 when $t = 1.5 \times 10^{-7}$ secs.

and $\frac{Kt}{r^2}$ = 0.02 when $t = 3 \times 10^{-7}$ secs.

The effect of including this smaller value of the thermal conductivity in the calculations is then to increase the time necessary for any particular temperature distribution to build up. Thus more time is given to the condensors to discharge the requisite amount of energy into the system. Bearing in mind the condition that distribution "a" now requires 1.5×10^{-7} secs. and "b" 3×10^{-7} secs., the energies liberated in this time are shown in Table XVI.

TABLE XVI

Column height	Heat required cals.		Heat supplied in (cals)	
	$\frac{Kt}{r^2}_a$ = 0.01	$\frac{Kt}{r^2}$ = 0.02	1.5×10^{-7}	3×10^{-7} secs.
0.19	0.068	0.27	0.090	0.19
0.34	0.072	0.29	0.074	0.15
0.66	0.096	0.38	0.057	0.11
1.0	0.121	0.48	0.051	0.10
1.69	0.156	0.62	0.027	0.05

ESTIMATION OF THE CONTACT RADIUS AFTER FLASH SINTERING FROM TEMPERATURE DISTRIBUTION CALCULATIONS AND ITS COMPARISON WITH THE VALUE OBTAINED FROM ELECTRICAL RESISTANCE MEASUREMENTS.

Two temperature distributions have been considered, one defined by $\frac{Kt}{r^2} = 0.01$ (a) and by $\frac{Kt}{r^2} = 0.02$ (b). From Table XVI it can be seen that for the first two column heights a temperature distribution intermediate between "a" and "b" can be achieved. For the remaining three column heights insufficient energy is released within the requisite time to attain either of these distributions. The first point which emerges then is that the compact 0.19 cm. in height can attain a distribution of higher temperatures than any of the other compacts and that the trend is to lower temperatures with increasing column height. Thus if high temperatures cause flow and this increases the contact area after flash sintering the contact radii should decrease with increasing column height. The contact radii obtained from electrical resistance measurements with the exception of those relating to column heights 0.66 cm. and 1.0 cm. showed the same trend. The values were (from Table VIII).

Column height	Contact radii calculated from electrical resistance after flash sintering.
0.19	2.3×10^{-4} cm.
0.34	1.92×10^{-4} cm.
0.66	1.84×10^{-4} cm.
1.0	1.89×10^{-4} cm.
1.69	1.74×10^{-4} cm.

It can been seen that the radii for column heights 0.66 and 1.0 cm. are not very different so that their exception to the trend of decreasing contact radii with increasing column height is not very marked. In this connection it is significant that the rate of heating of these compacts was nearly the same. (See Tables XV and XVI).

To obtain an estimate of the contact radii from the temperature distribution calculations, assume that for the shortest column height, 0.19 cm., distribution "b" ($\frac{Kt}{r^2} = 0.02$) was attained. (The heat required for this distribution was 0.27 cals. in 3×10^{-7} secs. and in this time 0.19 cals. were delivered). From Fig. 47 it can be seen that at a distance 0.05 r from the centre of the contact the temperature was 3,500°C (assuming T_m to be 4000°C). "r" the limiting value of the contact radius was 2×10^{-3} cm., therefore 0.05 r corresponds to 1×10^{-4} cm.

The temperature at a distance 0.1 r from the centre of the contact for the same distribution is not shown on this figure but it cab ne estimated from Fig. as approximately 2,600°C (for 0.1 r, $(\frac{a}{r})^3$ is 0.001). 0.1r 0.01r is equivalent to a radius of 2×10^{-4} cm. If softening or melting occurs at a temperature of 2600°C and under the pressures existing in the compact, flow might be expected at this temperature, a new circle of contact of radius 2×10^{-4} cm. could be formed.

The value calculated from electrical resistance measurements after flash sintering was 2.3×10^{-4} cm. for the compact considered

above (0.19 cm. high). In view of the assumptions involved in the calculations, viz. perfect spheres in open packing and 2,600°C as a flow temperature, the fairly close agreement between these contact radii is likely to be fortuitous. However, it is further evidence that the heat supplied by flash sintering is related to a process such as growth of the contact area between particlesand that the rate of heating approximates to that required to produce a contact of the same dimensions as that estimated from electrical resistance measurements.

For the other compacts, the heat input can be seen (Table XVI) to fall more and more below that required for the distribution which was considered to be attained by the shortest compact. Thus the trend of decreasing contact areas with increasing column heights (Table VIII) is confirmed by calculations based on energetic considerations.

Summary of the results of Part I with respect to the nature of graphite surface.

There is no evidence for the presence of an impurity film on the surface of graphite particles which constitutes a barrier to electronic conduction. Intercrystalline boundaries, dislocations, etc. however, will constitute defects and at these defect sites, impurity groups are probably to be found to satisfy what would otherwise be free valencies. In powdering block graphite, valency bonds must be ruptured and the number of impurity defects increased

since the freed valencies will satisfy themselves from the atmosphere. This is reflected in the increased positive thermo-electric power of the powder as compared to block material. Flash sintering slightly reduces the number of impurity defects. This is accomplished not simply by expelling the foreign atom or group. In the latter case the freed valency would have to satisfy itself again from the atmosphere. The fact that the thermo-electric power of the sintered material remains less positive than the pre-sintered powder indicates that some defects have been "annealed". The evidence of electrical resistance measurements and the results of heat transport calculations suggests that a plastic flow process occurs. Plastic flow in which groups of fused hexagons slipped into new positions could anneal impurity or other valence defects by allowing new carbon-carbon bonds to form. High local temperatures would expel the impurity and simultaneous plastic flow allow a few link up to take place.

Surface films and the function of graphite.

The above considerations must be discussed in conjunction with the work of Savage (43) on the lubricating properties of graphite. Savage found that when graphite was heated in vacuo, gases which were mostly water vapour were given off. The graphite was kept under vacuum and subjected to friction experiments and it was found that friction was much higher than normal and that considerable wear of graphite occurred. It was then suggested that the well known

lubrication properties of graphite are due to the presence of films of water molecules rather than to ease of shear between layer planes. Savage's results show that there can be little doubt of the importance of gaseous impurities to the good lubrication properties of graphite. It does not seem likely, however, that these properties are unconnected with the remarkable ease with which graphite shears. No evidence has been found for example, for the presence of surface films on molybdenum disulphide (59). This compound has a layer structure, is easily sheared and rivals graphite in lubricating properties. If an impurity group held at a defect site on a graphite surface is expelled under conditions where the freed valency must remain unsatisfied as in Savage's experiment, and if the graphite is then brought into contact with a clean metal surface, between the unsatisfied valency and the metal electrons a chemical bond could be created. Friction between the two surfaces would then be high since numerous defect sites will exist. Not only friction will be high but wear of graphite should also be heavy. As the surfaces move the defect - metal bond will cause fragmentation of the carbon hexagons which in turn will expose more free valencies.

As described in the Introduction to Part I, if a film between two metal surfaces is to act as a lubricant it must keep both metal surfaces apart. In this connection, water molecules, the major graphite surface impurity, have been reported as having little or no effect on the friction between metal surfaces (37).

By separating the metal surfaces the lubricant film causes a

marked increase in the electrical contact resistance. In the present work there was no evidence of a surface film increasing the contact resistance and estimates of conduction activation energies emphasised the absence of a current barrier on the graphite surface.

It is suggested that the gaseous impurities, e.g. water vapour which contribute to the lubricating action of graphite do so by satisfying free valencies as defect sites thereby preventing chemical bonding between the metal and graphite surfaces.

Their action would thus be indirect, the main factor in lubrication being the ease of shearing between the carbon layer planes.

CONCLUSION.

Flash sintering reduces the electrical resistance of graphite powders by increasing the contact area between particles. The contact sites are then stabilised and no longer flow under medium pressures. Reproducible measurements of electrical properties can be carried out on such powders after flash sintering and their increased resistance with respect to block material can be accounted for purely in terms of constriction of flow.

On powdering graphite rod in air the thermo-electric power changes from negative to positive values indicating that conduction in such powders is mainly by holes. These are likely to be created by electro-negative defects, e.g. $>C=O$, $>C-OH$ groups bound to broken carbon-carbon bonds and other such groups not bonded by primary valence forces present on the surface of the particles. These impurities however, do not constitute a closely knit impurity film through which electrical conduction is measurably reduced.

With the proviso that the π band is somewhat depleted, leading to "hole" conduction, the general and well established band theory of graphite can be applied to its powders.

Flash sintering is a technique which is applicable to the graphite compounds since only points of high electrical resistance are raised to very high temperatures. This will permit the electrical properties of the compound to be stabilised without causing general decomposition.

PART II

ANISOTROPIC THERMO-ELECTRIC EFFECTS IN GRAPHITE.

CHAPTER 8.

PART II : INTRODUCTION.

Crystallographic anistropy may lead to anistropy in physical properties.

Anistropic electrical resistance.

Bismuth has a hexagonal structure and a specific resistance normal to the basal plane between 109 and 139 times that measured in the plane (60). Antimony also shows anistropy of electrical resistance but of a very special kind. It is the only hexagonal crystal yet measured in which the resistance normal to the basal plane is less than that measured along it. The effect of pressure on the electrical resistance is to make antimony more "normal" and at 1200 $kg./cm^2$ and $75^{\circ}C$ the resistance has become greater normal to the plane than parallel to it. Where Bismuth is concerned, however, the effect of pressure is to increase the ratio of specific resistances. At atmospheric pressure the ratio is 1.275 and at 1200 $kg./cm.^2$ it is 1.48. From one point of view the accentuation by pressure of the excess of resistance for flow perpendicular to the basal plane is not to be expected because one explanation for this excess has been that the cleavage plane constitutes a type of flaw in the crystal which makes the passage of current more difficult. Increase of pressure would then be expected to diminish the separation of the cleavage planes and hence decrease the resistance (60). However pressure will effect the whole crystal and pressure induced changes in interatomic distances will bring different elastic

forces into play changing the Debye temperature. The phonon distribution will thus be altered and hence also the electrical resistance [electrical resistance in a metal can be explained largely in terms of electron-phonon interactions, phonons being the quanta associated with lattice waves (61)]. The direction in which the electrical resistance should alter along any particular crystal axis however, is not obvious.

The specific resistance of graphite along the basal plane is only about 3.9×10^{-5} ohm. cm. (62). In a direction normal to this plane values as high as one ohm. cm. have been reported. It will be appreciated that measurements of specific resistance in a direction normal to the basal plane is very difficult. Single crystals are rare and along the hexagonal axis, thicknesses are measured in fractions of a millimetre. Again, the presence of defects such as screw dislocations will influence the measurement profoundly, (63).

Temperature variation of electrical resistance.

Antimony is the only metal yet measured which shows an anisotropic temperature co-efficient of resistance. Only the magnitude of the co-efficients, however, are different. The average co-efficient along the basal plane in the temperature range 0 - 100°C is 0.0057 and for flow across this plane the value is 0.0048, the resistances in both cases increasing with temperature.

In the case of graphite, both the order of magnitude of the temperature co-efficient and its sign have been reported as different. Along the basal plane the value is given as $+9 \times 10^{-3}$ °C while normal to this

plane the value is -4×10^{-2} °C (64). Thus the material should behave as a metal within the plane and a semi-conductor normal to it.

Values of the physical properties of graphite reported to be anisotropic are shown in Table XVII.

TABLE XVII

	basal plane	hexagonal axis	Ref.
Thermal Expansion deg. C^{-1} 10^{-6}	6.6	26.0	64
Specific resistance ohm. cm.	3.9×10^{-5}	1.0	"
Thermal Conductivity watt $cm.^{-1} {}^{o}C^{-1}$	4.0	0.8	"
Hardness (Moh's scale)	6.5	0.5	"
Magnetic Susceptibility 10^{-6} e.m.u/g.	- 0.5	- 28.5	"

Magnetoresistance.

The electrical resistivity q of a metal is observed to increase by Δ q when the specimen is measured in a magnetic field H.

$$\frac{\Delta q}{q} = aH^2$$

"a" is a different constant for each metal.

A transverse effect is measured with the field at right angles to the direction of current flow and the longitudinal effect is measured with the field parallel to it. In the case of cadmium the longitudinal effect is about half the transverse effect, (65). The magnetoresistance effect is greater in semiconductors than in metals. It depence not only on the relative orientations of the current and magnetic field, but also on the direction in which the current flows through the crystal.

This dependance of the magnetoresistance on crystal orientation relative to the magnetic field can be explained in terms of variations in the effective mass of the current carriers. The effective mass m* (defined in Chapter I) is not, like ordinary mass, a scalar quantity and in an applied electric or magnetic field will have a different value for each component of acceleration (61). In Chapter I only a one dimensional treatment is given. Ref. (61) gives a more complete treatment. Values of effective mass can be obtained directly from cyclotron resonance experiments. In this way it has been shown that in the case of Silicon and Germanium m* is very anisotropic for both electrons and holes.

	conduction electrons		conduction holes	
	m^*l/m	m^*t/m	m_1^*/m	m_2^*/m
Si	0.97 ± 0.02	0.19 ± 0.01	0.16	0.52
Ge	1.58 ± 0.04	0.082 ± 0.001	0.042	0.34

m is the mass of a free electron

m^*_l, m^*_t } the value of m in any crystal orientation can be obtained in terms of these two quantities.

m^*_1, m^*_2 } these are the values averaged over different crystal orientations.

The above values are from reference (66).

The ratio of effective mass to rest mass of a free electron has been measured for both electrons and holes in graphite as 0.03 for electrons and 0.06 for holes (63). The dependance of effective mass on crystal

orientation, however, does not appear to have been investigated.

Thermo-electric power in anisotropic media.

An intrinsic semi-conductor is a two carrier system in which the number of electrons in the condiction band is equal to the number of holes in the valence band. An equation for the thermo-electric power, S, in such a system has been derived by Tauc, (67).

$$S = -\frac{k}{e}\left\{\frac{c-1}{c+1}\cdot\frac{E_G}{2kT} + \frac{2(c-1)}{c+1} + \frac{3}{4}\ln\left(\frac{m_n}{m_p}\right)\right\}$$

where k is Boltzmann's constant

c is the ratio of electron to hole mobility

m_n and m_p are the effective masses of electrons and holes respectively.

E_G is the forbidden gap width

e is the electronic charge

T is the absolute temperature

The above equation was derived assuming classical statistics to be applicable. This, however, may not be true when the gap width is of the order of kT at temperatures well below the melting point. With such a narrow gap width the material may become degenerate and Fermi-Dirac statistics may have to be employed. The above equation illustrates how sensitive is the thermo-electric power of intrinsic semi-conductors to changes in the mobilities of the charge carriers.

It has been found that in anisotropic bodies, the Peltier effect can occur in homogeneous regions if there are junctions of differently directed crystals, (68). Johnson (69) points out that in a material of

hexagonal structure such as tellurium, the effective mass and mobility ratio have one set of values associated with motion parallel to the a axis and another set of values associated with motion in the plane perpendicular to the a axis. Considering the thermo-electric power of an intrinsic semi-conductor as represented by the equation given above, if the term $\frac{3}{4}\ln \frac{m_n}{m_p}$ is neglected, the ratio of thermo-electric power measured parallel and perpendicular to the a axis is given by

$$\frac{S_{11}}{S_{\perp}} = \frac{(C_{11} - 1)(C_{\perp} + 1)}{(C_{11} + 1)(C_{\perp} + 1)}$$

where C_{11} and $C_{\perp}$ are the ratios of electron to hole mobility as measured parallel and perpendicular to the a axis respectively.

In the following part of this work thermo-electric power anisotropy in graphite is demonstrated. Because of this anisotropy it was possible to construct a thermocouple from graphite in its two main crystallographic orientations. These were in the nature of pioneering experiments. As a development of this work a less primitive graphite thermocouple embodying the same principle has since been constructed by Ubbelohde, Blackman and Dundas, (70).

CHAPTER 9

PART II : EXPERIMENTAL

Preparation of Materials.

Natural Ceylon graphite was obtained through the courtesy of the Morgan Crucible Company. The artificial graphite was obtained from A.E.R.E. Harwell. A block of natural graphite was chosen in which the cleavage plane was easy to distinguish. This was apparant by visible "strata" lines running along the side of the block. By pressing a razor blade gently into the graphite parallel to the strata lines, large flakes could be teased apart. If the same procedure was attempted along a plane perpendicular to this direction, no cleavage occurred and considerable resistance was offered to the blade. When specimens were cut from the block and allowed to stand in bromine vapour most of the swelling occurred in a direction perpendicular to the plane in which the flakes were laid down. Since swelling along the c axis of graphite is known to occur under these conditions and also because of the other observations noted above, the strata lines of the block were considered to lie along the basal plane of the graphite structure, consequently the hexagonal axis was taken to be perpendicular to this plane.

Methods of cutting natural graphite.

It was obviously desirable to cut the block graphite as finely as possible. Any distortion of the cut edges would clearly affect the orientation of a particular specimen. Although an instrument

employing a fine jet of diamond dust would probably have been the best cutting tool, such an instrument was not available at the time and other means had to be found. A small hacksaw blade was tried as this was the method used by other workers in cutting orientated pyrolytic graphite (71), but this was not found to give adequate control. The main problems arose in cutting along the hexagonal axis. After penetrating some way into the block the graphite on either side of the cut frequently shivered into small brick-like specimens. Cutting in the other direction was much simpler as the graphite cleaved easily. The edges of some specimens cut across the cleavage plane had uneven surfaces and if these surfaces were filed considerable "jarring" of the file occurred. In one case small pieces of the file were found on the graphite surface. This was a striking indication of the hardness of graphite along the basal plane. A razor blade was found to give better control and all the specimens employed were cut in this way. They measured about 1.5 cm. long by about 0.3 cm. square.

Distortion of the cut edges.

As mentioned earlier, cutting could not be achieved without some change in the orientation of the material around the edge of the cut. In an attempt to eliminate this "misorientated" graphite, a specimen was heated very carefully in a stream of oxygen and allowed to glow for a few seconds. It was reasoned that distorted graphite layers would constitute defect sites and oxidation would begin preferentially there: the energy required to remove such defect carbon being less than that required when carbon is part of a more regular arrangement.

In the latter case resonance energy would contribute considerably to its stabilization. The oxidation, however, could not be finely enough controlled. The surface of the whole specimen assumed a sooty texture. However oxidation did serve to accentuate the orientation of the material. After this treatment the lamellae could be seen to be close packed and fairly regular.

Provided the distorted regions of graphite around the cut edges did not assume such thicknesses that an appreciable temperature gradient could exist across them, then no spurious thermal EMF's could arise. It was assumed in the following work that no such spurious effects did in fact occur.

Graphite purity.

Because of the obvious danger of destroying the crystalline order of the samples they could not be chemically purified. Impurities, mostly iron and silica are known to be present in natural graphite and such impurities must have had some effect on the measurements. However, it is believed that an anisotropic thermo-electric effect is clearly demonstrated.

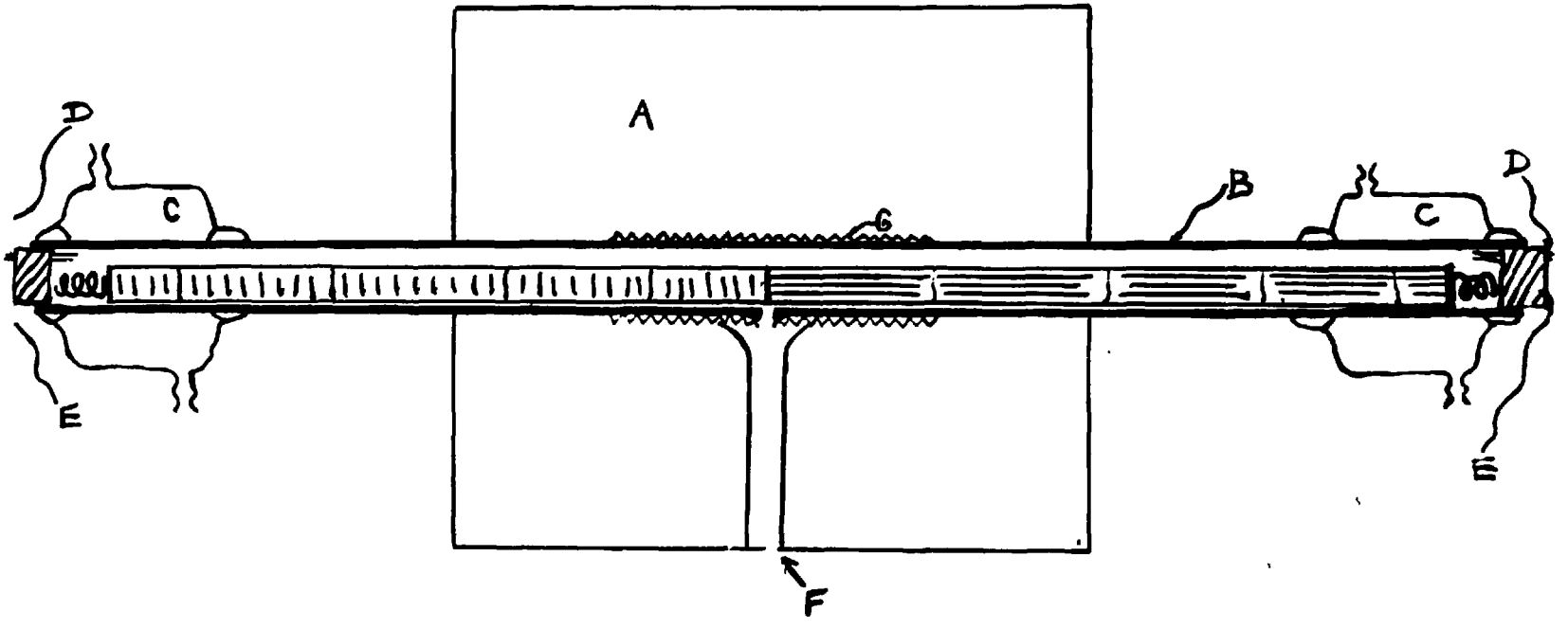


FIG. 50

Procedure.

The thermo-electric power was measured as a function or orientation in the glass cell shown in Fig. 14a. The "Self thermo-EMF" was then determined in the following manner. The "a" and "c" blocks were mounted in electrical contact in impervious tubes of mullite with copper electrodes at the cold junction which were water cooled. Fig. 50 shows the arrangement. 'A' was a ceramic brick which carried the mullite tube 'B'. The "c" versus "a" junction was viewed through a hole 'F' in the mullite tube for pyrometer measurements at high temperature. Temperatures below 1000°C were measured by means of a chromel alumel thermocouple inserted through 'F'. 'C' was a water condensor at each cold junction and the thermal EMF was measured by means of the potential leads 'E' on a Doran poteniometer. An electrical heating coil 'G' provided the heating in experiments up to 700°C. For measurements at high temperatures an oxygen-coal gas flame was employed, since a high temperature electrical furnace of convenient shape was not available at that time. To minimise any risks of diffusion of oxygen or water through the hot mullite the flame impinged on a platinum sheet protected by a coating of alumina. The flame was inserted into 'A' through a hole (not shown) drilled in the brick. B.O.C. white spot nitrogen was admitted as required through 'D'.

CHAPTER 10.

PART II : RESULTS.

Thermal EMF measurements along the main crystallographic axis.

The values obtained for the anisotropic thermo-electric power of graphite showed considerable variation, although the specimens were all cut from the same block of natural graphite. Figs. 51, 52, 53 and 54 show values that were obtained. In each case it is seen that a more positive value was observed along the c axis. Fig. 55 shows the effect with artificial graphite. When it appeared that an anisotropic thermo-electric effect was detectable the junction described in the experimental was constructed.

Results of heating the thermo-junction by an electrical coil.

When the junction was heated electrically to 700°C the results were regular and the straight line graph shown in Fig. 56 was obtained. Good qualitative agreement was found when the above experiment was performed on another set of crystal cut from the same block.

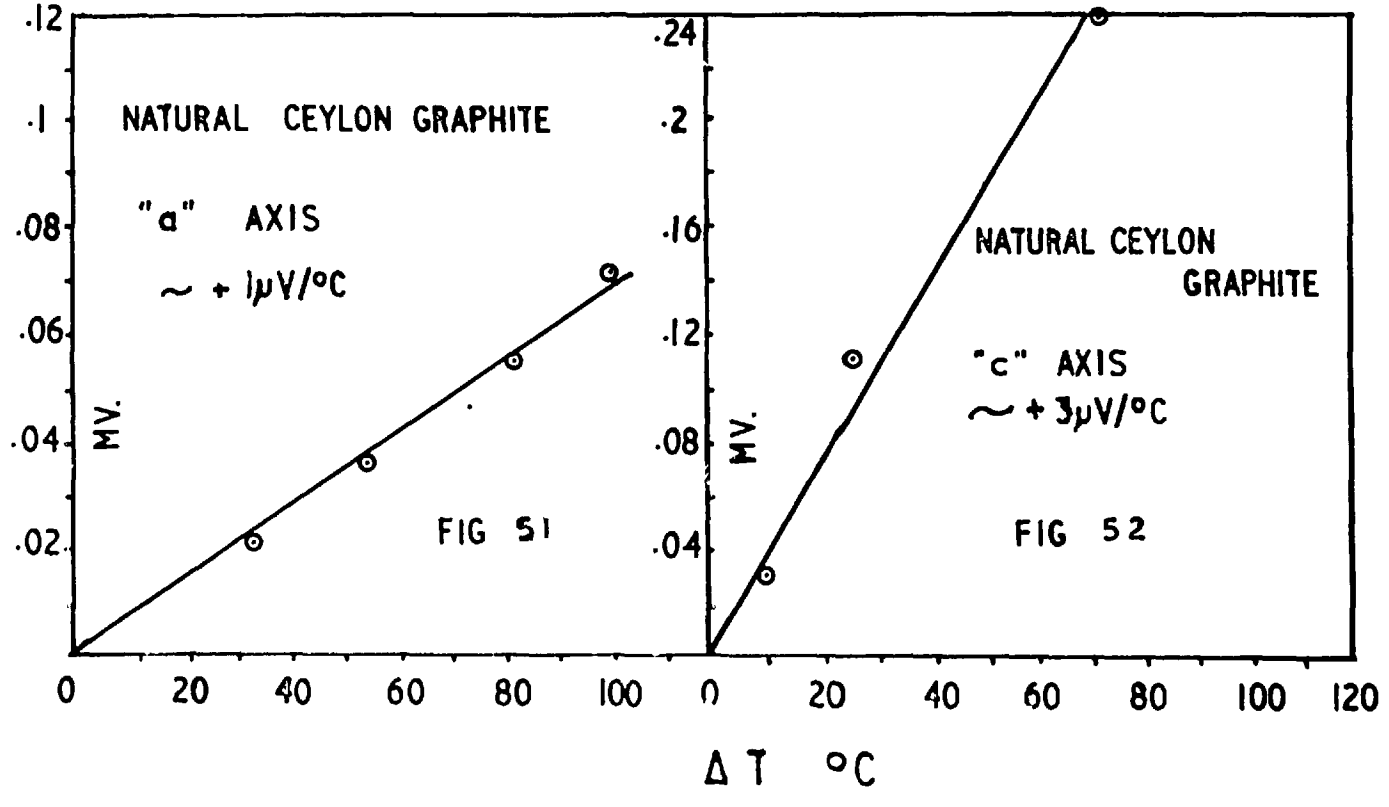
Results of heating the junction by an oxygen-coal gas flame.

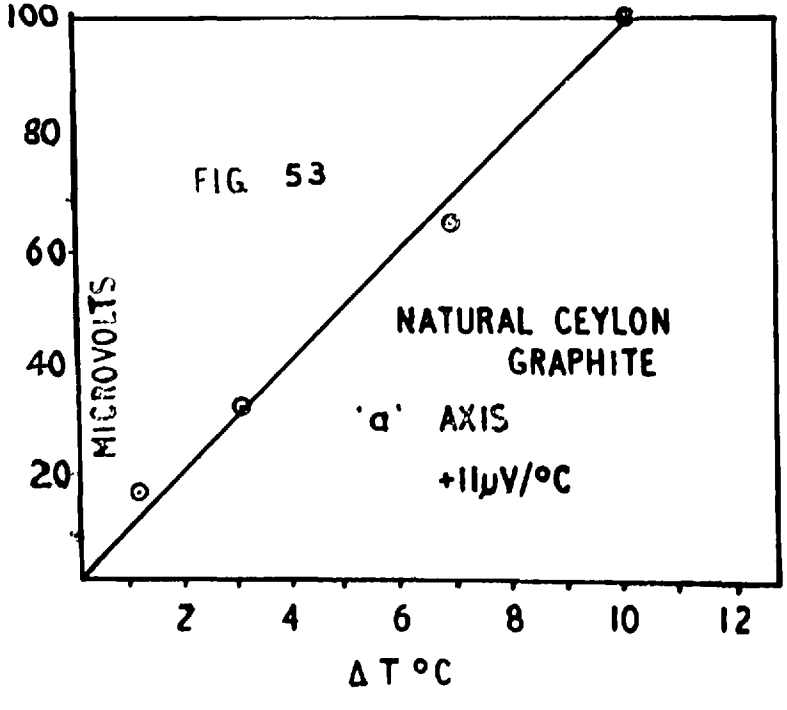
As may be seen from Fig. 57, when the thermo-junction was heated by means of an oxygen-coal gas flame impinging on the mullite tube the shape of the EMF temperature plot differed in a marked way from the straight line obtained under electrical heating conditions. Although the experimental conditions could not be rigoroudly controlled the main features of the experiment are clear.

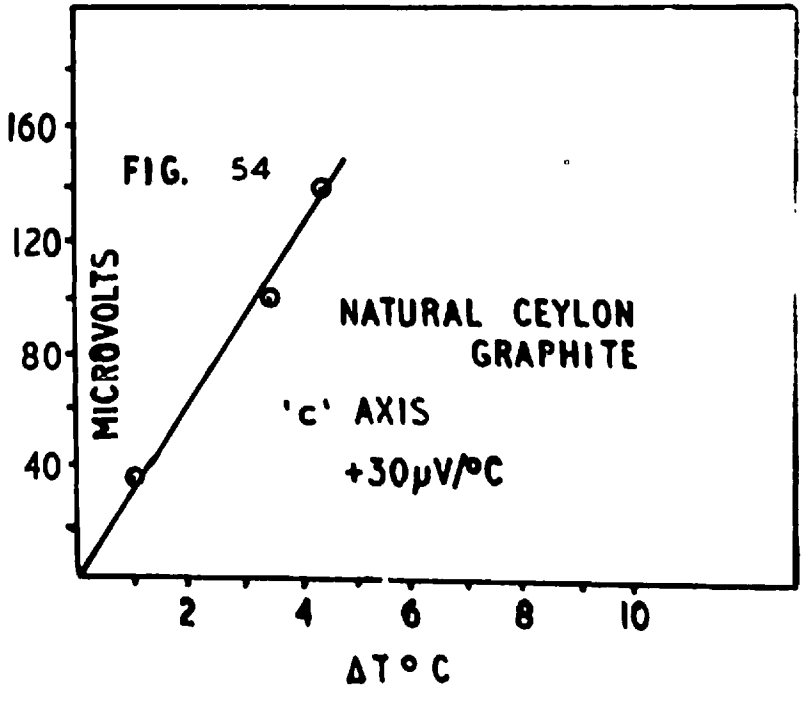
They are -

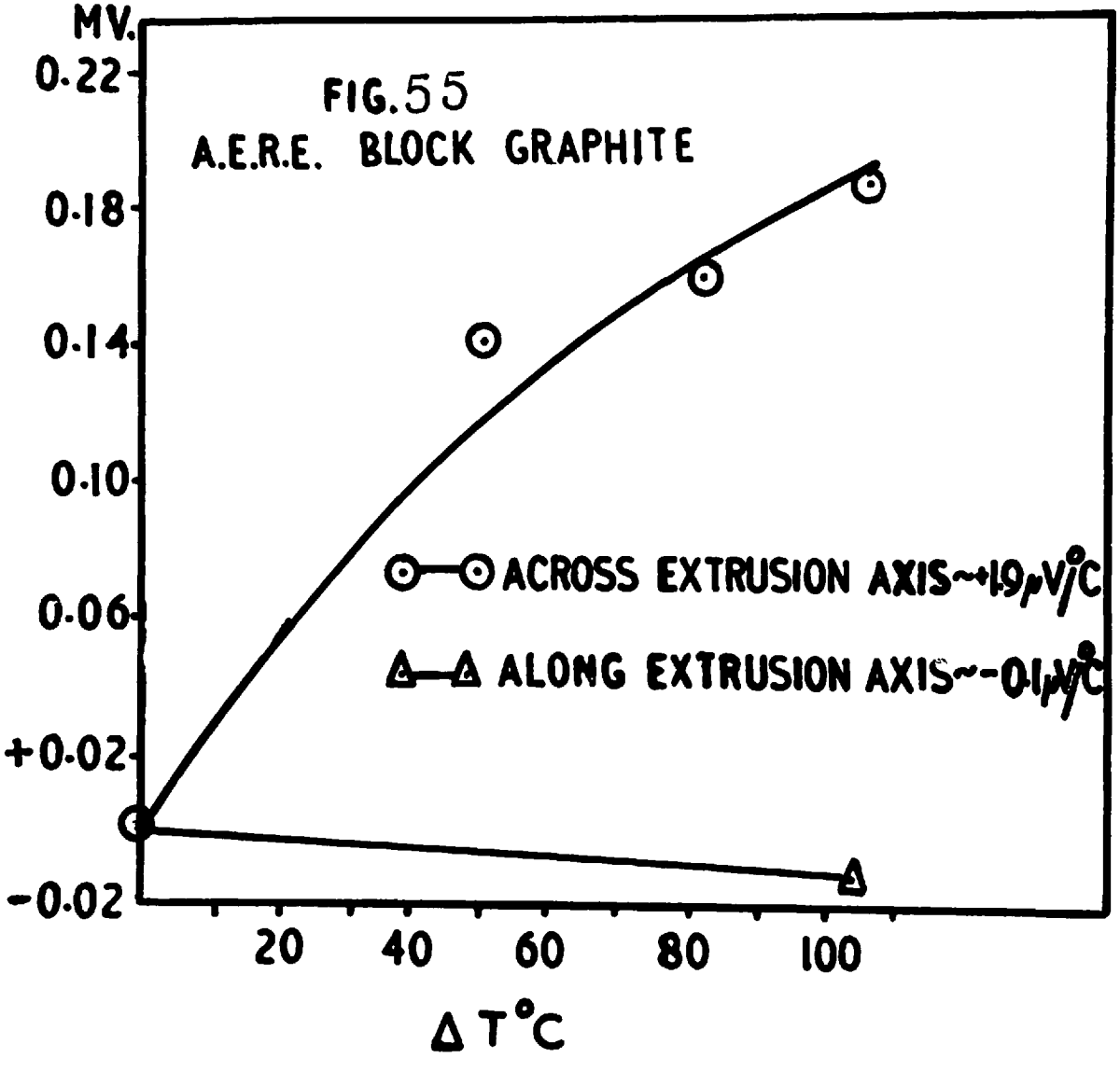
i) Around 300°C the EMF goes through a maximum which is followed by a steady decline and eventually a reversal of sign occurs.

ii) If nitrogen is passen over the heated graphite the maximum at 300°C does not occur although the curve shows a kink in this region. Above 700°C the curve levels off and then begins to fall in an irregular manner.


.12
.1
.08
.06
.04
.02
MV.
NATURAL CEYLON GRAPHITE
"a" AXIS
~ + 1μV/°C
FIG 51
.24
.2
.16
.12
.08
.04
MV.
NATURAL CEYLON GRAPHITE
"c" AXIS
~ + 3μV/°C
FIG 52
0 20 40 60 80 100
0 20 40 60 80 100 120
Δ T °C


100
80
60
40
20
MICROVOLTS
FIG. 53
NATURAL CEYLON
GRAPHITE
'a' AXIS
+11μV/°C
2
4
6
8
10
12
Δ T °C


160
120
80
40
MICROVOLTS
FIG. 54
NATURAL CEYLON
GRAPHITE
'c' AXIS
+30μV/°C
2
4
6
8
10
Δ T ° C


MV.
0·22
0·18
0·14
0·10
0·06
+0·02
-0·02
FIG.55
A.E.R.E. BLOCK GRAPHITE
ACROSS EXTRUSION AXIS~+1·9μV/°C
ALONG EXTRUSION AXIS~-0·1μV/°C
20
40
60
80
100
Δ T°C

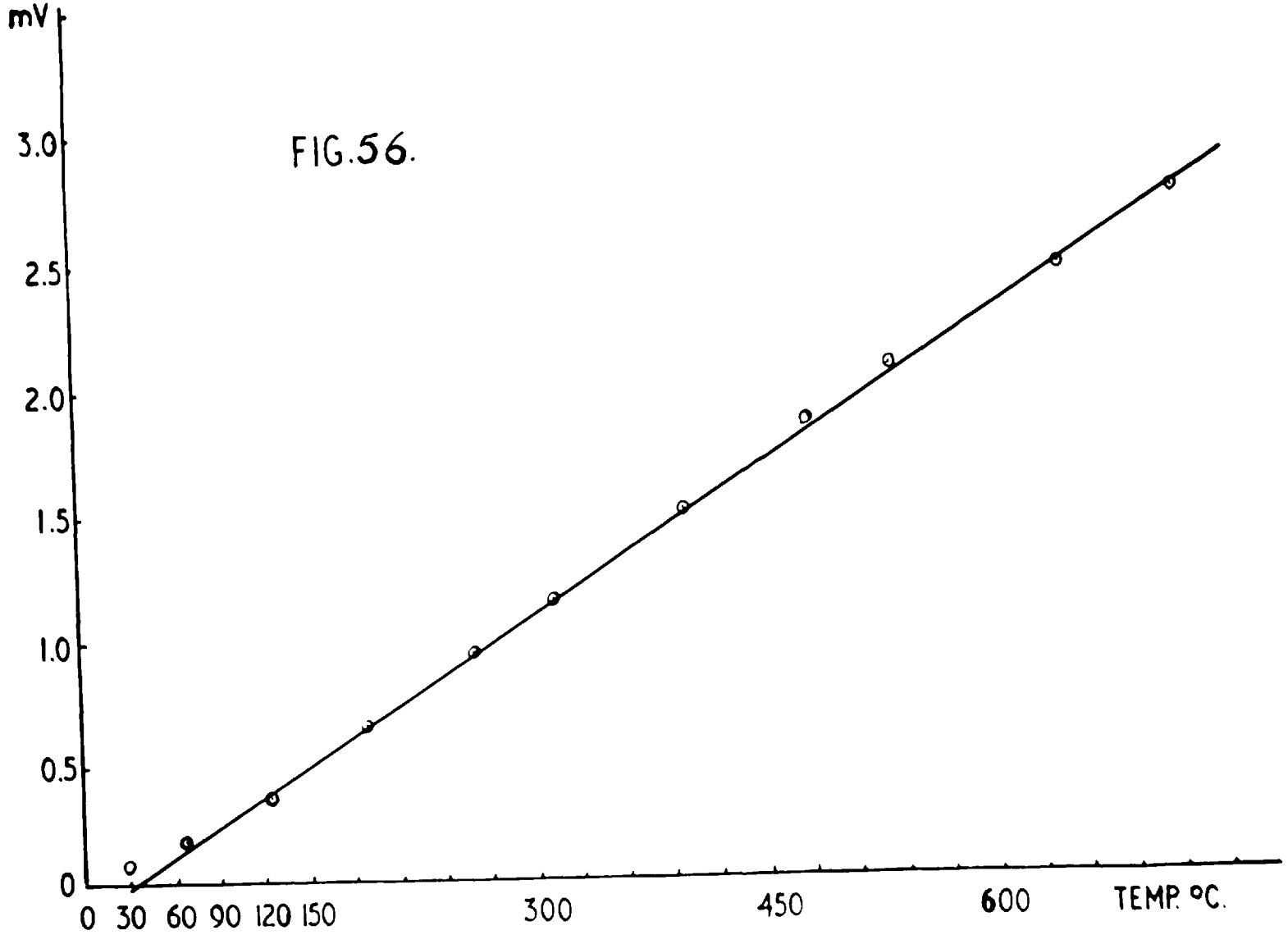


FIG.56.

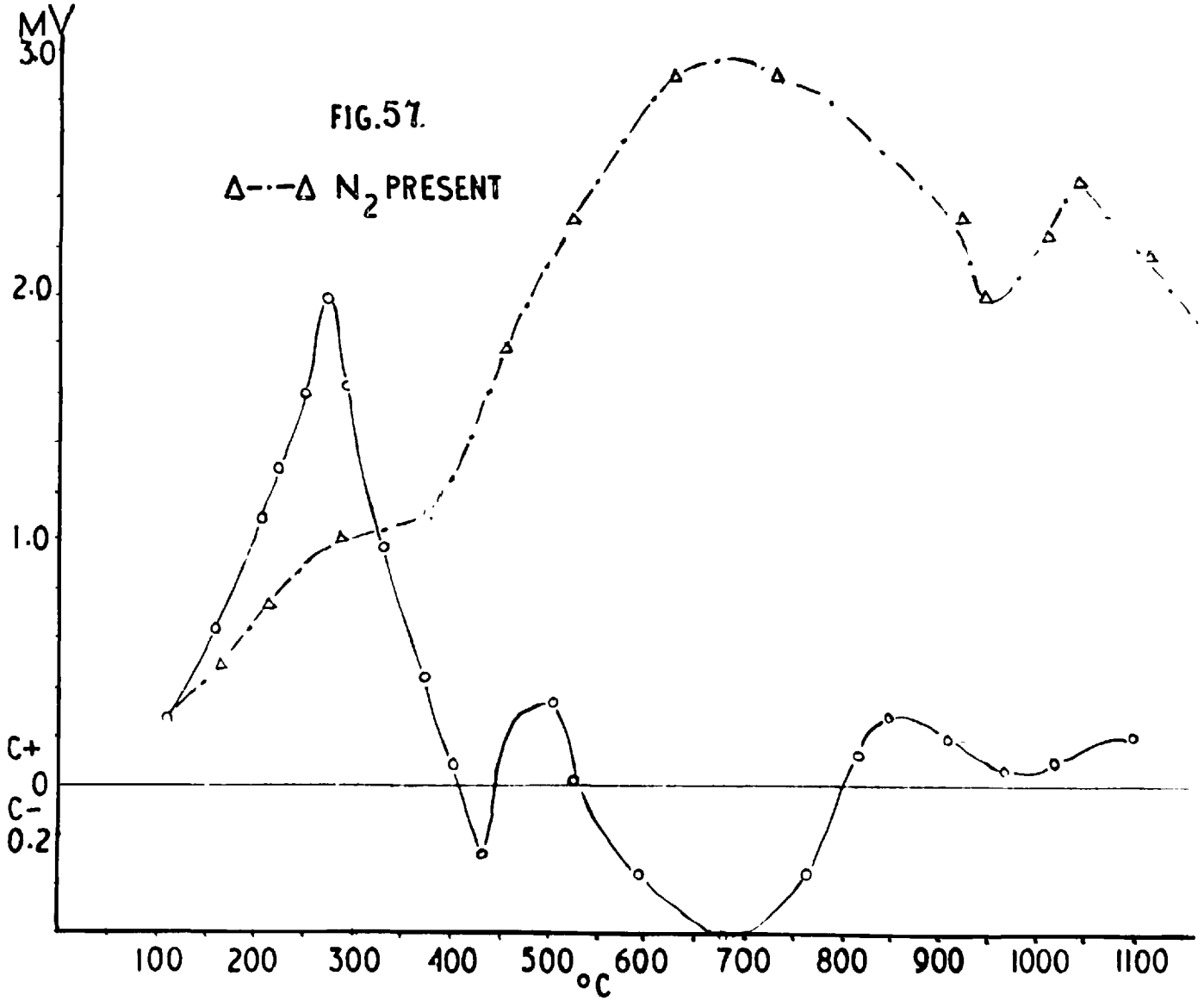


FIG.57.

Δ---Δ N_2 PRESENT

CHAPTER 11.

PART II : DISCUSSION.

A positive thermo-electric power or Hall co-efficient in graphite can be associated with vacant energy levels at the top of the π band. These vacancies can be caused in a number of ways, for example, chemisorbed electronegative species, certain valency defects, intercalated acceptor atoms may all to different degrees deplete the π band by localising electrons in their immediate vicinity. One well establish case is that of bromine graphite where it has been shown (72) (36) that the negative Hall co-efficient and thermo-electric power changes to positive values as the bromine content increases.

The thermo-electric power measurements in the previous chapter showed that the value measured along the c axis is more positive than that measured along the a axis. In both cases the effect is small and this may be attributed to approximately equal numbers of holes and electrons producing effects in opposite directions which tend to cancel one another out. (23).

The fact that with well orientated graphite the thermo-electric effect was positive along both a and c axes may be attributed to impurities in the material increasing the contribution of holes by depleting the π band. The ash content of this graphite was about 5% by weight and purification was not attempted in case the crystallinity was destroyed in the process.

If a axis and c axis graphite are considered to represent two different materials the anisotropic thermo-electric can be simply

interpreted as due to differences between the heights of the topmost filled electronic levels in each. The more positive value found for the c axis specimens suggests that by analogy with bromine graphite the Fermi level in this material is depressed to a greater extent.

If a junction is then made from these "different" materials it will behave like a junction of two dissimilar metals. As the temperature of the junction is raised electrons will flow from the a to the c specimens because the work function is less for the a specimen. The work function is the energy required to remove an electron from a point inside (corresponding to the Fermi level) to a point outside the material. The work function will therefore be greater for the material with a lower Fermi energy.

The above remarks were made on the assumption that a and c axis graphite are different materials. However it is meaningless to speak of two different band systems within a homogenous crystal. The interpretation can be rationalised by dispensing with this "double band" system and postulating only one band system in which the behaviour of electrons is very dependant upon crystal orientation.

This is what is implied by Johnson (69) - see Chapter 8 - when he states that in hexagonal crystals the effective mass and mobility of the charge carriers will be different along different crystal axis. It will be true in any crystal in which the constant energy surfaces in momentum space are not spherical. Asymmetrical E v k relationships are not unusual. In a particular crystal direction there may be energies permitted to the electron which in another orientation are forbidden. This results in band overlap, a common feature in metals. The

effective mass m* of an electron is intimately associated with the E v k relationship. It is defined by (see Chapter I)

$$m^* = \frac{h^2}{4\pi^2 \frac{d^2E}{dk^2}}$$

In systems where E v k relations are very anisotropic the effective-mass of the carrier (electron or hole) will depend in a marked manner on crystal orientation.

The Brillouin zone of graphite is very compressed along the hexagonal axis (73), thus there will be different E v k curves for different crystal directions. Only if the zone were a perfect sphere would the energy discontinuity occur at the same value of k irrespective of direction. Variation in effective mass should be therefore expected in graphite.

The anisotropic crystal structure of hexagonal crystals will also lead to values of the carrier mean free path, considered as the path between two lattice scattering collisions, which also depend upon crystal orientation. This will lead to variations in mobility.

The anisotropic thermo-electric power of graphite is believed to result from variations in the effective mass and mobility of the charge carriers for the reasons given above.

It is worth noting that while variations in the magnitude of the thermal EMF's were observed in different samples (probably due to variations in impurity concentrations) the ratios of the thermo-electric power S, measured parallel and perpendicular to the a axis, were nearly the same, in agreement with the formula given in Chapter 8.

$$\frac{S_{11}}{S_{\perp}} = \frac{(C_{11} - 1)(C_{\perp} + 1)}{(C_{11} + 1)(C_{\perp} + 1)}$$

where C is the ratio of the electron to hole S mobility.

From Figs. 51 & 52

$$\frac{S_{\perp}}{S_{11}} = \frac{+3 \ \mu V/^{\circ}C}{+1 \ \text{"}} = 3 : 1$$

and from Figs. 53 & 54

$$\frac{S_{\perp}}{S_{11}} = \frac{30 \ \mu V/^{\circ}C}{11 \ \text{"}} = 2.7 : 1$$

As a development of this work Ubbelohde Blackman and Dundas (70) have recently constructed a graphite thermocouple using a and c axis specimens of pyrolytic graphite. This graphite was highly orientated and was obtained in a high state of purity by cracking methane. Representative values for the thermo-electric power measured were about $-9\mu V/^{\circ}C$ for a axis and $+6\mu V^{\circ}/C$ for c axis specimens.

The Effect of chemical attack on the self thermo EMF in graphite.

From Fig. 56 it can be seen that there is a maximum in the EMF curve and that it declines thereafter eventually changing sign. This is most likely due to chemical attack on the junction. When the junction was protected by nitrogen the decline of the EMF was postponed to higher temperatures; although even with nitrogen present there would appear to be a sufficient concentration of attacking groups present to kink the EMF curve.

The maximum in the EMF curve observed probably marks the onset of oxidation and the possibility thus arises of measuring rates of carbon or graphite oxidation by changes in thermo-electric power.

PART III

THE PREPARATION AND PROPERTIES OF SOME GRAPHITE COMPOUNDS.

CHAPTER 12

PART III : INTRODUCTION

In 1841 Schaufhäutl (74) found that graphite reacted with sulphuric and nitric acids. Since then it has been found to react with numerous other materials which have widely differing chemical properties. The reaction products are known as lamellar compounds because the foreign atom, ion or molecule is intercalated between the lamellae (aromatic layer planes) expanding them to distances which depend upon the nature of the reacting species. This expansion along the hexagonal axis is the most characteristic feature of the lamellar compounds of graphite.

The main types of lamellar compounds are those in which graphite reacts with acids to give acid salts, e.g. graphite bisulphate (75) (76) (77) (78); in which halogens are intercalated directly, e.g. graphite bromine, (79)(80) (81), in which reaction with alkali metal occurs, e.g. potassium graphite (82) (83) (84) (85) and where reactions with metal halides such as ferric chloride takes place in which the whole halide molecule is intercalated. These latter compounds have been called molecular graphite compounds (86) (87) (88 The compounds relevant to the work to be described are graphite bromine, the alkali graphite and the molecular compounds.

Graphite-Bromine.

In 1933 A.Frenzel (79) found that graphite took up 83.5% of its own weight of bromine if left standing in bromine vapour. Rüdorff (80) demonstrated that the limiting weight of bromine taken

up corresponds to an empirical formula of C_8Br. The X-ray diffraction pattern of this compound yielded only ool lines and the inter-lamellar spacing suggested was 7.05Å units. Table XVIII.

Hennig (81) found that "residue" compounds of graphite bromine could be prepared by first allowing the graphite to take up the maximum amount of bromine and then standing it in air. Most of the bromine was desorbed in this way but a small amount of it remained firmly held. The X-ray diffraction pattern of this compound was not different from that of graphite and Hennig concluded as in the case of his bisulphate residue compound that the trapped reactant was located at lattice imperfections.

The Alkali Graphites.

Fredenhagen and Cadenbach (82) prepared compounds of graphite with potassium, rubidium and ceasium and observed that although sodium will not react with graphite, it will react with amorphous carbon.

Schleede and Wellman (83) and Rüdorff and Schulz (84) investigated the structure of the alkali graphite compounds and their values of the interlamellar spacings are given in Table XVIII They found the bronze compound of potassium graphite to have the formula C_8k and two blue compounds corresponded with the formulae $C_{24}k$ and $C_{36}k$.

In the work to be described as unsuccessful attempt was made to prepare sodium graphite from an amalgam of sodium and potassium. Recently, a reaction between sodium and graphite has been reported

in which the product has the formula $C_{64}Na$ (85). It was prepared by heating graphite and sodium together for four hours at 400°C.

MOLECULAR COMPOUNDS OF GRAPHITE.

Rüdorff and Schulze(87) observed that when graphite was heated to above 200°C with two or three times its own weight of ferric chloride a dark green lamellar compound was formed. They found various compounds could be prepared depending upon the temperature of the reaction. Two products corresponding to an empirical formula $C_{10}FeCl_3$ and $C_{30}FeCl_3$ were isolated. The expended interlamellar spacing was 9.37Å, Table XVIII.

Graphite-Aluminium Chloride.

It has been reported that graphite does not react with aluminium chloride (87). Croft, however, found that a reaction did take place and that aluminium chloride was intercalated by graphite (88). In the present work it was found that the aluminium chloride graphite compound could only be prepared with natural graphite. Croft did not attempt the preparation with artificial graphite. His compound and the one described in the present work were prepared by heating aluminium chloride and natural graphite together under vacuum at 260°C. In both cases, the compound contained 25% aluminium chloride by weight corresponding to an empirical formula of $C_{33}AlCl_3$. Croft made no measurements on his product but in the work to be described estimates of the interlamellar distances were made from X-ray diffraction data and some information about the electronic structure of the compound obtained.

Before this work was completed Rüdorff and Zeller (89) and Hennig (90) published other information about a graphite aluminium

chloride compound. Rüdorff concluded that oxygen or chlorine gas was necessary for the formation of the compound. Hennig showed that when artificial graphite and aluminium chloride were heated to 210°C in the presence of chlorine, a blue compound having the formula $C_n cl^- 3Alcl_3$ could be prepared with n varying between 30 and infinity. Rüdorff (89), however, stated that the chlorine acts catalytically and is not bound into the graphite with aluminium chloride. His analysis showed an exact chlorine to aluminium ratio of 3:1. Oxygen acts, according to Rüdorff, by combining with some $Alcl_3$ to form Alocl causing chlorine to be liberated which then catalyses the intercalation of $Alcl_3$ into graphite. His X-ray evidence and the results of his chemical analysis indicated that three main compounds are formed as the temperature of preparation is raised progressively from 265° to 440°C. These three compounds were all prepared from artificial graphite in the presence of chlorine and had the following approximate compositions -

1) C_9Alcl_3 in which every layer contained aluminium chloride. The colour of this compound was deep blue.
2) $C_{18}Alcl_3$ in which every other layer contained cluminium chloride and the colour was grey-black.
3) $C_{36}Alcl_3$ in which aluminium chloride was in every fourth layer and the colour was no different from graphite.

The inter-lamellar distance estimated by Rüdorff for aluminium chloride between two graphite lamellae was 9.52Å in his C_9 compound.

In his C_{36} compound he found the distance to be 9.60Å. The value arrived at independently in the present work was 9.75Å for a $C_{33}AlCl_3$ compound.

There are thus two sets of conditions under which a graphite aluminium chloride compound may be prepared. In the one instance there is the method of Croft using natural graphite heated under vacuum conditions with aluminium chloride at 260°C. This process produces a compound having the empirical formula $C_{33}AlCl_3$ (88).

The other method is that of Rüdorff (89) and Hennig (90) which may be applied to both artificial and natural graphite. In this case the graphite is heated with aluminium chloride and under free chlorine at temperatures ranging from 265° - 400°C. Three main compounds are produced, the formulae of which Rüdorff gives as C_9AlCl_3, $C_{18}AlCl_3$ and $C_{36}AlCl_3$.

It seems likely that these two methods lead to different types of compound. Rüdorff has recently (91) suggested that active chlorine may be intercalated in the form of $[AlCl_4]^-$ groups although the quantity of it is very difficult to establish.

The role of defects in compound formation.

Before carbon lamellae may be separated, some non-graphitic bonds must be broken (89). These valency defects could be removed by chlorine which might explain its function in the compound preparation. In this connection it may be relevant that natural graphite has a very well developed crystal structure with crystallites which are much larger than those of artificial graphite. With the more ordered

structure of natural graphite such non-graphitic cross linking bonds would be less common than in the case of artificial material. The problem of breaking them as an essential preliminary to intercalation may then be of little importance where natural graphite is concerned. This might be one explanation for the fact that a graphite-aluminium chloride compound can be prepared in the absence of chlorine from natural graphite, but that chlorine is necessary where artificial graphite is concerned. In the more familiar compounds of graphite, e.g. the alkali and halogen graphites, cross linking defects can presumably be removed by bonding with the reactant itself.

There can be little doubt that valency defects of the type mentioned above do exist in graphite. In conjunction with other defects such asscrew dislocations (63) they probably provide a path along which current may flow in single crystal graphite. Variations in the extent of such defect structures could account for the variations observed in measurements of the specific resistance along the hexagonal axis

Although their role in compound formation is still largely unknown, they may be associated with the fact that while the compound can be decomposed a small amount of the reactant is firmly held and cannot be recovered from the graphite (81).

Bonding in molecular compounds of graphite.

Croft was successful in intercalating a large number of substances into graphite (92). These were chlorides of the Transition and Group III elements. $CuBr_2$ and $AlBr_3$ were also found to react. He concluded that the valence state of the cation of a transition metal chloride determines whether or not a reaction with graphite will occur. Thus Pt cl_4, Pd cl_4, Bb cl_5 and Cu cl_2 are readily occluded but Pt cl_2, Pd cl_2, Sb cl_3 and Cu cl do not react even under a wide variety of experimental conditions. He suggests that two conditions are necessary for intercalation. Firstly electronic interaction between a cation and graphite must be possible and secondly the electron affinity of the cation must be sufficient to promote such interaction. The metal ion of cupric chloride for example possesses one singly occupied 3d orbital in which an electron transferred from graphite might be accommodated. No such accommodation is available however in the saturated 3d shell of the cuprous iron nor is it possigle to intercalate cuprous chloride. Where the chloride of iron are concerned only ferric chloride can be intercalated in graphite although both the ferrous and ferric ion could accommodate electrons transferred from graphite in their unfilled 3d shells. The fact that ferric chloride reacts with graphite and ferrous chloride does not is attributed by Croft to the greater electron affinity of the ferric ion. In the case of aluminium chloride graphite he suggests that Sp^3 bonding exists between the cation and graphite, two electrons being donated by the graphite.

This is the type of bonding which exists in aluminium chloride dimers in the vapour state.

Table XVIII

COMPOUND	INTER-LAMELLAR DISTANCE
C_8K	5.40Å
C_8Rb	5.65Å
C_8C_3	5.94Å
C_8Br	7.05Å
$C_{10}Fecl_3$	9.37Å
C_9Alcl_3	9.52Å
$C^+_{24}\ HSO^-_4 2H_2O$	7.98Å

ELECTRONIC PROPERTIES OF THE GRAPHITE COMPOUNDS.

G. Hennig (81) has determined the electrical resistance, its temperature co-efficient and the Hall co-efficient of graphite bisulphate at various stages of oxidation. The resistance decreases rapidly and the Hall co-efficient changes from negative to positive as the concentration of ions increases. The compounds were prepared by electrolysis and reduction could be brought about by reversing the electrodes. Hennig found however that reduction was not complete and some ions remained trapped presumably at lattice imperfections.

Hennig and his co-workers however carried out their investigations on the so-called "residue" compounds of graphite. In these compounds the carbon to reacting species atom-ratio was very large. The foreign atoms were present in little more than trace amounts. Hennig utilised this type of compound to avoid the crumbling of the graphite which generally occurs as the concentration of occluding species increases. This crumbling is associated with the considerable c axis expansion which takes place when graphite forms a compound. However because of the very small amounts of foreign elements present in the "residue" compounds, a definite stoichiometry is difficult to ascribe to them and indeed it might be argued that they are not compounds in the exact sense of the word.

McDonnel, Pink and Ubbelohde (36) in studying the electronic properties of the potassium graphite prepared the fully intercalated material C_8K. This substance having an exact stoichiometry and a

unique structure is a true lamellar compound of graphite. Because of the problem of crumbling, Ubbelohde et al used graphite powder as a starting material and compared the electrical resistance before and after compound formation. They found that reaction with potassium produced a marked decrease in electrical resistance. The temperature co-efficient of resistance of the compound was observed to be positive, suggesting metallic behaviour. On the basis of this low electrical resistance and positive temperature co-efficient the same authors postulated a pseudo-metallic hypothesis whereby potassium donates an electron to the aromatic pool of graphite.

In view of the large decrease of electrical resistance observed on forming C_8k from graphite it was important to establish whether the crystalline powder of the starting material exhibited large inter-particle resistance as with some metal powders due to impurity films on the surface. If this were so, compound formation might markedly reduce this contact resistance and the effects observed might be explained in this way. In Part I of this work experiments were described which showed that the inter-particle resistance in graphite powders depended simply on the area of contact. The low electrical resistance of C_8k powder as compared with graphite powder is therefore an intrinsic feature of the compound. Ubbelohde et al (36) also showed that a large decrease of electrical resistance occurred when graphite powder was allowed to take up bromine. They suggested that graphite could behave in an amphoteric manner, accepting an electron from potassium and donating one to bromine.

The electronic properties of the molecular compounds have received little attention. In what follows some results are described for aluminium-chloride graphite.

CHAPTER 13

PART III : EXPERIMENTAL

The aluminium chloride-graphite work to be described was embarked upon soon after Croft published the first paper describing the successful preparation of the compound. The main features of his preparation were confirmed and then the compound was investigated with the aim of determining its structure from X-ray measurements and gaining information about its electronic properties. Thermo-electric power and electrical resistance measurements were carried out.

In all the work of this section X-ray diffraction played a major part. The criterion of compound formation was always that the reaction product should have a unique structure. Thus for example it will be shown that when a sodium-potassium alloy is reacted with graphite, X-ray diffraction photographs of the product showed patterns corresponding to potassium graphite and to metallic sodium indicating that only the potassium of the alloy formed a lamellar compound.

Because of the scarcity of information about the structure of Bromine graphite an X-ray diffraction investigation was made of this compound prepared from highly crystalline natural material. Some preliminary measurements were made on the resistance changes which take place along the a and c axis of graphite when bromine is absorbed. Thermo-electric power measurements were also carried out on a highly orientated aggregate of natural graphite crystals after exposure to bromine vapour.

A Graphite Monochromator for X-rays.

It was found that a specimen of natural graphite when exposed to X-rays gave an intense 008 reflection, See Appendix I. This reflection has a high θ value (66.81°) and in subsequent work use was made of it to provide monochromatic radiation. A flake of Travancore graphite was mounted on the platform of a "Unicam" filter and the platform adjusted until the high angle reflection was obtained. The advantage of using graphite was that it did not undergo chemical change as readily as other crystal monochromators and was thus more suited to long exposure work. The monochromator was mounted between the window of the X-ray machine and the collimator of the camera.

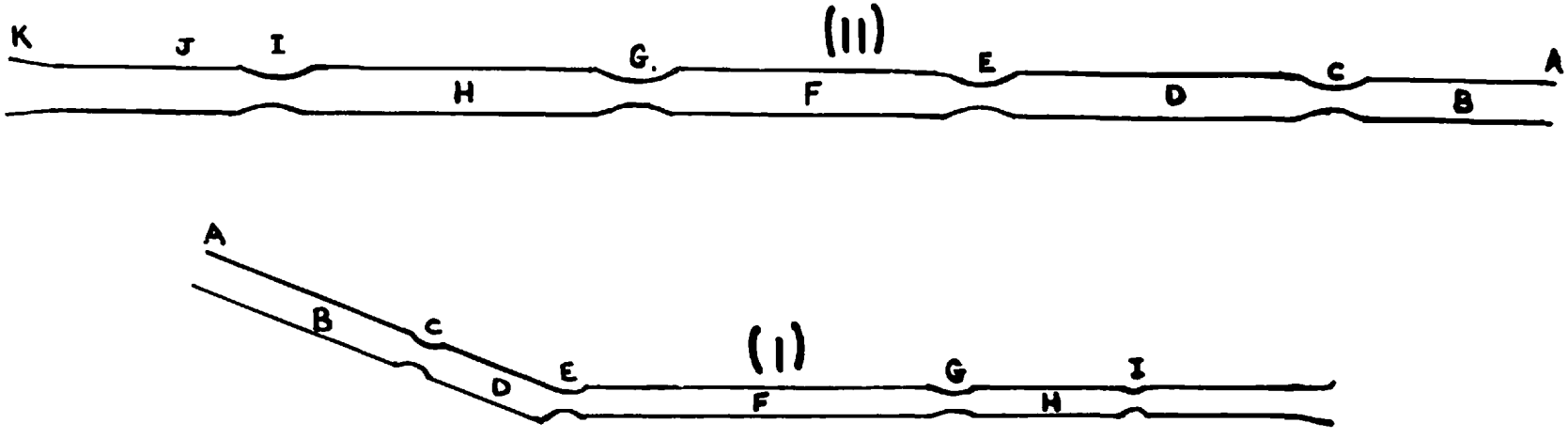


FIG. 58

The Preparation of aluminium-chloride graphite.

Materials.

High purity aluminium chloride was obtained from B.D.H. Graphite for the preparation was supplied by the Natural History Museum, South Kensington. It was natural graphite from Madagascar and consisted of platelets about 2 mm. in diameter. The ash content of this material was reduced from 5% to 1% by refluxing with concentrated hydrochloric acid. The preparation was also attempted with articicial graphite powder (passing 300 mesh) supplied by A.E.R.E., Harwell.

Procedure.

The glass apparatus is shown in Fig. 58 ii. The graphite was put into compartment D and a cone inserted in K. The system was then evacuated through B and the graphite baked at 400°C for five hours to expel moisture and adsorbed gases. Nitrogen was then admitted and the cone removed. Aluminium chloride was introduced into H in a flow of nitrogen. The quantities used were 7 g. aluminium chloride to 2 g. graphite. The cone at K was replaced and a furnace placed around H.

The system was evacuated and a seal made at I. The aluminium chloride was sublimed over into F and then into D. D was removed by seals made at E and C. The graphite and aluminium chloride were heated in a muffle furnace to 260°C and kept at that temperature for 24 hours. At the end of this period the tube was partially removed from the furnace and the excess aluminium chloride condensed in the cold end.

Analysis.

The aluminium chloride-graphite was fumed with concentrated sulphuric acid and then heated gently to expel excess acid. It was finally ignited and the aluminium chloride estimated as the oxide Al_2O_3.

The compound was investigated by X-ray diffraction.

The Preparation of Bromine Graphite.

Materials.

Analar Bromine was obtained from M. & B. Chemicals Ltd. Natural Madagascar graphite was obtained from the Natural History Museum and Ceylon graphite from the Morgan Crucible Company Limited.

Procedure.

The compound was prepared by allowing the graphite to stand over bromine in a dessicator at room temperature.

In an attempt to obtain a well defined X-ray diffraction photograph a crystalline fibre of Ceylon graphite was inserted into a thin walled capillary tube and dipped in liquid bromine. Both ends of the tube were then sealed in a flame.

Analysis.

The bromine content of the compound was determined by direct weighing. The compound was investigated by X-ray diffraction.

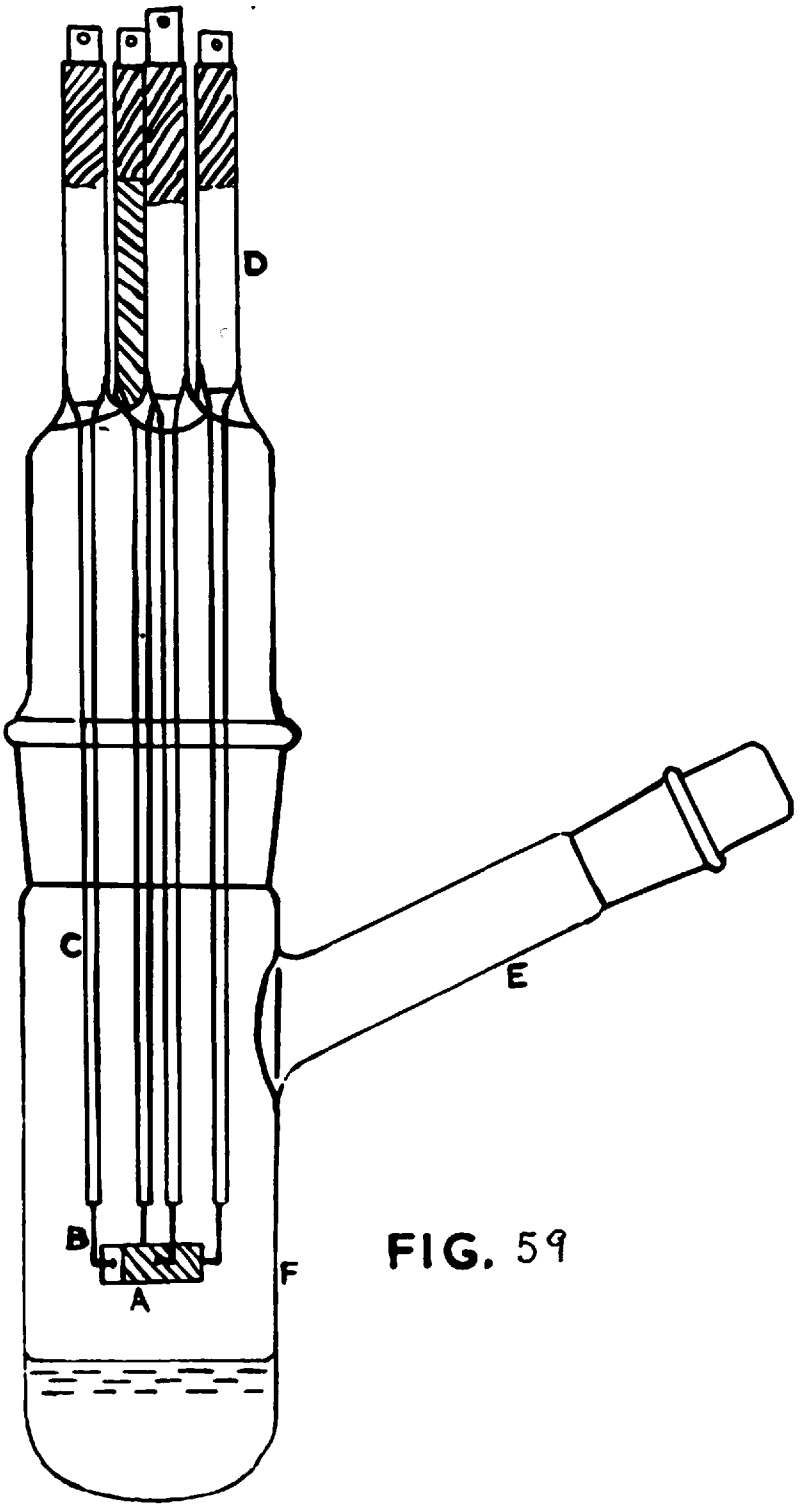


FIG. 59

Electrical resistance measurements on Bromine-graphite.

In an attempt to measure the influence of bromine on the electrical resistance of graphite measured along the a and c axis of the same crystal the apparatus without the graphite crumbling, bromine was dissolved in carbontetrachloride so that a controlled partial pressure could be employed. A well orientated block of natural graphite carrying four electrodes - two for each crystallographic axis - was enclosed in a glass vessel over the bromine/carbon-tetrachloride solution.

Materials.

A highly orientated aggregate of natural crystallites was supplied by the Morgan Crucible Co. It measured 2 mm. x 0.3 cm. x 0.2 cm. Analar Bromine was obtained from M. & B. Chemicals and Analar carbon tetrachloride from Hopkins & Williams.

Procedure.

Experiments were carried out using the apparatus shown in Fig. 59. The graphite A was mounted between four electrodes such that each pair lay along a main crystal axis. The electrodes were thick copper rods which terminate in thick platinum stirrups. These stirrups B were inserted into holes drilled in the graphite. The electrode assembly was mounted in the pyrex vessel F fitted with a B55 cone and socket joint and a side arm E. The electrodes were sliding fits in the four glass tubes D and were sealed at the exit by black wax. A solution of bromine in carbon tetrachloride at the temperature of melting ice was poured into the vessel through E. The reaction was carried out at this temperature my immersing F in a Dewar vessel containing crushed ice. By this means in was hoped to obtain

electrical resistance measurements under various partial pressures of bromine.

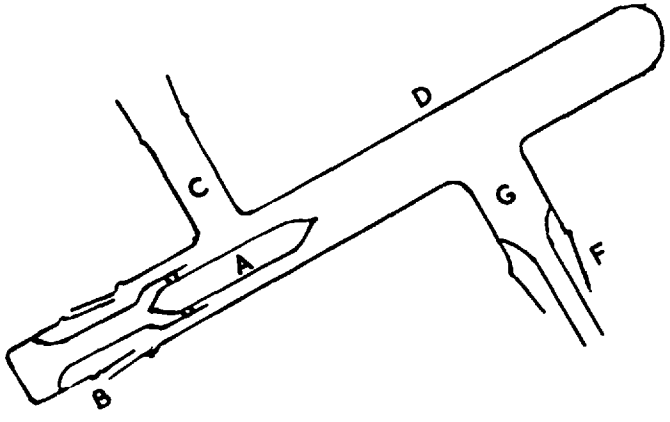
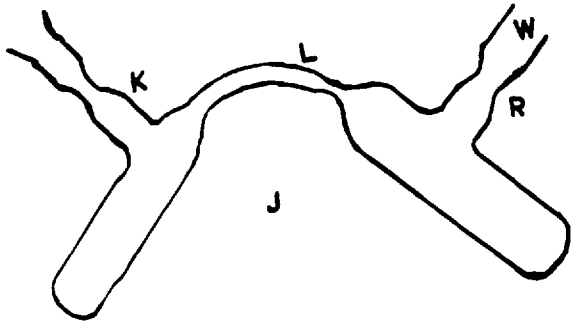


FIG.60



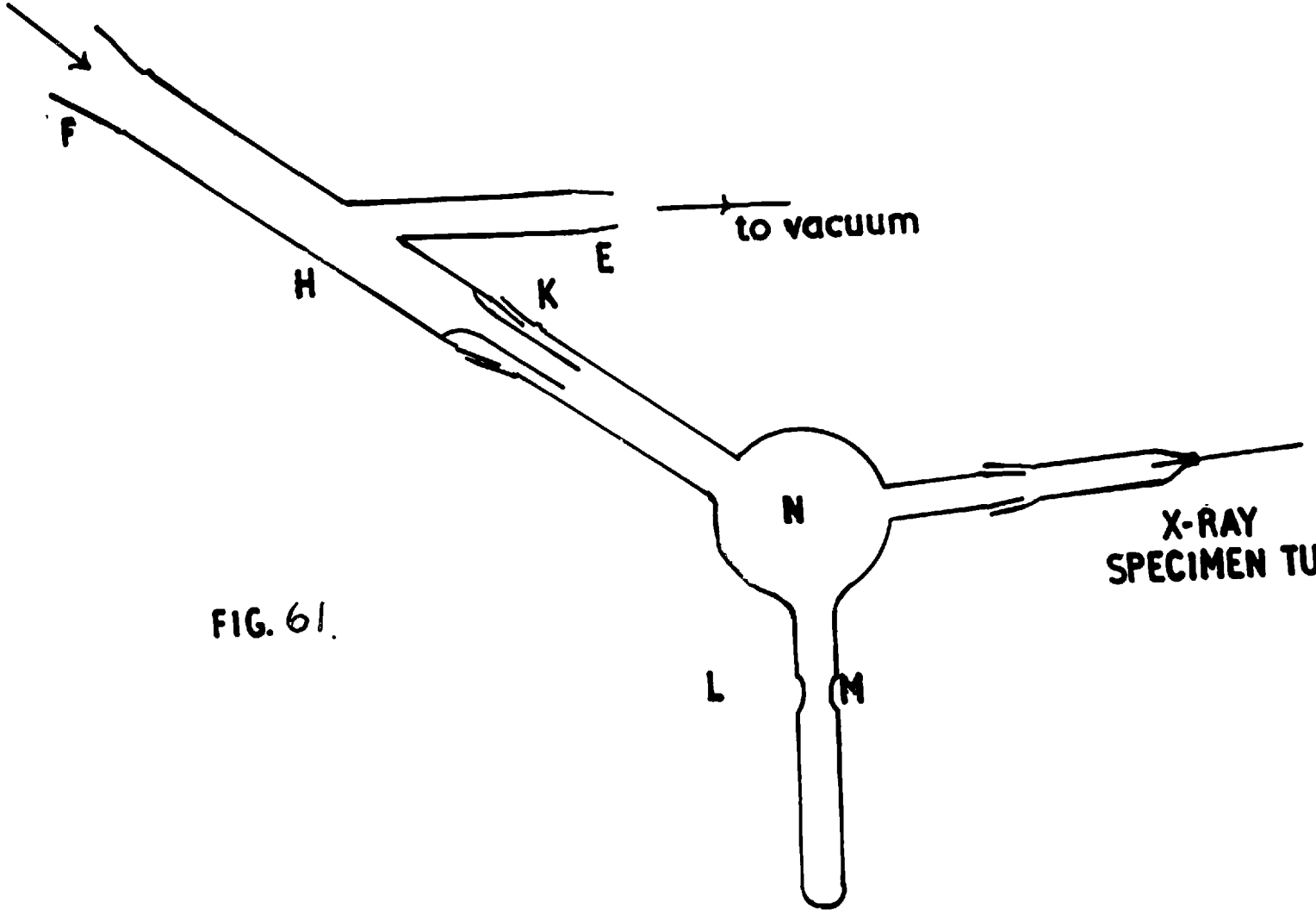


FIG. 61.

The reaction between graphite and a sodium-potassium alloy.

Materials.

An alloy of sodium and potassium containing 52.8% potassium by weight was obtained from Imperial Chemical Industries. This alloy is liquid at room temperature and was supplied under nitrogen in pyrex glass ampoules. A.E.R.E, Harwell graphite (10 mesh) was used.

Procedure.

The apparatus for carrying out the reaction is shown in Fig. 60. A scratch mark was cut on the ampoule A with a file and a piece of soft iron wrapped around one end. The other end was held in a teflon washer wedged into the cone B. A side entry C was positioned so that when the cone and ampoule were inserted into the tube D it was directly above the scratch mark. A stopper was inserted in the side entry and the system evacuated through E with the vessel J replacing the vessel N. Fig. 61. Nitrogen was admitted and the stopper in C removed. A glass rod was heated in an oxygen flame until the end was white hot. It was then inserted into the side entry and pressed hard against the scratch mark. The top piece of the ampoule cracked and fell off and was towed away by a magnet to the further end of the tube D. The nitrogen flow was stopped and the stopper re-inserted in the side entry. The system was then evacuated. The tube D was turned, swivelling on the cone and socket F and the alloy flowed down through the internal seal G to protect it from the grease of the joint, along the tube H and into the vessel J. A seal was then made at K and J removed. The vessel J consisted of two ampoules connected to one another. Before attaching J

to the vacuum system a weighed quantity of graphite was introduced into one of the ampoules via W to permit the formation of a C_4M compound where M represents one mole of alloy, and a seal made at R.

When J had been removed from the vacuum system it was tilted so that the allow flowed over into the graphite ampoule. When all the alloy had been transferred a seal was made at L.

The product was examined by X-ray diffraction.

Potassium graphite.

This compound was prepared in order that its thermal expansion might be measured and also that its X-ray diffraction pattern should serve as a reference for the work with the sodium/potassium alloy.

The preparation followed the well established method described by Fredenhagen and Cadenbach (82). Details of the method are given in Appendix 2. The compounds prepared were identified by their X-ray diffraction diagram.

Manipulation of Unstable Materials.

The Nitrogen Dry Box.

The Box C is shown in Plate I It was constructed in order that pyrophoric materials could be handled in an oxygen free atmosphere.

It was made from wood and consisted of an inner and outer chamber. B.O.C. "White spot" nitrogen which had been further purified by passing if through a heated tube containing potassium graphite was admitted to the inner chamber and nitrogen not purified in this way was admitted to the outer one. The pressure of the nitrogen in the inner chamber

was maintained slightly higher than that outside so that any leakage which occurred would take place outwards. Having two chambers considerably reduced the chance of oxygen contemination from the atmosphere of the laboratory.

The two chambers were geometrically similar. The interior could be viewed through perspex windows in both. Access to the interior was by elbow-length surgical gloves sealed to the outside walls. Two holes in the inner chamber wall were covered by sheets of thick rubber. Each sheet had a slot running down it and when the gloved hand was thrust through this slot the rubber sheet firmly gripped the forearm. When the gloved hands had been inserted into the inner chamber the two chambers became effectively sealed from one another. The rubber gloves were attached to the outside walls by first sealing them by means of rubber solution to thick rubber washers. These washers were then placed over holes cut in the wood and held in place by brass rings placed on top of them and screwed into the wood. The rubber sheet covering the holes in the inner chamber walls was held in place by the same means.

Nitrogen was admitted through tubes in the corners of each chamber. A small electric fan was installed to facilitate circulation of nitrogen. The inside chamber also contained a strip-light for illumination and a small electrically heated coil of wire for sealing off glass capillary tubes. The lids of each chamber could be removed for the insertion of sealed capsules of unstable materials and any other apparatus that was required. A dish of phosphorous pentoxide was set in the inner chamber

to remove moisture from the walls. Resistor units were installed so that the box could be heated and moisture in the wood expelled. The interior of both chambers was painted with white hard gloss paint to facilitate illumination and to seal cracks in the wood. All the connections through the walls were sealed with "plastic wood".

Vacuum transfer of unstable materials.

A sample of unstable material such as potassium graphite which had been prepared under vacuum conditions was opened either in the nitrogen box or under vacuum by the following method. This method was mainly employed to divide a specimen among a number of sample tubes.

Procedure.

The tube containing the unstable material was opened in the same way as the ampoule of sodium-potassium alloy already described. In this case, however, the vessel J, Fig. 60, was replaced by the vessel N as shown in Fig. 61. This was a pyrex flask fitted with a B19 socket K and four "fingers" each terminating in a B19 cone. The sample tubes L were connected to these cones and sealed with Apiezon black wax. When the tube had been opened and the system re-evacuated the powder could then be admitted to each of the sample tubes in turn by rotating the vessel about K. In some cases one of the fingers was fitted with a glass tube which had been drawn down to a capillary at one end and when powder was admitted a number of specimen tubes for X-ray diffraction could be obtained by sealing off different sections of the capillary.

When the powder had been distributed between the sample tubes, they were sealed off under vacuum at the constriction M.

The method described above proved satisfacoty except for the preparation of X-ray specimen tubes. Because the system had to be evacuated the capillary walls were of necessity thick. The absorption and scatter of X-rays which resulted from this, and the fact that the powder in the capillary could not be tamped, greatly increased the exposure time. More usually, X-ray specimen tubes were filled in the Nitrogen box.

CHAPTER 14

PART III : RESULTS

Aluminium chloride-graphite.

The compound obtained on heating natural graphite with aluminium chloride showed no apparent difference to the original graphite. The colour and shape of the flakes did not appear to be altered in any way. However when heated above 280°C these flakes rapidly expanded along the hexagonal axis and then disintegrated to form a material of sooty texture. Plates III and IV show photographs of flakes before and after exfoliation. When the exfoliation was carried out in a narrow glass tube, aluminium chloride condensed on the walls.

Analysis.

Aluminium chloride was estimated as Al_2O_3 in the manner described in the previous section.

$$\frac{Al_2O_3}{2AlCl_3} = \frac{\text{wt. of oxide}}{\text{wt. of chloride}} = \frac{101.94}{266.94}$$

$$\text{wt. of chloride} = \frac{266.94 \times \text{wt. of oxide}}{101.94}$$

$$\text{wt. of compound} - \text{wt. of chloride} = \text{wt. of carbon}$$

$$\frac{\text{Moles carbon}}{\text{Moles chloride}} = \frac{\text{wt. of carbon} \times 133.47}{12 \times \text{wt. of chloride}}$$

wt. of cpd. g.	wt. of oxide	wt. of chloride	wt. of carbon	Moles C / Moles $AlCl_3$
0.1590	0.0165	0.043	0.116	30
0.1864	0.0181	0.047	0.139	33



PLATE III

Aluminium-chloride-graphite flakes



PLATE IV

Aluminium-chloride-graphite flakes
after exfoliation.

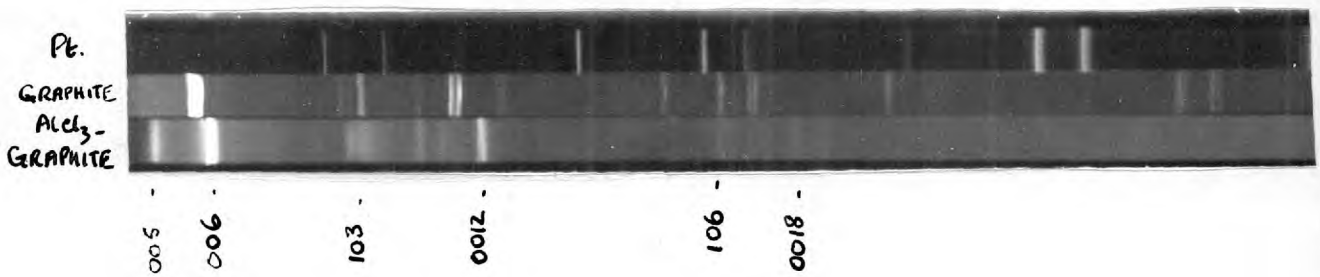
The Inter-lamellar distance in Aluminium chloride graphite.

An X-ray diffraction photograph of the compound $C_{33}AlCl_3$ is shown in Plate V together with one of the original graphite and a platinum reference. The reflections were measured and the corresponding spacings calculated. It was found that the spacings could be ascribed to the following indices.

TABLE XIX

Sin θ	d Å	Visual Intensity	Index h k l
0.1942	3.969	S	005
0.2396	3.217	VS	006
0.3624	2.127	fs	100
0.3738	2.062	fs	103
0.4236	1.819	fs	0011
0.4454	1.730	W	106
0.4792	1.608	S	0012
0.6278	1.227	W	110
0.6615	1.165	fs	1114
0.6897	1.117	VW	0018

S = strong; VS = very strong; fs = fairly strong; W = weak.

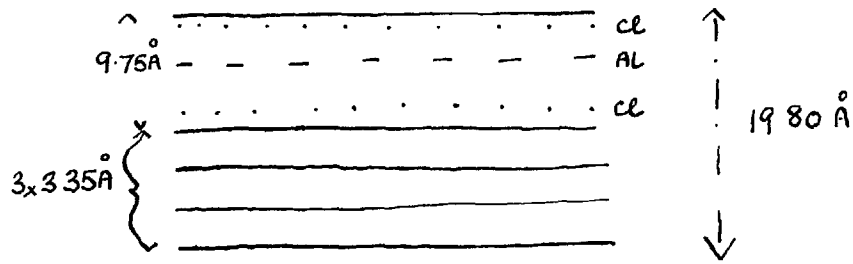


Monochromatic Radiation

12 Hours 45 kv. 50 ma.

PLATE V

The "a" dimension of the Unit cell was taken to be 2.45Å, i.e. the same as that of graphite (this is true for all the lamellar compound) and from the ool reflections the "c" dimension was calculated as 19.80Å. The "c" dimension of the unit cell can then accommodate three unexpanded graphite spacings of 3.35Å and one expended spacing of 9.75Å, viz.



Thermo-electric power of aluminium chloride graphite.

The aluminium-chloride compound was prepared from Madagascar flake graphite. The thermo-electric power of this graphite was +7μv/°C and that of both the C_{30} and C_{33} compounds was +32μv/°C, Fig. 62.

The effect of flash sintering on the electrical resistance and on its temperature variation of aluminium chloride-graphite.

The irregularities in the packing of the flakes made accurate determination of the specific resistance of aluminium chloride-graphite impossible. This was the same effect as described in Part I. However the order of resistances obtained was such as to suggest that there was not a marked difference between the specific resistance of natural flake graphite and its compound with aluminium chloride.

Specific resistance =

$$\left(\frac{1}{\text{specific conductance}}\right) \frac{\text{Resistance in ohms x cross sectional area in cm.}}{\text{column height in cm.}}$$

For Madagascar graphite Table V Part I the scatter of results lay between the limits 5.3×10^{-3} ohm.cm. (94 $ohm.^{-1}cm.^{-1}$) and 1.0×10^{-2}ohm.cm. (184 $ohm.^{-1}cm.^{-1}$).

For aluminium chloride-graphite ($C_{33}AlCl_3$) the results lay between 1.2×10^{-2}ohm.cm. (83.5 $ohm.^{-1}cm.^{-1}$) and 1.86×10^{-2} (53.7 $ohm^{-1}cm^{-1}$).

(The results compared are those obtained after flash sintering.)

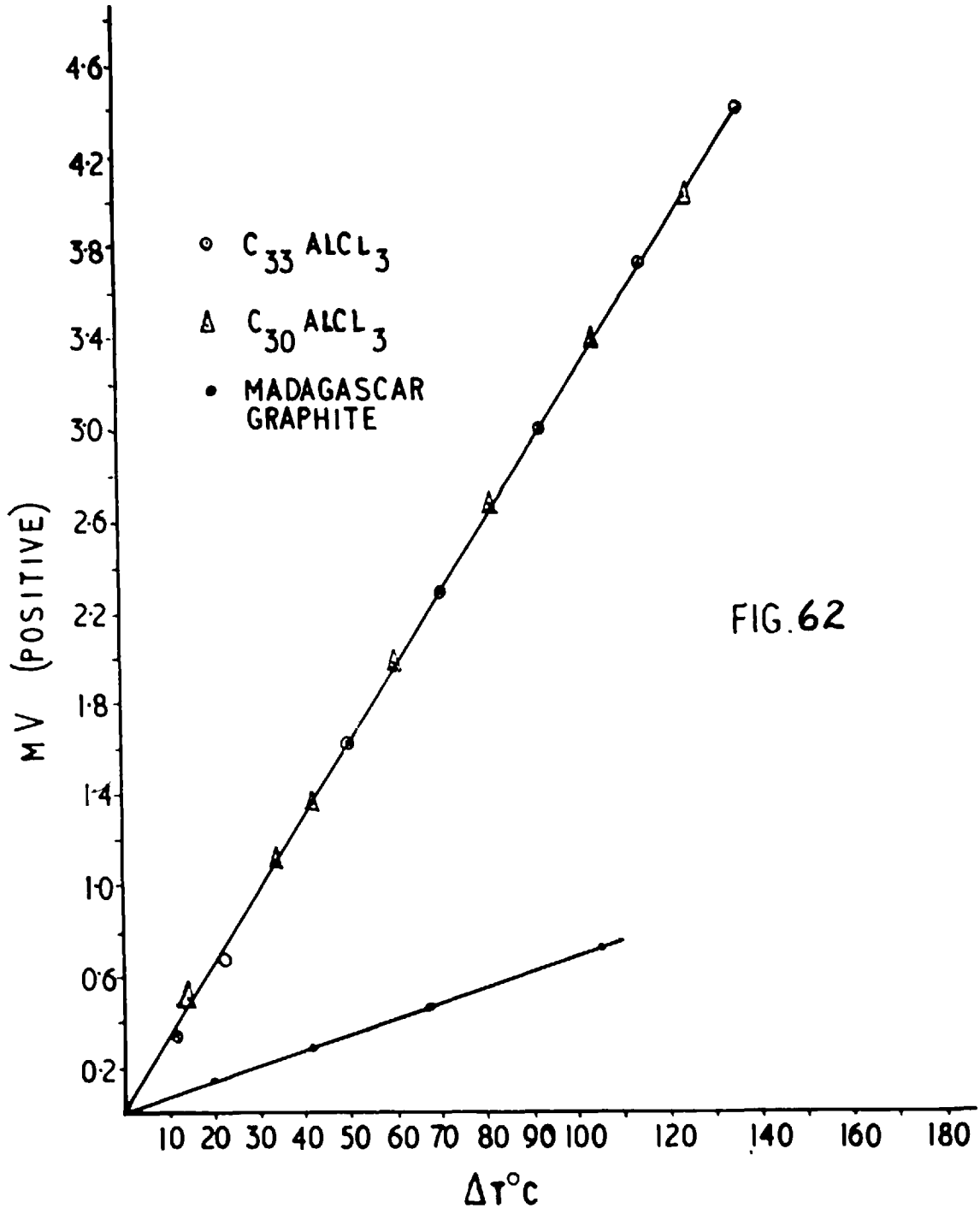
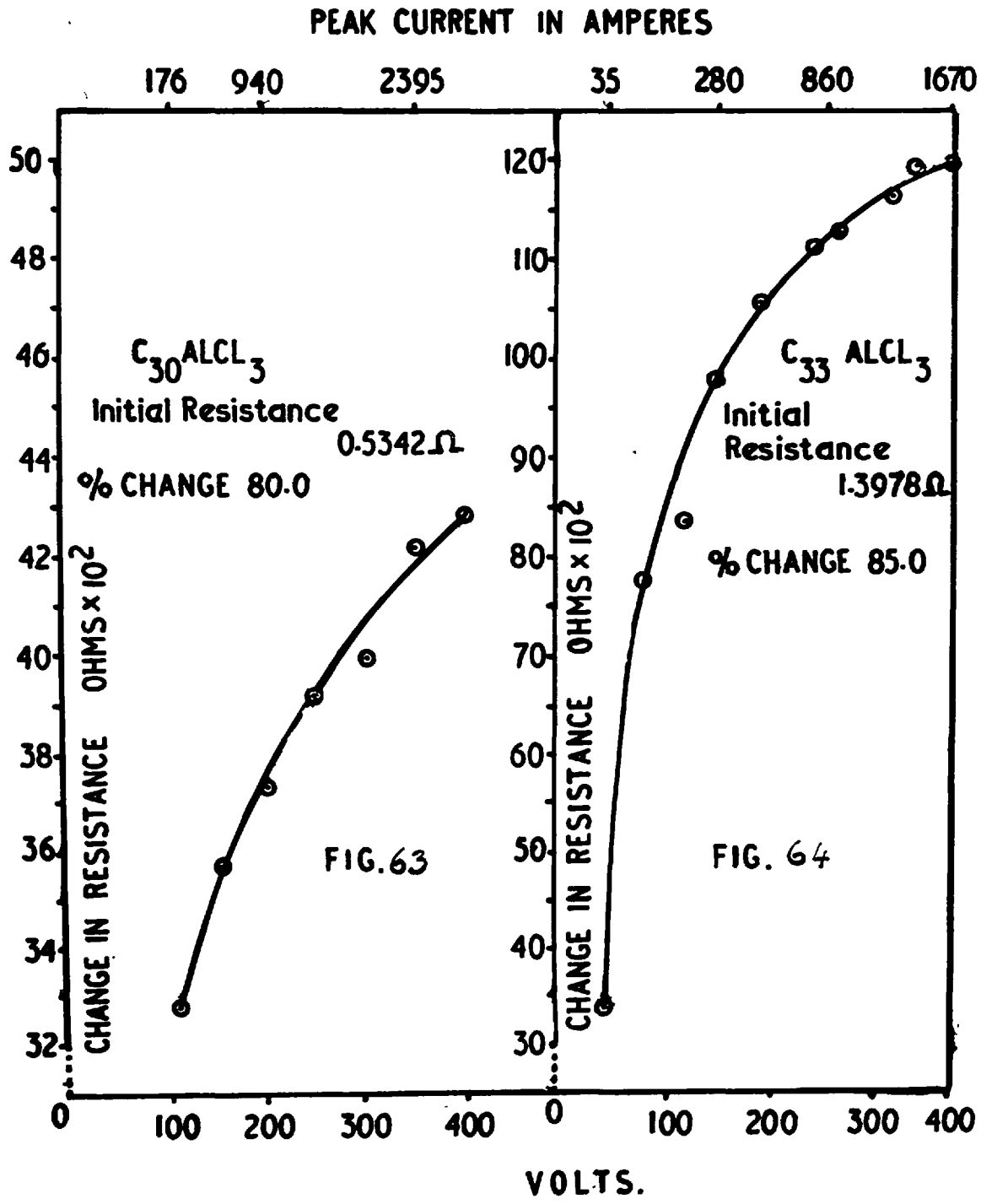
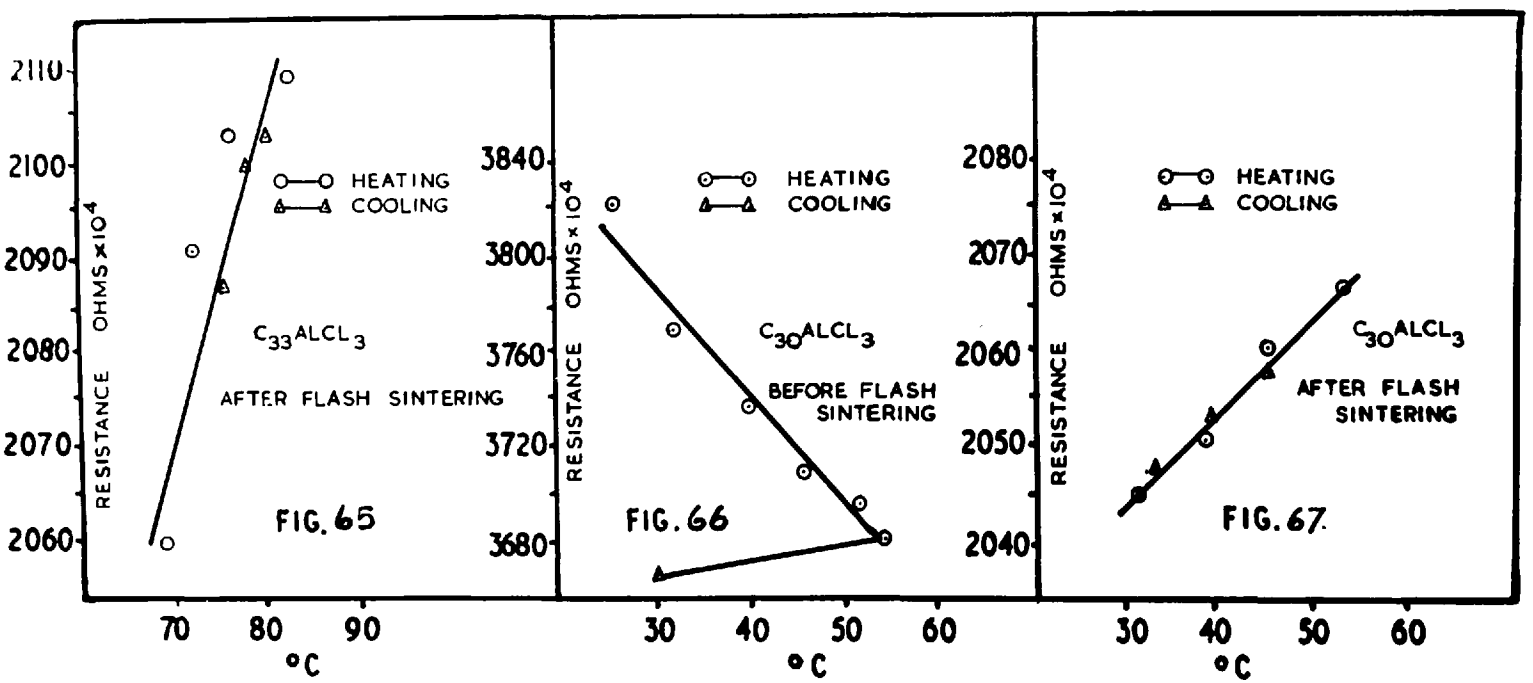

4·6
4·2
3·8
3·4
3·0
2·6
2·2
1·8
1·4
1·0
0·6
0·2
MV (POSITIVE)
C33 ALCL3
C30 ALCL3
MADAGASCAR GRAPHITE
10 20 30 40 50 60 70 80 90 100 120 140 160 180
ΔT°C

FIG. 62

Flash sintering decreased the electrical resistance of compacts of the compound in a very marked way. Figs. 63 and 64 show two of the curves obtained. Total resistance decreases in the range 40 - 85% were observed. The temperature variation of the electrical resistance was difficult to measure before flash sintering due to drifting values, Fig. 66. After flash sintering, however, the resistance consistently increased with increasing temperature. Figs. 65 and 67.


PEAK CURRENT IN AMPERES
176
940
2395
35
280
860
1670
$C_{30}ALCL_3$
Initial Resistance
0.5342Ω
% CHANGE 80.0
CHANGE IN RESISTANCE OHMS x 10^2
FIG.63
C_{33} $ALCL_3$
Initial
Resistance
1.3978Ω
% CHANGE 85.0
CHANGE IN RESISTANCE OHMS x 10^2
FIG. 64
VOLTS.


2110
2100
2090
2080
2070
2060
RESISTANCE OHMS×10⁴
HEATING
COOLING
C33ALCL3
AFTER FLASH SINTERING
70
80
90
°C
FIG. 65
3840
3800
3760
3720
3680
RESISTANCE OHMS×10⁴
HEATING
COOLING
C30ALCL3
BEFORE FLASH SINTERING
30
40
50
60
°C
FIG. 66
2080
2070
2060
2050
2040
RESISTANCE OHMS×10⁴
HEATING
COOLING
C30ALCL3
AFTER FLASH SINTERING
30
40
50
60
°C
FIG. 67

The change in electrical resistance of "a" and "c" axis graphite when exposed to bromine vapour.

Table XX summarises the results obtained using the apparatus shown in Fig. 59. The original graphite resistances measured were

a axis 9.9×10^{-4} ohm.cm. Conductance = 1000 $ohm^{-1}cm^{-1}$

c axis 4.4×10^{-1} ohm.cm. conductance = 2.5 $ohm^{-1}cm^{-1}$

TABLE XX

t min.	$\frac{\rho a}{\rho o^a}$	$\frac{\rho c}{\rho o^c}$	Mole fraction bromine in CCl_4
1	0.806		0.02
36	0.740	0.65	
82	0.697		
240	0.680	0.60	

ρ_o is the initial resistance before exposure to bromine.

ρ is the resistance after time 't'

$\frac{\rho}{\rho_o}$ is therefore the relation resistance after time 't' min.

After 240 minutes the graphite crystal aggregate crumbled and the experiment had to be discontinued.

As a development of this work Blackman Mathews and Ubbelohde (93) have recently succeeded in measuring the resistance changes along the two main axes of highly crystalline pyrolytic graphite which take place in bromine and potassium graphite formation. They found the resistance along the c axis in bromine graphite to be about two thirds the original resistance while the resistance along the a axis fell to about one tenth

its original value.

Where potassium graphite was concerned their results showed that the a axis exhibited approximately the same decrease as in the case of bromine graphite, but the c axis resistance decreased by a factor of 200.

Bromine Graphite.

Bromine graphite was prepared from natural graphite and analysed by direct weighing.

wt. of graphite 0.9835

wt. of Bromine graphite 1.8528

$$\frac{\text{Moles Carbon}}{\text{Moles Bromine}} = \frac{0.9835}{12} \times \frac{80}{0.8293} = 7.9$$

From the increase in weight the formula was taken as C_8Br

Inter-lamellar distance in Bromine-graphite.

Plate VI shows the X-ray diffraction photograph of bromine graphite Only ool reflections were obtained, viz.

Spacing dÅ	h k l
10.38	002
5.17	004
3.46	006
1.71	0012



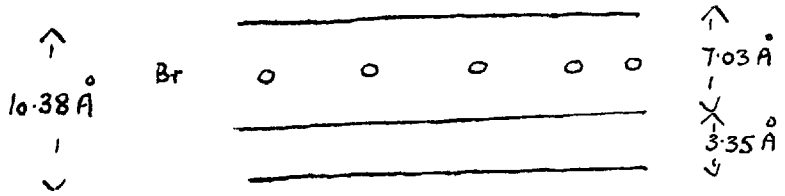
Monochromatic Radiation

10 hours 45 kv. 50 ma.

~~Bromine~~ Bromine-Graphite

Plate VI

The 10.38 spacing may be represented by one unexpanded graphite spacing and one expended to 7.03Å to accommodate bromine, viz.



Exfoliation of Bromine Graphite.

When heated to 150°C a flake of bromine graphite expanded rapidly along the hexagonal axis. This expension is some cases was over fifty times the original thickness. A feature which distinguished the exfoliation of bromine graphite from that of the aluminium chloride compound was that whereas in the latter case the flake was completely shattered in the case of bromine graphite when heating was discontinued, the expanded lamellae slowly closed until the original size and shape were regained. Plate VII shows a flake before heating and Plate VIII a flake in the process of exfoliation.

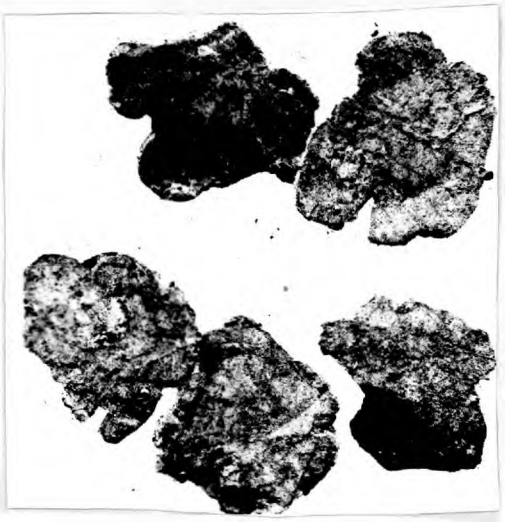


PLATE VII

Bromine-graphite flakes

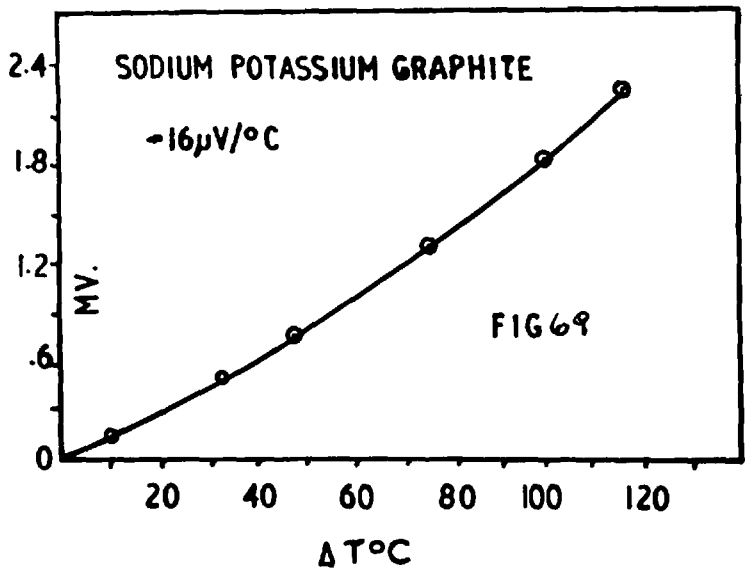


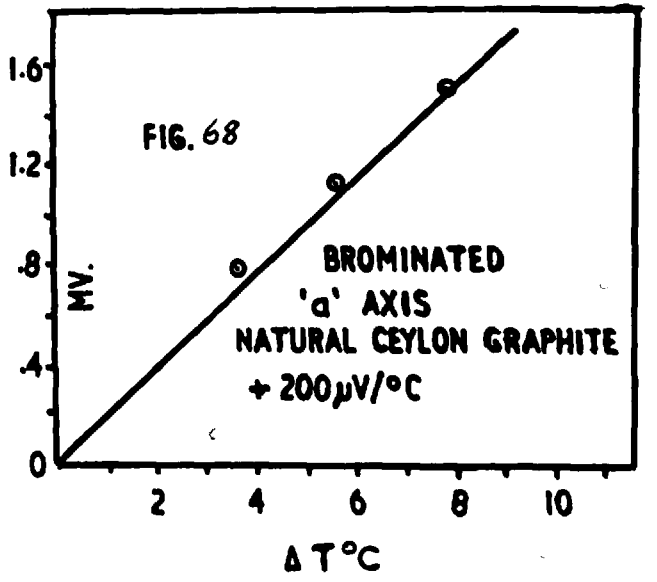
PLATE VIII

Bromine-graphite flake during exfoliation.

Thermo-electric power.

The thermo-electric power of bromine graphite in the form of powder and flake has been investigated by McDonnel Pink and Obbelohne (36). In the present work thermo-electric power was measured along the plane of a highly orientated aggregate of natural graphite crystallites which had been exposed to bromine vapour. A large positive EMF of 200μv/°C was obtained, Fig. 68.


SODIUM POTASSIUM GRAPHITE
+16μV/°C
FIG 69
MV.
2.4
1.8
1.2
.6
0
20
40
60
80
100
120
Δ T°C


FIG. 68
BROMINATED
'a' AXIS
NATURAL CEYLON GRAPHITE
+ 200μV/°C
MV.
1.6
1.2
.8
.4
0
2
4
6
8
10
Δ T°C

The reaction between sodium-potassium alloy and graphite.

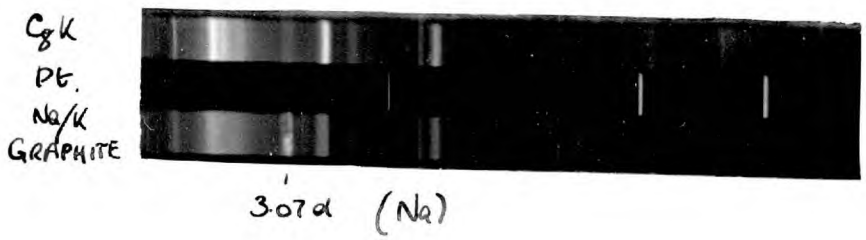
When the sodium-potassium alloy was poured into the graphite compartment, Fig. 60, heat was immediately evolved and it was observed that the liquid alloy "wet" the graphite. The graphite became silvery white then blue-green and finally a dull brown colour. The product was not however homogeneous. Some particles of powder had a dull white coating. The tube containing the product was sealed under vacuum and heated to 250°C for five hours. The tube was opened in the nitrogen box and some brown particles hand picked for examination by X-ray diffraction and thermo-electric power measurements.

Nitrogen connections to the cell shown in Fig. 14 were made inside the box and when some of the brown material had been poured in, the cell was removed to the thermostat.

The X-ray diffraction patterns of the product of the reaction.

Plate IX shown the X-ray photographs obtained. Potassium graphite C_8K and platinum photographs were also taken for comparison and reference. The spacings observed were -

C_8K		Na/K graphite
d	h k l	d
5.40	004	5.40
4.19	101	4.19
3.02	105	3.01
2.04	116	1.99
1.23	220	1.23
1.12	228	1.12
		3.07



Sodium Potassium-Graphite

Monochromatic Radiation

12 hours 45 kv. 50 ma.

PLATE IX

It can easily be seen that with the exception of the 3.07Å spacing all the others given by the product of the alloy - graphite reaction correspond to those of potassium graphite. The 3.07 spacing is one of pure sodium (011 Index) which is further borne out by the spotty nature of this reflection. Plate IX.

The thermo-electric power of the reaction product.

Fig. 69 shown the thermal EMF curve obtained. The cold junction was negative and the thermo-electric power taken as the slope of the line was - 16μv/°C.

CHAPTER 15

PART III:DISCUSSION

Aluminium chloride-graphite

The fact that after heating graphite with aluminium chloride under vacuum an X-ray diffraction pattern was obtained from the material which could be consistently indexed on the basis of an expanded graphite c spacing was positive evidence that reaction had occurred.

The above evidence, taken in conjunction with the fact that the flakes could be made to exfoliate on heating, liberating aluminium chloride was proof that an aluminium chloride-graphite lamellar compound had been formed.

The c dimension of the unit cell obtained from X-ray data was 19.80Å. This distance can accommodate one expanded spacing of 9.75Å and three normal graphite spacings of 3.35Å each. In the pure crystalline state, aluminium chloride is laid down in a layer structure with hexagonal symmetry. The c dimension of the unit cell is 17.92Å(49) with a distance of 1.34Å between the chlorine and aluminium layers.

The sum of the carbon-chloride-aluminium-chlorine-carbon distances works out as 9.65A, taking the distance between carbon and chlorine to be the sum of the van der Waal's contact radii ie 1.675Å(half the graphite ring thickness)+ 1.80Å(the radius of a chlorine atom,--Cl^- has effectively the same radius--(50a)). This is close to the observed value of 9.75A and lends support to

the hypothesis that aluminium chloride is laid down in graphite in much the same way as in the pure crystalline state.

The type of bonding involved in this compound cannot be completely specified at this stage. The evidence of the thermo-electric power however shows that the contribution of holes to conduction processes has been increased, the value of the thermo-electric power changing from $+7\mu v/^{\circ}C$ for the original graphite to $+32\mu v/^{\circ}C$ in the compound. This could be brought about by transfer of charge from the graphite π electron system to the aluminium chloride molecules.

The fact that the compound exfoliates violently and gives up its aluminium chloride on heating to 280°, i.e. only some $20^{\circ}C$ above the temperature of preparation suggests that the forces stabilising the compound are not very great and that the dissociation vapour pressure of the compound at a temperature T_2 is equal to the vapour pressure of aluminium chloride at the preparation temperature T_1 where $T_2 = T_1 + 20^{\circ}C$. In this respect the compound approximates to a solid solution and may be compared with bromine graphite when a solid solution is even more closely resembled. The latter compound is only stable in the presence of bromine vapour but if it is allowed to stand in air, bromine is steadily given off until only a "residue" compound remains. (81).

The weak bonding between graphite and aluminium chloride is further indicated by the fact that the inter-lamellar spacing calculated from X-ray diffraction results is not much different (0.11Å greater) from the sum of the bond distances across an aluminium chloride layer and

the sum of the repulsion radii of two graphite carbon atoms. If appreciable electron interaction took place between aluminium chloride and the carbon lamellae the inter-lamellar spacing calculated from X-ray data would be expected to be smaller than that estimated from a straight sum of inter-atomic distances.

It seems likely that aluminium chloride and the carbon layer planes form bonds of the polarisation type found, for example, between bromine and smaller ring systems (94). The proximity of electro-negative chlorine atoms to the easily polarised π electrons of the aromatic ring system could lead to some transfer of charge to the chloride molecule. Weyl (95) and Hennig (96) suggest that charge transfer interactions can take place over considerable distances by way of associated anions. In the crystalline state of aluminium chloride the chlorine atoms are octahedrally co-ordinated to the aluminium in $3S\ 3p^3 3d^2$ orbitals and long distance charge transfer of the type mentioned above might occur from the graphite to the vacant d orbitals of aluminium through the chlorine anions. Charge transfer interactions of this type would create electron traps in the carbon layer planes, sites in the vicinity of which electrons could reduce their potential energy and so tend to become localised.

Electrical Resistance and flash sintering.

Flash sintering had a marked effect on the electrical resistance of the compound. Before flash sintering drift of resistance was very pronounced and a reproducible temperature variation of resistance could not be measured because of it. Fig. 66. Figs. 63 and 64 show

the change of resistance observed on flash sintering. Resistance decreases of the order of 80% were observed; compare the 40% decrease of the original graphite, Table V. Part of the large resistance decrease of the compound on flash sintering is possibly due to removal of aluminium chloride adsorbed on the contact surfaces of the graphite flakes. Although precise values could not be obtained it seems likely that there is no great difference between the specific conductance of natural flake graphite and a compound of this material with aluminium chloride. The scatter of specific conductances for the compound and the original graphite lay between 54 and 84 $ohm.^{-1}cm.^{-1}$ and between 94 and 180 $ohm.^{-1}cm.^{-1}$ respectively.

From the previous remarks concerning the weakness of electron interaction between the intercalated aluminium chloride molecules and the graphite layer planes, in this compound intercalation may be anticipated as having only a slight influence on the electrical conductivity. In polycrystalline graphite, electrical conduction is mostly "a" axis conduction (45) and this will be especially true where aggregates of natural flakes are concerned. In Part I an instance was observed where the electrical resistance of a natural flake graphite increased with temperature like a metal. This is the type of variation observed along the "a" axis in single crystals. A similar type of variation was observed in the aluminium-chloride compound.

In "a" axis conduction the current is borne along the layer planes and with only slight electron interaction between the aluminium chloride molecules which are between the layers little change might be

expected on compound formation.

The thermo-electric evidence suggested that the contribution of holes to the conduction process had been increased. An increase in the number of holes would increase the total number of carriers and hence the electrical conductivity. The results obtained from conductivity measurements did not enable small changes to be detected but they did suggest that the electrical conductivity of graphite is not greatly affected by forming a lamellar compound with aluminium chloride. The ferric chloride-graphite compound has also been reported as having a conductivity little different from that of graphite (87). Conduction processes in graphite are not simple. In the first instance graphite is a two carrier system and the total conductivity thus depends upon four factors

1) The number of conduction electrons
2) The mobility of conduction electrons
3) The number of conduction holes
4) The mobility of conduction holes

i.e. the conductivity σ is given by

$$\sigma = n_s e\mu_s + n_p e\mu_p$$

where "μ" represents the mobility and "n" the number of charge carriers. Sunscripts s and p refer to electrons and holes respectively and "e" is the electronic charge (61). Secondly the marked differences in conductivities along each of the major graphite axis makes interpretation of conductivity changes on compound formation difficult. Recently Ubbelohde Blackman and Mathews (93) have shown that c axis conduction

can be increased by a factor of 200 in the case of potassium-graphite while the a axis conductivity increases ten times.

With regard to the molecular compounds aluminium chloride-graphite and ferric chloride graphite, it is possible that if intercalation increases the number of holes in the π band the effect of this increase in increasing the conductivity is offset by greater scattering caused by the presence of bulky molecules between the layers. The increased positive thermo-electric power which suggested the presence of extra holes in the π band and which raised the question of why the condictivity was not increased can be interpreted however in terms of a reduced electron mobility, (Chapter 8). This latter interpretation may be of particular relevance where the acceptor molecule in question utilises weak charge transfer bonds as has been suggested earlier in the case of aluminium chloride-graphite. In the case of these weak bonds it may be no longer true to assert that an acceptor molecule creates holes in the π band since the new energy levels associated with the charge transfer bond may lie sufficiently far above those of valence electrons to ensure that electrons will not be removed from the valence levels. A similar situation occurs in Germanium where Read and Schokkely have shown (97) that plastic deformation may lead to a dislocation in the interior of the crystal and a row of what they call "dangling" bonds along the edge of the dislocation. These dangling bonds constitute acceptor sites but the attractive forces associated with them are not strong enough to break an electron pair bond between atoms. The energy levels of these acceptor sites lie mich closer to the conduction band in Germanium and so it is the conduction electrons which are removed to

pair with "dangling bonds." This reduces the conductivity. The main effect of such an acceptor molecule may be to cause polarisation of electrons which would reduce their mobility. It is possible that while graphite compounds containing "excess" electrons, represented by potassium graphite and those compounds containing "excess" holes represented by bromine graphite are well established, a third group of compounds, represented by aluminium chloride-graphite, exists in which the total number of charge carriers with respect to the original graphite is unaltered and the mobility of electrons reduced. Such a group of compounds would be expected to show enhanced hole contributions to the thermo-electric power and Hall co-efficient while exhibiting a somewhat reduced electrical conductivity.

The graphite compound with chlorine and aluminium chloride.

In a paper published concurrently with this work (89) Rudorff found that graphite would readily react with graphite if chlorine gas was present. He found that a number of different compounds were formed each containing differing amounts of aluminium chloride. He was not able, however, to determine the amount of active chlorine. Hennig then investigated the effect of chlorine and concluded that it was bound in stoichiometric amounts with the aluminium chloride molecules in the ratio of 1:3 (90). Hennig postulated a complex of the form

$$C_n^{+}Cl^{-}3AlCl_3$$

in which the negative charge is associated with chlorine and n varies

between 30 and infinity. He measured the Hall effect of the compound and found that it indicated increased hole conduction. Most of Hennigs measurements were performed on compounds containing very little $AlCl_3$ e.g. on compound in which the ratio of carbon atoms to aluminium chloride molecules was of the order of 200:1. For these dilute compounds he found an increase in electrical conductance. It seems fairly certain that the aluminium chloride compounds prepared in the presence of chlorine and the ones described in the present work are distinct from one another. Hennig's dilute compounds do not represent true equilibrium compounds being prepared simply by allowing decomposition to proceed for different periods of time. His technique was to prepare a compound at 210°C by heating artificial graphite and aluminium chloride together under one atmosphere of chlorine for 24 hours. The compounds he chose for measurement were prepared from this compound by heating it to 450°C under vacuo and holding that temperature for different times. He points out that some decomposition was observed at 150°C but does not state whether his compound exfoliated or not. In the present work the compound prepared exfoliated violently at 280°C. The measurements of Hennig undoubtedly show the effect of incorporating chlorine and aluminium chloride into graphite but the observations might be better attributed to the "impurity" effect of chlorine and aluminium chloride in graphite rather than to compound formation involving these molecules.

In Rüdorff's X-ray investigation of his compounds he observed that the structure of the $C_{36}AlCl_3$ compound was such that the unit cell consisted of one occupied layer with an expanded spacing of 9.60Å and three normal graphite spacings of 3.35Å. This may be compared with the structure deduced for the compound $C_{33}AlCl_3$ in the present work in which the unit cell consisted of three normal graphite spacings and one expanded spacing of 9.75Å. Measurements of the electronic properties of Rüdorff's lamellar compounds would be interesting to compare with the results obtained in the present work, since they might be expected to show differenced due to the presence of active chlorine in his compound. It is known that chlorine itself can form a lamellar compound with graphite (98) the formula being C_8Cl and with aluminium chloride and chlorine both present, the primary bond is probably between the carbon macro-molecules and chlorine, electron transfer in which the chlorine becomes negatively charged largely determining the binding energy of the compound. The bonding between the active chlorine and aluminium chloride may be due to charge transfer interactions in which the d orbitals of aluminium are involved.

From the evidence obtained in this work, it may be said that

1) Natural flake graphite forms a compound with aluminium chloride when the two are heated together in vacuo at 260°C. The empirical formula corresponds to $C_{33}AlCl_3$.

2) From X-ray diffraction measurements the C dimension of the unit cell of this compound is 19.80Å long. This corresponds to one

expanded graphite spacing of 9.75Å and three normal graphite spacings of 3.35Å. Thus the inclusion of aluminium chloride expands the graphite lamellae from 3.35 to 9.75Å.

3) The electrical conductance of the compound is of the same order as the original graphite.

4) The thermo-electric power of the compound is significantly more positive that the original graphite indicating that aluminium chloride acts as an acceptor molecule.

5) The carbon lamellae rapidly expand and the whole structure disintegrates when a flake of the compound is heated to 280°C in air or nitrogen when aluminium chloride in given off which will then condense on a cold surface.

6) The bonding between aluminium chloride and the graphite carbon is weak and probably corresponds to polarisation forces.

Bromine-Graphite.

In a bromine atmosphere graphite takes up bromine and releases it again in an atmosphere of air. Trace amounts of bromine, however, are retained in the graphite, e.g. flakes of bromine graphite which were left in air for two weeks still exfoliated when heated to about 150°C. Plates VII and VIII. These trace amounts probably correspond to bromine which has been bound at imperfections or substituted at sites where hydrogen was still present. However, the large diamagnetism of graphite is destroyed when bromine is intercalated (36) indicating significant interaction between the bromine species and the graphite π electrons. In the present work it was observed when a graphite bar was connected in series with a galvonometer using platinum leads, and one end of the bar was wet with bromine, a current was produced in the circuit. Thie current quickly fell but it strongly suggests that bromine negative ions are formed in graphite and that they diffuse rapidly throughout the material.

A well orientated piece of crystalline graphite did not yield an X-ray diffraction pattern capable of supplying much structural information once it had been exposed to bromine. The material had been prepared for examination by allowing a sliver of natural graphite contained in a specimen tube and with its a axis lying parallel to the specimen tube to take up bromine before sealing the tube. However, the bromine must have destroyed the crystallinity of the

graphite for most of the reflections obtained were weak. As was also observed by Rüdorff, only ool lines were obtained. The C dimension of the unit cell was found to be 10.38Å corresponding to one expanded spacing of 7.03Å and a normal graphite spacing of 3.35Å.

Electrical resistance of bromine graphite.

The influence of bromine on the electrical resistance of well-orientated graphite can be seen from Table XVIII. McDonnell Pink and Ubbelohde (36) first showed that bromine decreased the electrical resistance of powdered graphite. In this work it has already been demonstrated that this must have been a true intrinsic effect of the solid and not due to a decrease in the inter-crystalline resistance. It was then of importance to know which orientation in the crystal was most affected by compound formation. The results given in Table XVIII give some indication of the effect. They are not conclusive but it must be stressed that it is extremely difficult to obtain specimens of well orientated graphite large enough to permit this type of investigation. The specimen had to be large enough to permit electrodes to be attached along each main crystal orientation. The results obtained before the specimen crumbled were not numerous but they are considered to be of interest since the effect of bromine was measured in the two main crystal directions on the same specimen. It was intended to study the effect of bromine at different partial pressures by using different mole fractions of bromine in carbon tetrachloride. Table XVIII shows

shows that immediately the bromine/carbon tetrachloride mixture was admitted to the vessel the resistance of the graphite began to fall. But after 240 minutes the specimen crumbled and electrical contact was lost. Up to then it could be said, however, that the resistance continually decreased and that the relative decrease along the c axis was somewhat greater than that observed along the a axis. The c axis resistance after bromination was about two thirds the original resistance. The decrease of electrical resistance along the a axis of the crystal is considered to be due to an increase in the total number of current carriers, brought about by a bromine atom removing an electron from the band of graphite and thusincreasing the number of holes in that band, while by acting as a bridge structure between two adjacent carbon lamellae it might also provide a path across which electrons might flow in c axis conduction, thus reducing the c axis resistance.

This work on bromine graphite described in the Chapter was the beginning of an investigation in which it was hoped to clarify the influence of compound formation on the anisotropic properties of single crystal graphite. It was severely limited by the fact that good graphite crystals are very difficult to obtain. However, by the use of pyrolytic graphite which can be so well crystallised that it exhibits all the known anisotropic effects of single crystal graphite, Ubbelohde, Blackman and Mathews (93) have recently succeeded in measuring accurately the electrical resistance changes which take place on compound formation. They found that in

bromine graphite the c axis resistance was reduced by about one third and the a axis resistance fell to about one tenth its original value. They also observed that most of the total resistance decrease occurs in the preliminary stages of bromination. This confirme the effects observed in the present work where the resistance was found to decrease immediately on the introduction of a bromine/carbon tetrachloride mixture in which the bromine mole fraction was 0.02.

Thermo-electric power measurements.

Fig. 73 shows the results obtained when the thermal EMF of a well orientated piece of brominated natural graphite was measured along the a axis. The EMF was strongly positive and equal to $+200\mu v/^{o}C$. This is clear evidence of hole conduction.

Conclusions.

The intercalation of bromine between two carbon lamellae involves an expansion of the interlamellar distance from 3.35 to 7.03Å. Rüdorff quotes a value of 7.05Å.

The electrical resistance of graphite along each main crystallographic axis decreases immediately on exposure to bromine vapour. In bromine graphite, a axis conduction is mainly in the π band by holes; c axis conduction takes place possibly by means of bromine bridges and may be compared to long range charge transfer whereby charge is transferred to cations, in this case the graphite lamellae, by associated anions.

The bond between bromine and graphite in the lamellar compound does not appear to be a strong one. Bromine will, however, be more firmly bound at defect sites and edge atoms and this bromine probably represents the small fraction or residue always retained by graphite. Although bromine is readily given off and the compound resembles a solid solution, electron transfer from the carbon macro-molecules to the bromine in the lamellar compound is significant. This is indicated by the fact that the marked diamagnetism of graphite is destroyed (36), the thermo-electric power becomes markedly positive and the electrical conductivity is increased on compound formation. The evidence suggests that bromine in bromine graphite consists of ionized bromine atoms Br^{-} and bromine molecules acting as spacers between these ions, only two out of every eleven bromine atoms being ionized (96). This observation could be used to reconcile the apparent weakness of the bonding between graphite and bromine with the fact that considerable electronic interaction takes place. The bromine "spacer" molecules are probably not significantly bonded to graphite. Their main function is to keep the Br^{-} ions apart and by reducing the repulsion forces keep the potential energy of the system to a minimum. When the external bromine pressure falls these "spacer" molecules might evaporate leaving the more firmly bonded bromine ions behind. In the absence of "spacers" however inter-ionic repulsion forces may cause the potential energies of the system to increase resulting in the expulsion of most of the ionized bromine.

The reaction between sodium potassium and graphite.

No lamellar compound of graphite with sodium at the time of this work had been prepared. Recently (85) a claim has been made that small quantities of sodium can be occluded in graphite, however the fact still remains that sodium does not react with graphite with anything like the ease of potassium, rubidium or caesium. By presenting sodium to graphite in intimate association with potassium it was thought that potassium by reacting with graphite first would separate the lamellae and make possible the intercalation of sodium.

The alloy when admitted into the graphite compartment wet the graphite immediately. It was a most interesting reaction to watch. A considerable quantity of heat was given out and as the reaction proceeded the graphite changed colour frequently passing from silver through green and blue to dark brown. This colour sequence probably represents the formation of intermediate lamellar compounds. It was also observed that a dull white lumpy solid was deposited throughout the powder. This was assumed to be unreacted sodium.

The X-ray diffraction photograph of the dark brown product is shown in Plate IX. Potassium graphite (C_8K) prepared and photographed for comparison is shown as well. With the exception of one spacing all the others correspond to those of the potassium compound. The exception is a spacing characteristic of pure sodium. It would appear then that potassium reacts with graphite and leaves sodium adsorbed on the outside of the powder.

There is no obvious reason why sodium and graphite should not react or only react with extreme difficulty. In the smaller aromatic molecules, adducts are formed with lithium, sodium and potassium (99) (100); no other alkali metals appear to be investigated, and the type of bond formed is generally taken to be of the $M^{+}Ar^{-}$ type. This is most probably the type of bond formed in the compound prepared from the sodium/potassium alloy. The thermo-electric power was negative indicating transfer of charge from the metal to the aromatic network as found also for potassium graphite (36).

Ubbelohde (63) by comparing the alkali graphite with the alkali fluorides, F^{-} is about the same size as C^{-}, could find no clear thermo-dynamic reason why a sodium-graphite compound should not exist. The greater ionization energy of sodium with respect to potassium, rubidium, and caesium, would be compensated for by the greater crystal energy of sodium-graphite were it formed. While the electron affinity of fluorine is sufficient to form fluorides with all the alkali metals, where carbon macro-molecules are concerned the energy terms involved in compound formation are more nearly in balance. Ubbelohde thus concluded that the free energy of formation is small and that variables such as the extent of defect structures present could determine whether in the case of sodium-graphite the free energy of formation was positive or negative.

APPENDIX I

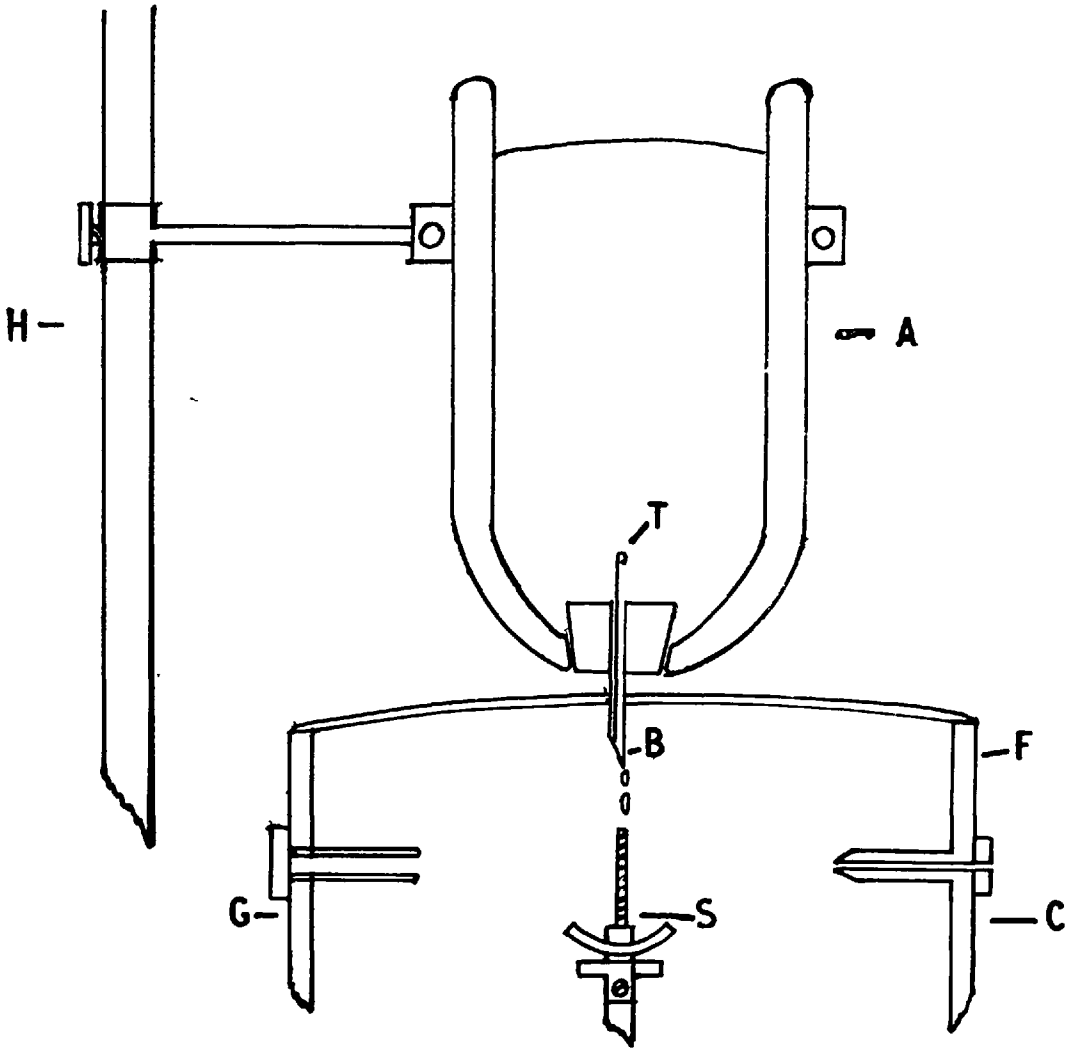
The Thermal Expansion of Graphite.

The thermal expansion of graphite was measured concurrently during the work described in Part III. It was hoped that by comparing the expansion of graphite along the hexagonal axis with that of potassium graphite in the same direction some information might be obtained about the type of bonding between potassium and the carbon layer planes. However, potassium graphite required too long an exposure time for a liquid introgen "drip" to be practicable and the investigation had to be abandoned. The apparatus used and the results obtained for graphite are recorded below.

Experimental.

The graphite measured was a piece of natural Travancore material. It was not purified in any way in order to preserve crystallinity and hence shorten the exposure time. X-ray diffraction photographs were taken at room temperature and -196°C. Details of the apparatus used in carrying out the liquid introgen "drip" are shown in Fig. 70. The container for liquid introgen was a large Dewar vessel with a hole at the bottom in the middle of which a hypodermic needle was located by means of a cork. This vessel was clamped over the specimen with a fine wire passing down the needle and poised about 1 mm. above the capillary. F is the film holder. The "drip" was commenced some 15 minutes before starting the low temperature exposure in order to allow thermal

FIG. 70



equilibrium to be attained. For each measurement, two low temperature and two room temperature exposures were taken. Two diffraction photographs of a platinium rod were also included in each film. The position of the graphite reflection chosen to indicate expansion was then measured by calibrating the film in its vicinity from the known θ values of the nearest platinum lines. The filme were measured using the instrument described in Part III. A nickel filter was employed in some exposures.

Results.

The reflections obtained from the graphite flake were so intense due to its high degree of crystallinity that exposure times were of the order of 1 minute. The preferred orientation of the individual crystallites made it possible to set the flake so that only certain reflections were obtained. Measurements were made on the 008 reflection since this had a ool indices and therefore represented the interlayer spacing uniquely. Its high θ value meant that for a given expansion its movement was considerably greater than those ool reflections of lower orders and could be expected to give more accurate results. Previous published results had all been made using the lower orders of ool since the intensity of the 008 had not been found high enough to permit accurate measurement.

The results obtained are shown below. Diffraction photographs are reproduced in PLATES XX and XXI

The values for the "c" dimension represent the mean of four sets of determinations. The mean deviation was 1×10^{-3} for the room



PLATE X

Unfiltered

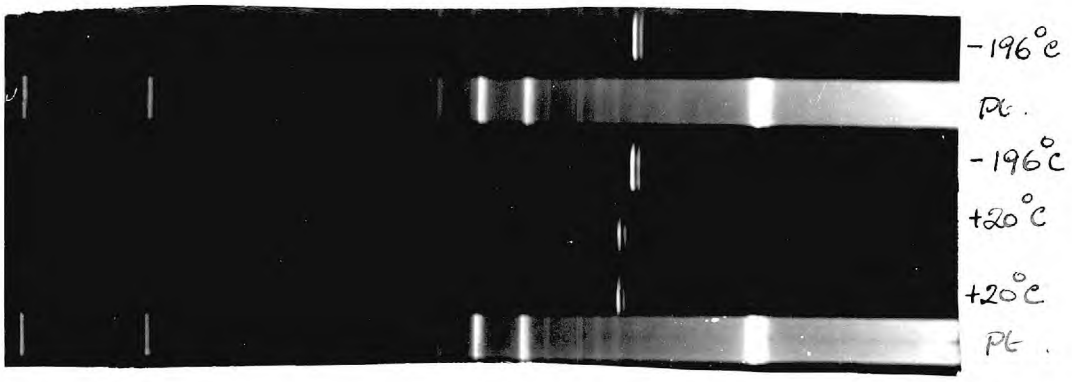
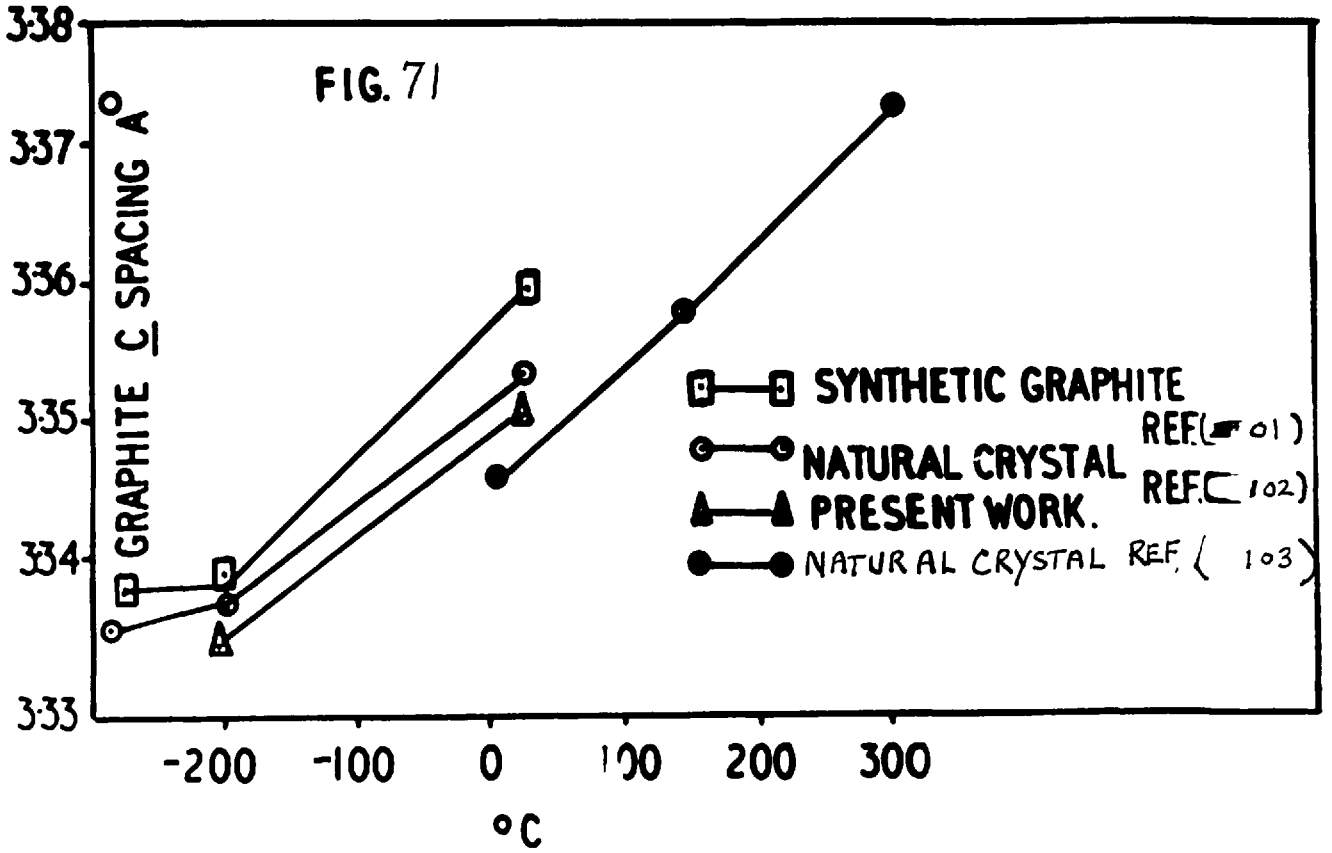


PLATE XI

Nickel filter


FIG. 71
3·38
3·37
3·36
3·35
3·34
3·33
GRAPHITE C SPACING A°
-200
-100
0
100
200
300
°C
SYNTHETIC GRAPHITE REF.(101)
NATURAL CRYSTAL REF.(102)
PRESENT WORK.
NATURAL CRYSTAL REF.(103)

temperature exposures and for those made at liquid nitrogen temperatures was 4×10^{-4}.

Reflection	Temperature	c dimension Å
008	20°C	6.7028
	-196°C	6.6708

$$\alpha_{\parallel} = \frac{1}{c} \frac{\Delta c}{\Delta T}$$

$$= 2.21 \times 10^{-5}$$

Fig. 71 shows these results and the results of other workers for the change of the c spacing with temperature.

Discussion.

The thermal expansion of graphite is much greater along the c axis than parallel to the basal plane. This may be readily understood because of the lack of strong binding forces between the layers. It is of interest to enquire into the nature of the inter-layer binding forces when intercalated species are present.

Measurements of thermal expansion along the c axis of a lamellar compound will give some information about the strength of bonds between the intercalated species and the carbon macromolecules, a reduced expansion as compared to the original graphite suggesting that the foreign species serves as a link holding the layer planes more strongly together. Variations in thermal expansion values throughout a series of compounds involving foreign electron acceptors and electron donors will give a comparative measure of the extent of electron interaction in each case.

APPENDIX II

The preparation of potassium graphite.

Materials. Potassium was supplied by B.D.H. and graphite by A.E.R.E. Harwell. The graphite was supplied as powder sieved between 60 and 120 mesh.

Purification of Potassium: Method described by Lewis (101)

The potassium was supplied under oil and was purified by first dissolving off most of the oil with petroleum ether. The next stage in the purification was carried out using the apparatus illustrated in Fig. 68 (i). After washing with petroleum ether the potassium was introduced into B. Tube B was then drawn off at A with nitrogen flowing until just before the final seal was made. The system was then evacuated by means of a two stage rotary pump and a solicone oil diffusion pump. The potassium in B was melted down through D into F, i.e. through two successive capillaries C and E. A seal was made at E, and B and D drawn off. A furnace was then placed around F and at a low temperature any remaining oil distilled into H. Tube F was finally removed by sealing off at G. Before the next stage the potassium was melted into one end of the ampoule F.

Procedure.

Apparatus for carrying out the reaction was similar to that used in the aluminium chloride-graphite preparation shown in Fig. 68ii but was constructed from one cone of X8 G.E.C. soda glass which had a

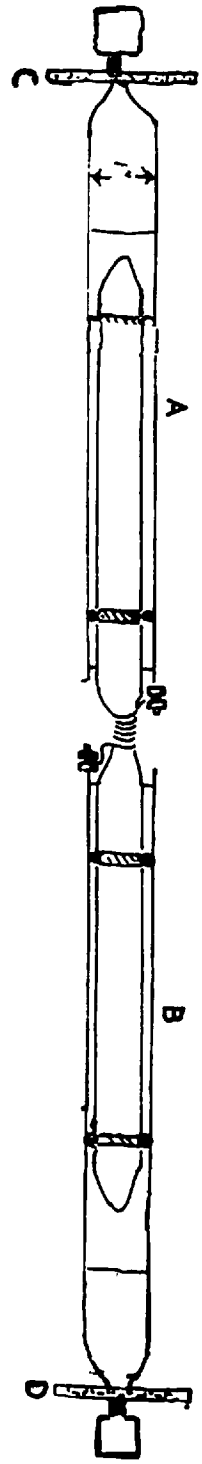


FIG. 72

flashed-on inner layer of Na_{10} which is resistant to attack of alkali-metal vapour. This was sealed at J to a socket K tapered and ground from the same glass. An amount of graphite, sufficient to form a C_8K compound, was tapped into compartment H. The inside of the socket was kept covered to avoid contact with graphite. The tube was then connected by a wax seal to the vacuum train. Nitrogen was passed through and the potassium ampoule broken and inserted into B, open end first. The tube was then sealed at A and the system evacuated as before. The graphite was then degassed by heating to 500°C. The potassium was distilled first into B and then into D, these compartments being removed in turn. The potassium was then in F and the tubes F and H with the capillary separating them at G were removed by sealing off at I. F and H were held in a metal cradle as shown in Fig. 72. A coil of michrome wire was joined to A and B such that about 10 turns were in the centre of the capillary. The cradle was then placed in a furnace. The furnace consisted of two windings of equal resistance with a centre tapping. The asbestos washers C.D. on the ends of the cradle closed the furnace. The furnace was electrically heated using constant voltage and Variac transformers. The part of the furnace surrounding the graphite was held at 400°C and that surrounding the potassium at 360°C. Temperatures were measured by Anschutz thermometers inserted into pockets in the furnace.

The reaction was completed in 24 hours, the product being a bromze coloured compound. A blue compound of potassium with

graphite was prepared by a colleague using a similar technique but lower temperatures, i.e. the graphite was maintained at 400°C and the potassium at 284°C.

The structures of the potassium graphites are well established and in the present work the compounds prepared were identified by X-ray diffraction.

REFERENCES

1. "Solid State Physics" : A.J. Dekker; Macmillan (1958) p. 302.
2. "Electrical and Magnetic Properties of Solids" : N. Cusack; Longmans (1957) p. 100.
3. "Semiconductors" : D.A. Wright; Methuen (1955) p. 51.
4. Frahklin, R.E. Proc. Roy. Soc. (Lond.) A209, 196 (1950.
5. Bacon, G. Act. Cryst. 1 337 (1948).
6. Bacon, G. Act. Cryst. 3= 137, 320, (1950).
7. Warren, B. Phys. Rev. 59, 693 (1941)
8. Biscoe, J. and Warren B. J. App. Phys. 13, 364 (1942)
9. Pinnick, H. Phys. Rev. 94, 319 (1954)
10. Trzebratowski, W. Roez. Chem. 17, 73 (1937)
11. Bernal, J.D. Proc. Roy. Soc. A106 749 (1924)
12. Hassel, O. Mark H., Z.Phys. 24 317 (1924)
13. Finch, G., Wilman, H. Proc. Roy. Soc. A155 345 (1936).
14. Lipson, H. Stokes, A. Nature 149 328 (1942)
15. Laidler, D. Taylor, A., Nature 146 130 (1940).
16. "Valence": C.A. Coulson, Oxford (1952).
17. "Graphite and its Crystal Compounds" : A.R. Ubbelohde and F.A. Lewis, Oxford, (1960) p. 71 and p. 10.
18. Coculson, C.A., Nature 159 265 (1947).
19. Wallace, P.R., Phys. Rev. 71 622 (1947).
20. Johnston, D., Proc. Roy. Soc. A227 349 359 1955.
21. Primak, W., Fuchs, L., Phys. Rev. 95, 22 (1954)
22. Soule, D., Phys. Rev. 112, 698, 708 (1958).

23. Kmetko, E., J. Chem. Phys. 21, 2152 (1853)

24. Mrozowski, S., Phys. Rev. 85, 609 (1952); 86, 105 (1952)

25. Kinchin, G.H., Proc. Roy. Soc. (Lond.) A217 9 (1953)

26. Uebersfeld, J. and Erb. Proc. 3rd Carbon Conf. Buffalo (1959).

27. Pinnick, H.T., J. Chem. Phys. 20, 756 (1952).

28. Brooks, H. J. Chem. Phys. 8 939 (1940)

29. Ganguli and Krishnan, K., Proc. Roy. Soc. A177 168 (1941)

30. Loebner, E., Phys. Rev. 84 153 (1951).

31. Gottstein, Ann. Physik 43 1079 (1914).

32. Fokuda, Saito, Elektrotech. J. Japan 2 129 (1938).

33. Hove, J. and Smith, A., Phys. Rev. 104, 892 (1956).

34. Smith, A. and Rasor, N., Phys. Rev. 104, 885 (1956).

35. Berman, R. Indust. Carbon Conf., London (1958).

36. McDonnell, M., Pink, R., Ubbelohde, A.R., J. Chem. Soc. 191 (1951).

37. "The Friction and Lubrication of Solids": Bowden, J., Oxford, 1945.

38. Bowden, J. and Williamson, Proc. Roy. Soc. A246 (1958).

39. Strout, J., Phil. Trans. Roy. Soc. 161, 77 (1871).

40. Knowles, A., Indust. Carbon Conf. London, (1958).

41. Hertz, J., Reine Angew Math. 92 156.

42. "The Friction and Lubrication of Solids": p. 62.

43. Savage, R. Ann. N.Y. Acad. Sci. 53 862 (1951).

44. Whitehead, Proc. Roy. Soc. A201 109 (1950)

45. Mrozowski, S., Proc. 3rd Carbon Conf. Buffalo (1959).

46. An Advanced Treatise of Physical Chemistry, Partington: Longmans.

48. Blackwood, J., Rev. Pure Appl. Chem. 4 251 (1954).

47. W. Jost, Diffusion Academic Press, N.Y. 1952).

49. Handbook of Chemistry and Physics; Rubber Publishing Co. 41st Ed..

50. Williamson and Adams, Phys. Rev. 111 2 (1919).

50a The nature of the Chemical Bond L PAULING CORNELL. 1948 p 189

51. Copp and Ubbelohde, A.R., Trans. Far. Soc. 44 646 (1948).

52. International Critical Tables.

53. Berman, R., Proc. Phys. Soc. 65A 102 9 (1952).

54. Alterthum, H., Fehse, W. and Pirani M.E. Elektrochem. 31 313 1925.

55. Glockler, G., J. Chem. Phys. 22 159 (1954).

56. Bassot, J. Bronnstoff, Chem. 22 127 (1942).

57. "Measurement of Inductance", Champbell and Childs; McMillan (1935).

58. Powell and Schofield, Proc. Phys. Soc. 51 153 (1939).

59. Johnson, R. Godfrey, D., Bisson, E., Naca Tech, Note 578 (1948).

60. "Physics of High Pressure"; P. Bridgeman, Bell (1931) Ch. 9.

61. "Electrical and Magnetic Properties of Solids"; N. Cusack. Longmans (1957) p.190.

62. Pirani; Fehse, Z. Elektrochem. 29 168 (1923).

63. "Graphite and its Crystal Compounds"; Ubbelohde, A.R. and Lewis, F.A. Oxford (1960). p. 98

64. Grisdale, R., Bell Syst. Tech. Jour. 30 April 1951.

65. Kapitza, Proc. Roy. Soc. A123 292 1929.

66. Dresselhaus, Kip and Kittel, Phys. Rev. 98 368 (1955).

67. Tauc. J. Phys. Rev. 95 1394 (1954).

68. Samoilouitch A, Korenblit, L., Fortschr. Phys. 1 486 (1954).

69. Johnson, V., Progress in Semiconductors, Vol. I, 1956, p.87.

70. Ubbelohde, A,R., Blackman, L., Dundas, P., Proc. Roy. Soc. A255 293 (1960)

71. Watt, W., Brown, A. Indust. Carbon Conf. 1958. London, p.86.

72. Hennig, G., J. Chem. Phys. 19 922 (1951)

73. Brennan, R. J. Chem. Phys. 20 40 (1952)

74. Schaufhautl, P. J. Prakt. Chem. 21 155 (1841)

75. Brodie, B. Phil. Trans. Roy. Soc. 149 249 (1859)

76. Rüdorff, W. Z. Phys. Chem. B45 42 174 (1939)

77. Thiele, H. Tech. Ind. Schweiz. Chem. ZTG 18 47 (1935)

78. Hofmann and Rüdorff, W. Trans. Far. Soc. 34 1017 (1938)

79. Frenzel, A. and Hofmann, U., Z Elektrochem. 40 511 (1934)

80. Rüdorff, W. Z. Anorg. Chem. 245 383 1941.

81. Hennig, G. J. Chem. Phys. 20 1438, 1443 (1952)

82. Fredenhagan and Cadenbach, Z Anorg. Chem. 158 249 (1926)

83. Schleede, A. and Wellmann M. Z. Phys. Chem. 188 1 (1932)

84. Rudorff, W. and Schulze, E. Z.Anorg. Chem. 277 156 (1954)

85. Asher, R. J.Inorg. Nucl. Chem. 10 238 (1959)

86. Thiele, H. Z.Anorg. Chemie 206 407 (1932)

87. Rudorff, W. and Schulze, H. Z.Anorg. Chem. 245 121 (1940)

88. Croft, R.C. Nature 172 725 (1953)

89. Rüdorff, W. and Zeller, R. Z.Anorg. Chem. 279 182 (1955)

90. Dzurus, H. and Hennig, G. J. Chem. Phys. 27 275 (1957): Jacs. 79 1051 (1957).

91. Rüdorff, W. and Landela, A. Z.Anorg. Chem. 293 327 (1958)

92. Croft, R.C. Aust. J. Chem. 9 184 (1956)

93. Ubbelohde, A.R., Blackman, L. and Matthews, J., Proc. Roy. Soc. A 256 15 (1960)

94. Slough, W. and Ubbelohde, A.R. J. Chem. Soc. 782 911 982 (1957)

95. Weyl, W. J. Phys. Chem. 55 507 (1951)

96. Hennig, G. Phys. Rev. 95 1088 (1954)

97. Read, W. Phil. Mag. 45 775 (1954) 46 111 (1956)

98. Juza, R. Jonck, P. and Schmeckenberger, A. Z.Anorg. Chem. 292 34 (1957)

99. Holmes Walker, A. and Ubbelohde, A.R. J. Chem. Soc. 720 (1954)

100. Gracey, J. and Ubbelohde, A.R. J. Chem. Soc. 4089 (1955)

~~101. Lewis, F.A. J. Soc. Chem. Ind. 1504 (1957)~~

101. Walker, Ind. Eng. Chem. 45 1171 (1953)

102. Baskin Meyer, Phys. Rev. 100 544 (1955)

103. Nelson, Riley, H. Proc. Phys. Soc. 57 (1945)

104. Lewis, F.A. J. Soc. Chem. Ind. 1504 (1957)

(*Reprinted from Nature, Vol.* 179, *pp.* 193–194, *January* 26, 1957)

ANISOTROPIC THERMO-ELECTRIC EFFECTS IN GRAPHITE

By Prof. A. R. UBBELOHDE, F.R.S., and J. ORR

Department of Chemical Engineering, Imperial College of Science and Technology, London

WITHIN recent years the concept[1] that graphite presents a transition between aromatic and metallic electrons has been elaborated in a number of theoretical and experimental studies. Various considerations suggest that graphite is much more markedly metallic in one principal direction in the crystals, along the *a* axis, than perpendicular to this direction, along the *c* axis. Structurally, apart from lattice defects graphite presents infinite planes of conjugated aromatic electrons along the *a* axis, whereas along the *c* axis the macro-aromatic molecules are merely bound by van der Waals types of forces, with a distance of separation of around 3·35 A. This weaker interaction is accompanied by marked anisotropy of a number of physical properties related to the electronic interactions. Thus the thermal expansions are respectively $6 \cdot 6 \times 10^{-6}$ along the metallic and $26 \cdot 0 \times 10^{-6}$ along the non-metallic directions[2] in the crystals, compared, for example, with about 14×10^{-6} and 65×10^{-6} for zinc. The hardness is $> 6 \cdot 5$ Mohs along the *c* axis and about 0·5 Mohs along the *a* axis[3]. Relative rates of oxidation along the *a* axis and *c* axis are in the ratio[3] 17 : 1. Magnetic anisotropy is shown by the marked diamagnetism along the *c* axis[4]. Thermal conductance, which is mainly due to lattice vibrations, is about 4·0 watt cm.$^{-1}$ deg. C.$^{-1}$ along the *a* axis and 0·8 units along the *c* axis[3].

These differences are perhaps no larger than may be expected for anisotropic crystal structures generally. However, a new and striking group of phenomena appear when electronic properties are examined. The specific electrical resistance has been previously measured[5] and found to be about $3 \cdot 9 \times 10^{-5}$ ohm cm. along the *a* axis and about 0·01 along the *c* axis. It is most significant that the temperature coefficient of resistance along the *a* axis is metallic in character, and is about 0·009 deg. C.$^{-1}$, whereas along the *c* axis the crystals behave as semiconductors, with a temperature coefficient of $-$ 0·04

deg. C.$^{-1}$. (Some theoretical interpretations[6] regard even the conductance along the *a* axis as of semi-conductor type, but with zero activation energy.)

These findings lend particular interest to other anisotropic electronic properties of graphite. By courtesy of the Morgan Crucible Co., we have been able to cut appropriate sections from comparatively large blocks of material in which the alignment, though not perfect, is not far from that for single crystals. Using sections about 1·5 cm. long by 3 mm. square, it is readily shown that the thermo-electric power of graphite against copper along the *c* axis is about + 30 μV./deg. C. compared with about + 11 μV./deg. C. along the *a* axis.

Measurements of thermo-electric power against copper cannot be conveniently extended to very high temperatures, for various reasons. However, it is perfectly possible to measure the self thermo-electric power of graphite to quite high temperatures, by forming thermo-junctions between blocks cut along the *a* and *c* axes respectively. This has now been done. The blocks were mounted in electrical contact in impervious tubes of mullite with copper electrodes at the cold junctions, which were water-cooled. Various exploratory researches showed that above about 250° C. the presence or absence of even traces of oxygen had a critical influence on the self-e.m.f. (*a*/*c*) of graphite. Using 'B.O.C. white spot' nitrogen with less than 10 p.p.m. of oxygen to exclude air, the self-e.m.f. of graphite has been measured up to about 1,200° C. Temperatures were measured by chromel/alumel couples in the lower regions, and by pyrometry in the higher regions. Results up to about 700° C. are quite regular, and are illustrated in Fig. 1. Above this temperature, despite all precautions, a falling off in thermo-electric power was generally observed. There are reasons to believe that this falling off was due to adventitious oxidation, despite the protective stream of nitrogen, since values of thermo-electric power were occasionally obtained which lay on the prolongation of the curve at lower temperatures (not shown). Deliberate injection of oxygen into the nitrogen stream depresses the e.m.f. The point is possibly of some technical importance, since if the self thermo-e.m.f. of graphite in the complete absence of oxygen continues to follow the low-temperature curve, then *a*/*c* combinations of graphite could form very useful thermo-electric junctions at very high temperatures. They might even be used for forming micro-power units in special circumstances.

Interpretation of these findings must necessarily be provisional at the present stage, but it accords

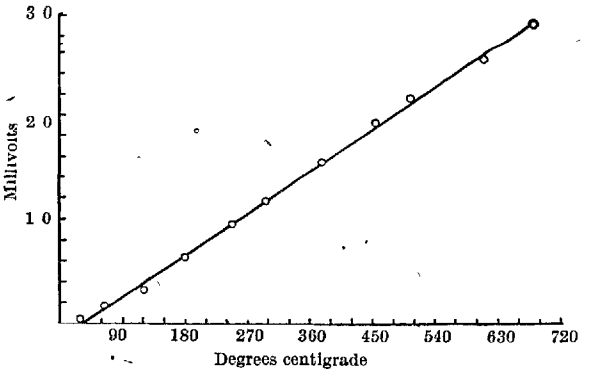


Fig 1. Self thermo-e.m f. of graphite, *a* block–*c* block

with the general view, also based on other anisotropic properties, that graphite behaves as a metallic conductor along the *a* axis and as a semi-conductor with finite energy gap along the *c* axis. The fact that the *c* blocks are positive relative to the *a* blocks can perhaps be explained as follows :

The electronic levels along both axes may be represented as in Fig. 2*A*.

In the combination described, a '*c*' block/'*a*' block junction behaves like a semiconductor-metal contact, provided no *n*-type impurities are present in the '*c*' block to donate electrons to the vacant conduction bands or that there are few such centres compared with the number of electrons in the conduction band of the '*a*' block. The topmost filled levels of the '*a*' block will be higher than those of the '*c*' block. When contact is made, these levels will be adjusted until no difference exists.

As the temperature of the '*c*' block/'*a*' block junction is raised, electrons will flow from the '*a*' to the '*c*' specimen because the work function is less for the '*a*' specimen (Fig. 2*B*).

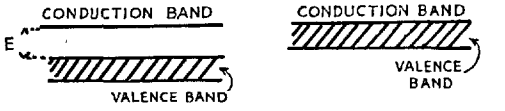


Fig. 2*A*

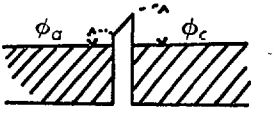


Fig 2*B*

The thermo-electric power against copper shows that in both blocks the conduction appears to be mainly by means of holes in the valence band, with a greater number of holes for movement in the '*c*' direction than in the '*a*'. The origin of these holes need not be discussed here.

In the light of this tentative interpretation, the influence of oxygen is significant. It seems highly probable that oxygen attaches itself in the first instance to all defect sites and free valencies in the macro-aromatic molecules which form layers in the graphite crystals. As a result, at each group quinone electrons are withdrawn from the co-operative aromatic pool in each macro-molecule, in a manner well known when smaller aromatic molecules form quinones. This raises the work function of the macro-quinones in the planes of the macro-aromatic molecules so that the thermo-e.m.f. of '*a*' block against '*c*' block is reduced.

This interpretation of the effect of oxygen throws an interesting light on relative rates of oxidation along and perpendicular to the *a* axis, quoted above. The effect of oxygen on the thermo-electric power of graphite concords with previous interpretations of the effect of electron acceptors in lamellar compounds[7] as in bromine graphite.

[1] Ubbelohde, ***Nature*, 132**, 1002 (1933).

[2] Beckhurst, I., *Proc. Roy. Soc.*, A, **102**, 340 (1923). Erfling, H. D., *Ann. Phys.*, **34**, 136 (1939).

[3] Values depend somewhat on methods of measurement. Those quoted are given by Grisdale, Pfister and van Roosbroeck, *Bell Syst. Tech. J.*, **30**, 271 (1951).

[4] Krishnan, *Phil. Trans. Roy. Soc.*, A, **231**, 235 (1933).

[5] *c* axis. Washburn, *Ann. Phys.*, **48**, 236 (1915). Krishnan and Ganguli, *Nature*, **144**, 667 (1939) *a* axis. Pirani and Fehse, *Z. Elektrochem.*, **29**, 168 (1923). Nishiyama, *Sci. Rep. Tohoku. Imp. Univ.*, **21**, 171 (1932).

[6] Coulson, *Nature*, **159**, 265 (1947). Wallace, *Phys. Rev.*, **71**, 622 (1947).

[7] McDonnell, Pink and Ubbelohde, *J. Chem. Soc.* (39), 191 (1951)

Printed in Great Britain by Fisher, Knight & Co., Ltd., St Albans

REPRINTED FROM THE
PROCEEDINGS OF THE PHYSICAL SOCIETY, B, VOL. LXX, p. 928, 1957
All Rights Reserved
PRINTED IN GREAT BRITAIN

Contact Effects resulting from Compression and Flash Sintering in Graphite Powders

By F. A. LEWIS†, J. ORR AND A. R. UBBELOHDE
Department of Chemical Engineering, Imperial College

MS. received 13*th March* 1957, *and in final form* 27*th June* 1957

Abstract. Experiments are described on contact resistance effects in graphite powders : (i) as these are progressively compressed up to 3600 kg cm^{-2} in the cold : this produces a marked decrease of electrical resistance, though it seems unlikely that much compression of the actual crystal lattice of graphite is effected ; (ii) when loosely pressed powder is subjected to flash discharges from a bank of charged condensers ('flash sintering') : this is in order to explore possible mechanisms of sintering that avoid any prolonged heating of the graphite at high temperatures.

In the case of powdered polycrystalline graphite, both (i) and (ii) lead to a marked lowering and stabilization of the electrical resistance. Their influence on the thermoelectric power is discussed. 'Flash sintering' promises to be a useful and accessible technique in studying the conductance of crystal compounds of graphite. The results throw a significant light on the nature of the conductance barriers in graphite powders.

§ 1. INTRODUCTION

PREVIOUS work (McDonnell, Pink and Ubbelohde 1951) has shown that the formation of crystal compounds has marked effects on the electronic properties of graphite. Such effects have been interpreted on a model which attributes both electron donor and electron acceptor properties to the amphoteric layers of fused carbon rings. Intercalation between the layers of acceptor groups such as bromine or aluminium chloride (Orr and Ubbelohde, to be published) reduces the number of electrons in a full band in the carbon macromolecule, whereas intercalation of donors such as the alkali metal atoms injects electrons into the empty band lying just above it. Either process greatly increases the electrical conductivity, and also influences other electronic properties, such as the thermoelectric power (McDonnell, Pink and Ubbelohde 1951) and the Hall effect (Currie *et al.* 1956).

In pursuing this line of investigation on the chemical physics of aromatic systems, one major difficulty springs from the circumstance that most methods yet evolved for preparing lamellar crystal compounds of graphite lead to powders. When properties such as the electrical conductance are studied, it is necessary to determine how far these are influenced by contact effects between particles of the powder, and surface and edge effects between individual crystallites in each particle. Interpretation of such contact effects in terms of fundamental electronic processes in disordered crystals is of considerable theoretical as well as practical importance.

† Now at Department of Chemistry, Queen's University, Belfast, N. Ireland.

In powder metallurgy the process of inducing true lattice joins between particles of powder is known as sintering ; this may also induce crystal growth. Conventional procedures for sintering particles of graphite would require the use of a high temperature, often exceeding 1500°C. Apart from other objections this makes conventional high temperature sintering inapplicable to crystal compounds, which would decompose at much lower temperatures. The present paper records studies of two possible alternative routes for removing uncertainties arising from contact effects in powdered graphite, with the object of extending suitable techniques to the crystal compounds in due course.

Compression in the cold to high pressures can increase the bulk density of powdered graphite to values approaching and exceeding that of the original polycrystalline block from which the powder was prepared. A parallel increase in electrical conductance is found, as is described below. The extent of the change indicates that electron contact barriers between crystallites of graphite are comparatively unimportant and that increasing the density mainly serves to decrease the effective path of flow of the current. This behaviour contrasts with certain other metal powders in which particles may be coated by skins of oxide which have considerably higher resistance than the metal.

Flash sintering appears to remove certain reactive regions at contact points between the particles, probably by inducing local bond rearrangement leading to welding. This has interesting consequences for the electronic properties of loosely contacted graphite powder and suppresses the drift of these properties with time.

§ 2. Experimental

2.1. *Materials*

For measurements under pressure, a block of polycrystalline graphite kindly provided by the Atomic Energy Research Establishment, Harwell was powdered, and the fines passing a 300 mesh sieve were used. The original cylindrical block graphite had a specific resistance along its extrusion axis of $1 \times 10^{-3}\Omega$ cm and across the extrusion axis of $3 \times 10^{-3}\Omega$ cm. Its apparent density was $2{\cdot}00\,\mathrm{g\,cm^{-3}}$, determined by flotation. The bulk density was $1{\cdot}68\,\mathrm{g\,cm^{-3}}$. This powder was also used for many of the flash sintering experiments. In addition, raspings from a rod of Acheson graphite were used for some of the measurements of thermoelectrical power.

Air was not excluded during powdering, so that any free valencies produced by disrupting carbon macromolecules would almost certainly oxidize to peroxide, quinone or OH groups.

2.2. *Pressure Measurements*

Previous studies of the effects of compression in the cold on the electrical conductance of powders have not been extensive, and have frequently been limited to particles coated with skins of different chemical composition and considerably lower conductance. When such skins can be avoided, as appears to be the case in the present studies, the effects of compression on the electronic properties are of considerable fundamental interest. There is, however, a technical difficulty in applying high pressure to powders. If a fluid is used to ensure uniform application of pressure on each particle of the powder, films of the fluid can creep between contacts and influence their electrical properties

by their own resistance. If dry powders are compressed, non-uniform pressures on individual particles tend to be built up by a system of forces and by friction at the walls of the container used. These forces involve proportionately more serious lack of uniformity if the pressure is exerted on small areas and long lengths of a column of powder, as is desirable with a good conductor in order to attain conveniently measurable electrical resistances. Ways of meeting these difficulties in the case of powdered graphite are described in what follows.

Figure 1 shows the resistance cell used for definitive measurements, evolved after many exploratory trials on powdered graphite. Measurement of electrical resistance and apparent density could be carried out simultaneously with this apparatus.

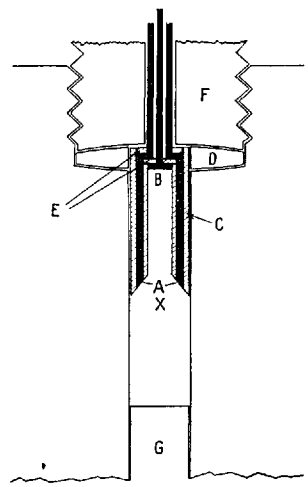


Figure 1.

The cell into which the powder was compressed was a close fit in the top of a high pressure cylinder. The lower end A of a copper cylinder formed one electrode of the cell. The top electrode B was a disc at the end of a copper rod. The electrodes were insulated from one another and from the steel cylinder walls by thin tubes of ethoxyline resin (silica filled). The outer insulating tube C fitted tightly into the lens ring D which helped to align the cell. Both electrodes were shouldered so that the high pressure thrust was transmitted, through insulating washers E, also made from silica filled ethoxyline resin, to the screwed plug F. Above these shoulders the electrodes consisted of a coaxial cylinder and rod. Soldered connections were made to these above the plug F after the cell was in position. Electrical resistance was measured directly by a Smith's low resistance bridge. In order to vary the column length of powder, the maximum length of the cell (5·0 cm) could be reduced, by screwing further short copper cylinders of the same diameter (0·75 cm) into the top electrode.

The cell constant and the resistance of the leads were first measured using salt solutions and mercury. Any changes of cell dimensions before and after application of pressure were measured by the cathetometer and by recalibration of the cell constant with pressures below 3000 kg cm^{-2}. Any irreversible changes in cell dimensions led to errors in the electrical resistance measurements of less than 1%. Corrections for reversible volume changes of the cell materials were of

the same magnitude. Errors of this order do not affect the conclusions discussed below.

The powder under investigation was pressed into the cell by a piston G moving in the high pressure cylinder. A vernier on this piston moved against a graduated scale and was viewed by a remote optical system. The volume occupied by a known mass of graphite (usually about 15 g) could thus be calculated. For each measurement the given pressure was alternately released and reapplied until the electrical resistance had reached a limiting value indicated by no change in resistance on further application of pressure. This operation is analogous to that of tamping. By this means greater reproducibility of results is ensured. Moreover, if the pressure was steadily increased in one single thrust without tamping, damage to the lower electrode and insulating sleeves of the cell resulted due to the powder becoming densely packed at X (figure 1) before the space between the electrodes was filled uniformly.

Because of the uncertainties in the packing of the powder, the usual plot of resistance against column length to test for any appreciable contact resistance between the copper electrodes and the column of powder (McDonnell, Pink and Ubbelohde 1951) cannot be very precise. However, the ratio of the resistance to length of column was found to be practically independent of column length, indicating that any contact resistance between copper and graphite powder could be neglected in the present experiments.

In the course of cycles of observations on electrical resistance and on pressure, which were measured simultaneously, it was noted that as the total compression increased fewer tamping thrusts were necessary before the electrical resistance at the given pressure reached its limiting value. Values of the electrical resistance for unit length were reproducible to within 5% at any given pressure, for different samples of the same powder. Hysteresis was observed in both volume and resistance readings when the pressure was released.

2.3. *Results for Powders under Pressure*

Figure 2 (*a*) records a typical run of pressure measurements. Volume changes were recorded simultaneously. Volume changes at higher pressure (which

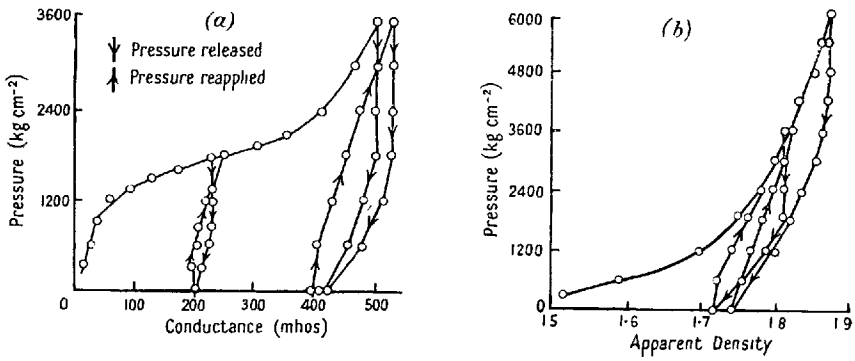


Figure 2.

would have destroyed the resistance cell) were determined in a parallel run after removing the cell electrodes and insulation, and are recorded in figure 2(*b*).

2.3. *Flash Sintering Experiments*

Figure 3(*a*) illustrates the apparatus used for measurements on the electrical resistance and on the thermo electric voltage of columns of powdered graphite. The material was packed in a Pyrex tube A and was maintained between two cylindrical copper electrodes B1, B2, of cross sectional area 0·085 cm^2. These electrodes were a sliding fit in the Pyrex tube and were faced with thin platinum sheet, hard soldered to the copper, so that the barrier contact was between bright platinum and graphite. Each of these copper electrodes formed one arm of a copper–graphite thermocouple. To measure its temperature by means of a

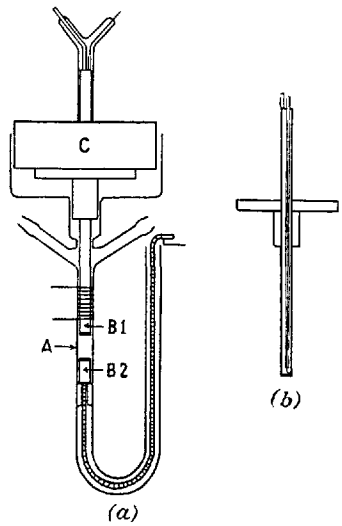


Figure 3.

copper–eureka thermocouple the top electrode carried the eureka wire down its centre and was insulated from it by a glass capillary. A section through this electrode is shown in figure 3(*b*). For resistance measurements, most of the apparatus could be immersed in a bath with thermostat control to $\pm 0{\cdot}05°$ c and no heating coil was used. For special purposes, the sample in the Pyrex tube could be maintained under oxygen-free nitrogen, but this was not found necessary in the experiments described below.

To measure thermoelectric power, a heating coil of 'brightray' wire was wound on the outside of the glass cell in the vicinity of the top electrode so that a controlled temperature difference could be maintained between the two electrodes. The powder column itself and the lower electrode were at the temperature of the thermostat bath in which the cell was immersed. A lead weight C exerted a pressure of 13 kg cm^{-2} on the upper electrode.

The thermoelectric power between the two copper electrodes was measured on a Doran potentiometer to 0·005 mv.

The columns of graphite powder represented in figure 3(*a*) were not tamped but instead the electrode and weight were gently set on top of the powder immediately after it was poured into the cell. Reasons for avoiding tamping were :

(i) when the columns of powder were tamped, the resistance of any given column height could not be easily reproduced. This was attributed to variations

in the degree of tamping and possibly in the preferred orientation of particles ; these were difficult to eliminate. There was also a prolonged drift of resistance with time after tamping, which made measurement very inconvenient. The resistance decreased progressively, suggesting slip followed by welding at points of contact between particles.

(ii) By using untamped columns the effect of flash sintering on poor contact points of high resistance could be more readily followed. Figure 4 (*a*) records measurements of resistance plotted against column length for untamped powders. A curve is obtained instead of the straight line plot normally expected for uniformly packed columns. As the column height increased the packing became progressively less close, and the effective resistance per unit length increased.

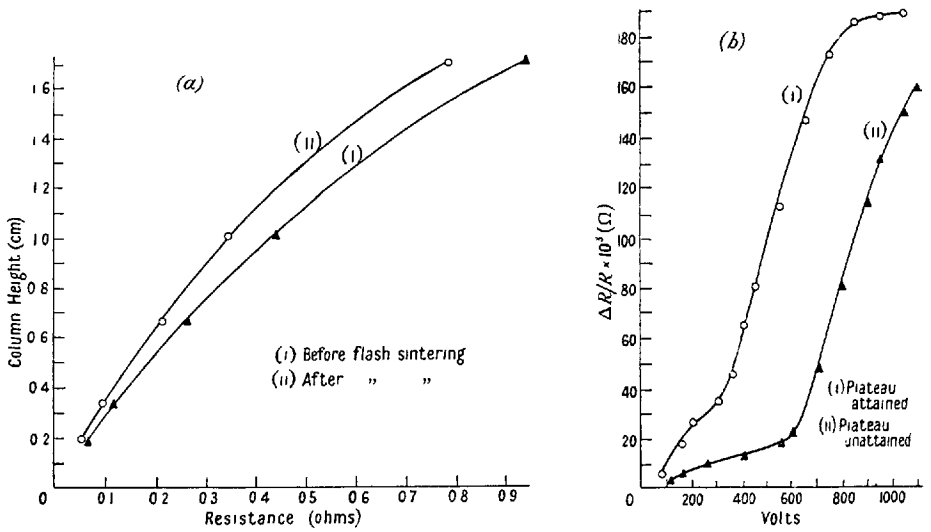


Figure 4.

With the packing precautions as described, quite steady readings of resistance were, however, obtained. After obtaining the highest resistances and column lengths recorded in figure 4 (*a*) the temperature coefficient of total resistance was determined for the longest columns, to minimize any leads effects. Thermoelectric measurements were also made at various bath temperatures. A plot of thermo-e.m.f. against temperature interval between the two carbon–copper junctions gave a straight line (not shown). From its slope the thermoelectric power was obtained as recorded in the table.

2.4. *Effects of Flash Sintering*

The column lengths of graphite powder (figure 4 (*a*)) packed as above were subjected to flash sintering, by discharging a bank of condensers through them of progressively increasing total energy starting with various initial voltages. At first the resistance of the column decreased progressively. A stage or plateau was then reached, after which little further change could be effected by repeated discharges of the same energy or by increasing the total energy still more (figure 4 (*b*). For long columns of large resistance the discharge energy available to us was insufficient to reach this stage. Finally, for discharges considerably more powerful than the plateau values the resistance increased again, due to

Electronic Properties of Graphite before and after Flash Sintering

Sample (A.E.R.E.)	(1)	(2)	(3)
Compact block graphite parallel to extrusion axis.	1000	1·2	−0·1
Compact block graphite perpendicular to extrusion axis.	333	1·2	+1·9
Compact block graphite powdered before flash sintering.	62·5	1·4	+23·0
Compact block graphite powdered after flash sintering.	140	1·2	+20·0

(1) Specific conductance (Ω^{-1} cm^{-1}); (2) Temperature coefficient of conductance $\times 10^3$; (3) Thermoelectric power (μv deg^{-1}).

scattering of the carbon from contact with the platinum, and some vaporization of carbon.

Photomicrographs of the polished platinum caps before and after flash discharge failed to reveal any change of contact surface with the graphite powder, which might help to explain the decrease of resistance. Measurements of resistance are also plotted in figure 4 (*a*) against column length for samples subjected to flash discharges. Calculations of the temperature coefficient of resistance are also recorded in the table. After flash sintering, the graphite itself when tipped out showed no obvious differences from the original powder.

§ 3. Discussion

Various findings recorded in this paper can be discussed conveniently on the basis of the contacts between edges and corners of small 'perfect' crystallites of graphite. In the particles of powder these may be only a little thicker than macro-aromatic molecules of fused carbon rings forming each layer of the perfect crystallite. Various chemical differences may be expected at the edges of such crystallites or macro-aromatic molecules.

(i) Free carbon valencies may be bonded to oxygen atoms. An analogy is when hexaphenylethane interacts with atmospheric oxygen. Bonded oxygen may be present as peroxide bridges or quinone groups. There may also be OH groups if the hydrogen which is often present in graphite has not been completely expelled during its original baking, or if water is absorbed chemically from the atmosphere when the polycrystalline lump is ground and sieved.

(ii) Neighbouring macro-molecules may be jointed by actual carbon bonds, probably under considerable strain, again as in hexaphenylethane and similar molecules. More than one bond may join macro-molecules of carbon in favourable cases.

The effects of cold pressing on the bulk density of graphite powders suggests that random stacking of the crystallites in the original powdered sample appears to be modified to give a very considerable degree of alignment at high pressures. Figure 2 (*b*) indicates that the maximum apparent bulk density achieved in the cold was higher than that (1·68 g cm^{-3}) of the block with preferred orientation

from which the powder was prepared. Considerable strain energy appears to be stored in the compressed powder, which expands again on releasing the pressure. Detailed examination of the hysteresis curves in figure 2 indicated that actual compression of the crystal lattice is unlikely at the pressures achieved. This concurs with estimates of the compressibility of graphite (Riley 1945, Basset 1941).

The effects of cold pressing on the resistance and volume occupancy of graphite powders can be summed up by the conclusion that any electron barriers at contact points between neighbouring crystallites in a particle, or between particles, are only small, and are much less, for example, than between particles of metal where skins of oxide intervene at contact points. Though the electron barriers are only small at contacts between graphite particles, the crystal disorder leads to a scattering of electron waves and thus increases the resistance. Compression probably aligns the crystallites somewhat and reduces the current path ; this factor lowers the resistance to some extent. Detailed comparison with the original extruded block graphite was not feasible because of its preferred orientation. Allowing for this, the conductance of the cold-compressed powder is of the same order as for the original block.

Flash sintering permits local rearrangement of disordered atoms at the scattering points. Practically all the energy dissipated in a discharge with plateau voltage and capacity is liberated in a very short time, of the order of 5 microseconds. If heat conductance during this interval can be neglected, contact points of high scattering resistance will be raised to very high temperatures for a short period. Assuming all the electrical energy is liberated at the contact points, and that these points are thereby raised to 4000°c, it is calculated from the heat content of graphite that the carbon undergoing sintering around these contact points forms 0·1% of the total mass. This could well correspond with the extent of change occurring in actuality.

The flow of graphite powder under pressure shows certain analogies with the discharge process, since mechanical strain energy is probably released by sudden slipping at contact points, which thereby become momentary hot spots. The drift of resistance in tamped columns under light pressures can in fact be compared with a progressive chemical polymerization, in which the macro-molecules of graphite weld together at the hot spots each time a slip occurs. This corresponds with the melting and solidification in other frictional processes ; the high melting point of graphite around 4000°c permits hot spots to attain exceptionally high temperatures.

These conclusions about the contact in graphite powders can be further elucidated from a consideration of the aromatic character of the macro-molecules in graphite. At the edges these cannot hold more than one or two impurity groups such as $=O$, $-OH$, etc. By analogy with the behaviour of smaller aromatic molecules, such groups will form part of the aromatic ensemble of the macro-molecule, by electronic conjugation. Unlike powdered metals, powdered graphite cannot therefore readily form thick barrier layers of low conductance, separating individual crystallites. This conclusion is highly important in developing the study of crystal compounds of graphite obtainable only in powder form.

The effects of flash sintering on the electronic properties give additional and more detailed information, particularly in the case of electronic properties of the

macro-molecules which are more sensitive to edge effects than the overall conductance. In a model of graphite discussed by Mrozowski (1952) it is pointed out that valency defects at specific carbon atoms in graphite remove corresponding electrons from the full band of the perfect crystal, to lower energy levels. Such valency defects if not too numerous increase the conductance, and affect other electronic properties of graphite correspondingly.

The present experiments are primarily concerned with edge defects. The first point to note is that whilst the thermoelectric power of the original block graphite against copper lay between $-0{\cdot}1$ and $+1{\cdot}9\mu$v deg^{-1} according to the orientation, the same material in powdered form in a lightly packed column shows a thermo electric power of $+23{\cdot}0\mu$v deg^{-1}. This comparatively large change would be expected if a large increase in edge defects and possible edge oxides occurs on powdering, thus depleting the band in the graphite crystallites.

Because of the increased conductance path in the powder, direct comparisons of the conductance in block and powder do not give immediate information about changes in the Π bands. However, differences between the temperature coefficients of conductance for block and powdered graphite again indicate a greater depletion of the Π band in the powders.

The length of column was not found to alter appreciably after flash sintering. But the effective conductance paths are probably shortened by the elimination of electron scattering at contacts between impurity groups and by the direct formation of carbon–carbon bonds. Flash sintering removes a considerable proportion of defect sites, as is confirmed by the changes in electronic properties in the table. The temperature coefficient of resistance drops to the value for block graphite and the thermoelectric power becomes less positive, as defects which deplete the Π band decrease in number.

Acknowledgments

The authors wish to thank the referees for drawing their attention to the experiments of Bowden and Williamson (1954), with contacts of gold. These would not form thick oxide films separating the metal conductors, and it is interesting that the findings of these authors lend broad support to our present conclusions for graphite particles.

Thanks are due to the Central Electricity Board for their support of this research.

References

Basset, J., 1941, *C. R. Acad. Sci., Paris*, **213**, 829.

Bowden, F. P., and Williamson J. B. P., 1954, *Research Correspondence*, Vol. 7, Number 10, October 1954.

Currie, L. M., Hamister, V. C., and MacPherson, H. G., 1956, *Proceedings of the International Conference on the Peaceful Uses of Atomic Energy* (New York : United Nations) Vol. 8, p. 451.

McDonnell, F. R. M., Pink, R. C., and Ubbelohde, A. R., 1951, *J. Chem. Soc.*, 191.

Mrozowski, S., 1952, *Phys. Rev.*, **85**, 609, **86**, 1056.

Riley, D. P., 1945, *Proc. Phys. Soc.*, **57**, 486.